

Università degli Studi di Salerno



Dipartimento di Chimica e Biologia "A. Zambelli"

Ph. D. Course in Chemistry - XXXII Cycle

Ph. D. Thesis in Chemistry

New perspectives in phase transfer catalysis

Tutor:

Dr. G. Della Sala

Co-tutors:

Prof. P. Neri

Prof. L. Bernardi (Università di Bologna)

PhD Coordinator:

Prof. R. Zanasi

Doctorate Student:

Marina Sicignano

8800100026

2016-2019

Alla mia famiglia

Abstract

The increasing demand for the stereoselective synthesis of bioactive compounds in both industrial and academic research has led to the rapid development of a variety of diastereo- and enantio-selective processes using phase transfer catalysis conditions. Because of its advantages, such as mild reaction conditions, simple procedures, scalability, use of inexpensive and recyclable catalysts, high selectivity and yields, phase transfer catalysis (PTC) is considered a green alternative to many homogeneous techniques. Therefore, this catalytic strategy has found widespread application in organic synthesis for the construction of several natural and unnatural compounds.

In this regard, this research project has been mainly aimed at the design and development of new stereoselective methodologies under mild phase transfer catalysis conditions for the synthesis of novel potentially bioactive products. In the first part of the thesis, the well-known cation-binding catalytic properties of crown ethers have been further explored in previously unreported arylogous Michael additions of weakly activated and unactivated phthalides, achieving new products with high stereoselectivity and yields by using inexpensive achiral catalysts and mild reaction conditions. Phthalides attracted our interests because of their large diffusion in natural sources, their broad range of biological activities, such as anti-inflammatory and anti-bacterial properties, and the consequent extensive use in medicinal chemistry, but also for their usefulness in organic synthesis as versatile building blocks.

Next, the synthesis of enantioenriched novel products catalyzed by chiral quaternary ammonium salts has been investigated. The commercial availability, high efficiency and broad applicability of these catalysts make them ideal candidates for the discovery of new asymmetric phase transfer

transformations. In this context, the first asymmetric alkylation of 3-carboxylic-*t*-Bu-ester phthalides has been developed, giving easy access to a novel class of potentially useful enantioenriched compounds.

Moreover, during my stay in the laboratories of Prof. José Alemán, at the Universidad Autónoma de Madrid, the asymmetric introduction of the SCF₃ group at C-4 position of both azlactone and isoxazolidin-5-one substrates has been developed, affording novel enantioenriched thiofluorinated compounds with high enantiocontrol of the newly generated quaternary chiral centers. The first example of enantioselective synthesis of a valuable α -SCF₃- $\beta^{2,2}$ -amino acid has been also described. Knowing the attractive features of fluorine-containing molecules, relevant applications of these new chiral thiofluorinated products in the pharmaceutical and medicinal field could be envisaged.

TABLE OF CONTENTS

<i>List of publications</i>	12
<i>List of abbreviations</i>	13
1. Introduction	15
1.1 Phase Transfer Catalysis	16
1.2 Phase Transfer Catalysts	22
1.3 Asymmetric Phase Transfer Catalysis	30
1.3.1 Chiral phase transfer onium salts	31
1.3.2 Chiral macrocyclic phase transfer catalysts	48
1.4 Aims of the work	55
2. Diastereoselective synthesis of substituted	
Phthalides	58
2.1 Phthalides	59
2.2 Stereoselective methods for the construction of the lactone ring	62
2.3 Stereoselective alkylation methods at C-3 site of phthalides	65
2.3.1 Stereoselective alkylations at C-3 site of activated phthalides	66
2.3.2 Stereoselective alkylations at C-3 site of unactivated or weakly activated phthalides	72
2.4 Diastereoselective Michael addition of weakly activated	
Phthalides	74
2.4.1 Specific objectives	74
2.4.2 Results and discussions	76
2.4.3 Conclusions	84
2.5 Diastereoselective Michael addition of unactivated phthalides	85
2.5.1 Specific objectives	85

2.5.2 Results and discussions	86
2.5.3 Mechanistic insights and DFT calculations	99
2.5.4 Conclusions	104
2.6 Asymmetric Michael addition of weakly activated phthalides	105
2.6.1 Specific objectives	105
2.6.2 Results and discussions	105
2.6.3 Conclusions	110
3. Enantioselective alkylation of 3-substituted Phthalides	111
3.1 Enantioselective alkylation of 3-carboxylic-<i>t</i>-Bu-ester-phthalides	112
3.1.1 Specific objectives	112
3.1.2 Results and Discussion	113
3.1.3 Conclusions	128
4. Novel asymmetric trifluoromethylthiolation reactions	129
4.1 Thiofluorinated compounds	130
4.2 Asymmetric trifluoromethylthiolation of azlactones	137
4.2.1 Specific objectives	137
4.2.2 Results and discussions	139
4.2.3 Mechanistic speculations	153
4.2.4 Conclusions	155
4.3 Asymmetric trifluoromethylthiolation of isoxazolidin-5-ones	156
4.3.1 Specific objectives	156
4.3.2 Results and discussions	158
4.3.3 Conclusions	166

5. Summary	167
5.1 Final conclusions	168
6. Experimental section	171
6.1 General procedures	172
6.2 Diastereoselective Michael addition of weakly activated phthalides	173
6.2.1 Synthesis of 3-aryl phthalides 75b-f	174
6.2.2 General Procedure for the arylogous Michael reaction of 3-aryl phthalides	175
6.2.3 Analytical data of products 78aa-fd	177
6.2.4 Procedure for the reaction of 75a with 76a catalyzed by TBAB and KOH	182
6.2.5 X-ray crystallography	183
6.3 Diastereoselective Michael addition of unactivated phthalides	185
6.3.1 Synthesis of substrates	185
6.3.2 General Procedure for the arylogous Michael reaction of unactivated phthalides	187
6.3.3 Analytical data of arylogous Michael adducts of phthalides	187
6.3.4 Arylogous Michael reaction of 79a and 76a with neutral work-up	196
6.3.5 ¹ H NMR monitoring of arylogous Michael reaction of 79a and 76a in the absence of BSA	197
6.3.6 Study of degradation of trans-chalcone under the reaction conditions at different temperatures	198
6.3.7 Study of possible <i>anti</i> to <i>syn</i> conversion under reaction conditions	199

6.3.8 <i>X</i> -ray crystallography	200
6.3.9 Computational data	202
6.4 Asymmetric Michael addition of weakly activated phthalides	209
6.4.1 General procedure for the asymmetric AMR of 3-Ph-phthalide	210
6.4.2 General procedure for the synthesis of compound 89aa	211
6.5 Enantioselective alkylation of 3-substituted-Phthalides	211
6.5.1 Synthesis of phase transfer catalyts 94e, 94o-s	212
6.5.2 Synthesis of 3-carboxylic- <i>t</i> -butyl-ester-phthalides 91a, 91c-e	214
6.5.3 Synthesis of compound 91b	217
6.5.4 Synthesis of compounds 97 and 98	219
6.5.5 Typical procedure for the synthesis of racemic compound 93a	219
6.5.6 General procedure for the enantioselective alkylation of 3-carboxylic- <i>t</i> -butyl-ester-phthalide	220
6.5.7 Analytical data of asymmetric 3,3-disubstituted phthalides	220
6.5.8 <i>X</i> -ray crystallography	227
6.6 Asymmetric trifluoromethylthiolation of azlactones	228
6.6.1 Synthesis of azlactones substrates	229
6.6.2 Typical procedure for the synthesis of racemic compound 130a	231
6.6.3 General procedure for the enantioselective trifluoromethylthiolation of azlactones	231
6.6.4 Analytical data of asymmetric trifluoromethylthiolated compounds	232
6.7 Asymmetric trifluoromethylthiolation of isoxazolidin-5-ones	239
6.7.1 Synthesis of <i>N</i> -Boc α -substituted isoxazolidin-5-one	239
6.7.2 General procedure for the synthesis of compounds 105, 108, 118 and 136	244
6.7.3 Typical procedure for the synthesis of racemic compounds 134a	245

6.7.4 General procedure for the asymmetric Trifluoromethylthiolation of Isoxazolidin-5-ones	245
6.7.5 General procedure for the synthesis of 2-trifluoromethylthio- $\beta^{2,2}$ -amino acid 137a	257
6.7.6 <i>X</i> -Ray data	258

List of publications

M. Sicignano, A. Dentoni Litta, R. Schettini, F. De Riccardis, G. Pierri, C. Tedesco, I. Izzo, G. Della Sala, *Highly Diastereoselective Crown Ether Catalyzed Arylogous Michael Reaction of 3-Aryl Phthalides*, *Org. Lett.*, **2017**, *19*, 4383-4386.

R. Schettini, M. Sicignano, F. De Riccardis, I. Izzo, G. Della Sala, *Macrocyclic Hosts in Asymmetric Phase-Transfer Catalyzed Reactions*, *Synthesis*, **2018**, *50*, 4777-4795.

M. Sicignano, R. Schettini, L. Sica, G. Pierri, F. De Riccardis, I. Izzo, M. Bholanath, Y. Minenkov, L. Cavallo, G. Della Sala, *Unprecedented Diastereoselective Arylogous Michael Addition of Unactivated Phthalides*, *Chem. Eur. J.*, **2019**, *25*, 7131–7141.

V. Capaccio, M. Sicignano, R. I. Rodriguez, G. Della Sala, J. Alemán, *Asymmetric Synthesis of α -Trifluoromethylthio- β -Amino Acids under Phase Transfer Catalysis*, *Org. Lett.*, **2019**, DOI:10.1021/acs.orglett.9b04195.

M. Sicignano, R. I. Rodriguez, V. Capaccio, F. Borello, G. Della Sala, J. Alemán, *Expanding the Realm of Phase Transfer Catalysis: Asymmetric Trifluoromethylthiolation of Azlactones*, manuscript in preparation.

M. Sicignano, R. Schettini, M. L. Marino, G. Pierri, I. Izzo, F. De Riccardis, L. Bernardi, G. Della Sala, *Asymmetric phase transfer catalyzed alkylation of 3-carboxylic-*t*-Bu-ester-phthalides*, manuscript in preparation.

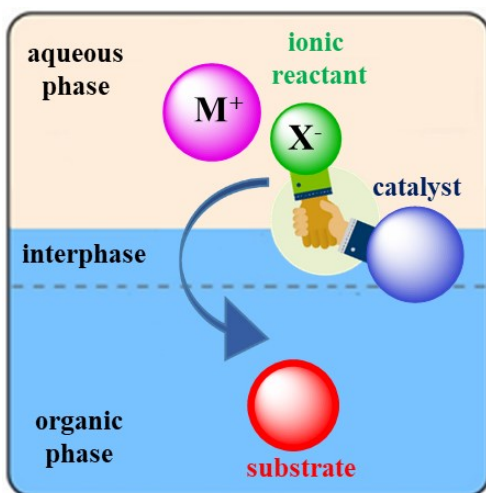
List of abbreviations

PTC	Phase Transfer Catalysis
LL	Liquid-Liquid
SL	Solid-Liquid
BINOL	1,1'-Bi-2-naphthol
APTC	Asymmetric Phase Transfer Catalysis
Ph	Phenyl
Bn	Benzyl
Me	Methyl
Et	Ethyl
MIRC	Michael Initiated Ring Closure
t-BuOH	<i>tert</i> -butanol
THF	Tetrahydrofuran
(DHQD)₂PHAL	Hydroquinidine 1,4-phthalazinediyl diether
CN	cyano
LDA	Lithium diisopropylamide
TIPS	Triisopropylsilyl ether
TBDPS	<i>tert</i> -Butyldiphenylsilyl ether
MBH	Morita-Baylis-Hillman
Cbz	carboxybenzyl
Boc	<i>tert</i> -butoxycarbonyl
Ar	Aryl
AMR	Arylogous Michael reaction

DMF	<i>N,N</i> -Dimethylformamide
DCE	Dichloroethane
18C6	18-crown-6
15C5	15-crown-5
DCH18C6	dicyclohexyl-18-crown-6
BTEAC	benzyltriethylammonium chloride
TBAC	tetrabutylammonium chloride
MTBE	Methyl <i>tert</i> -butyl ether
Tf	Triflate

Chapter 1

Introduction



Phase Transfer Catalysis

1. Introduction

1.1 Phase Transfer Catalysis

The transformations of organic starting materials into target products require, in most cases, a great number of synthetic steps involving the use of different solvents, catalysts, additives, etc. with the consequent production of several waste materials. Therefore, the planning of a chemical strategy able to minimize eco-unfriendly issues should be crucial. In this regard, the *Phase Transfer Catalysis* (PTC) is one of the most versatile and green methodologies of organic synthesis for the construction of useful chemical products.¹ Because of its several advantages, this approach is widely employed both in academic and industrial processes. In particular, the typical benefits of this technique, such as extremely simple procedures and work-up, high selectivity and yields, mild reaction conditions, low energy consumption, absence of water-sensitive reagents, makes it especially suitable for industrial applications.² The PTC is a mechanistically unique methodology because the use of the phase transfer catalyst allows the chemical activation of the substrates together with transport phenomena. Under these conditions, a rate enhancement can take place for reactions between reagents partitioned in two immiscible phases, as is the case with inorganic water-soluble reagents and lipophilic substrates.³ Since the majority of PTC reactions concern the transfer of an anion from an aqueous phase (LL-PTC) or solid phase (SL-PTC) into an organic phase, the most common phase transfer catalysts are salts containing an organic and

¹ M. Makosza, *Pure Appl. Chem.*, **2000**, 72,1399-1403.

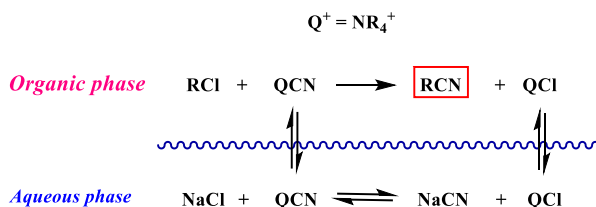
² J. Tan, N. Yasuda, *Org. Process Res. Dev.* **2015**, 19, 1731-1746.

³ F. Montanari, D. Landini, F. Rolla, *Topics in Current Chemistry*, **1982**, 101,147-200.

moderately lipophilic cation, such as ammonium and phosphonium salts, or macrocyclic cation-binding agents such as crown ethers and cryptands.⁴ They, in fact, promote the migration of the anionic species across the two immiscible phases by forming lipophilic ion pairs.

The term “*phase transfer catalysis*” was introduced by Starks in 1971.⁵

A classic example of PTC is the reaction between 1-chlorooctane and aqueous sodium cyanide (**Scheme 1.1**).⁶ Under neat conditions, no substitution occurs in the absence of any catalyst even with heating the mixture for two days, whereas just 1 wt % of the appropriate ammonium salt is enough to catalyze the full conversion to 1-cyanooctane in 2 hours. The catalyst allows the transfer of cyanide anion into the organic phase releasing it in a more reactive form and promoting the displacement reaction with the alkyl halide. Finally, with the migration of the displaced chlorine anion into the aqueous phase, a new catalytic cycle starts.



Scheme 1.1 Mechanistic scheme of the phase transfer catalyzed substitution reaction between 1-chlorooctane and sodium cyanide

⁴ M. Fedorynski, M. Jezierska-Zieba, B. Kakol, *Drug Research*, **2008**, 65, 647-654.

⁵ C. M. Starks, *J. Am. Chem. Soc.*, **1971**, 93, 195-199.

⁶ a) C. M. Starks, C. L. Liotta, M. E. Halpern, *Phase-Transfer Catalysis: Fundamentals, Applications, and Industrial Perspectives*, Chapman & Hall: New York, **1994**; b) C. M. Starks, C. L. Liotta, *Phase Transfer Catalysis: Principles and Technique*, Academic Press, INC: New York, **1978**.

It is important to note that PTC reactions always involve two general steps:

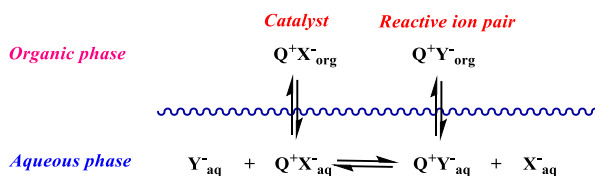
- 1) The *transfer step*
- 2) The *intrinsic reaction step*

The first includes the anion transport from the aqueous or solid phase into the organic phase, while the second one encompasses the reaction sequence occurring in the organic phase and leading to the desired product. High rates of both steps are necessary to obtain favorable PTC processes. Several parameters strongly affect the kinetics of phase transfer reactions such as the type and the lipophilicity of the catalyst, the temperature, the agitation rate, the dielectric constant of the solvent, the tightness of the cation-anion pair, the amount of water in the inorganic phase, the anion hydration-degree in the organic phase, and others. Clearly, some parameters affect much more one step than the other. For example, *transfer* rate-limited reactions are heavily affected by stirring rate, while this factor has less influence on *intrinsic* rate-limited processes. Therefore, in order to achieve optimal results, it is very important to identify the rate-limiting step. However, despite the key role of phase transfer catalysis in organic synthesis, some mechanistic aspects remain unclear to date. The difficulty of the study is mainly due to the great number of parameters that must be considered for a biphasic system.⁷

In typical PTC reactions, the anionic species are introduced in the heterogeneous system as inorganic salts or are generated *in situ* by treatment of a weakly acidic organic precursor with a strong inorganic base. For a simple liquid-liquid, aqueous-organic reaction, Starks proposed the first general mechanism (**Scheme 1.2**). The onium catalyst $Q^+ X^-$ partitioned between the two immiscible phases, comes in contact with the inorganic salt in the aqueous phase, giving an anion exchange that releases the active

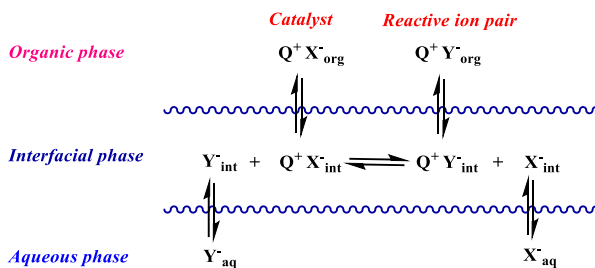
⁷ K. Maruoka, *Asymmetric Phase Transfer Catalysis*, WILEY-VCH Verlag GmbH & Co. KGaA: Weinheim, **2008**.

species Q^+Y^- . The new catalytic ion pair migrates into the organic phase and promotes the reaction. Then, the anionic product X^- moves into the aqueous phase restarting the catalytic cycle.⁸



Scheme 1.2 Schematic Starks mechanism

Later on, a modified extraction mechanism *across the interphase* was proposed by Brändström and Montanari⁹ in order to give a mechanistic rationale for the good activity of strongly lipophilic catalysts, which are sparingly soluble in the aqueous phase.¹⁰ This pathway does not require the complete migration of the catalyst into the aqueous phase, but the anion exchange between the catalyst Q^+X^- and the inorganic salt M^+Y^- takes place in the interfacial area, also referred as *interphase* (**Scheme 1.3**).



Scheme 1.3 Schematic Interfacial mechanism

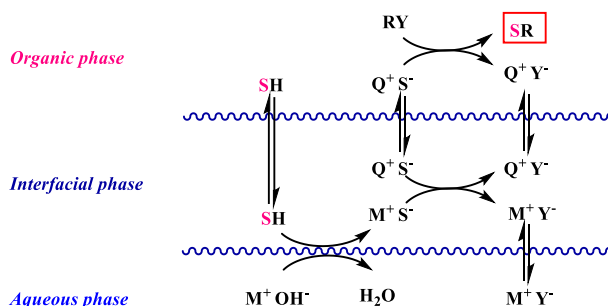
⁸ G. Pozzi, S. Quici, R. H. Fish, *Journal of Fluorine Chemistry*, **2008**, 129, 920-929.

⁹ A. Brändström, *Adv. Phys. Org. Chem.*, **1977**, 15, 267-330.

¹⁰ D. Landini, A. Maia, F. Montanari, *J. Am. Chem. Soc.*, **1978**, 100, 2796-2801.

This altered mechanism is more likely to occur with more lipophilic catalysts, such as large water-insoluble quaternary onium salts R_4N^+ containing long alkyl chains or lipophilic acyclic or cyclic polyethers.

An *interfacial* LL-PTC mechanism was also suggested by Makosza for reactions where aqueous solution of alkali hydroxide $M^+ OH^-$ are used to generate the active anionic species S^- starting from slightly acidic substrates SH (**Scheme 1.4**).¹¹ After the ion exchange step in the interphase, the lipophilic ion-pair $Q^+ S^-$ migrates into the organic phase promoting the intrinsic organic reaction with the electrophile RX.



Scheme 1.4 Schematic Interfacial mechanism in the presence of slightly acidic substrates

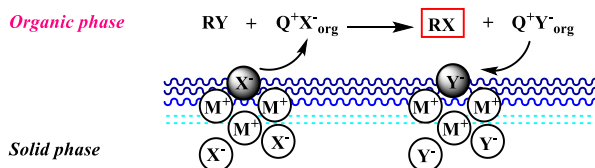
However, according to mechanistic studies, the simple extraction mechanism and the interfacial mechanism should be considered as two extreme cases of several intermediate LL-PTC pathways.¹² In addition, some reactions can also take place with both mechanisms.

Unlike LL-PTC reactions, involving two immiscible aqueous-organic phases, in SL-PTC systems, the solid inorganic salt is suspended in the organic solvent. The two methods, although analogous, have some differences. Reactions that do not occur in liquid-liquid phases, may be

¹¹ M. Makosza, *Pure Appl. Chem.*, **1975**, *43*, 439–462.

¹² H. M. Yang, H. S. Wu, *Catal. Rev. Sci. Eng.*, **2003**, *45*, 463–540.

accelerated in solid-liquid conditions.¹³ This is the case of some fluorine and acetate induced phase transfer reactions because the absence of water increases the reactivity of poorly nucleophilic anions. The SL-PTC is a powerful methodology especially useful to avoid undesired water effects, such as hydrolysis side reactions and slow reaction rates. Crown ethers are usually claimed better catalysts than onium salts for solid-liquid processes. As represented in **Scheme 1.5**, the phase transfer Q^+ species (a quaternary onium salt, a polyethylene glycol- or a crown ether-cation complexed) delivers the anionic reactant X^- as a lipophilic ion pair $Q^+ X^-$ from the surface of the solid salt into the organic phase. Then, the intrinsic reaction takes place and the co-product Y^- comes back into the solid phase.¹⁴ In several examples, quaternary onium salts are reported to be unable to exchange anions directly with anhydrous solid salts.¹⁵



Scheme 1.5 Schematic solid-liquid phase transfer mechanism

Two negative features affect the SL-PTC methods: a) the transfer step is usually rate-limiting because the solid-liquid diffusion is slow, b) the product Y^- covers the solid surface hindering the anion migration into the organic system. However, a series of experiments show that very little amounts of water (ranging from 0.5 to 5% based on the solid salt) increase the rates of

¹³ M. Makosza, M. Fedorynski, *Handbook of Phase Transfer Catalysis*; Y. Sasson, R. Neumann, Eds., Academic & Professional: London, **1997**, 35, 135-167.

¹⁴ D. Albanese, D. Landini, A. Maia, M. Penso, *Ind. Eng. Chem. Res.*, **2001**, 40, 2396-2401.

¹⁵ a) S. Dermeik, Y. Sasson, *J. Org. Chem.*, **1985**, 50, 879-882. b) H. A. Zahalka, Y. Sasson, *J. Chem. Soc., Chem. Commun.*, **1984**, 1652-1654. c) E. V. Dehmlow, H. C. Rath, *J. Chem. Res.*, **1988**, 12, 384-385.

SL reactions if compared to anhydrous conditions. The reason is that small quantities of water cover the surface of the solid crystal forming a thin aqueous film named *omega phase*. This new region acts as a sponge adsorbing the catalyst from the organic phase and enhancing the rate of anionic transport. Generally, under these conditions, even onium salts work effectively. Nevertheless, if the optimal amounts of water are exceeded, the reaction rates drastically decrease owing to the anion hydration.

1.2 Phase Transfer Catalysts

The phase transfer catalysis is a versatile powerful anion-activating method. Thanks to the weak coulombic interactions with bulky cationic species Q^+ , such as onium or polyether-metal cation, the reactivity of Y^- anions is usually high. This effect is greater when solid-liquid PTC conditions or concentrated aqueous alkaline solutions in liquid-liquid systems are used. As a result of the reduced interaction, these anions are considered “*naked*” species. An active PT catalyst must ensure the formation of a *loose* ion pair and a favorable partition equilibrium between the two immiscible phases. Key requirements when choosing a PT agent are the stability under reaction conditions, structural features, availability, cost and activity.¹⁶ The most widely used catalysts are quaternary onium salts (*quats*) and neutral ligands such as crown ethers, cryptands and polypodands.¹⁷ Lipophilicity and extraction capability of onium salts strongly increase with the length of the chains. However, if the alkyl groups are too bulky, the rate of the anion extraction decreases since the approach of the positive atom to the *interface* becomes more hindered. An optimal balance between the accessibility of the

¹⁶ S. D. Naik, L. K. Doraiswamy, *Alche Journal*, **1998**, *44*, 612-646.

¹⁷ D. R. Joshi, N. Adhikari, *World J. Pharm. Res.*, **2019**, *8*, 508-515.

positive charge and lipophilicity is necessary.¹⁸ Tetramethyl-, tetraethyl- and tetraisopropyl-ammonium cations are too hydrophilic and usually ineffective catalysts, whereas tetrabutylammonium salts, due to their moderate organophilicity and high availability, are very common PT catalysts. High performances are reported with tetraalkylammonium quats containing pentyl- esyl- and longer chains up to decyl- groups. Examples of ammonium and phosphonium salts are reported in **Figure 1.1**.

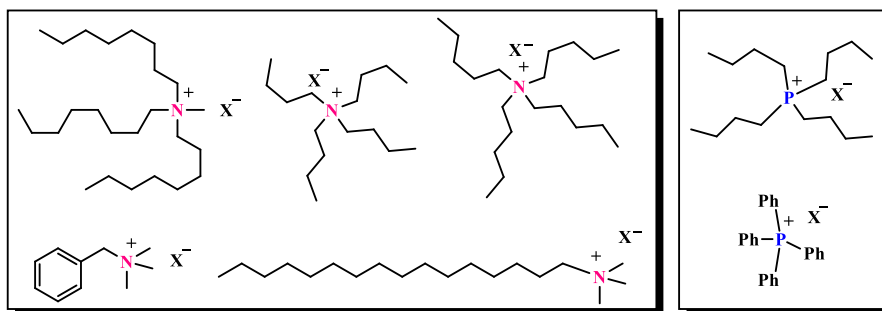


Figure 1.1 Examples of ammonium and phosphonium salts

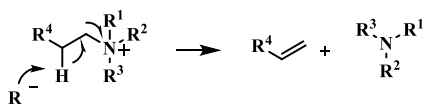
In addition, the catalyst efficiency is also influenced by the nature of the anions.¹⁹ In fact, with small and highly hydrated anions such as OH^- and F^- , which are slowly transported into the organic phase, unsymmetrical open-faced and accessible quats, such as $\text{C}_{16}\text{H}_{33}\text{NMe}_3^+$ and BnNEt_3^+ , provide the best results because the cation approach to the interphase is facilitated. However, quaternary onium salts are not very stable under strongly basic conditions such as 50% NaOH or KOH aqueous solutions, especially at higher temperatures, leading to Hofmann eliminations, nucleophilic substitutions and Stevens rearrangements decomposition products (**Scheme**

¹⁸ M. Rabinovitz, Y. Cohen, M. Halpern, *Angew. Chem. Int. Ed. Engl.*, **1986**, 2, 960-970.

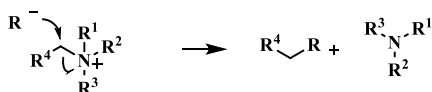
¹⁹ D. Albanese, *Catal. Rev.*, **2003**, 45, 369-395.

1.6).²⁰ In detail, these issues occur under milder reaction conditions with phosphonium salts limiting their use.

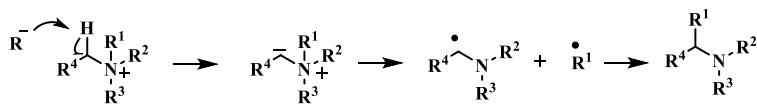
Hoffman Elimination



Nucleophilic Substitution



Stevens Rearrangement



Scheme 1.6 Examples of typical decomposition of quaternary ammonium salts

Generally, macrocyclic ligands such as crown ethers and cryptands show higher stability in basic media at high temperature, though they are more expensive and sensitive to acidic conditions. Thanks to their ability to form highly stable complexes with cations, these ligands are widely applied as phase transfer catalysts. Indeed, Pedersen's discovery of crown ethers is one of the major milestones of organic chemistry.²¹ The selective complexation of alkali and alkaline earth metals by crown ethers can be considered as a supramolecular host/guest type interaction enabled by the molecular organization of the electron-donating oxygen atoms in the macrocycle. The stability constants of such complexes strongly depend on the compatibility between the ionic radius of the cation and the macrocycle's cavity size.

²⁰ a) D. E. Patterson, S. Xie, L. A. Jones, M. H. Osterhout, C. G. Henry, T. D. Roper, *Org. Process Res. Dev.*, **2007**, *11*, 624-627; b) L. Vial, M. H. Gonçalves, P. Y. Morgantini, J. Weber, G. Bernardinelli, J. Lacour, *Synlett*, **2004**, 1565-1568.

²¹ C. J. Pedersen, *Angew. Chem. Int. Ed. Engl.*, **1988**, *27*, 1021-1027.

Accordingly, it is well-known that Li^+ , Na^+ , K^+ and Cs^+ cations are highly compatible in shape and size with 12-crown-4, 15-crown-5, 18-crown-6 and 21-crown-7 respectively, as depicted in **Figure 1.2**.

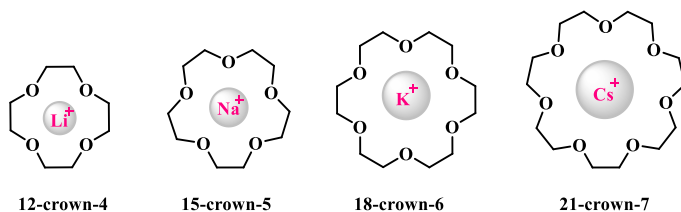


Figure 1.2 Crown ethers and alkali metals complexation

Examples of common cryptands are reported in **Figure 1.3**. Thanks to a macrobicyclic effect, high complexation constants with metal ions are usually ensured. Nevertheless, these compounds are more expensive than crown ethers.

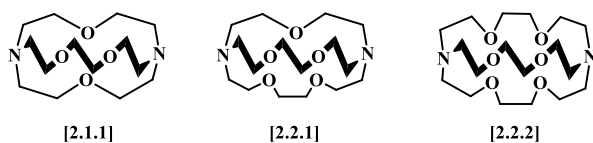


Figure 1.3 Examples of cryptands

Podands and polypodands are also used as phase transfer catalysts (**Figure 1.4**). They are inexpensive and non-toxic but generally show lower activity than macrocycles and onium salts due to lower extraction constants. In order to decrease their hydrophilicity, some lipophilic structural motifs are, introduced.

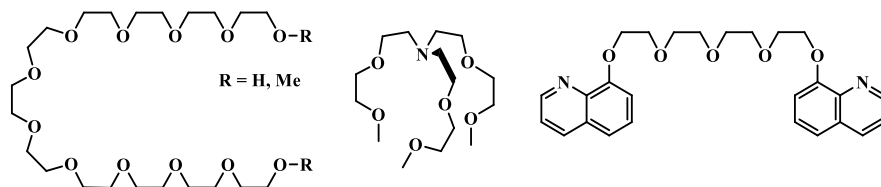


Figure 1.4 Examples of podands and polypodands

Crown ethers and cryptands exhibit excellent catalytic activity, especially, in solid-liquid phase transfer systems, so much to be considered as the optimal catalysts in many heterogeneous processes.²² Under LL-PTC conditions, the activity of crown ethers is often limited by the reduced lipophilicity and less favorable partition equilibrium if compared to bulky quats. In order to increase their organophilicity, alkyl chains and/or aromatic rings are generally introduced in the simple polyether skeleton. Typical sterically hindered crown ethers are showed in **Figure 1.5**.

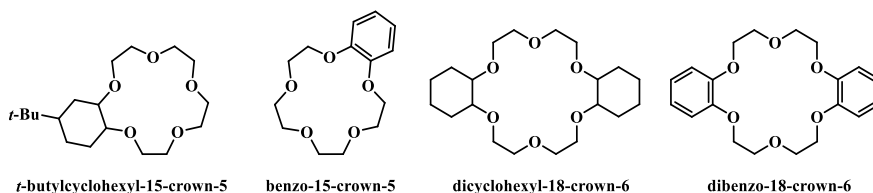


Figure 1.5 Examples of lipophilic crown ethers

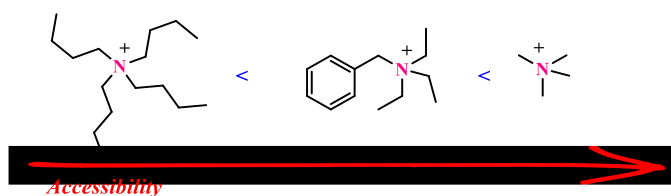
Moreover, the extraction constants of cation-binding ligands can be extremely different from those of quat salts.²³ Specifically, crown ethers are better performing with soft, more polarizable anions such as Γ^- and SCN^- due

²² a) M. C. Vander Zwan, F. W. Hartner, *J. Org. Chem.*, **1978**, *43*, 2655-2656. b) A. Maia, D. Landini, S. Petricci, *Supramol. Chem.*, **2000**, *11*, 289-292; c) L. Xia, Y. Jia, S. Tong, J. Wang, G. Han, *Kinet. Catal.*, **2010**, *51*, 69-74.

²³ D. Landini, A. Maia, F. Montanari, F. M. Pirisi, *J. Chem. Soc., Perkin II* **1980**, 46-51.

to the better partition ability, while onium salts are more efficient with hard, smaller counteranions as Cl^- and N_3^- .²⁴

Unlike the extraction mechanism promoted by onium salts, the complexation process of macrocyclic catalysts involves the generation of large lipophilic M^+ -crown species associated with the corresponding counteranion. However, in both cases, the formation of loose or tight ion pairs is involved. The tightness of the ion pair strongly affects the reactivity of the anionic species. Loose ion pairs are favored by sterically hindered cationic species, hampering the direct ion contact. On the other hand, very sterically accessible cations lead to the formation of tight or contact ion pairs, limiting the anionic reactivity.^{6,25} In particular, the cation accessibility of quaternary onium salts decreases with bulkier chains leading to looser ion pairs, as simply represented in **Scheme 1.7**.



Scheme 1.7 Accessibility trend of quaternary ammonium cations

Crown ethers form M^+ -crown/anion complexes tighter than bulky ammonium salts since the metal cation is easily accessible above and below the macrocycle plane. On the contrary, cryptands lead to the highest cation-anion separation because the metal cation is unaccessible being completely encapsulated into the macrobicyclic cavity (**Figure 1.6**).⁶

²⁴ A. Maia, *Pure & Appl. Chem.*, **1995**, 67, 697-702.

²⁵ M. Halpern, *Phase-Transfer Catalysis, Ulmann's Encyclopedia Of Industrial Chemistry*, Wiley-VCH Verlag GmbH & Co. KGaA, Weinheim, **2012**, 495-501.

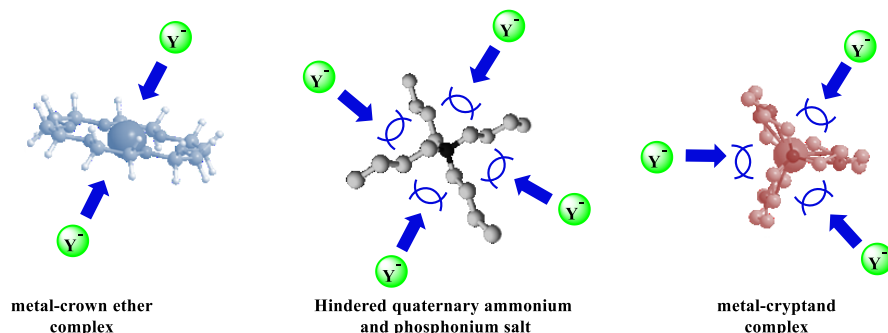
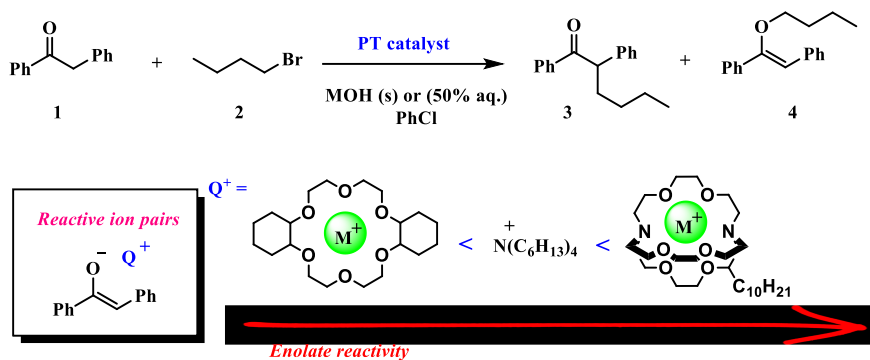


Figure 1.6 Accessibility of cation center

In this context, a kinetic study conducted for the phase transfer catalyzed alkylation reaction of deoxybenzoin **1** showed that the enolate reactivity strongly depends on the type of ligand involved.²⁶ In particular, the highest rate constants were achieved with [2.2.2]-Cryptand. This catalyst provided the highest cation-anion separation and, consequently, the most reactive anion. Lower reactivities were, instead, observed with hexylammonium chloride and even less with DCH-18-crown-6 under the same reaction conditions (Scheme 1.8).

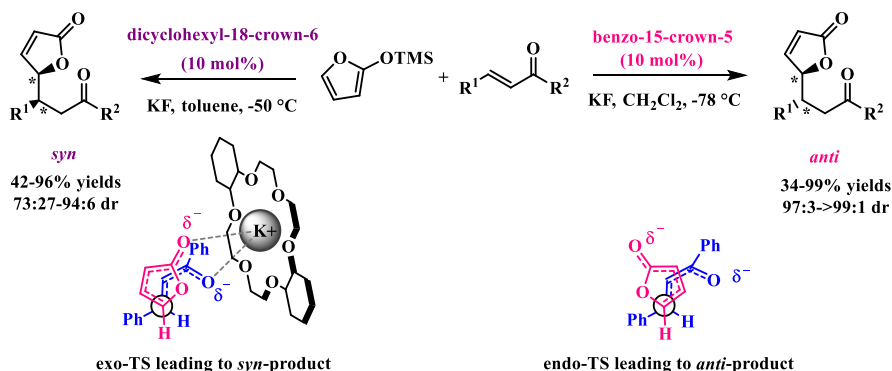


Scheme 1.8 Reactivity of the alkylation reaction of deoxybenzoin

²⁶ A. Gobbi, D. Landini, A. Maia, S. Petricci, *J. Org. Chem.* **1998**, *63*, 5356-5361.

Additionally, it was observed that the ion pair separation degree affects the regioselectivity too. In fact, DCH-18-crown-6 led exclusively to the *C*-alkylated product **3**, whereas some amounts of *O*-alkylation product **4** were obtained with [2.2.2]-Cryptand. In general, *O*-alkylations are usually favored by factors inducing looser ion pairs, such as less accessible cations and more polar solvents.⁶

In some cases, the type of phase transfer catalysts may strongly affect the stereoselectivity of the reaction. During our previous studies on macrocycle phase transfer catalyzed reactions, crown ethers provided excellent performances in the diastereoselective Mukaiyama-Michael reaction of butenolides to α,β -unsaturated ketones.²⁷



Scheme 1.9 Switchable Diastereoselective Mukaiyama–Michael Reaction of butenolides

Interestingly, it was found that choosing the appropriate solvent and macrocycle size, very high *syn*- or *anti*-diastereoselectivity could be achieved. In particular, through DFT calculations, it was rationalized that such switchable diastereoselectivity is the result of different degrees of ion

²⁷ G. Della Sala, M. Sicignano, R. Schettini, F. De Riccardis, L. Cavallo, Y. Minenkov, C. Batisse, G. Hanquet, F. Leroux, I. Izzo, *J. Org. Chem.*, **2017**, *82*, 6629-6637.

separation in the dienolate anion/cation ion pair (**Scheme 1.9**). Apolar solvents and sterically accessible cations favor tighter ion pairs leading to *syn*-diastereomers through stable chelated transition state. Scarcely accessible cations and polar solvents result instead in loose ion pairs so that the cation is far removed and can not be involved in the transition state. In this latter case, without the assistance of the cation, a different approach of the nucleophile is favored affording the *anti*-product.

1.3 Asymmetric Phase Transfer Catalysis

The increasing demand for enantiomerically enriched compounds in both industrial and academic research has led to the rapid development of a variety of enantioselective processes using chiral phase transfer catalysts. Because of its advantages, such as mild reaction conditions, simple procedure, large-scale potential, the PTC is considered a green alternative to many homogeneous systems. Therefore, phase transfer catalysts have found widespread application in asymmetric organic synthesis.²⁸ Cinchona alkaloid-derived ammonium salts were first used as pioneering chiral phase transfer catalysts and, still today, are some of the most employed. The reasons for their extensive use are the unique structural properties, low cost, excellent commercial availability and the possibility to readily prepare large libraries of derivatives. Other widely employed chiral phase transfer catalysts are the synthetic, structurally rigid C_2 -symmetrical bis(binaphthyl)ammonium salts, known as Maruoka catalysts. The main features are their typically structural robustness even under strongly basic conditions and, the possibility to use lower catalyst loading. Moreover, chiral

²⁸ a) T. Ooi, K. Maruoka, *Angew. Chem. Int. Ed.*, **2007**, *46*, 4222 – 4266; b) S. Shirakawa, K. Maruoka, *Angew. Chem. Int. Ed.*, **2013**, *52*, 4312 – 4348; c) J. Vachon, J. Lacour, *Chimia*, **2006**, *60*, 266-275.

cation-binding macrocycles have been tested as asymmetric phase transfer catalysis. Among them, crown ethers have received more attention due to their peculiar features.

1.3.1 Chiral phase transfer onium salts

Cinchona alkaloids are natural bioactive compounds extracted from a genus of flowering plants belonging to the *Rubiaceae* family, available in four structural types, each one characterized by a hindered tertiary amine, a hydroxyl group at 9 position and a vinyl functionality (**Figure 1.7**). Chiral cinchona alkaloid ammonium salts can be easily prepared through alkylation of the tertiary amine group.

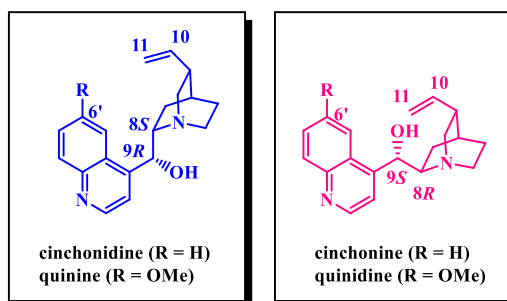
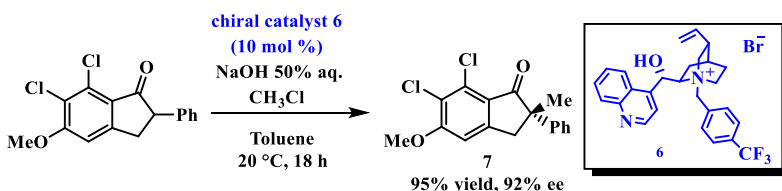


Figure 1.7 The main four kinds of *Cinchona* alkaloid

The first application of *Cinchona* quaternary ammonium salts as chiral phase transfer catalysts was developed by the Merck research group in 1984.²⁹ Dolling and coworkers reported the first example of PTC process using *N*-p-trifluoromethylbenzylcinchoninium bromide **6** as the chiral catalyst for the methylation of 2-phenylindanone **5** under LL-PTC conditions (50% NaOH

²⁹ a) U. -H. Dolling, P. Davis, E. J. J. Grabowski, *J. Am. Chem. Soc.*, **1984**, 106, 446-447; b) D. L. Hughes, U. -H. Dolling, K. M. Ryan, E. F. Schoenewaldt, E. J. J. Grabowski, *J. Org. Chem.*, **1987**, 52, 4745-4752.

aqueous, toluene). The desired product **7** was obtained with high yield and enantioselectivity as represented in **Scheme 1.10**. The involvement of a *tight* ion pair between the chiral catalyst and the indanone enolate is responsible for the asymmetric induction. As shown in **Figure 1.8**, the authors suggested the participation of hydrogen bonding and π - π stacking interactions in stabilizing the reactive ion pair **8** and directing the stereoselective attack of methyl chloride.



Scheme 1.10 Asymmetric phase transfer catalytic methylation of an indanone derivative

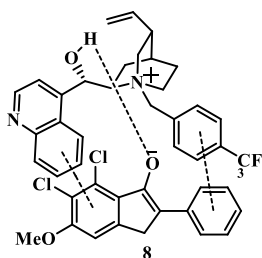
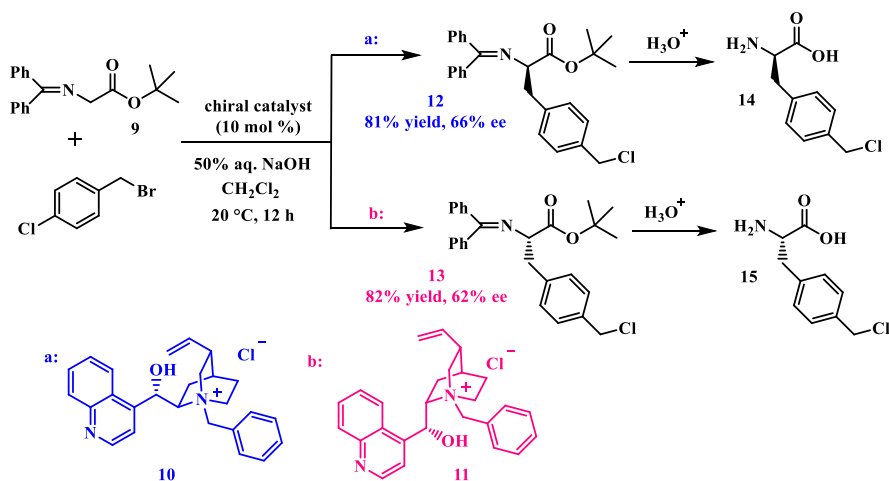


Figure 1.8 Ion pair intermediate

Five years later, O'Donnell and coworkers employed a similar chiral quaternary ammonium salt for the enantioselective alkylation of *N*-(diphenylmethylene)glycine *tert*-butyl ester **9** under LL-PTC conditions.³⁰ Through this very attractive and innovative approach, it was possible to prepare both the enantiomeric forms of amino acids using pseudoenantiomeric chiral catalysts. In detail, employing quaternary

³⁰ M. J. O'Donnell, W. D. Bennett, S. Wu, *J. Am. Chem. Soc.*, **1989**, *111*, 2353-2355.

ammonium *Cinchonine*-derivative **10**, the amino acid product **14** with absolute *R* configuration was achieved after acid hydrolysis. The product **15** with *S* absolute configuration was afforded with *Cinchonidine*-based ammonium salts **11**. In both cases, high yields and moderate enantiomeric excesses were achieved (**Scheme 1.11**).



Scheme 1.11 Enantioselective alkylation of amino acid derivatives by O'Donnell and coworkers

Subsequently, O'Donnell and coworkers proved that the active catalytic form in this PTC approach was formed directly in situ through the rapid alkylation of the hydroxyl group at C-9 of the catalyst under base reaction conditions.³¹ In particular, they speculated that the *O*-alkylated-*Cinchonidine*-based ammonium salts were the real catalyst of the asymmetric reaction. Thus, in order to confirm this hypothesis, the catalyst **16** (**Figure 1.9**) was prepared independently and submitted to the usual reaction conditions in presence of benzyl bromide. The same enantiomeric excess (60% ee) was obtained employing *N*-benzyl cinchonidinium chloride

³¹ M. J. O'Donnell, S. Wu, J. C. Huffman, *Tetrahedron*, **1994**, *50*, 4507-4518.

11 or *N,O*-benzyl cinchonidinium bromide **16** showing that the *O*-alkylated species was, actually, the active catalyst.

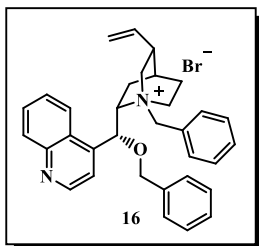
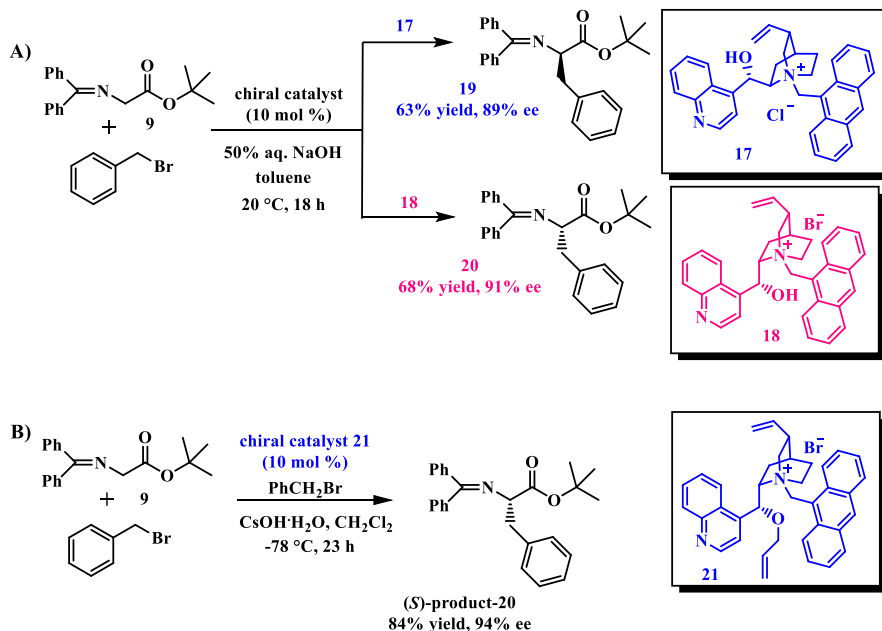


Figure 1.9 Structure of *N,O*-dibenzyl cinchonidinium bromide

In 1997, the research groups of Lygo³² and Corey³³ opened independently a new era of asymmetric phase transfer catalysis. Both research groups observed an improvement of enantioselectivity in the alkylation reaction of glycine ester derivative upon replacement of the *N*-benzyl group with a more hindered anthracenylmethyl moiety on the quaternary nitrogen atom. Lygo's group achieved enantiomeric excesses up to 91% using free C-9-OH-*N*-anthracenylmethyl derivatives (**Scheme 1.12 A**). Whereas, considering the previous study on *O*-alkylated derivatives, Corey's group promoted the same reaction with the novel *O*-allyl-*N*-anthracenylmethyl cinchonidinium salt **21** at very low temperature and solid CsOH·H₂O obtaining a higher asymmetric induction in presence of benzyl bromide (**Scheme 1.12 B**). Excellent enantioselectivities up to >99% were achieved with the same catalyst using different alkylating and allylating agents.

³² B. Lygo, P. G. Wainwright, *Tetrahedron Lett.* **1997**, *38*, 8595-8598.

³³ E. J. Corey, F. Xu, M.C. Noe, *J. Am. Chem. Soc.* **1997**, *119*, 12414-12415.



Scheme 1.12 Asymmetric alkylations of 26 by Lygo (A) and Corey (B)

The novel catalyst structure **21** was designed by Corey considering the bridgehead nitrogen of the chiral ammonium salts as an imaginary tetrahedron composed of four faces indicated as F1, F2, F3 and F4 (**Figure 1.10**). The ammonium cation adopts a favorite conformational arrangement and the nucleophilic enolate generated during the PTC reaction is coordinated with preferential orientation in order to minimize the steric hindrance. According to this model, the negatively charged oxygen atom of the enolate interacts with the positive nitrogen atom of the catalyst through the only open face F4 due to steric effects. The approach to the F1 face is, in fact, prevented by the large quinuclidine moiety, whereas the F2 and F3 faces are cluttered by -OR and benzyl groups respectively. The attractive interaction between the positive charge of the cation and the negative charge of the enolate stabilizes, instead, the resulting tight ion pair. In addition, the *si*-face of the nucleophilic *E*-enolate is hindered by the quinoline group when

Cinchonidinium-derivative is employed and consequently the approach of the alkylating agent takes place on the *re*-face of the enolate affording the *S*-product. The origin of the observed stereoselectivity is, thus, ascribed to a combination of conformational and steric factors.

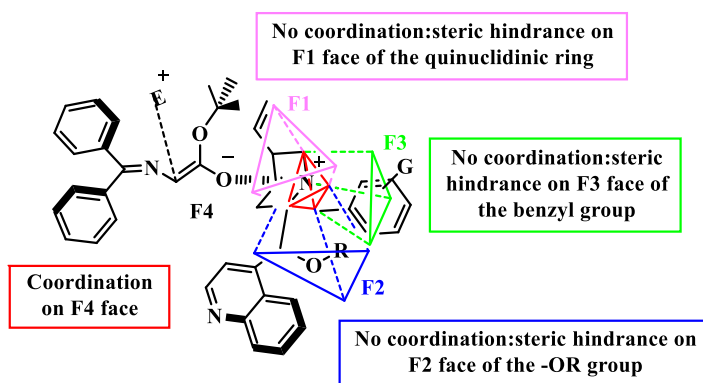


Figure 1.10 Origin of stereoselectivity in cinchona PTCs

The substrate-catalyst coordination approach proposed by Corey was later confirmed by DFT calculations of the modeled transition state for the allylation reaction of *tert*-butyl glycinate benzophenone Schiff base-catalyzed by the *O*-allyl-*N*-antracenylnmethyl cinchonidinium salts.³⁴ As depicted in **Figure 1.11**, the lowest energy transition state (*S*)-TS **22** is stabilized by an oxy-anion electrostatic interaction between the enolate (positioned with the π -face perpendicular) and the quaternary ammonium salts. That oxy-anion interaction is the key to understanding the high asymmetric induction found. In fact, thanks to this stronger interaction in (*S*)-TS, the enolate-electrophile system fits better into the pocket of catalyst over the (*R*)-TS leading to the *S*-product.

³⁴ T. C. Cook, M. B. Andrus, D. H. Ess, *Org. Lett.*, **2012**, *14*, 5836-5839.

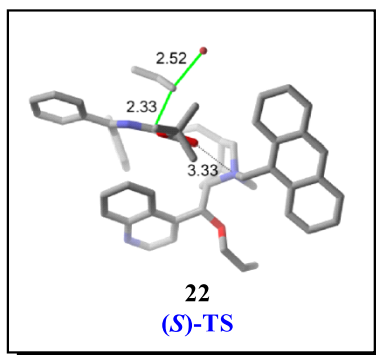


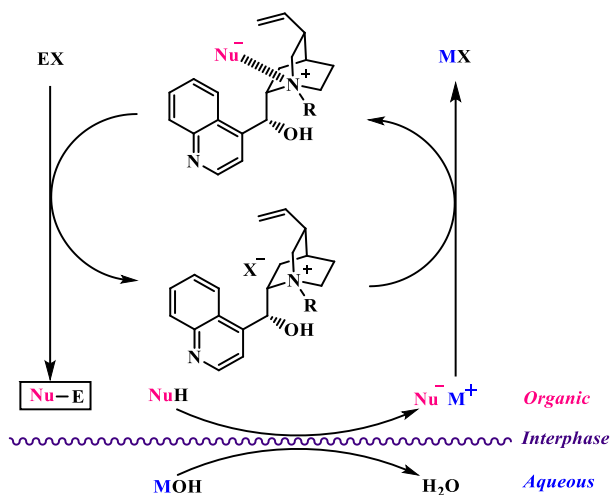
Figure 1.11 Lowest energy transition state (*S*)-TS

The asymmetric methylation of 2-phenylindanone **5** using *N*-p-trifluoromethylbenzylcinchoninium bromide **6** developed in 1984²⁸ was also submitted to the theoretical investigation by Pliego research group in 2013.³⁵ Through DFT calculations of the modeled lower energy transition states, it was demonstrated that the previous hypothesized model including hydrogen bond and π - π stacking interactions was not correct (See **Figure 1.7**). In detail, it was found that the favored transition state was stabilized both by hydrogen bond interaction between the negative charge of the carbonyl oxygen of the nucleophile and the hydroxyl group at 9 position of the catalyst and by electrostatic interaction of the leaving chlorine anion with the positive nitrogen atom of the catalyst. Therefore, a surprisingly crucial role of the leaving group was revealed.

In general, the most typical APTC reactions involve the functionalization of activated α -carbon of carbonyl compounds and other enolizable substrates under basic conditions. The generally assumed interphase mechanism for this type of reaction, catalyzed by chiral *Chincona*-alkaloids ammonium salts, is reported below (**Scheme 1.13**). The first step is the deprotonation of

³⁵ E. de Freitas Martins, J. R. Jr Pliego, *ACS Catal.*, **2013**, 3, 613-616.

the pro-nucleophile by the inorganic base at the interface forming the corresponding metal enolate. This latter undergoes a rapid ion-exchange with the catalyst and provides a lipophilic chiral ammonium enolate. This tight ion pair migrates from the interface into the organic layer where it reacts with the electrophile and affords the enantioenriched product. Finally, the regenerated ammonium salt comes back into the interface restarting the catalytic cycle. It is very important to emphasize that high asymmetric inductions are obtained as long as the chiral onium enolate is rapidly formed and very reactive so that the non-stereoselective alkylation of the metal enolate is prevented. Furthermore, the lipophilic ion pair has to be tight enough in order that an effective asymmetric induction on the enolate can be exerted by the chiral cation. Lastly, effective shielding of one of the two enolate enantiotopic faces is needed to control the absolute configuration of the product.



Scheme 1.13 Interphase mechanism in the presence of a cinchonidine derived quaternary ammonium salt

Since their advent, *Cinchona* alkaloid-derived quaternary ammonium salts have played a decisive role in the field of asymmetric phase transfer catalysis, mainly due to their excellent commercial availability and low cost. They have been applied with great results to a variety of asymmetric transformations, including α -alkylations,³⁶ Michael additions,³⁷ aldol,³⁸ Darzens³⁹ and epoxidation⁴⁰ reactions. These chiral catalysts, thanks to their privileged structure, can be easily modified leading the way for useful libraries of different chiral quaternary ammonium salts. The extensive literature on this topic has shown that the reaction types and substrates are extremely sensitive to the structure of catalysts. Therefore, choosing from a rich assortment is of key importance for a catalyst screening process during the study of a novel methodology. The modifications of *Cinchona* alkaloid-derived quaternary ammonium salts are easily achieved through the introduction of different substituents at the bridgehead nitrogen atom, at the

³⁶ For examples see: a) M. J. O'Donnell, *Aldrichimica Acta*, **2001**, *34*, 3–15; b); M. J. O'Donnell, *Acc. Chem. Res.*, **2004**, *37*, 506–517; c) E. J. Corey, Y. Bo, J. Busch-Petersen, *J. Am. Chem. Soc.*, **1998**, *120*, 13000–13001.

³⁷ For examples see: a) K. Hermann, H. Wynberg, *J. Org. Chem.*, **1979**, *44*, 2238–2244; b) R. S. E. Conn, A. V. Lovell, S. Karady, L. M. Weinstock, *J. Org. Chem.*, **1986**, *51*, 4710–4711; (c) F. Y. Zhang, E. J. Corey, *Org. Lett.*, **2000**, *2*, 1097–1100; d) F. -Y. Zhang, E. J. Corey, *Org. Lett.*, **2001**, *3*, 639–641; e) T. Perrard, J.-C. Plaquevent, J.-R. Desmurs, D. Hébrault, *Org. Lett.*, **2000**, *2*, 2959–2962; f) E. J. Corey, F.-Y. Zhang, *Org. Lett.*, **2000**, *2*, 4257–4259.

³⁸ For examples see: a) A. Ando, T. Miura, T. Tatematsu, T. Shioiri, *Tetrahedron Lett.*, **1993**, *34*, 1507–1510; b) T. Shioiri, A. Bohsako, A. Ando, *Heterocycles*, **1996**, *42*, 93–97; c) M. Horikawa, J. Busch-Peteren, E. J. Corey, *Tetrahedron Lett.*, **1999**, *40*, 3843–3846; d) A. Ando, T. Miura, T. Tatematsu, T. Shioiri, *Tetrahedron Lett.*, **1993**, *34*, 1507–1510.

³⁹ For examples see: a) J. C. Hummelen, H. Wynberg, *Tetrahedron Lett.*, **1978**, *19*, 1089–1092; b) S. Arai, T. Shioiri, *Tetrahedron Lett.*, **1998**, *39*, 2145–2148; c) S. Arai, Y. Shirai, T. Ishida, T. Shioiri, *J. Chem. Soc. Chem. Commun.*, **1999**, 49–50; d) S. Arai, Y. Shirai, T. Ishida, T. Shioiri, *Tetrahedron*, **1999**, *55*, 6375–6386; e) S. Arai, T. Shioiri, *Tetrahedron*, **2002**, *58*, 1407–1413.

⁴⁰ For examples see: a) H. Wynberg, B. Greijdanus, *J. Chem. Soc. Chem. Commun.*, **1978**, 427–428; b) L. Alcaraz, G. MacDonald, J. P. Ragot, N. Lewis, R. J. K. Taylor, *J. Org. Chem.*, **1998**, *63*, 3526–3527; c) A. G. M. Barrett, F. Blaney, A. D. Campbell, D. Hamprecht, T. Meyer, A. J. P. White, D. Witty, D. J. Williams, *J. Org. Chem.*, **2002**, *67*, 2735–2750; d) W. Adam, P. B. Rao, H. -G. Degen, A. Levai, T. Patonay, C. R. Saha-Möller, *J. Org. Chem.*, **2001**, *67*, 259–264; e) B. Lygo, D. C. M. To, *Tetrahedron Lett.*, **2001**, *42*, 1343–1346; f) S. Arai, H. Tsuge, M. Oku, M. Miura, T. Shioiri, *Tetrahedron*, **2002**, *58*, 1623–1630.

C-6 of the quinolinic moiety as well as at C-9 of the alkaloid structure. Examples of hydrogenation of the olefin moiety together with the protection of the hydroxyl group also are broadly reported.

In the early 2000s, dimeric cinchona-derived quaternary ammonium salts were designed by the groups of Jew, Park⁴¹ and Najera⁴², obtained by introducing different chemical spacers, such as aromatic rings, linking the bridgehead nitrogen of the two cinchona units. Libraries of dimeric chiral ammonium salts have been easily built by changing the chemical nature of the spacer, e.g. naphthyl or anthracenyl group (**Figure 1.12**). As a result, remarkable catalytic and chiral efficiency was achieved in many of the studied reactions.⁴³

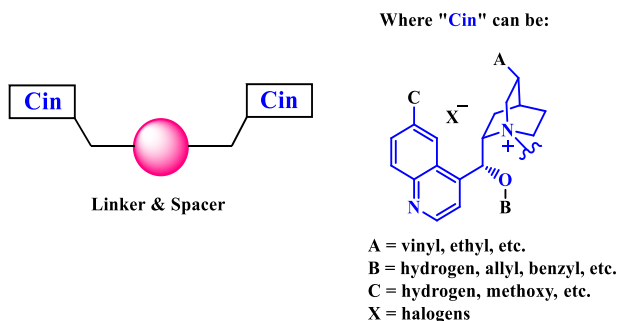


Figure 1.12 General structure of dimeric Cinchona-phase transfer catalysts

Catalytic bifunctional *Cinchona* quaternary ammonium salts, able to activate the nucleophile and the electrophile simultaneously in a highly stereoselective way, have also been largely employed in asymmetric PTC.

⁴¹ S. -S. Jew, B. -S. Jeong, M. -S. Yoo, H. Huh, H. -G. Park, *Chem. Commun.* **2001**, 1244-1245.

⁴² R. Chinchilla, P. Mazon, C. Najera, *Tetrahedron: Asymmetry* **2002**, *13*, 927-931.

⁴³ a) H. -G. Park, B. -S. Jeong, M. -S. Yoo, J. -H. Lee, M. -k. Park, Y. -J. Lee, M. -J. Kim, S. -S. Jew, *Angew. Chem.*, **2002**, *114*, 3162-3164; b) H. -G. Park, B. -S. Jeong, M. -S. Yoo, J. -H. Lee, M. -k. Park, Y. -J. Lee, M. -J. Kim, S. -S. Jew, *Angew. Chem. Int. Ed.*, **2002**, *41*, 3036-3038; c) S. -S. Jew, H. -G. Park, *Chem. Commun.*, **2009**, 7090-7103.

Though the hydroxy group at 9 position may act itself as a hydrogen-bond donor, in several examples it has been replaced with more efficient activating groups such as urea (A), thiourea (B) or squaramide (C) functionalities (**Figure 1.13**).⁴⁴ Thanks to the new mode of activation ensured by the bifunctional-phase transfer chiral catalyst, high levels of selectivity and stereocontrol have been achieved in many studied reactions.

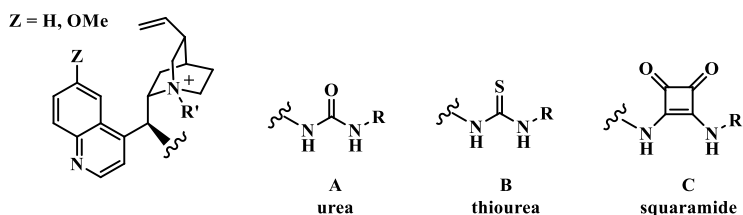
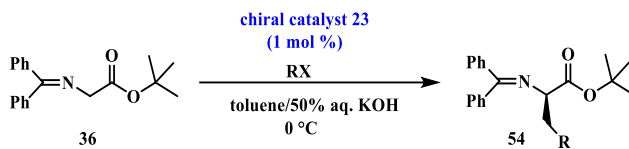


Figure 1.13 General structure of bifunctional cinchona-phase transfer catalysts

Although the excellent performances achieved with *Cinchona* alkaloids ammonium salts, the need to expand the horizons of asymmetric phase transfer catalysis has induced several groups in developing novel structures for chiral ammonium catalysts.

In this perspective, in 1999, Maruoka and coworkers designed and prepared synthetic, structurally rigid new chiral C_2 -symmetrical *bis*(binaphthyl)ammonium salts derived from commercially available (*S*)- or (*R*)-BINOL in several steps, (**Figure 1.14**), and successfully applied them in

⁴⁴ For examples see: a) K. M. Johnson, M. S. Rattley, F. Sladojevich, D. M. Barber, M. G. Nunez, A. M. Goldys, D. J. Dixon, *Org. Lett.* **2012**, *14*, 2492–2495; b) J. Novacek, M. Waser, *Eur. J. Org. Chem.* **2013**, 637–648; c) E. Sorrentino; S. J. Connon, *Org. Lett.*, **2016**, *18*, 5204–5207; d) Z. -P. Wang, Q. Wu, J. Jiang, Z. -R. Li, X. -J. Peng, P. -L. Shao, Y. He, *Org. Chem. Front.*, **2018**, *5*, 36–40; e) C. Cornaggia, F. Manoni, E. Torrente, S. Tallon, S. J. Connon, *Org. Lett.*, **2012**, *14*, 1850–1853; f) B. Wang, T. Xu, L. Zhu, Y. Lan, J. Wang, N. Lu, Z. Wei, Y. Lin, H. Duan, *Org. Chem. Front.*, **2017**, *4*, 1266–1271; g) N. Lu, Y. Fang, Y. Gao, Z. Wei, J. Cao, D. Liang, Y. Lin, H. Duan, *J. Org. Chem.*, **2018**, *83*, 1486–1492.



Entry	Catalyst	RX	Yield (%)	ee (%)
1	23 a	BnBr	73	79 (<i>R</i>)
2	23 b	BnBr	81	89 (<i>R</i>)
3	23 c	BnBr	95	96 (<i>R</i>)
4	23 d	BnBr	91	98 (<i>R</i>)
5	23 e	BnBr	90	99 (<i>R</i>)
6	23 e	BnBr	72	99 (<i>R</i>)
7	23 e	EtI	89	98 (<i>R</i>)
8	23 e	allylBr	80	99 (<i>R</i>)
9	23 e	(2,6)-dimethyl-BnBr	98	99 (<i>R</i>)
10	23 e	4-Benzoyl-BnBr	86	98 (<i>R</i>)

^aWith 0.2 mol% of (S,S)-20e. ^bWith saturated CsOH at -15°C.

Table 1.1 Enantioselective alkylation of glycine ester benzophenone Schiff base-catalyzed by *C*₂-symmetrical bis(binaphthyl)ammonium salts

When structurally less rigid *C*₂-symmetric chiral quaternary ammonium salts (**24**, **Figure 1.15**) were used in the enantioselective alkylation reaction of *N*-(diphenylmethylene)glycine *tert*-butyl ester, only low yields and enantiomeric excesses were achieved confirming, thus, the crucial role of the steric hindrance. Quite surprisingly, quaternary ammonium salts possessing flexible alkyl moieties **25** instead of a binaphthyl group proved to be effective furnishing the alkylation product almost quantitatively and with excellent enantioselectivity in presence of only 0.01-0.1 mol% of catalyst.⁴⁷

Several biaryl ammonium cations were reported by Maruoka's research group including *atropos* monobiphenyl adducts **26**⁴⁸ and *C*₂-symmetric

⁴⁷ M. Kitamura, S. Shirakawa, K. Maruoka, *Angew. Chem., Int. Ed.*, **2005**, *44*, 1549-1551.

⁴⁸ Z. Han, Y. Yamaguchi, M. Kitamura, K. Maruoka, *Tetrahedron Lett.* **2005**, *46*, 8555-8558.

ammonium salts catalysts containing two chiral biphenyl units **27**.⁴⁹ Aryl substituents at the 4,4'- and 6,6'-positions of the *bis*-binaphthyl core were also introduced (**28**, **Figure 1.15**).⁵⁰ Finally, phosphonium salts **29**⁵¹ and bifunctional-type catalysts **30**⁵² were also prepared.

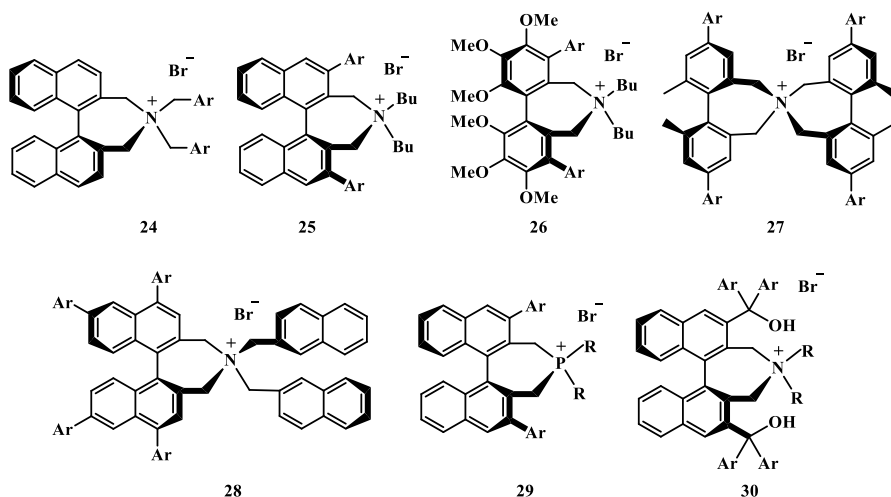


Figure 1.15 Representative Maruoka catalysts

In general, Maruoka catalysts have proven to be highly efficient chiral catalysts widely applied both in academic research and in large-scale methodologies for the synthesis of biologically active compounds.⁵³ In fact,

⁴⁹ T. Ooi, Y. Kubota, K. Maruoka, *Synlett*, **2003**, 12, 1931-1933.

⁵⁰ a) T. Hashimoto, K. Maruoka, *Tetrahedron Lett.* **2003**, 44, 3313-3316; b) T. Hashimoto, Y. Tanaka, K. Maruoka, *Tetrahedron: Asymmetry* **2003**, 14, 1599-1602.

⁵¹ a) For examples see: R. He, C. Ding, K. Maruoka, *Angew. Chem. Int. Ed.*, **2009**, 48, 4559-4561; b) C.-L. Zhu, F.-G. Zhang, W. Meng, J. Nie, D. Cahard, J.-A. Ma, *Angew. Chem. Int. Ed.*, **2011**, 50, 5869-5872.

⁵² For examples see: a) T. Ooi, D. Ohara, K. Fukumoto, K. Maruoka, *Org. Lett.*, **2005**, 7, 3195-3197; b) X. Wang, Q. Lan, S. Shirakawa, K. Maruoka, *Chem. Commun.*, **2010**, 46, 321-323; c) Y. Liu, S. Shirakawa, K. Maruoka, *Org. Lett.*, **2013**, 15, 1230-1233.

⁵³ For examples see: a) P. G. Bulger, *Comprehensive Chirality*, E. M. Carreira, H. Yamamoto Eds.; Elsevier: Amsterdam, **2012**, 9. b) F. Xu, *Sustainable Catalysis: Challenges and Practices for the Pharmaceutical and Fine Chemical Industries*; P. J. Dunn, K. K. Hii, M. J. Krische, M. Williams Eds.; Wiley: Hoboken, NJ, **2013**; c) R. Albert, K. Hinterding, V. Brinkmann, D. Guerini, C. Müller-Hartwig, H. Knecht, C. Simeon, M. Streiff, T. Wagner,

if compared with the cinchona alkaloids quaternary ammonium salts, the chiral binaphthol-based phase transfer catalysts are typically more stable, even when strongly basic conditions are used, mainly due to the lack of β -hydrogens, preventing Hoffman elimination side reactions. Thus, the opportunity to lower the catalyst loading, in many cases, offsets the relatively high cost of Maruoka catalysts due to their several synthetic steps.

In general, cost-effectiveness and large-scale availability are key features to consider in choosing the optimal candidate catalyst for industrial applications.⁵⁴

In 2003, new chiral phase transfer ammonium salts characterized by configurationally labile (*tropos*) biphenyl moieties with stereogenic exocyclic appendages were developed by Lygo's group (**31**, **Figure 1.16**).⁵⁵

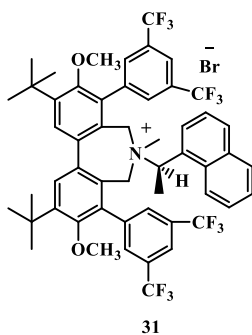


Figure 1.16 Lygo's phase transfer catalyst

K. Welzenbach, F. Zécari, M. Zollinger, N. Cooke, E. Francotte, *J. Med. Chem.*, **2005**, *48*, 5373-5377; d) X. Jiang, B. Gong, K. Prasad, O. Repič, *Org. Process Res. Dev.*, **2008**, *12*, 1164-1169; e) S. R. Fix-Stenzel, M. E. Hayes, X. Zhang, G. A. Wallace, P. Grongsaard, L. M. Schaffter, S. M. Hannick, T. S. Franczyk, R. H. Stoffel, K. P. Cusack, *Tetrahedron Lett.*, **2009**, *50*, 4081-4083; f) M. Seki, Y. Kawase, *Process for stereoselective production of optically active pyrrolyl-succinic acid imide derivative*. JP 2011026201 A, **2011**; g) G. Humphrey, C. K. Chung, N. R. Rivera, K. M. Belyk, WO 2013148550 A1, **2013**.

⁵⁴ J. Tan, N. Yasuda, *Org. Process Res. Dev.*, **2015**, *19*, 1731-1746.

⁵⁵ B. Lygo, B. Allbutt, S.R. James, *Tetrahedron Lett.* **2003**, *44*, 5629-5632.

In addition, more recently, other structurally different onium phase transfer chiral catalysts were introduced including tartaric acid derivatives **36**,⁵⁶ C₂-symmetric chiral cyclic guanidine compounds **33**⁵⁷, cyclic ammonium salts **37**,⁵⁸ 1,2,3-triazolium catalysts **35**,⁵⁹ P-spiro chiral tetraaminophosphonium salts **32**,⁶⁰ chiral pentanidium derivatives **41**,⁶¹ chiral bis-guanidinium salts **34**,⁶² chiral cyclohexanediamine-derived bifunctional tetraalkylammonium compounds **39**⁶³ and chiral bifunctional quaternary ammonium **38**⁶⁴ and phosphonium **40a-b**⁶⁵ catalysts (Figure 1.17).

Although a wide range of efficient chiral catalysts have already been introduced and used for practical asymmetric transformations, the design and the application of new chiral phase transfer catalysts in organic remains an

⁵⁶ For example see: a) M. Waser, K. Gratzner, R. Herchl, N. Müller, *Org. Biomol. Chem.*, **2010**, *10*, 251-254; b) T. Shibuguchi, Y. Fukuta, Y. Akachi, A. Sekine, T. Ohshima, M. Shibasaki, *Tetrahedron Letters*, **2002**, *43*, 9539-9543; c) T. Ohshima, T. Shibuguchi, Y. Fukuta, M. Shibasaki, *Tetrahedron*, **2004**, *60*, 7743-7754; d) S. Arai, R. Tsuji, A. Nishida, *Tetrahedron Lett.*, **2002**, *43*, 9535-9537.

⁵⁷ T. Kita, A. Georgieva, Y. Hashimoto, T. Nakata, K. Nagasawa, *Angew. Chem. Int. Ed.*, **2002**, *41*, 2832-2834.

⁵⁸ S. E. Denmark, N. D. Gould, L. M. Wolf, *J. Org. Chem.*, **2011**, *76*, 4260-4336.

⁵⁹ For example see: a) K. Ohmatsu, M. Kiyokawa T. Ooi, *J. Am. Chem. Soc.*, **2011**, *133*, 1307-1309; b) K. Ohmatsu, A. Goto, T. Ooi, *Chem. Commun.*, **2012**, *48*, 7913-7915; c) K. Ohmatsu, Y. Hakamata, A. Goto, T. Ooi, *Heterocycles*, **2014**, *88*, 1661-1666.

⁶⁰ D. Uraguchi, Y. Asai, Y. Set, T. Ooi, *Synlett*, **2009**, 658-660.

⁶¹ a) T. Ma, X. Fu, C. W. Kee, L. Zong, Y. Pan, K.-W. Huang, C.-H. Tan, *J. Am. Chem. Soc.*, **2011**, *133*, 2828-2831; b) Y. Yang, F. Moineaud, W. Chin, T. Ma, Z. Jiang, C.-H. Tan, *Org. Lett.*, **2012**, *14*, 4762-4765; c) L. Zong, S. Du, K. F. Chin, C. Wang, C.-H. Tan, *Angew. Chem., Int. Ed.*, **2015**, *54*, 9390-9393; d) L. Zong, X. Ban, C. W. Kee, C.-H. Tan, *Angew. Chem., Int. Ed.*, **2014**, *53*, 11849-11853.

⁶² C. Wang, L. Zong and C.-H. Tan, *J. Am. Chem. Soc.*, **2015**, *137*, 10677-10682.

⁶³ For example see: a) J. Novacek, M. Waser, *Eur. J. Org. Chem.*, **2014**, 802-809; b) M. Tiffner, J. Novacek, A. Busillo, K. Gratzner, A. Massa, M. Waser, *RSC Adv.*, **2015**, *5*, 78941-78949; c) M. Perillo, A. Di Mola, R. Filosa, L. Palombi, A. Massa, *RSC Adv.*, **2014**, *4*, 4239-4246.

⁶⁴ H.-Y. Wang, J.-X. Zhang, D.-D. Cao, G. Zhao, *ACS Catal.*, **2013**, *3*, 2218-2221.

⁶⁵ For example see: a) S. Shirakawa, A. Kasai, T. Tokuda, K. Maruoka, *Chem. Sci.*, **2013**, *4*, 2248-2252; b) S. Shirakawa, L. Wang, R. He, S. Arimitsu, K. Maruoka, *Chem. Asian J.*, **2014**, *9*, 1586-1593; c) S. Shirakawa, K. Maruoka, *Tetrahedron Lett.*, **2014**, *55*, 3833-3839.

ever-timely goal of organic synthesis in order to push further the limits of this technique and expand the process applications.⁶⁶

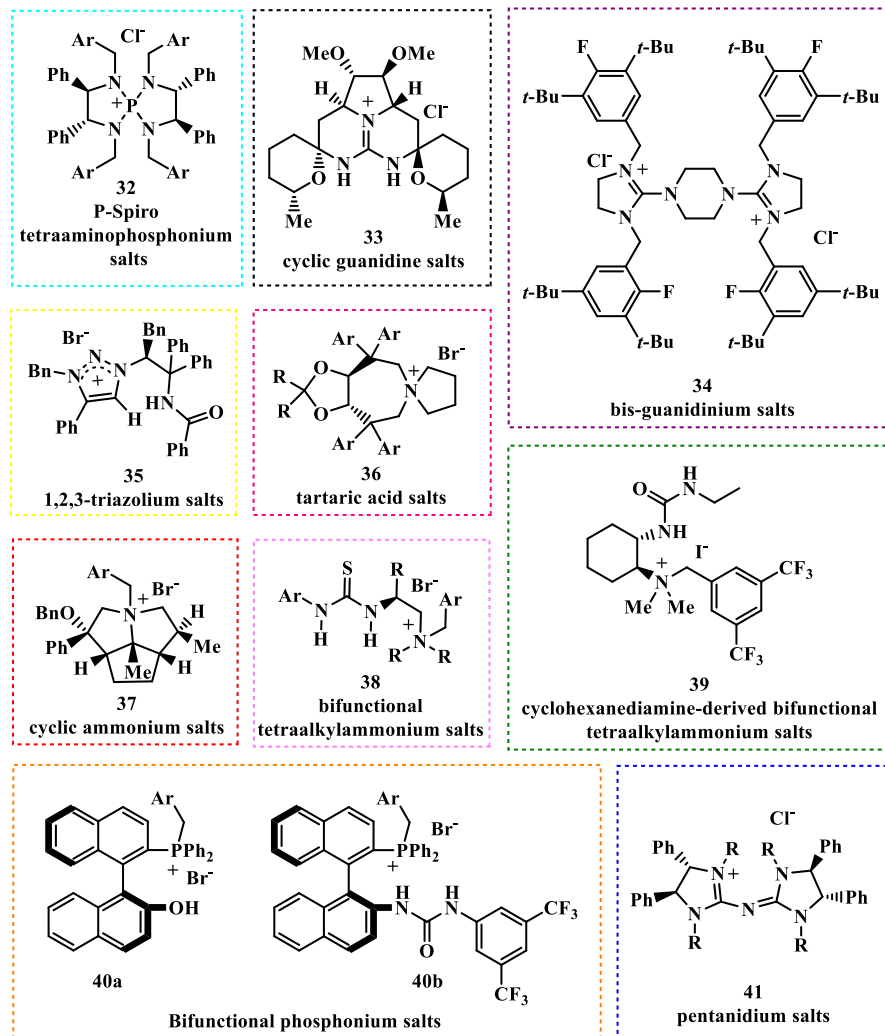


Figure 1.17 Novel phase transfer catalysts

⁶⁶ S. Kaneko, Y. Kumatabara, S. Shirakawa, *Org. Biomol. Chem.*, **2016**, *14*, 5367-5376.

1.3.2 Chiral macrocyclic phase transfer catalysts

The great interest in the synthesis of non-racemic enantioenriched compounds has also inspired the design and application of several chiral macrocyclic systems in the field of the asymmetric phase transfer catalysis. Compared to the extensively studied chiral ammonium salts and Maruoka catalysts, the macrocyclic chiral compounds have been less investigated, although they can be considered an intriguing alternative to the traditional catalysts. Among them, various chiral crown ethers have been developed and employed as phase transfer catalysts.

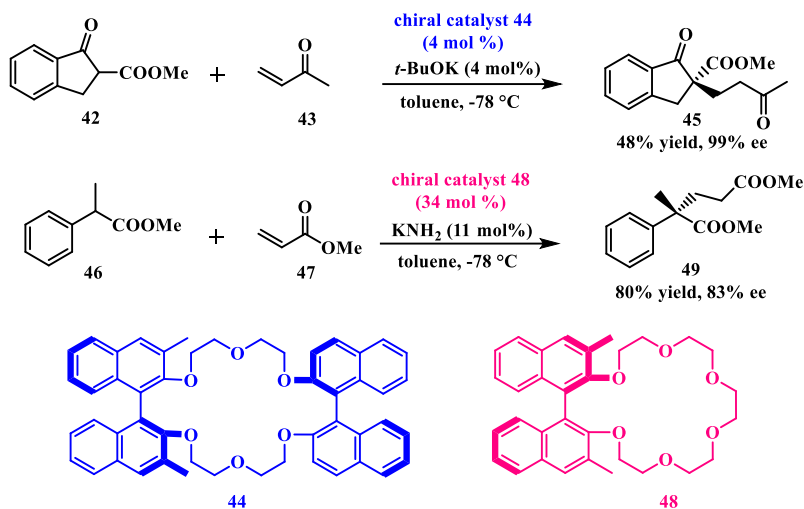
Despite the assured advantages of the ammonium salts like large-scale availability, the peculiar structural characteristics of coronands ensure better performances under specific reaction conditions. For example, in SL-PTC, crown ethers might be more efficient thanks to their high ability to extract inorganic salts from the solid form.

In general, macrocycles are attractive catalysts since their spatial rigid backbone enhances the molecular recognition ability through the formation of host-guest supramolecular assemblies with neutral or anionic species. Chiral macrocycles can interact with prochiral substrates forcing the preferred guest's orientation and discriminating between two different enantiotopic faces or groups. In this regard, the possibility to originate well-organized reactive ion pair induces excellent potential for the application in asymmetric phase transfer catalysis.⁶⁷

The first application of macrocycles was pioneered by Cram in 1981 who employed C_2 -symmetric binaphthyl-modified crown ethers in Michael addition reactions between methyl vinyl ketone **43** and 2-methoxycarbonyl-

⁶⁷ R. Schettini, M. Sicignano, F. De Riccardis, I. Izzo, G. Della Sala, *Synthesis*, **2018**, *50*, 4777-4795.

1-indanone **43** or between methyl 2-phenylpropanoate **46** and methyl acrylate **47** under solid-liquid conditions with good results (**Scheme 1.14**).⁶⁸



Scheme 1.14 Michael additions catalyzed by Cram's crown ethers

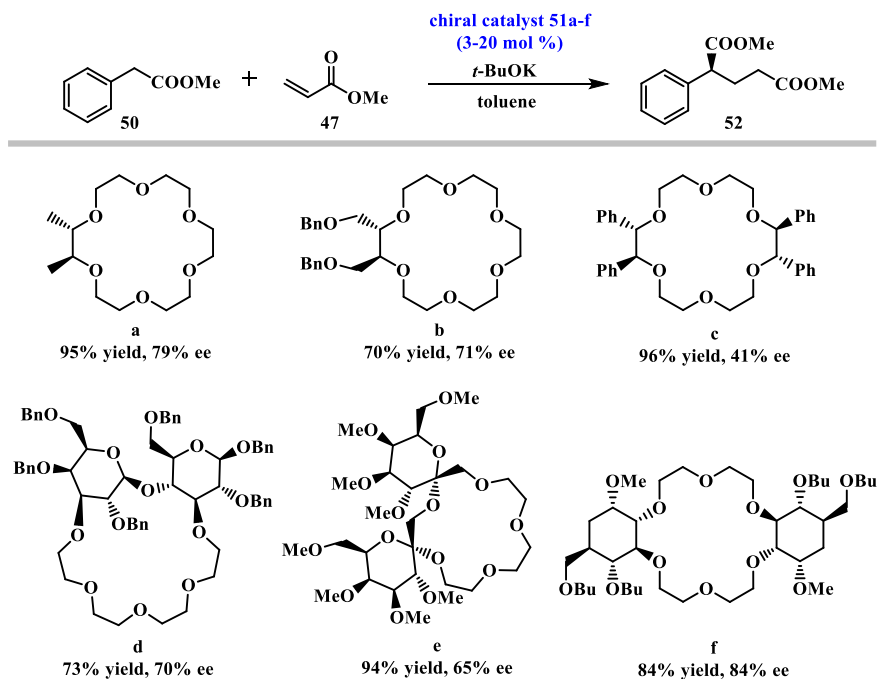
The authors suggested that the high enantiocontrol originates from the presence of the bulky binaphthyl structure which prevents the attack of the acceptor on the more shielded prochiral face of the oriented carbanion.

The addition of methyl phenylacetate **50** to methyl acrylate **47** was also investigated with several chiral crown ethers by other research groups achieving moderate to good enantioselectivity.⁶⁹ As shown in **Scheme 1.15**, carbohydrate-based crown ethers were also tested in the 1,4-addition with

⁶⁸ D. J. Cram, G. D. Y. Sogah, *J. Chem. Soc., Chem. Commun.*, **1981**, 625-628.

⁶⁹ a) M. Takasu, H. Wakabayashi, K. Furuta, H. Yamamoto, *Tetrahedron Lett.*, **1988**, 29, 6943-6946; b) S. Aoki, S. Sasaki, K. Koga, *Tetrahedron Lett.*, **1989**, 30, 7229-7230; c) E. V. Dehmlow, V. Knufinke, *Liebigs Ann. Chem.*, **1992**, 283-285; d) J. Crosby, J. F. Stoddart, X. Sun, M. R. W. Venner, *Synthesis*, **1993**, 141-145; e) E. Brunet, A. M. Poveda, D. Rabasco, E. Oreja, L. M. Font, M. S. Batra, J. C. Rodríguez-Ubis, *Tetrahedron: Asymmetry*, **1994**, 5, 935-948.

interesting results.⁷⁰ The best degree of enantioselectivity was, in fact, achieved by Töke and collaborators with the glucose-derived crown ether **51f**.

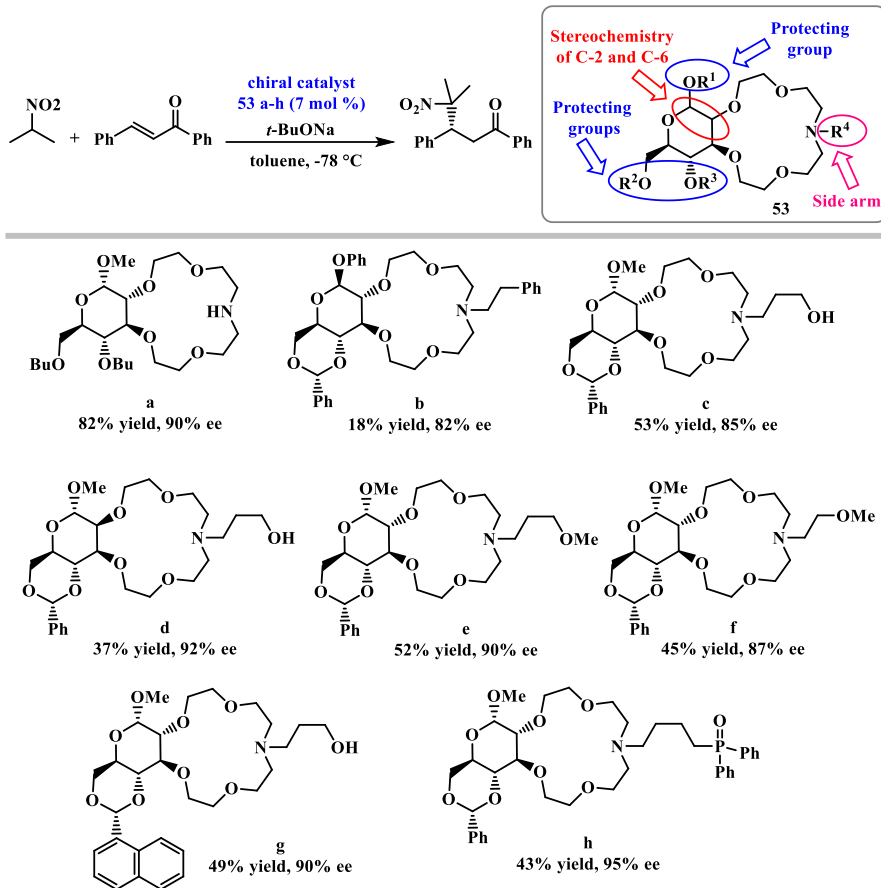


Scheme 1.15 Crown Ether Catalyzed Enantioselective Michael Additions of Phenylacetate to Methyl Acrylate

The idea to include carbohydrates into crown ether backbones arises from the opportunity to easily design large libraries of chiral macrocycles offered

⁷⁰ a) M. Alonso-López, M. Martín-Lomas, S. Penadés, *Tetrahedron Lett.*, **1986**, 27, 3551-2334; b) J. Jimenez-Barbero, M. Martín-Lomas, S. Penadés, *Tetrahedron*, **1988**, 44, 1535-1543; c) D. A. H. van Maarschalkerwaart, N. P. Willard, U. K. Pandit, *Tetrahedron*, **1992**, 48, 8825-8840; d) P. P. Kanakamma, N. S. Mani, U. Maitra, V. Nair, *J. Chem. Soc., Perkin Trans. I*, **1995**, 2339-2344; e) A. Dondoni, A. Marra, *Tetrahedron Lett.*, **2009**, 50, 3593-3596; f) L. Töke, P. Bakó, G. M. Keserű, M. Albert, L. Fenichel, *Tetrahedron*, **1998**, 54, 213-222; g) L. Töke, L. Fenichel, M. Albert, *Tetrahedron Lett.*, **1995**, 36, 5951-5954.

by the stereochemical diversity of these natural products and the presence of many derivatizable functional groups.



Scheme 1.16 Lariat sugar-based azacrown ethers catalyze the enantioselective addition of 2-nitropropane to *trans*-chalcone

Later on, some novel chiral sugar-based lariat azacrown ethers, with general structure **53**, were developed by Tőke and Bakó and tested in the enantioselective Michael addition of 2-nitropropane to *trans*-chalcone

(Scheme 1.16).⁷¹ High asymmetric inductions and moderate yields were showed. These catalysts were also successfully applied in Michael additions of malonate esters⁷², in epoxidations of chalcones with *tert*-butyl hydroperoxide under LL-PTC conditions,⁷³ in Darzens condensations⁷⁴ and in MIRC reactions with different Michael acceptors⁷⁵.

The side arm of lariat azacrown ether provides an additional binding site for the cation creating a three-dimensional cavity. The coordinating side arm helps to bring the complexed cation closer to the chiral macrocycle, resulting in an enhanced asymmetric induction on the associate prochiral substrate (Figure 1.18).

Moreover, chiral crown ethers were employed both in the enantioselective alkylation⁷⁶ and in the asymmetric conjugate addition⁷⁷ of glycine esters

⁷¹ For examples see: a) P. Bakó, T. Kiss, L. Tőke, *Tetrahedron Lett.*, **1997**, 38, 7259-7262; b) P. Bakó, Z. Bajor, L. Tőke, *J. Chem. Soc., Perkin Trans. 1*, **1999**, 3651-3655; c) P. Bakó, G. Keglevich, Z. Rapi, *Lett. Org. Chem.*, **2010**, 7, 645-656; d) T. Novák, J. Tatai, P. Bakó, M. Czugler, G. Keglevich, L. Tőke, *Synlett*, **2001**, 424-426; e) P. Bakó, A. Makó, G. Keglevich, M. Kubinyi, K. Pál, *Tetrahedron: Asymmetry*, **2005**, 16, 1861-1871.

⁷² a) Z. Rapi, A. Grün, T. Nemcsok, D. Hessz, M. Kállay, M. Kubinyi, G. Keglevich, P. Bakó, *Tetrahedron: Asymmetry*, **2016**, 27, 960-972; b) P. Bakó, Z. Rapi, A. Grün, T. Nemcsok, L. Hegedűs, G. Keglevich, *Synlett*, **2015**, 26, 1847-1851.

⁷³ a) A. Makó, Z. Rapi, G. Keglevich, Á. Szöllősy, L. Drahos, L. Hegedűs, P. Bakó, *Tetrahedron: Asymmetry*, **2010**, 21, 919-925; b) T. Bakó, P. Bakó, G. Keglevich, P. Bombicz, M. Kubinyi, K. Pál, S. Bodor, A. Makó, L. Tőke, *Tetrahedron: Asymmetry*, **2004**, 15, 1589-1595; c) P. Bakó, T. Bakó, A. Mészáros, G. Keglevich, A. Szöllősy, S. Bodor, A. Makó, L. Tőke, *Synlett.*, **2004**, 643-646; d) Z. Rapi, T. Szabó, G. Keglevich, Á. Szöllősy, L. Drahos, P. Bakó, *Tetrahedron: Asymmetry*, **2011**, 22, 1189.

⁷⁴ For examples see: a) P. Bakó, Á. Szöllősy, P. Bombicz, L. Tőke, *Synlett*, **1997**, 291-292; b) P. Bakó, E. Czinege, T. Bakó, M. Czugler, L. Tőke, *Tetrahedron: Asymmetry*, **1999**, 10, 4539-4551; c) A. Makó, Á. Szöllősy, G. Keglevich, D. K. Menyhárd, P. Bakó, L. Tőke, *Monatsh Chem.*, **2008**, 139, 525-535; d) T. Novák, P. Bakó, G. Keglevich, I. Greiner, *Phosphorus, Sulfur Silicon Relat. Elem.*, **2007**, 182, 2449-2456.

⁷⁵ For examples see: a) T. Nemcsok, Z. Rapi, G. Keglevich, A. Grün, P. Bakó, *Chirality*, **2018**, 30, 407-419; b) Z. Rapi, A. Grün, G. Keglevich, A. Stirling, P. Bakó, *New J. Chem.*, **2016**, 40, 7856-7865; c) Z. Rapi, T. Nemcsok, A. Grün, Á. Pálvölgyi, G. Samu, D. Hessz, M. Kubinyi, M. Kállay, G. Keglevich, P. Bakó, *Tetrahedron*, **2018**, 74, 3512-3526.

⁷⁶ a) Itoh, T.; Shirakami, S. *Heterocycles* **2001**, 55, 37; b) Yonezawa, K.; Patil, M. L.; Sasai, H.; Takizawa, S. *Heterocycles* **2005**, 66, 639.

⁷⁷ a) T. Akiyama, M. Hara, K. Fuchibe, S. Sakamoto, K. Yamaguchi, *Chem. Commun.*, **2003**, 1734-1735; b) F.-Y. Zhang, E. J. Corey, *Org. Lett.*, **2000**, 2, 1097-1100; c) V. I. Maleev, M.

derivatives affording amino acid products. However, only moderate enantioselectivities were achieved.

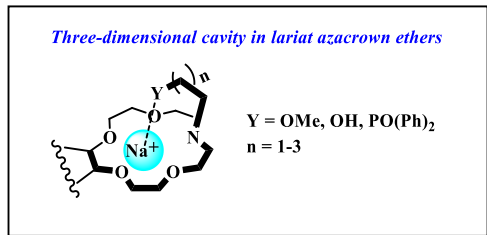


Figure 1.18 *Three-dimensional cavity in lariat azacrown ethers*

In general, if compared to the excellent performance of chiral ammonium salts, chiral crown ethers showed to be less efficient phase transfer catalysts in many of the studied methodologies.

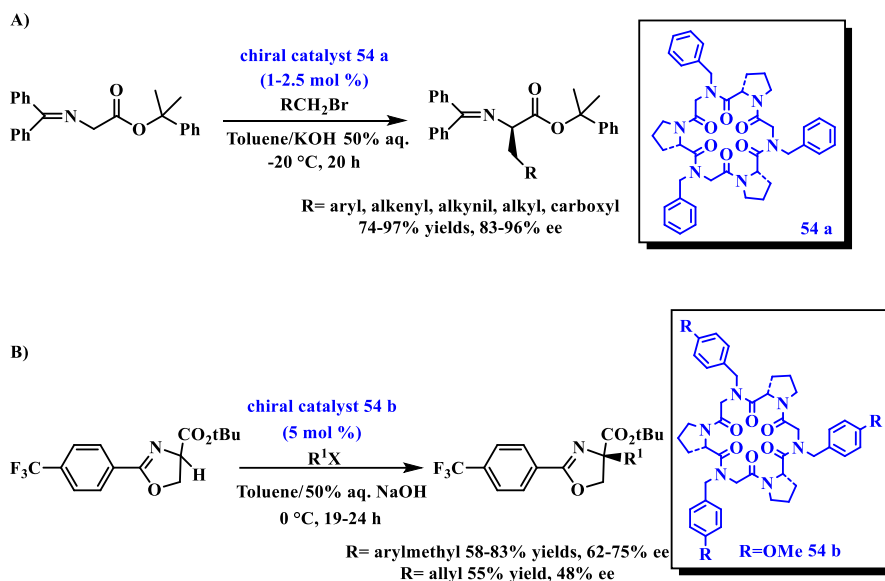
Recently, our group envisioned chiral cyclic peptoids as possible candidates for APTC. Peptoids are an emerging class of peptidomimetics, introduced in the early 1990s by the Zuckermann group,⁷⁸ characterized by a peptide-like backbone in which the side chain is attached to the nitrogen atoms instead of the α -carbon atoms, resulting in *N*-substituted glycine oligomers. Large libraries of structural different peptoids can be easily obtained through solid-phase synthesis, taking advantage of their modular structure. Proline-containing cyclopeptoids were, thus, tested in the enantioselective alkylation of *N*-(diphenylmethylene)glycine esters⁷⁹ (**Scheme 1.17 A**) and of serine-

North, V. A. Larionov, I. V. Fedyanin, T. F. Savel'yeva, M. A. Moscalenko, A. F. Smolyakov, Y. N. Belokon, *Adv. Synth. Catal.*, **2014**, 356, 1803-1810.

⁷⁸ R. J. Simon, R. S. Kania, R. N. Zuckermann, V. D. Huebner, D. A. Jewell, S. Banville, S. Ng, L. Wang, S. Rosenberg, C. K. Marlowe, D. C. Spellmeyer, R. Tan, A. D. Frankel, D. V. Santi, F. E. Cohen, P. A. Bartlett, *Proc. Natl. Acad. Sci. U. S. A.*, **1992**, 89, 9367-9371.

⁷⁹ a) R. Schettini, B. Nardone, F. De Riccardis, G. Della Sala, I. Izzo, *Eur. J. Org. Chem.*, **2014**, 7793-7797; b) R. Schettini, F. De Riccardis, G. Della Sala, I. Izzo, *J. Org. Chem.*, **2016**, 81, 2494-2505.

derived oxazoline esters⁸⁰ (**Scheme 1.17 B**) with moderate to high enantioselectivity proving to be a promising class of chiral phase transfer catalysts.



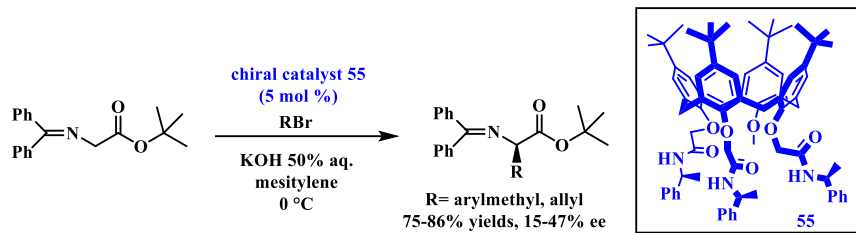
Scheme 1.17 Asymmetric alkylation of *N*-(diphenylmethylene) glycine esters (A) and serine-derived oxazoline esters (B) catalyzed by a hexamer cyclic peptoids

Additionally, Calix[*n*]arenes, a well-known class of macrocyclic compounds widely exploited in supramolecular chemistry⁸¹, were also applied for the first time in APTC to catalyze the asymmetric alkylation of glycine esters

⁸⁰ R. Schettini, A. D'Amato, F. De Riccardis, G. Della Sala, I. Izzo, *Synthesis*, **2017**, 49, 1319-1326.

⁸¹ For examples see: a) *Calixarenes and Beyond*; P. Neri, P. J. L. Sessler, M. -X. Wang, Eds., Springer: Dordrecht, **2016**; b) C. D. Gutsche, *Calixarenes, an Introduction*, Royal Society of Chemistry: Cambridge, **2008**; c) *Calixarenes 2001*, Z. Asfari, V. Böhmer, J. Harrowfield, J. Vicens, Eds., Kluwer: Dordrecht, **2001**. d) *Calixarenes in the Nanoworld*, J. Vicens, J. Harrowfield, Eds.; Springer: Dordrecht, **2007**.

derivatives.⁸² However, as shown in **Scheme 1.18**, the alkylated products were obtained with only low to moderate enantioselectivity.



Scheme 1.18 Asymmetric alkylation of *N*-(diphenylmethylene) glycine ester catalyzed by a calix[4]arene triamide

1.4 Aims of the work

Considering the remarkable advantages of phase transfer catalysis as a green high-performance strategy of organic synthesis, the main goal of this research project is to further explore the potentialities of this approach in new stereoselective processes for the synthesis of potentially bioactive products. In the first part of the thesis, the study has been focused on the application of simple achiral macrocycles in highly diastereoselective Michael additions. The idea is to exploit the well-established complexing properties of crown ethers in new phase transfer catalytic strategies, with a special preference for the use of mild conditions and inexpensive catalysts. In this regard, Chapter 2 describes the development of two novel crown ether-catalyzed Michael reactions for the synthesis of 3,3-disubstituted and 3-substituted Phthalides. Asymmetric synthesis of Michael adducts has also been investigated availing of α,β -unsaturated carbonyl compounds containing chiral auxiliaries.

⁸² N. A. De Simone, R. Schettini, C. Talotta, C. Gaeta, I. Izzo, G. Della Sala, P. Neri, *Eur. J. Org. Chem.*, **2017**, 5649-5659.

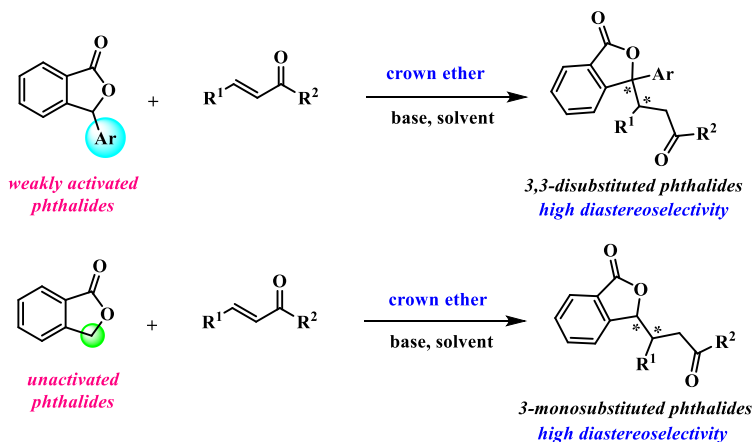
The second part of this research project concerns the employment of chiral quaternary ammonium salts for the synthesis of novel enantioenriched products. The commercial availability, low cost, high efficiency and broad applicability of chiral ammonium salts make them ideal candidates for the discovery of new asymmetric phase transfer transformations.

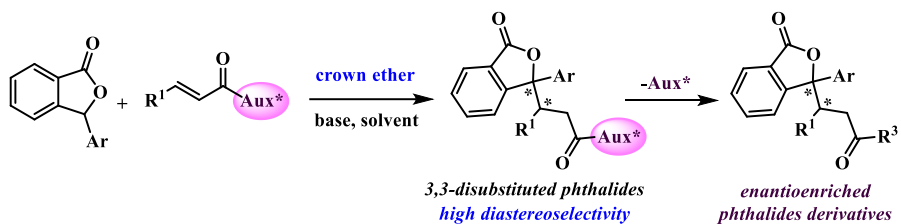
Thus, the first example of the enantioselective alkylation of activated Phthalides has been reported in Chapter 3, enabling the synthesis of novel products that are hardly accessible with the most commonly used methods.

Additionally, during my abroad period at the Universidad Autónoma de Madrid under the supervision of Prof. José Alemán, the scope of the research has been extended to the investigation of novel asymmetric trifluoromethylthiolation reactions under phase transfer catalysis conditions. The stereoselective introduction of SCF₃ functionality in organic compounds is an emerging application in organic synthesis attracting the interest of several research groups. In Chapter 4, the direct asymmetric trifluoromethylthiolation of azlactones and isoxazolidinones has been studied giving access to new enantioenriched thiofluorinated products.

In **Scheme 1.20**, the highlights of the next chapters are summarized.

Chapter 2:

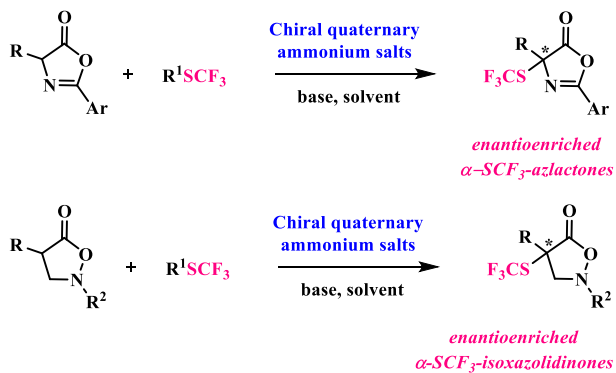




Chapter 3:



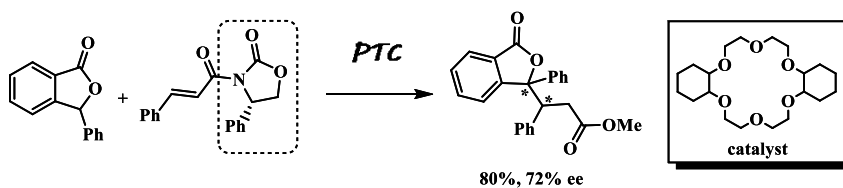
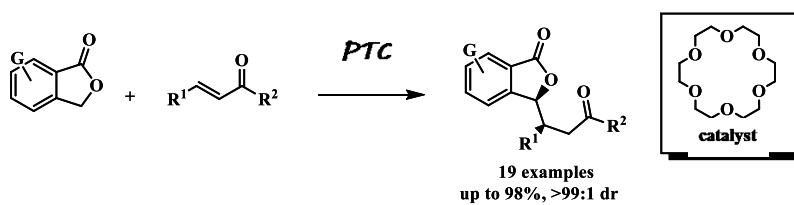
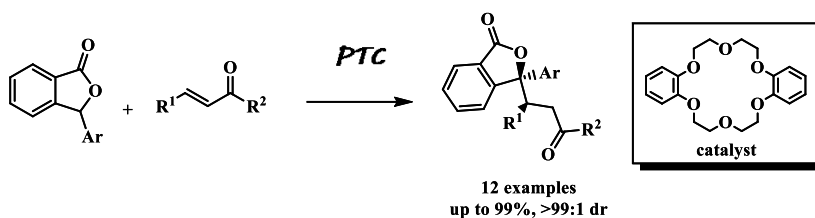
Chapter 4:



Scheme 1.20 The highlights of the research work developed during the PhD

Chapter 2

Diastereoselective synthesis of substituted Phthalides



2. Diastereoselective synthesis of substituted *Phthalides*

2.1 Phthalides

Isobenzofuran-1(3*H*)-ones, also known as phthalides, are aromatic heterocyclic compounds widely distributed in natural sources, mainly in plants and fungi, and exhibiting a broad range of important biological activities, such as anti-inflammatory, anti-oxidant, antibacterial, cytotoxic and vasodilating properties.⁸³ In addition, they are valuable building blocks for the synthesis of interesting biologically active products like anthracyclines, naphthoquinoid and anthraquinoid compounds.⁸⁴

Phthalides are structurally constituted by a bicyclic core derived from the fusion of a lactone (ring A) with an aromatic ring (ring B) (**Figure 2.1**), that could be considered cyclic esters of the corresponding 2-(hydroxymethyl)-benzoic acid.

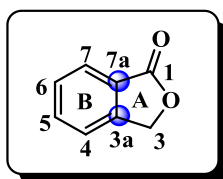


Figure 2.1 General structure of phthalides

⁸³ G. Lin, S. S. -K. Chan, H. -S. Chung, S. L. Li, *Stud. Nat. Prod. Chem.*, **2005**, 32, 611-669.

⁸⁴ A) V. Snieckus, *Chem. Rev.*, **1990**, 90, 879-933; b) D. Mal, P. Pahari, *Chem. Rev.*, **2007**, 107, 1892-1918; c) K. Rathwell, M. A. Brimble, *Synthesis*, **2007**, 643-662; d) A. S. Mitchell, R. A. Russell, *Tetrahedron*, **1995**, 51, 5207-5236; e) D. Mal, K. Ghosh, S. Jana, *Org. Lett.*, **2015**, 17, 5800-5803; f) Z. Fei, F. E. McDonald, *Org. Lett.*, **2007**, 9, 3547-3550; g) M. L. Patil, H. B. Borate, D. E. Ponde, V. H. Deshpande, *Tetrahedron*, **2002**, 58, 6615-6620; h) C. Cox, S. J. Danishefsky, *Org. Lett.*, **2000**, 2, 3493-3496; i) R. S. Mali, K. N. Babu, *J. Org. Chem.*, **1998**, 63, 2488-2492; l) J. N. N. Eildal, J. Andersen, A. S. Kristensen, A. M. Jørgensen, B. Bang-Andersen, M. Jørgensen, K. Strømgaard, *J. Med. Chem.*, **2008**, 51, 3045-3048.

Based on the structural characteristics and, specifically, on the type of substitution, these compounds are classified into three different categories (Figure 2.2):

- A. dimeric phthalides
- B. 3-substituted phthalides
- C. 3-unsubstituted phthalides

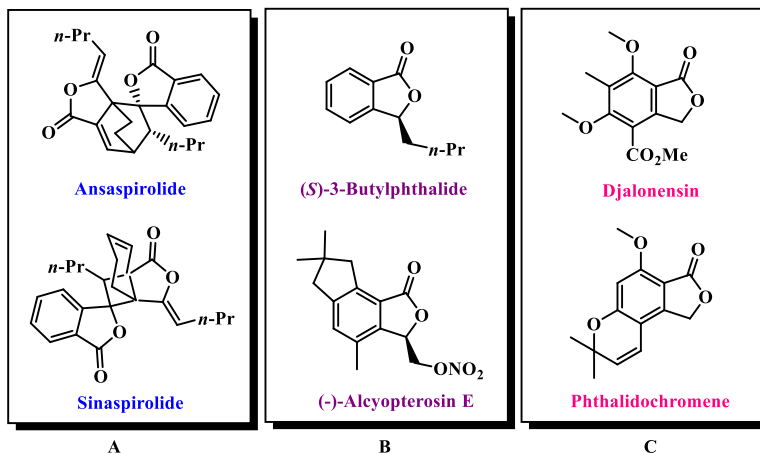


Figure 2.2 Examples of dimeric phthalides (A), 3-substituted phthalides (B) and 3-unsubstituted phthalides (C)

Dimeric phthalides are seen as Diels-Alder or [2+2] cycloadducts. Most of the natural phthalides with pharmacological activities belong to the group of 3-substituted derivatives. An example is 3-butylphthalide, a drug with anti-ischemic, anti-convulsant and anesthetic properties.⁸⁵ More than half of the about 300 phthalides isolated to date are 3-substituted derivatives with stereocenters located at C-3 or in other positions. A major fraction of them

⁸⁵ X. Diao, P. Deng, C. Xie, X. Li, D. Zhong, Y. Zhang, X. Chen, *Drug Metab. Dispos.*, **2013**, *41*, 430–444.

shows interesting biological activity.⁸⁶ In **Figure 2.3** have been reported some examples of naturally occurring bioactive phthalides.

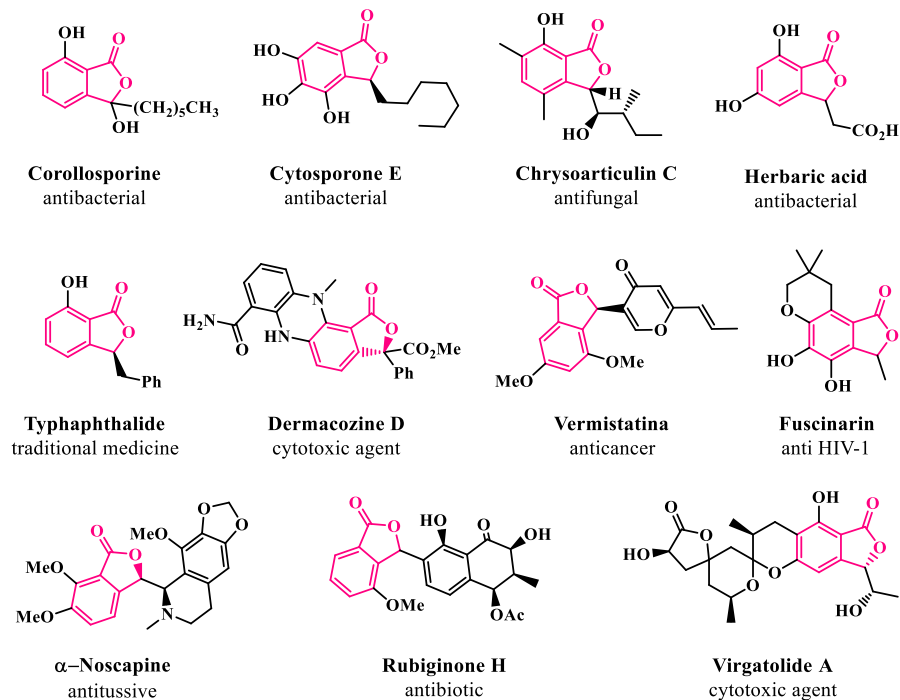


Figure 2.3 Selected examples of naturally occurring bioactive phthalides

Furthermore, a great number of synthetic phthalides have been prepared. Chemical modifications of the distinctive structure of these compounds have been designed to increase their promising pharmacological properties.⁸⁷ Selected examples of synthetic molecules used in medicinal chemistry are shown in **Figure 2.4**.

⁸⁶ A. León, M. Del-Ángel, J. L. Àvila, G. Delgado, *Progress in the Chemistry of Organic Natural Products*, 104, A. D. Kinghorn, H. Falk, S. Gibbons, J. Kobayashi, Eds., Springer, Cham, **2017**, 127–246.

⁸⁷ R. Karmakar, P. Pahari, D. Mal, *Chem. Rev.*, **2014**, 114 6213-6284.

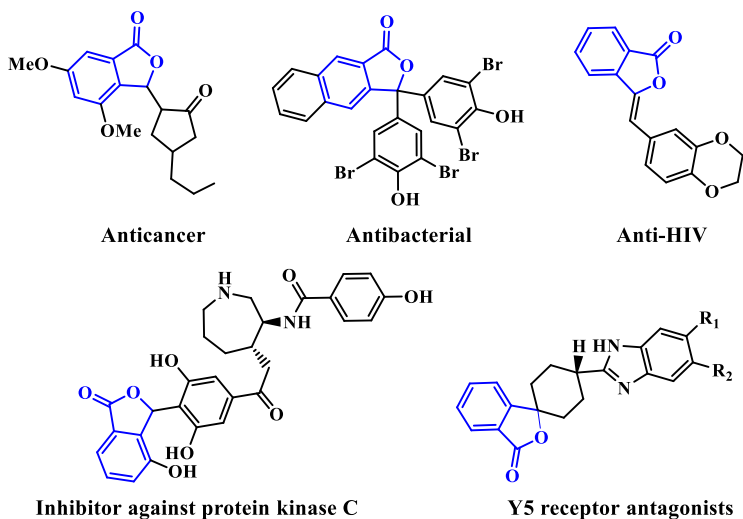
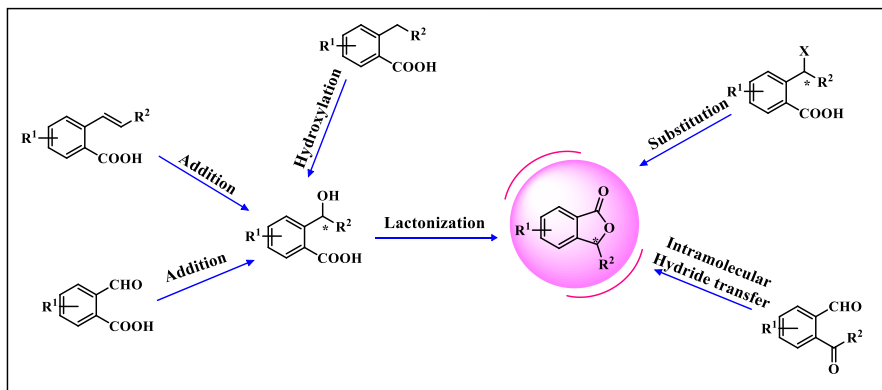


Figure 2.4 Selected examples of synthetic bioactive phthalides

2.2 Stereoselective methods for the construction of the lactone ring

Due to their intriguing chemical properties, the development of new catalytic methods for the synthesis of structurally different phthalides and, specifically, for the synthesis of 3-substituted phthalides triggered a great interest. In particular, major attention has been addressed to the stereocontrolled formation of new chiral centers. In this context, most of the strategies involve the stereocontrolled construction of the lactone ring starting from aromatic substrates. For this purpose, several approaches have been studied, including oxidation, condensation, lactonization, nucleophilic addition, hydrogenation and, also, hydride transfer reactions, each one starting from aromatic precursors. A schematic representation of the different methods is shown below (**Scheme 2.1**).

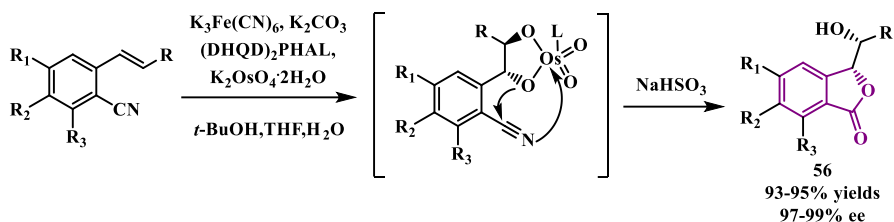


Scheme 2.1 Examples of stereoselective methods for the construction of the lactone ring

The lactonization reaction of the chiral hydroxy acid, or of its analogs, is the simplest and most used way to achieve enantioenriched phthalides. The hydroxy acid species can be obtained starting from the corresponding carboxyaldehyde or from the corresponding *o*-alkenyl carboxylic acid through, respectively, addition reaction to the aldehyde group or by Sharpless dihydroxylation. Alternatively, the hydroxylation of the 2-alkylbenzoic acid affords the hydroxy acid derivative.

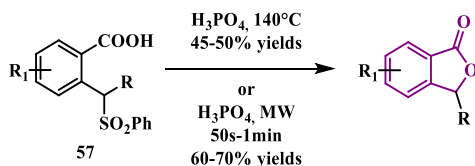
An example of asymmetric dihydroxylation reaction of cyano cinnamates and styrene derivatives was reported by Sudalai in 2012 for the synthesis of highly enantioenriched 3-substituted phthalides **56**. As showed in **Scheme 2.2**, excellent yields and enantioselectivity were achieved thanks to an unusual synergism between CN and osmate groups.⁸⁸

⁸⁸ R. S. Reddy, I. N. C. Kiran, A. Sudalai, *Org. Biomol. Chem.*, **2012**, *10*, 3655–3661.



Scheme 2.2 Synthesis of chiral phthalides **56** through asymmetric dihydroxylation reaction

The presence of a good leaving group can induce the formation of 3-substituted phthalides through an intramolecular substitution reaction carried out by the nearby carboxylic acid group. In this regard, interesting results were achieved both under microwave and conventional heating conditions, treating compound **57**, containing a sulfonic functionality, with a strong acid (**Scheme 2.3**).⁸⁹

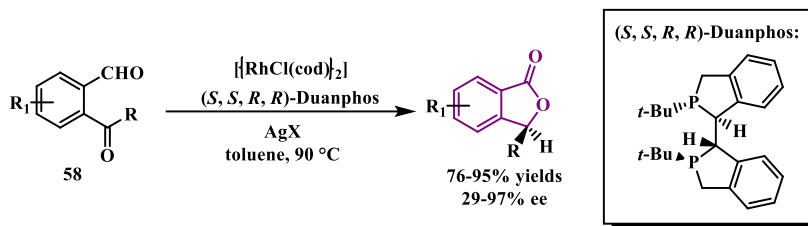


Scheme 2.3 Synthesis of 3-substituted phthalides through intramolecular reactions

A notable example of stereocontrolled construction of the lactone ring based on a hydride transfer reaction is the asymmetric rhodium-catalyzed intramolecular ketone hydroacylation reaction of ketobenzaldehydes **58** affording enantiomerically enriched phthalides, reported in 2010.⁹⁰

⁸⁹ B. T. S. Thirumamagal, S. Narayanasamy, *Tetrahedron Lett.*, **2008**, *49*, 512–515.

⁹⁰ M. C. Willis, *Angew. Chem. Int. Ed.*, **2010**, *49*, 6026–6027.

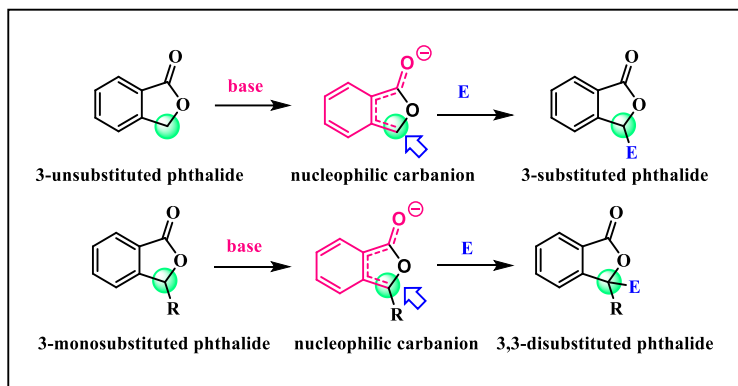


Scheme 2.4 Synthesis of chiral phthalides through hydride transfer reaction

2.3 Stereoselective alkylation methods at C-3 site of phthalides

An alternative route for the stereoselective synthesis of 3-substituted phthalides could be the stereocontrolled insertion of alkyl groups at the C-3 position of a 3-unsubstituted lactone. In this regard, the key point of the method is the weak acidity of the C-3 site, which could be exploited in reactions with electrophiles after the activation with bases. This approach, though synthetically attractive, has been much less investigated. It would involve the deprotonation of the weakly acid C-3 site with a sufficiently strong base generating the corresponding carbanion, that is expected to react with the selected electrophile leading to the desired 3-substituted phthalide product. This strategy can be used for both the synthesis of 3-substituted and 3,3-disubstituted phthalides starting from the 3-unsubstituted or the 3-monosubstituted substrate, respectively. Such approach could be defined as an “*arylogous synthetic method*” since the propagation of the electron-withdrawing effect of the carbonyl group to the C-3 position of the lactone ring takes place through the conjugated aromatic core (Scheme 2.5).

On the other hand, alkylation reactions of weakly activated or completely non-activated phthalides are more challenging due to their poor acidity.

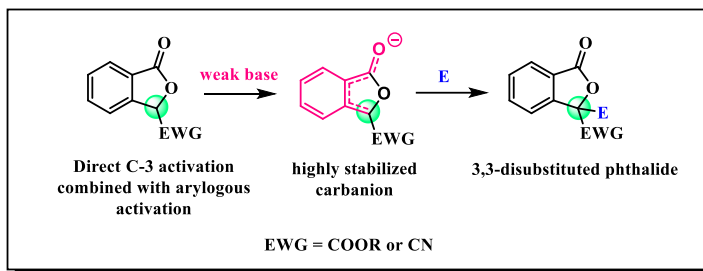


Scheme 2.5 Arylogous synthesis of 3-substituted and 3,3-disubstituted phthalides

Thus, C-3 unsubstituted phthalides appear to be not sufficiently activated to react with electrophiles at the α -site under mild reaction conditions. Indeed, harsh conditions like strong bases (LDA or metal alkoxides) and/or high temperatures are required with the subsequent formation of substantial amounts of byproducts and complete loss of the stereocontrol of the reaction.

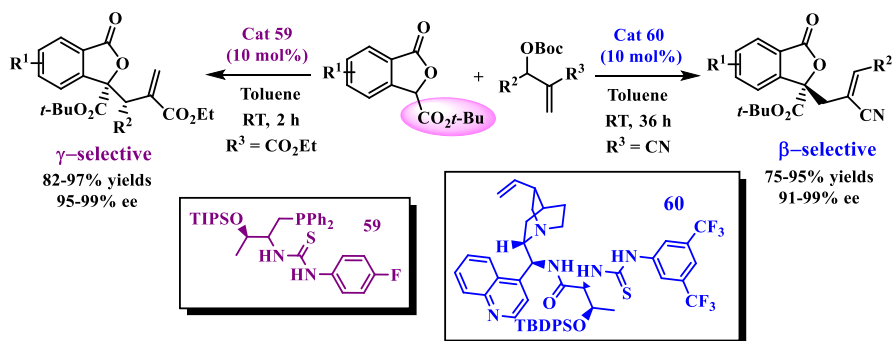
2.3.1 Stereoselective alkylations at C-3 site of activated phthalides

Enantioselective S_N2' allylic alkylations, Mannich reactions and Michael additions of 3-cyano- and 3-alkoxycarbonyl-phthalides have been reported in the literature, by using chiral weak base organocatalysts, leading to 3,3-disubstituted phthalides. However, it should be noted that such reactions are not true examples of arylogous synthetic processes because the C-3 position is directly activated by additional $-\text{COOR}$ or $-\text{CN}$ electron-withdrawing functionalities, that are required to increase its acidity.



Scheme 2.6 General Alkylation of activated phthalides

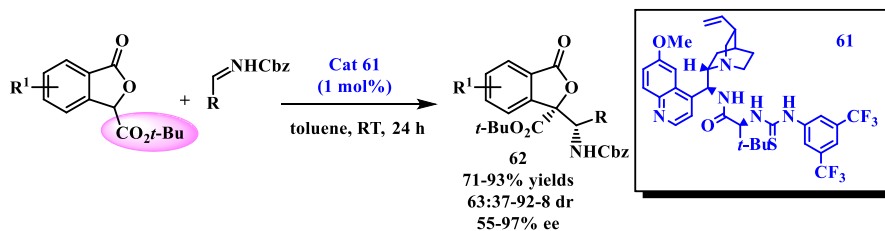
In 2012, the first asymmetric allylic alkylation of 3-carboxylic-*t*-Bu-ester-phthalide with MBH carbonates was studied.⁹¹ By using bifunctional chiral phosphines **59** or multifunctional tertiary amine-thioureas **60** as catalysts, γ -selective or β -selective allylic alkylation products were achieved with high yields and excellent stereo- and regio-selectivity. The authors suggested the involvement of either an S_N2' - S_N2' route or an addition-elimination process respectively, depending on the catalyst used and the structure of the allylic carbonates, to obtain optically enriched 3,3-disubstituted phthalide regioisomers (Scheme 2.7).



Scheme 2.7 Asymmetric allylic alkylation of 3-carboxylic-*t*-Bu-ester-phthalide with MBH carbonates

⁹¹ F. Zhong, J. Luo, G.-Y. Chen, X. Dou, Y. Lu, *J. Am. Chem. Soc.*, **2012**, *134*, 10222–10227.

A direct Mannich-type reaction employing activated phthalides as donors was reported for the first time by Lu's research group in 2012.⁹² The synthesis of 3,3-disubstituted phthalide derivatives **62** in excellent yields and good diastereo- and enantioselectivities was achieved in the presence of a multifunctional catalyst **61** as shown in **Scheme 2.8**.



Scheme 2.8 Asymmetric Mannich reaction of 3-carboxylic-*t*-Bu-ester-phthalide

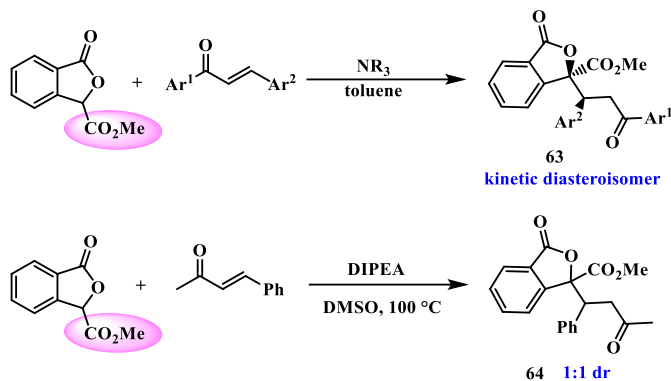
The Michael reaction of phthalides with electron-poor alkenes represents an expedient way to insert in stereoselective manner alkyl groups at the C-3 position of the lactone ring. Indeed, various examples of diastereo- and enantioselective Michael additions of activated phthalides are described in the literature.

The first example was the Michael addition of phthalide-3-carboxylic acid methyl ester to various α,β -unsaturated ketones.⁹³ When the reaction was carried out in the presence of tertiary amines as catalysts with aromatic Michael acceptors in toluene, a single diastereoisomer was initially obtained under kinetic control. Meanwhile, for prolonged reaction times a mixture of diastereoisomers in 1:1 ratio was achieved, probably due to the epimerization reaction of the kinetic product **63**. The use of tertiary bases, however, is not

⁹² J. Luo, H. Wang, F. Zhong, J. Kwiatkowski, L. -W. Xu, Y. Lu, *Chem. Commun.*, **2012**, 48, 4707-4709.

⁹³ T. Heisler, W. K. Janowski, R. H. Prager, M. J. Thompson, *Aust. J. Chem.*, **1989**, 42, 37-47.

applicable to α,β -unsaturated aliphatic ketones because of their poor reactivity. Furthermore, low yields and no diastereoselectivities were observed with intermediate reactive arylmethylketones, since harsh conditions, such as 100°C, were necessary to promote the Michael additions (Scheme 2.9).



Scheme 2.9 Michael addition of 3-carboxylic-methyl-ester-phthalide

The enantioselective version of the Michael addition between 3-carboxylic-methyl-ester-phthalide and *trans*-chalcone was also carried out by the same authors who reported the Mannich reaction, using cinchonine and cinchonidine as catalysts. The enantiomeric excesses obtained were 67 % and 65 % respectively with opposite chirality.

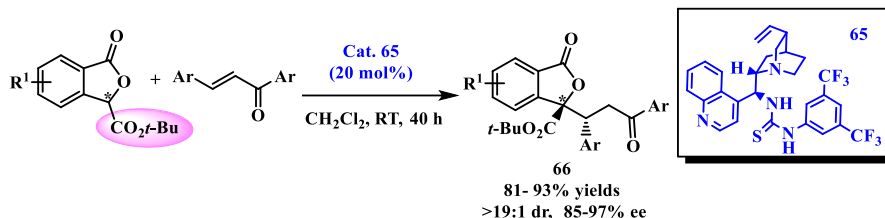
In 2013, Lu's research group reported two examples of asymmetric Michael additions of activated phthalides to *trans*-chalcones⁹⁴ and nitroolefins⁹⁵.

The reaction of 3-carboxylic-*t*-Bu-ester-phthalide with chalcones promoted by a quinidine-derived thiourea catalyst **65** led to the synthesis of

⁹⁴ J. Luo, C. Jiang, H. Wang, L. -W. Xu, Y. Lu, *Tetrahedron Lett.*, **2013**, *54*, 5261–5265.

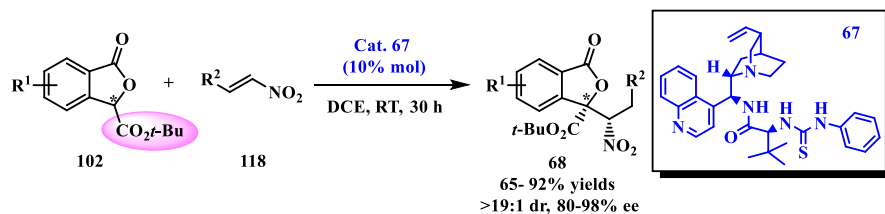
⁹⁵ J. Luo, H. Wang, F. Zhong, J. Kwiatkowski, L. -W. Xu, Y. Lu, *Chem. Commun.*, **2013**, *49*, 5775-5777.

enantioenriched 3,3-disubstituted phthalide derivatives **66** in excellent yields, diastereo- and enantioselectivities. (Scheme 2.10).



Scheme 2.10 Asymmetric Michael addition of 3-carboxylic-*t*-Bu-ester-phthalide to chalcones

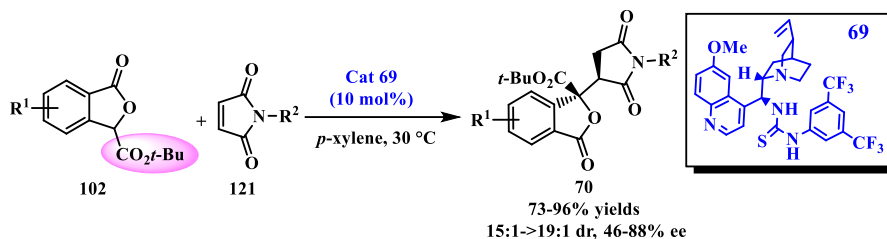
Very good results were achieved, also, in the reaction with nitroolefins promoted by amino acid-incorporating multifunctional catalyst **67**. As reported in Scheme 2.11, novel enantioenriched phthalides derivatives **68** were prepared in mild conditions.



Scheme 2.11 Asymmetric Michael addition of 3-carboxylic-*t*-Bu-ester-phthalide to nitroolefins

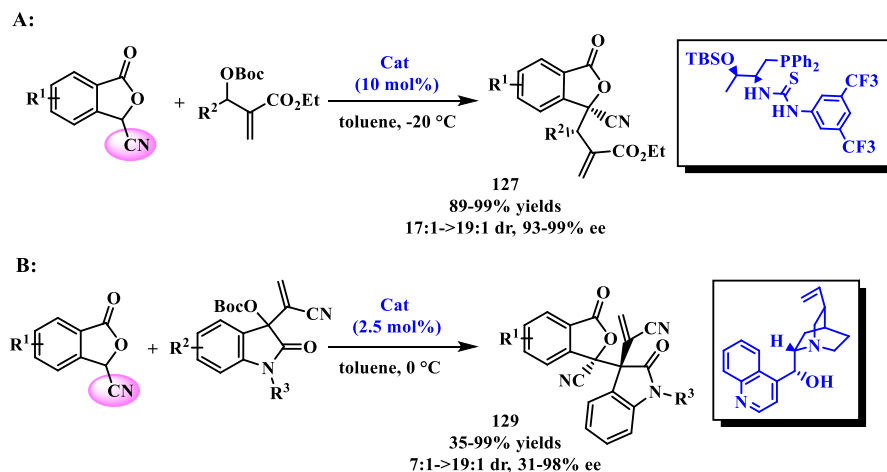
Recently, a highly stereoselective Michael addition/desymmetrization reaction of 3-substituted phthalides to maleimides was realized.⁹⁶ A series of 3,3-disubstituted phthalides **70** were prepared in moderate to good yields with high diastereoselectivities and good enantioselectivities employing a quinine-derived bifunctional thiourea **69** as chiral catalysts (Scheme 2.12).

⁹⁶ J. Wang, X. Li, J. -P. Cheng, *Sci. China Chem.*, **2019**, 62, 649-652.



Scheme 2.12 Asymmetric Michael addition of 3-carboxylic-*t*-Bu-ester-phthalide to maleimides

Moreover, 3-cyano-phthalides were also employed as activated substrates. Indeed, two examples of asymmetric allylation reactions using MBH carbonate derivatives for the synthesis of enantiomerically enriched functionalized 3-cyano-phthalide products were reported.⁹⁷ As summarized in **Scheme 2.13**, good stereoselectivity and yields were achieved in both studies.

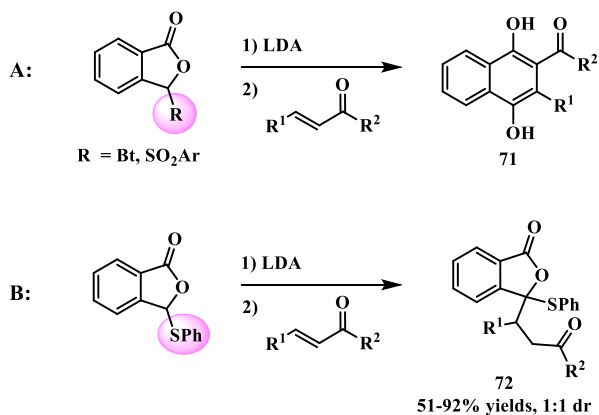


Scheme 2.13 Asymmetric allylation reactions of 3-cyano-phthalide to MBH carbonates (A) and MBH carbonates of isatin (B)

⁹⁷ a) Z. -P. Hu, Z. Zhuang, W. -W. Liao, *J. Org. Chem.*, **2015**, *80*, 4627–4637; b) W. Liu, Z. -P. Hua, Y. Yan, W. -W. Liao, *Tetrahedron Lett.*, **2018**, *59*, 3132–3135.

2.3.2 Stereoselective alkylations at C-3 site of unactivated or weakly activated phthalides

In various studies published by the research groups of Kraus, Katritzky and Hauser, phthalides characterized by a weakly activating group at C-3 site like thiophenyl, sulfonyl and benzotriazolyl functionalities were employed as substrated in Michael addition reactions. In all cases, the use of a sufficiently strong base as LDA in order to achieve the nucleophilic species and promote the attack to the electrophile was necessary, due to the poor acidity of the α -position. However, under strong base conditions, the activating groups behave as nucleofuges yielding naphthoquinols products **71** upon rearrangement of the Michael adducts.⁹⁸ Exclusively in the case of 3-phenylthio-phthalide, the Michael product **72** could be isolated in good yields but without getting any stereoselectivity.⁹⁹



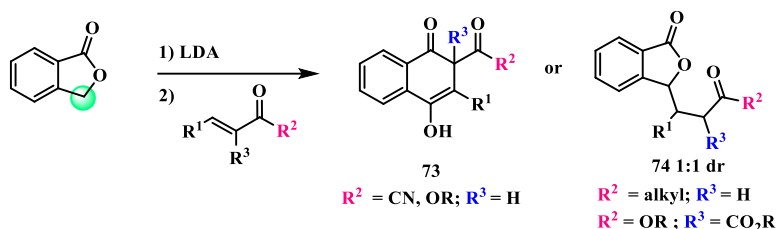
Scheme 2.14 Michael additions of phthalides weakly activated by cyano, benzotriazolyl, sulfonyl (A) and thiophenyl (B) functionalities

⁹⁸ a) G. A. Kraus, H. Sugimoto, *Tetrahedron Lett.*, **1978**, 19, 2263-2266; b) F. M. Hauser, R. P. Rhee, *J. Org. Chem.*, **1978**, 43, 178-180; c) M. Watanabe, H. Morimoto, K. Nogami, S. Ijichi, S. Furukawa, *Chem. Pharm. Bull.*, **1993**, 41, 968-970; d) A. R. Katritzky, G. Zhang, L. Xie, *Synth. Commun.*, **1997**, 27, 3951-3961.

⁹⁹ G. A. Kraus, H. Sugimoto, *Synth. Commun.*, **1977**, 7, 505-508.

3-Unsubstituted phthalides were also explored in Michael additions. However, the harsh reaction conditions required to ensure the anion generation and the subsequent attack to the electrophile provided 1,4-adducts as a mixture of diastereomers in low yields along with rearrangement and cyclization products.

In the work carried out by Broom, the LDA was used as a strong base to promote the conjugated addition of 3-unsubstituted phthalides to various Michael acceptors.¹⁰⁰ The type of product achieved strongly depends on the nature of the electrophile employed. As shown in **Scheme 2.15**, the 1,4-addition to α,β -unsaturated esters and nitriles generates a highly reactive enolate intermediate that attacks the lactone affording rearrangement products **73**. On the other hand, the intramolecular cyclization reaction does not occur with α,β -unsaturated ketones and dimethyl-ethylidenemalonate thanks to the greater stabilization of the anionic adduct. However, in all cases, the Michael product **74** was achieved with no stereocontrol.

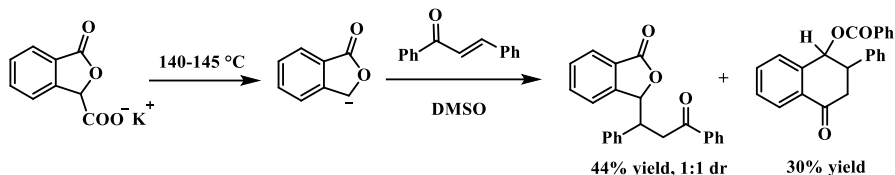


Scheme 2.15 Michael additions of 3-unsubstituted phthalide promoted by a strong base

The phthalide anion could be also generated by thermal decarboxylation of phthalide-3-carboxylic acid potassium salt resulting in conjugate addition to *trans*-chalcone, in dimethylsulfoxide, along with rearrangement by-

¹⁰⁰ N. J. P. Broom, P. G. Sammes, *J. Chem. Soc., Perkin Trans. 1*, **1981**, 465-470.

products.¹⁰¹ Also under those conditions, no stereoselectivity was obtained (Scheme 2.16).



Scheme 2.16 Decarboxylative Michael additions of 3-unsubstituted phthalide promoted by high temperature

2.4 Diastereoselective Michael addition of weakly activated phthalides

2.4.1 Specific objectives

As already mentioned, the examples of alkylation at C-3 site of the phthalide lactone ring hitherto reported in the literature are few. In this regard, considering the important pharmacological properties showed by these compounds, the development of new efficient stereoselective arylogous reactions has inspired our interest.

At the beginning of this PhD project research, the attention focused particularly on the investigation of stereoselective Michael addition of weakly activated phthalides. As mentioned before, reactions of 3-unsubstituted phthalides or weakly activated derivatives require harsh conditions such as strong bases and high temperatures, yielding Michael adducts without any control over diastereoselectivity or rearrangement products. Stereocontrolled Michael reactions could only be achieved with phthalides activated by ester or cyano group at C-3 position. This inevitably

¹⁰¹ J. A. Dibbens, R. H. Prager, C. H. Schiesser, A. J. Wells, *Aust. J. Chem.*, **1985**, *38*, 913-920.

limits the scope of accessible products to 3,3-disubstituted phthalides containing such electronwithdrawing groups.

With the aim to extend the scope of Michael donors in diastereoselective reactions to weakly activated phthalides, 3-aryl-derivatives were selected as potential candidates (**Figure 2.5**). These compounds are easy to prepare and have never been previously used in the arylogous Michael reactions (AMR).

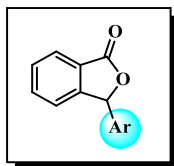
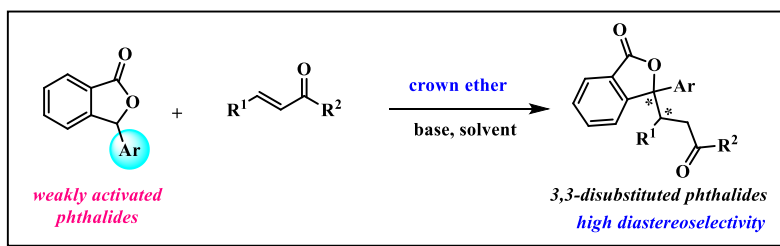


Figure 2.5 General structure of 3-aryl-phthalides

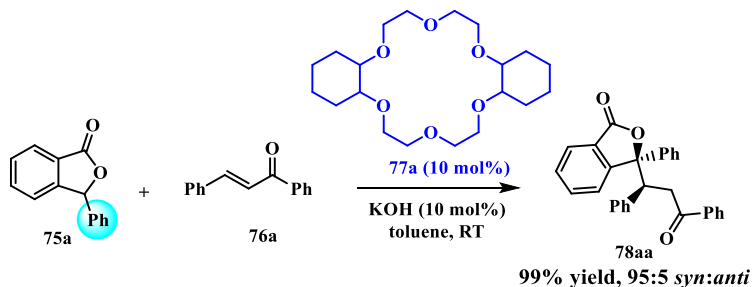
Having obtained very good results in the diastereoselective Mukaiyama-Michael reaction of butenolides catalyzed by crown ethers³¹, in view of the structural analogy between butenolides and phthalides, we decided to explore the use of crown ethers in the diastereoselective AMR of 3-aryl-phthalides under mild phase transfer catalysis conditions (**Scheme 2.17**).



Scheme 2.17 Diastereoselective crown ether-catalyzed arylogous Michael reaction (AMR) of 3-aryl-phthalides

2.4.2 Results and Discussion

Our investigation started using 3-phenylphthalide, a commercially available compound, as a model substrate. The attempted arylogous Michael reaction of 3-phenylphthalide **75a** with *trans*-chalcone **76a** promoted by triethylamine (1.0 eq.) in toluene did not give any traces of addition product after 24 hours. This confirmed the poorer activating ability of the phenyl group compared to *t*-butoxycarbonyl group. Subsequently, phase transfer crown ether-catalyzed conditions were employed (crown ether in presence of an inorganic base). However, using 1 equivalent of KOH and 10 mol% of dicyclohexane-18-crown-6 as phase transfer catalyst in toluene, complete degradation of reactants was observed. To our delight, the reaction of 3-phenyl-phthalide with *trans*-chalcone in the presence of catalytic amounts of KOH (10 mol%) and dicyclohexane-18-crown-6 (10 mol%) at room temperature cleanly yielded the desired adduct with high *syn*-diastereoselectivity (95:5 dr) (Scheme 2.18).

Scheme 2.18 AMR of **75a** with **76a**

The (R^* , S^*) relative configuration of the major diastereomer **78aa** was determined by the X-ray crystal analysis (Figure 2.6).

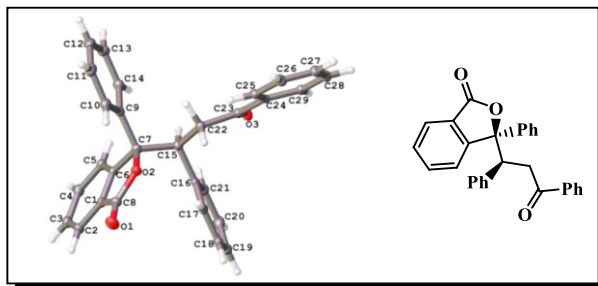
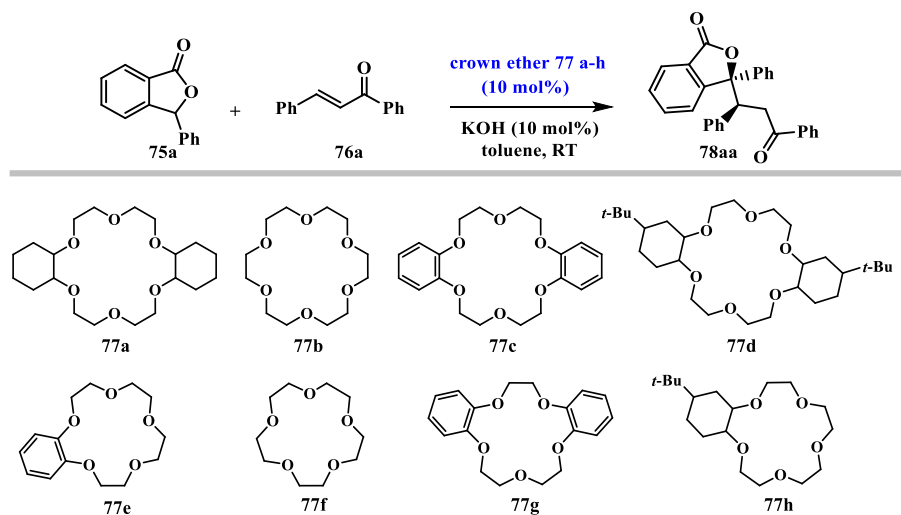


Figure 2.6 Single-crystal X-ray structure of 78aa

Then, the catalyst-effect was evaluated and structurally different macrocyclic catalysts derived from 18-crown-6 and 15-crown-5 were tested in the AMR (**Table 2.1**). It is worth noting that all the catalysts employed were commercially available.

In all cases, excellent yield and *syn*-diastereoselectivity were achieved. 18-Crown-6 (**77b**) and dibenzo-18-crown-6 (**77c**) exhibited higher diastereoselectivity than dicyclohexane-18-crown-6 (cf. **entries 2, 3** with **entry 1, Table 2.1**), whereas no improvements were observed with the more hindered catalysts **77d** (**entry 4, Table 2.1**). Performing the AMR with 15-crown-5 derivatives **77e–h** (**entries 5–8, Table 2.1**) slightly lower yields and stereoselectivities were obtained, probably due to the smaller cavities. The effect of the crown ether's structure both on the catalytic activity and the diastereoselectivity of the reaction was also investigated. As reported in **entry 9**, carrying out the addition in the absence of the macrocycle no product was achieved after long reaction times, confirming the essential role of the phase transfer catalyst. Although crown ethers **77b** and **77c** displayed comparable performances in toluene, dibenzo-18-crown-6 proved to be a more versatile catalyst, giving better diastereoselectivity in different solvents, such as CH_2Cl_2 (cf. **entry 10** with **entry 11, Table 2.1**), and was thus preferred for further investigations.



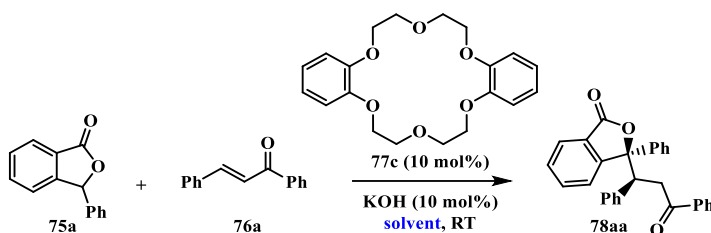
entry	catalyst	t (h)	yield (%) ^b	dr ^c
1	77a	5	99	95:5
2	77b	5	95	98:2
3	77c	5	95	98:2
4	77d	6	97	97:3
5	77e	20	94	96:4
6	77f	20	95	96:4
7	77g	20	90	95:5
8	77h	20	95	97:3
9	-	116	-	-
10 ^d	77b	20	98	92:8
11 ^d	77c	6	94	95:5

^aReaction conditions: **75a** (0.2 mmol), **76a** (0.20 mmol), KOH (0.020 mmol), catalyst **77** (0.020 mmol), toluene (1.0 mL). ^bIsolated yields. ^cDetermined by ¹H NMR analysis of the crude product. ^dReaction performed in CH₂Cl₂.

Table 2.1 Screening of crown ethers in the AMR of **75a** with **76a**^a

Subsequently, the solvent effect in the AMR of **75a** with **76a** catalyzed by **77c** was surveyed. As shown in **Table 2.2**, in aprotic polar solvents such as

CH₃CN and DMF, the yields and the diastereoselectivities were disappointing (**entries 2 and 3**). In particular, with DMF, the Michael adduct was achieved only in moderate yield and with longer reaction time. Good to high yields were obtained in reactions performed in halogenated and ethereal solvents, but the diastereoselectivities were slightly lower compared to toluene (**entries 4–8**). However, diethyl ether was an exception since a high *syn:anti* diastereoselectivity was observed in this solvent (**entry 6**).



entry	solvent	t (h)	yield (%) ^b	dr ^c
1	toluene	5	95	98:2
2	CH ₃ CN	4	74	79:21
3	DMF	68	58	72:28
4	CH ₂ Cl ₂	6	94	95:5
5	DCE	20	90	96:4
6	Et ₂ O	20	94	98:2
7	THF	44	83	94:6
8	MTBE	20	89	95:5
9	mesitylene	20	96	98:2
10	<i>o</i> -xylene	7	89	97:3
11	<i>m</i> -xylene	7	88	98:2
12	<i>p</i> -xylene	7	87	97:3

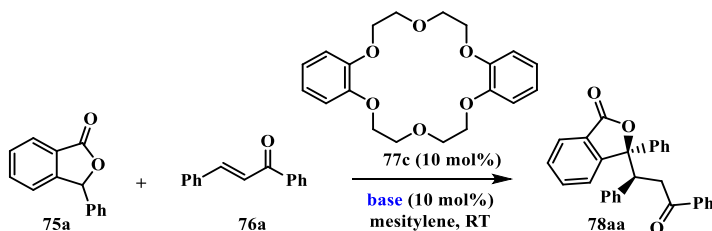
^aReaction conditions: **75a** (0.2 mmol), **76a** (0.20 mmol), KOH (0.020 mmol), dibenzo-18-crown-6 (0.020 mmol), solvent (1.0 mL). ^bIsolated yields. ^cDetermined by ¹H NMR analysis of the crude product.

Table 2.2 Screening of solvents in the AMR of **75a** with **76a**^a

Other aromatic solvents provided better results (**entries 9–12, Table 2.2**) with yields and diastereoselectivity similar to those achieved in toluene. A slight increase in the yield was obtained in mesitylene, which therefore was chosen as the preferred solvent for further studies.

Later, the influence of the base and the reaction temperature were evaluated.

The results are shown in **Table 2.3**.



entry	base	t (h)	yield (%) ^b	dr ^c
1	KOH	20	96	98:2
2	KF	144	-	-
3	PhOK	144	64	>98:2
4	K ₂ CO ₃	144	-	-
5	K ₃ PO ₄	144	91	>98:2
6	K ₂ HPO ₄	144	-	-
7	KH ₂ PO ₄	144	-	-
8 ^d	KOH	20	83	>98:2
9 ^e	KOH	116	61	>98:2

^aReaction conditions: **75a** (0.2 mmol), **76a** (0.20 mmol), base (0.020 mmol), dibenzo-18-crown-6 (0.020 mmol), solvent (1.0 mL). ^bIsolated yields. ^cDetermined by ¹H NMR analysis of the crude product. ^dReaction performed at 0 °C. ^eReaction performed at -20 °C.

Table 2.2 Screening of bases and temperatures in the AMR of **75a** with **76a**^a

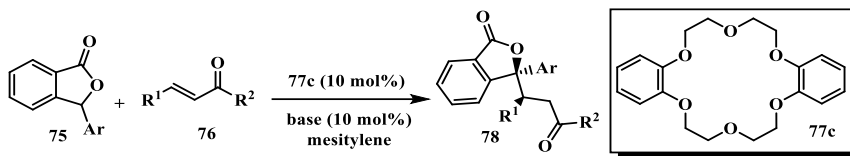
A large screening of bases was conducted, but most of them provided disappointing results. No traces of any product were observed in the reaction promoted by weak inorganic bases such as KF, K₂CO₃, K₂HPO₄, and

KH₂PO₄. Meanwhile, bases of intermediate strength, such as PhOK and K₃PO₄, promoted the formation of the Michael adduct **78aa** as a single diastereomer, albeit with long reaction times (**entries 3 and 5**). With PhOK, the yield was only moderate due to incomplete conversion even after long times, whereas a high yield was obtained with K₃PO₄, which proved to be a very effective base. The AMR performed with KOH at 0 °C (**entry 8**) also furnished a single diastereomer, with the advantage of a shorter reaction time compared to K₃PO₄, but with a slightly lower yield. At -20 °C with KOH, the yield decreased. Therefore, KOH at 0 °C and K₃PO₄ at room temperature were selected as the two most efficient basic conditions. The following scope of the reaction was studied under both conditions in mesitylene catalyzed by 10 mol% of dibenzo-18-crown-6.

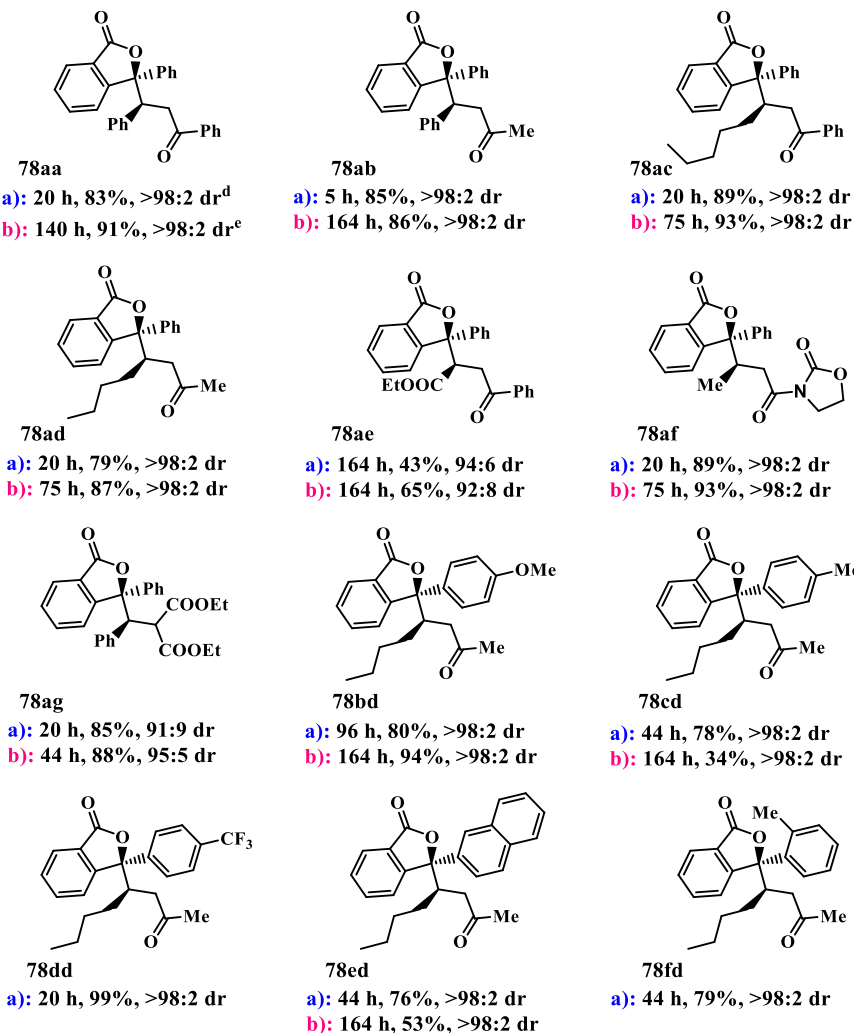
As shown in **Scheme 2.19**, the AMR was investigated with several Michael acceptors. Both aliphatic and aromatic α,β -unsaturated ketones and other unsaturated Michael acceptors as 3-crotonyl-2-oxazolidinone **76f**, and diethyl benzylidenemalonate **76g** were tested. The desired adducts **78aa–ag** were achieved with good to excellent yields and as single diastereomers in nearly all cases. Only with the ester group-containing Michael acceptors (**76e** and **76g**), a small amount of the minor *anti* products were detected.

Generally, the reactions promoted by KOH proceeded with shorter times even at 0 °C, while with K₃PO₄ the additions required prolonged times at room temperature. However, better yields were achieved with K₃PO₄. In addition, K₃PO₄-promoted reaction gave both higher yield and diastereoselectivity for product **78ag**.

As expected, the presence of electron-donating groups on the aromatic ring decreased the reactivity at the C-3 site of the lactone ring and, consequently, longer reaction times were needed to ensure high conversions.



a): KOH, 0 °C; b): K₃PO₄, RT



^aReaction conditions: **75** (0.20 mmol), **76** (0.20 mmol), base (0.020 mmol), **77c** (0.020 mmol), mesitylene (1.0 mL). ^bIsolated yields. ^cDiastereomeric ratios determined by ¹H NMR analysis of the crude product. ^dAt the 1.00 mmol scale, **78aa** was obtained with 90% yield and >98:2 dr after 20 h. ^eAt the 1.00 mmol scale, **78aa** was obtained with 92% yield and >98:2 dr after 44 h.

Scheme 2.19 Scope of the AMR of 3-Aryl Phthalides catalyzed by dibenzo-18-crown-6^{a,b,c}

For example, *p*-methoxyphenyl-substituted product **78bd** was achieved in good yield at 0 °C with KOH after 44 h, while excellent yield was obtained with K₃PO₄ at room temperature but in longer reaction time. The *p*-tolyl-substituted adduct **78cd** was produced with good yield in the presence of KOH at room temperature rather than at 0 °C in order to increase the reaction rate. K₃PO₄ turned out to be ineffective with *o*-tolyl substituent, and only KOH at 0 °C afforded the product **78fd** with good yield. On the contrary, the electron-withdrawing *p*-CF₃ substituent greatly increased the reactivity of the C-3 position forming the adduct **78dd** with excellent yield in short reaction time.

The (R*,S*) configuration was further confirmed by X-ray analysis of the crystallized major diastereomer **78ag** (Figure 2.7).

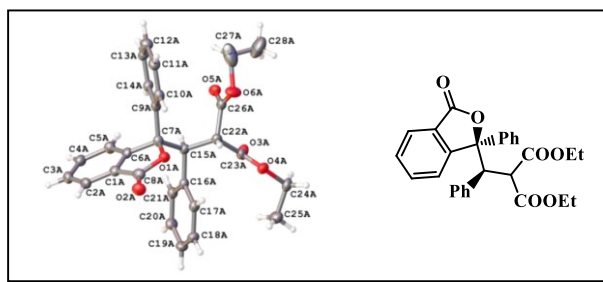


Figure 2.7 Single-crystal X-ray structure of **78ag**

A phase transfer catalytic mechanism involving the formation of an ion pair between the K⁺-crown ether complex and the arylogous enolate generated after deprotonation of phthalides (Figure 2.8) should be the most plausible for this process. In order to further confirm this hypothesis, a widely employed phase transfer catalyst such as tetrabutylammonium bromide was used to carry out the arylogous Michael reaction in the presence of a catalytic amount of KOH. Albeit less efficient than crown ethers (product **78aa** was

obtained with a lower yield, 70% yield, and diastereomeric ratio, 92:8 dr, at RT in 68 h) a good catalytic activity was encountered.

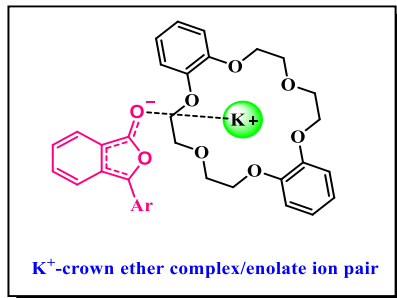


Figure 2.8 Schematic structure of K^+ -crown ether complex/ enolate ion pair

2.4.3 Conclusions

In this study, the first example of arylogous Michael reaction of weakly activated 3-aryl-phthalides promoted by catalytic amounts of crown ethers and solid KOH or K_3PO_4 , in mesitylene, was developed. Crown ethers have proven to be very efficient catalysts whereas tertiary amine organocatalysts failed. Thus, under mild reaction conditions, the conjugate additions of several 3-aryl-phthalides to different electrophilic Michael acceptors provided various 3,3-disubstituted-phthalides in good to excellent yields and as single diastereomer in nearly all cases.

Our methodology, subject of a publication,¹⁰² has recently been exploited in an efficient, cost-saving, and environmentally-friendly integrated photo-flow oxidative two-step process¹⁰³ including the synthesis of 3-substituted-

¹⁰² M. Sicignano, A. Dentoni Litta, R. Schettini, F. De Riccardis, G. Pierri, C. Tedesco, I. Izzo, G. Della Sala, *Org. Lett.*, **2017**, *19*, 4383-4386.

¹⁰³ D. Aand, S. Karekar, B. Mahajan, A. B. Pawar, A. K. Singh, *Green Chem.*, **2018**, *20*, 4584-4590.

phthalides and the following arylogous Michael reaction, which further confirmed its significance.

2.5 Diastereoselective Michael addition of unactivated phthalides

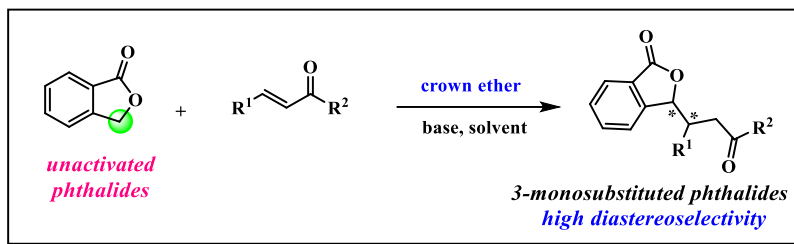
2.5.1 specific objectives

As a natural evolution of the previously described arylogous Michael reaction of 3-arylphthalides, we planned the application to unsubstituted phthalides in order to achieve the diastereoselective synthesis of the 3-alkylphthalides, which is a class of compounds widely represented in nature.

3-Unsubstituted phthalides are more challenging substrates because of their poor acidity at the C-3 site. As reported in the literature, high temperature and strong base conditions ensure the deprotonation of the α -site, but Michael adducts were generated with no diastereoselectivity and in low yields together with cyclic byproducts.

On the other hand, it is well known that the basicity of inorganic bases such as metal hydroxides, could be exceptionally enhanced under phase transfer catalysis conditions allowing the reactions of weakly acidic pro-nucleophiles with electrophilic species. In addition, the unnecessary use of anhydrous solvents and controlled atmospheres, the cost-saving and the easy scale-up, would make these mild reaction conditions extremely advantageous.

Therefore, here are described the studies on the first phase transfer catalyzed diastereoselective AMR of unactivated phthalides (**Scheme 2.20**).

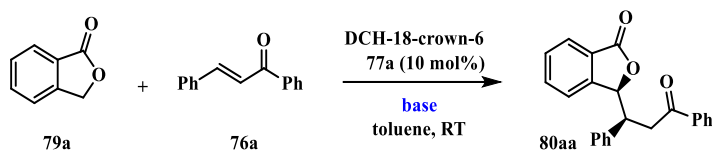


Scheme 2.20 AMR of unactivated phthalides under PTC conditions

2.5.2 Results and Discussion

As an initial approach, reaction conditions analogous to the previously described AMR of 3-arylphthalides were applied to the reaction of unactivated phthalides.

Catalytic amounts of KOH and dicyclohexane-18-crown-6 **77a** were used to promote the conjugate addition of the commercially available 1-isobenzofuranone **79a** to *trans*-chalcone **76a** at room temperature in toluene. Unfortunately, only traces of the desired Michael adduct were detected using 10 mol% and 20 mol% of KOH respectively, despite the long reaction times (**Table 2.4, entries 1 and 2**). Increasing the amount of KOH up to 1 molar equivalent, the isolated yield raised up to 45% after 6 hours, but this result could not be further improved by prolonging the reaction time (**entry 3**). In fact, monitoring the reaction by ^1H NMR, it was observed the complete disappearance of the phthalide after 6 hours, preventing further addition to the chalcone, and the concomitant appearance of a white precipitate probably due to the lactone ring-opening. However, albeit in low yield, the Michael product was obtained with high diastereoselectivity (95:5 dr).



entry	base (mol eq.)	t (h)	yield (%) ^b	dr ^c
1	KOH (0.10)	216	traces	-
2	KOH (0.20)	144	13	ND
3	KOH (1.0)	6	45	95:5
4	<i>t</i> -BuOK (1.0)	6	18	ND
5	PhOK (1.0)	96	No reaction	ND
6	K ₂ CO ₃ (1.0)	96	No reaction	ND
7 ^d	KOH (1.0)	6	55	93:7

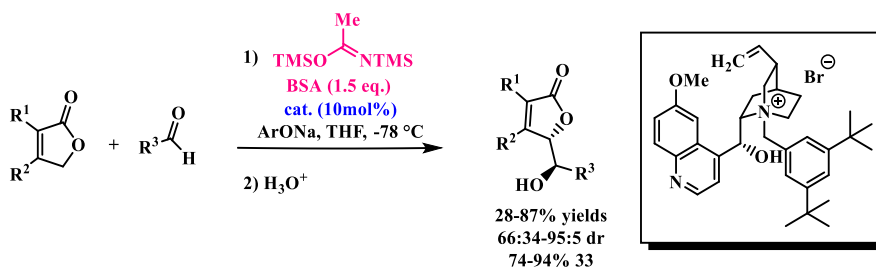
^aReactions were performed with **79a** (0.20 mmol), **76a** (0.20 mmol), base (x mmol), and DCH-18-crown-6 (0.020 mmol) in toluene (1.0 mL), unless otherwise noted. Workup was carried out by addition of HCl 1M/THF mixture (1:3, 4.0 mL). ^bYield of isolated product. ^cDetermined by ¹H NMR analysis of the crude product mixture. ^d1.0 molar equivalent (0.20 mmol) of DCH-18-crown-6 were used.

Table 2.4 AMR of **79a** to **76a** promoted by inorganic bases and DCH-18-crown-6^a

Bases of different strengths were also used, but still with disappointing results. As shown in **Table 2.4**, a low yield was achieved with *t*-BuOK due to the generation of several side products (**entry 4**), while no conversion was detected with PhOK and K₂CO₃ (**entries 5 and 6**). A test with stoichiometric amounts of KOH and crown ether was also performed. A slight increase of the yield to 55% was obtained but the decomposition of the starting material and, in this case, also of the *trans*-chalcone was not avoided (**entry 7**). Therefore, some modification of the reaction protocol in order to improve the conversion appeared to be necessary.

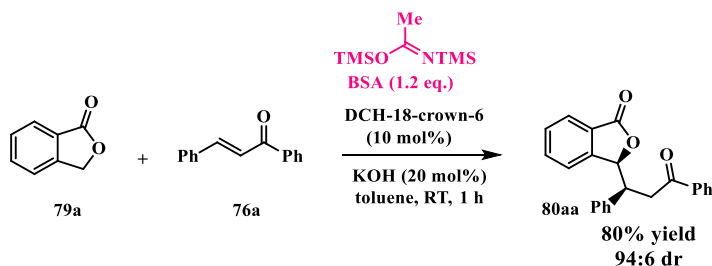
In an interesting work carried out by the group of Levacher, the addition in the reaction mixture of a silylating agent, specifically *N,O*-Bis(trimethylsilyl)acetamide (BSA), strongly accelerated the vinylogous

aldol reaction of butenolides catalyzed by chiral quaternary ammonium salts (Scheme 2.21).¹⁰⁴ The authors proposed the trapping of the aldol product to form a silyl ether, which was then cleaved during acidic work-up.



Scheme 2.21 Phase transfer catalyzed vinylogous aldol reaction of butenolides with BSA

Thus, taking inspiration from this study and considering the structural affinity between phthalides and butenolides, we explored the same silylating additive to promote the conjugated addition of unsubstituted phthalides, anticipating a possible entrapment of the supposed Michael enolsilane adduct. Using a small excess of BSA (1.2 eq.) in the presence of 20 mol % of KOH and 10 mol % of crown ether, after 1 hour the desired 3-monosubstituted phthalide product was indeed isolated with high yield (80%) and high diastereomeric ratio (94:6 dr) (Scheme 2.22).



Scheme 2.22 Diastereoselective AMR of phthalide to *trans*-chalcone promoted by BSA

¹⁰⁴ A. Claraz, S. Oudeyer, V. Levacher, *Adv. Synth. Catal.*, **2013**, 355, 841–846.

The relative configuration of the major diastereoisomer resulted to be *syn*, as determined by X-ray analysis (**Figure 2.9**).

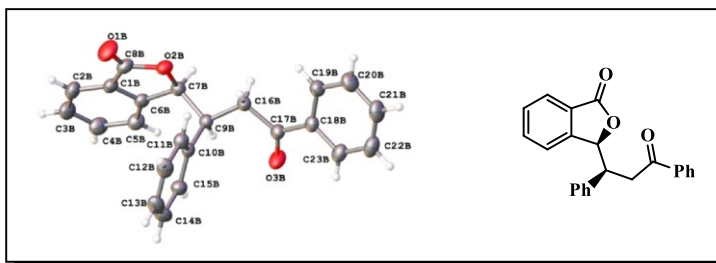
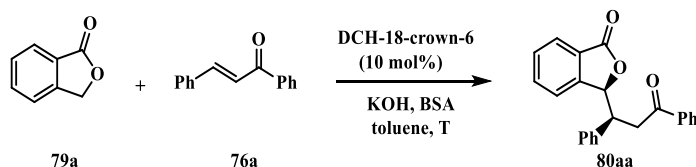


Figure 2.9 Single-crystal X-ray structure of **80aa**

The use of different amounts of KOH was, then, investigated. Lowering the amount of inorganic base to 10 mol %, a slower addition was observed resulting in a low conversion even after long reaction time (**Table 2.5, entry 1**). Whereas, using 1 equivalent of KOH, only moderate yield was achieved due to the formation of several byproducts (**entry 3**).

The investigation of other parameters, such as the amount of BSA and the temperature was subsequently evaluated. 1.5 Eq. of BSA provided the best compromise between yield and dr (86 %, 94:6) since the diastereoselectivity decreased to 90:10 dr in presence of 2.0 eq. of BSA whereas the yields decreased with lower amounts of silylating additive (**Table 2.5, entries 3-5**). A large screening of the temperature was performed too. Moving down from room temperature to -40 °C, the diastereomeric ratio remained unaffected, while a substantial increase of the yield up to 98% was achieved (**Table 2.5, entries 6-8**). This large yield variation should be ascribed to the progressive reduction of the chalcone decomposition at lower temperatures. In fact, no degradation of the Michael acceptor was detected after 48 hours by submitting the *trans*-chalcone at -40 °C under the typical reaction condition

and in the absence of the phthalide **79a**, while a total consumption after 1 hour was observed at room temperature. However, the further reduction of the temperature resulted in incomplete conversion and lower diastereoselectivity (**entries 9 and 10**). Therefore, further investigations were performed at -40 °C.



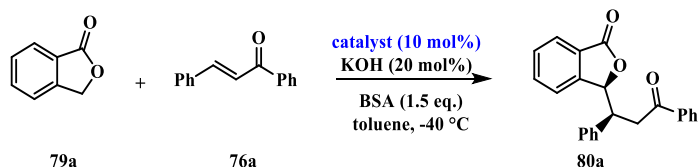
entry	KOH (mol eq.)	BSA (mol eq.)	T (°C)	t (h)	yield (%) ^b	dr ^c
1	0.1	1.2	RT	48	30	95:5
2	0.2	1.2	RT	1	80	94:6
3	1.0	1.2	RT	1	42	95:5
4	0.2	1.5	RT	1	86	94:6
5	0.2	2.0	RT	1	90	90:10
6	0.2	1.5	0	1	93	94:6
7	0.2	1.5	-20	1	94	94:6
8	0.2	1.5	-40	2	98	94:6
9	0.2	1.5	-50	3	91	92:8
10	0.2	1.5	-78	15	87	90:10

^aReactions were performed with **79a** (0.20 mmol), **76a** (0.20 mmol), KOH (x mmol), BSA (y mmol), and DCH18C6 (0.020 mmol) in toluene (1.0 mL), unless otherwise noted. Workup was carried out by the addition of HCl 1M/THF mixture (1:3, 4.0 mL). ^bYield of isolated product. ^cDetermined by ¹H NMR analysis of the crude product mixture

Table 2.5 AMR of phthalide **79a** to *trans*-chalcone with BSA^a

At a later stage, the effect of the catalyst structure was thoroughly inspected. First, the decisive role of the phase transfer catalyst in this reaction was validated by conducting the conjugate addition of phthalide to *trans*-

chalcone at $-40\text{ }^{\circ}\text{C}$ in toluene, with KOH and BSA, in the absence of crown ether, and detecting only traces of the 3-substituted-phthalide product after 48 hours (**Table 2.6, entry 2**). At this point, several phase transfer catalysts were screened, as shown in **Table 2.6**. A large increment of the diastereoselectivity to 99:1 *syn:anti* was achieved with 18-crown-6 after 15 hours reaction (**entry 3**). The longer reaction time needed to accomplish full conversion in comparison to DCH-18-crown-6 could be explained considering the lower lipophilicity of 18-crown-6, entailing a less favorable extraction constant.



entry	catalyst	t (h)	yield (%) ^b	dr ^c
1	DCH18C6	2	98	94:6
2	-	48	traces	-
3	18C6	15	97	99:1
4	15C5	2	90	50:50
5 ^d	18C6	168	71	94:6
6 ^{d,e}	15C5	48	86	80:20
7 ^f	18C6	144	6	80:20
8	BTEAC	4	87	92:8
9	TBAC	48	69	88:12
10	Crypt-222	7	87	55:45

^aReactions were performed with **79a** (0.20 mmol), **76a** (0.20 mmol), KOH (0.040 mmol), BSA (0.30 mmol), and catalyst (0.020 mmol) in toluene (1.0 mL) at $-40\text{ }^{\circ}\text{C}$, unless otherwise noted. Workup was carried out by addition of HCl 1M/THF mixture (1:3, 4.0 mL). ^bYield of isolated product. ^cDetermined by ^1H NMR analysis of the crude product mixture. ^dNaOH (0.040 mmol) was used in place of KOH. ^eReaction was performed at room temperature. ^fCsOH (0.040 mmol) was used in place of KOH.

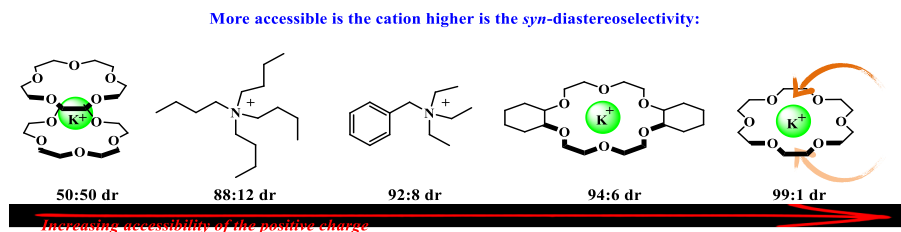
Table 2.6 Screening of catalysts^a

A considerable effect of the macrocyclic size on the diastereoselectivity was also detected. In fact, using the smaller 15-crown-5 instead of 18-crown-6 derivatives, a decline of *syn*-preference was observed, resulting in 1:1 diastereomeric ratio (**entry 4**). To better understand the influence of the cation-crown ether system on the stereoselectivity, NaOH was also employed as inorganic base with both 18-crown-6 and 15-crown-5 at -40 °C (**entries 5 and 6**). Under both conditions very sluggish reactions were observed, thus, in order to achieve a good conversion, higher temperature (25 °C) was employed. Interestingly, in both cases the *syn*-diastereoselectivity was lower than with KOH/18-crown-6 system, but better if compared to 1:1 diastereomeric ratio obtained with KOH and 15-crown-5. Finally, the reaction performed with CsOH and 18-crown-6 generated the product with very low yield due to the formation of many byproducts (**entry 7**).

Moreover, other types of phase transfer catalysts such as quaternary ammonium salts and cryptands were evaluated. As summarized in **Table 2.6**, quaternary ammonium salts provided values of *syn*-diastereoselectivity intermediate between those achieved with KOH/18-crown-6 and KOH/15-crown-5 (cf. **entries 8 and 9** with **entries 3 and 4**). In particular, benzyltriethylammonium chloride (BTEAC) afforded good yield and diastereomeric ratio, whereas poorer results and longer reaction time were obtained with the bulkier tetrabutylammonium chloride (TBAC). The [2.2.2]-Cryptand (crypt-222) led to the Michael adduct efficiently in short reaction time, but as an almost equimolar *syn:anti* diastereomeric mixture (**entry 10**).

As discussed in **section 1.2**, the steric accessibility of the cation affects the ion pair separation degree thereby influencing the stereoselectivity of the phase transfer reaction. Similarly, in our case, the formation of looser or

tighter ammonium or K^+ -crown/phthalide ion pairs could be responsible for the different diastereoselectivity observed. In fact, if we compare results achieved with structurally different catalysts (**Scheme 2.23**), it is well-clear that the increasing steric accessibility of the cation enhances the *syn*-diastereoselectivity.



Scheme 2.23 Trend of the *syn*-diastereoselectivity with different catalysts

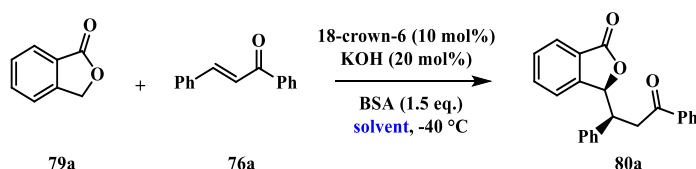
The low diastereoselectivity observed with 15-crown-5 could be explained by assuming the formation of 2:1 “sandwich” K^+ complexes in which the cation accessibility is poor and well-separated ion pairs are promoted.¹⁰⁵ On the other hand, the high accessibility of the potassium above and below the macrocycle plane of K^+ -18-crown-6 complexes supports rather tight ion pairs in apolar solvents affording high *syn*-diastereoselectivity. With quaternary ammonium salts, instead, lower levels of *syn*-diastereoselectivity were detected. This result reflects the poorer steric accessibility of the cation compared to K^+ -18-crown-6 system. In particular, the diastereoselectivity was slightly higher with BTEAC than with TBAC, owing to the higher hindrance of the larger butyl groups in the latter ammonium salt. Since K^+ is completely wrapped inside the macrobicyclic cavity of [2.2.2]-cryptand, the

¹⁰⁵ a) Cation Binding by Macrocycles: Complexation of Cationic Species by Crown Ethers; Y. Inoue, G. W. Gokel Eds.; Dekker: New York, 1990; b) Y. Ishii, Y. Soeda, Y. Kubo, *Chem. Commun.*, 2007, 2953–2955.

resulting high cation-anion separation degree well explains the low 55:45 *syn:anti* diastereomeric ratio obtained with this catalyst.

To highlight the origin of the *syn*-diastereoselectivity, DFT calculations were conducted. A detailed explanation about the effect of the catalyst on the stereoselectivity will be, in fact, discussed in the mechanistic part below.

Next, interesting results were achieved with the solvent screening (**Table 2.7**).



entry	Solvent (ϵ_r) ^e	t (h)	yield (%) ^b	dr ^c
1	Toluene (2.4)	15	97	99:1
2	Mesitylene (2.4)	15	96	>99:1
3	Et ₂ O (4.3)	2	89	97:3
4	THF (7.5)	2	90	88:12
5	CH ₂ Cl ₂ (9.0)	1	88	69:12
6	ACN (36.6)	8	71	50:50
7 ^d	DMF (38.2)	48	72	43:57

^aReactions were performed with **79a** (0.20 mmol), **76a** (0.20 mmol), KOH (0.040 mmol), BSA (0.30 mmol), and 18-crown-6 (0.020 mmol) in the appropriate solvent (1.0 mL) at -40 °C, unless otherwise noted. Workup was carried out by the addition of HCl 1M/THF mixture (1:3, 4.0 mL). ^bYield of isolated product. ^cDetermined by ¹H NMR analysis of the crude product mixture. ^dReaction performed at room temperature. ^e ϵ_r : dielectric constant of the solvent.

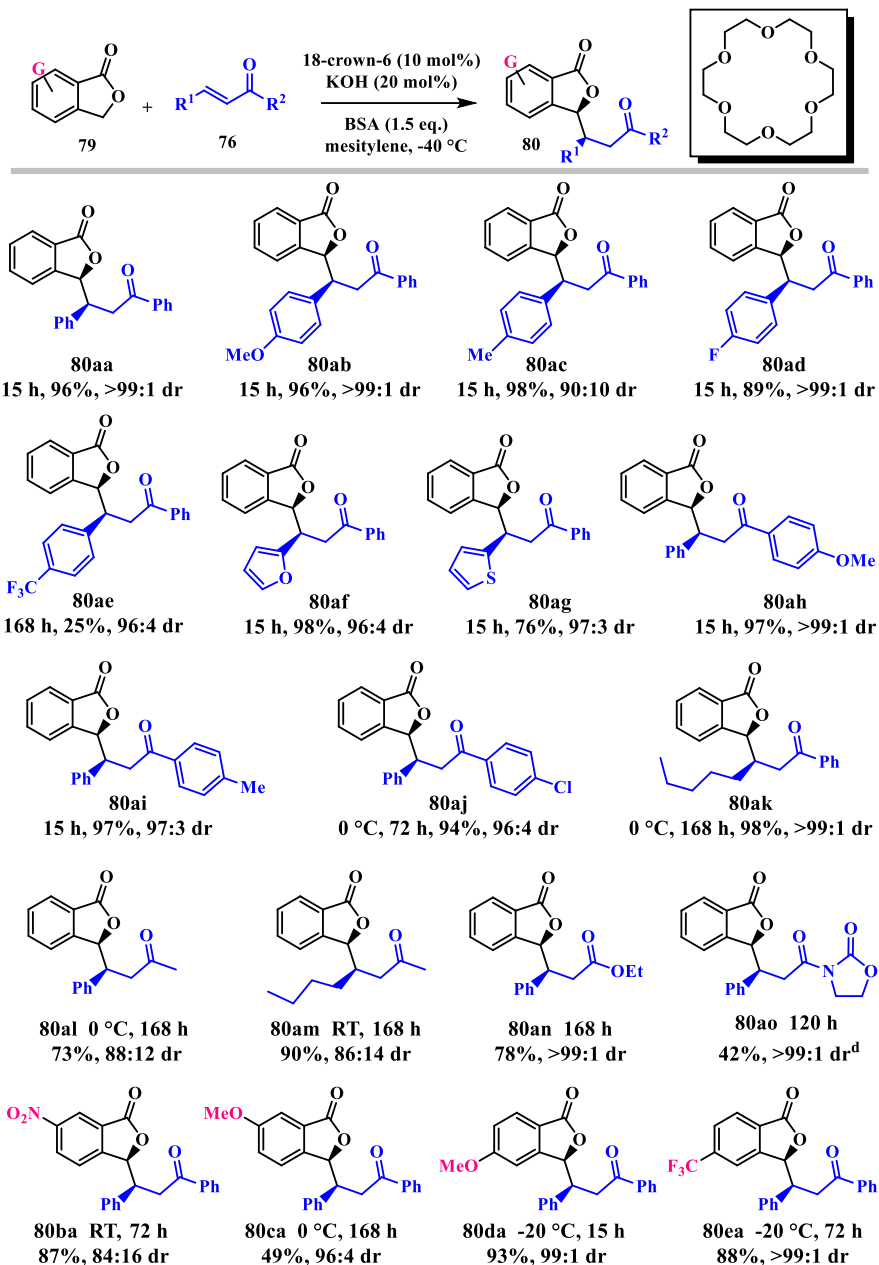
Table 2.7 Screening of solvents^a

Mesitylene turned out to be the best solvent, giving the product as a single diastereomer in very high yield (**entry 2**). Moreover, a close relationship between the diastereomeric ratio and the solvent dielectric constant (ϵ_r) was observed. In particular, an enhancement of the *anti* diastereoisomer fraction

was observed as the solvent dielectric constant increased. In fact, a slight preference for the *anti* diastereoisomer was achieved in DMF ($\epsilon_r = 38.2$) (Table 2.7, entry 7). It should be noted that in this solvent the conjugate addition was too sluggish at $-40\text{ }^\circ\text{C}$, and so the temperature was brought to $25\text{ }^\circ\text{C}$. A 50:50 *syn/anti* mixture was instead observed in acetonitrile (entry 6), whereas only a moderate preference for the *syn*-adduct was observed in CH_2Cl_2 (entry 5).

In ethereal solvents characterized by lower dielectric constants, good *syn*-diastereoselectivities and high yields were detected (entries 3 and 4). Finally, as mentioned before, the highest *syn*-diastereoselectivity was obtained in very low dielectric constant solvents, such as toluene and mesitylene. This behavior, as well as for the catalyst's structure effect, could be rationalized by taking into account the degree of tightness of the ion-pair involved. In fact, in apolar solvents, tight ion pairs could be assumed promoting high *syn*-diastereocontrol, whereas polar solvents such as ACN and DMF should encourage the formation of more solvent-separated ion pairs leading to poor diastereoselectivity. However, a detailed explanation of the solvent effect on the diastereoselectivity will be done below.

At this point, with the optimized reaction conditions in hand, the scope of the AMR of unactivated phthalides was extensively studied. Aromatic and aliphatic α,β -unsaturated carbonyl compounds as well as variously functionalized phthalides were tested, leading to excellent levels of *syn*-diastereoselectivity and good to high yields. In some cases, the *syn*-diastereoisomer was obtained as a single product. In addition, further optimization of the temperature was performed with some substrates in order to achieve better conversions and diastereomeric ratios.



^aReactions were performed with **79** (0.20 mmol), **76** (0.20 mmol), KOH (0.040 mmol), BSA (0.30 mmol), and 18-crown-6 (0.020 mmol) in mesitylene (1.0 mL) at -40 °C. ^bYield of isolated product. ^cDiastereomeric ratios were determined by ¹H NMR analysis of the crude product mixture. ^dDCH18C6 (0.020 mmol) was used in place of 18C6.

Scheme 2.24 *Scope of the AMR of unactivated phthalides^{a-c}*

As shown in **Scheme 2.24**, variously substituted *trans*-chalcones were surveyed. Excellent yields and diastereoselectivities were achieved after 15 hours with *p*-substituted *trans*-chalcones **76b,c,h,i** bearing electron-donating groups, as well as with 2-furanyl and 2-thiophenyl heteroaromatic substrates **76f** and **76g**.

Similar results were observed with *p*-fluorosubstituted chalcone **76d**, whereas with other electron-poor chalcones longer reaction times were needed to ensure good conversions. More precisely, the *p*-Cl substituted chalcone **76j** displayed a good reactivity at 0 °C, forming the desired Michael adduct with 97% yield and 96:4 diastereomeric ratio. On the contrary, the *p*-CF₃ substituted Michael adduct **80ae** was produced with only 25% yield at -40 °C owing to the low conversion. The same reaction performed at room temperature gave only a slight increase of the yield to 38%, with lower diastereoselectivity (88:12 dr). However, high to excellent diastereomeric ratios were achieved with all the *trans*-chalcones tested (94:6 to >99:1), regardless of the electronic effect of the substituent.

Higher temperatures and longer reaction times were required for Michael acceptors bearing aliphatic groups attached either on the carbonyl carbon or at the β-position, due to their lower reactivity in the AMR. Nevertheless, good to optimal yields and diastereoselectivities were obtained. In particular, the adduct **80ak** was produced as a single diastereomer with 98% of yield. A very interesting result was achieved in the conjugate addition to ethyl cinnamic ester **76n**, with the formation of the expected product **76an** in high yield and as a single diastereomer. To the best of our knowledge, this is the first example of Michael addition of 3-unsubstituted phthalides to an unsaturated ester. The *N*-cinnamoyl-2-oxazolidinone **76o** was also investigated as a substrate in the AMR, but its lower reactivity required the use of the more lipophilic DCH-18-crown-6 and longer reaction time. A

single diastereomer was produced also in this case, albeit with only moderate yield.

Finally, the effect of different substituents on the aromatic phthalide core was evaluated. Four differently arene-functionalized phthalides **79b-e** were synthesized and studied in the AMR. As reported in **Scheme 2.24**, both electron-donating and electron-withdrawing groups at C-6 and at C-5 positions were well tolerated in the Michael addition achieving high to excellent diastereoselectivities and good to high yields. Because of their lower reactivity compared to the unfunctionalized phthalide, further screening of the temperatures was done in order to establish the best conditions. 6-Nitrophthalide afforded the corresponding Michael product **80ba** with 87% yield and 84:16 *syn:anti* at room temperature, while with 6-methoxy-phthalide the product **80ca** was isolated with moderate yield at 0 °C. The best reaction temperature for both 5-methoxy- and 5-trifluoromethyl-phthalide resulted to be -20 °C, affording the Michael products **80da** and **80ea** with excellent levels of diastereoselectivities and high yields.

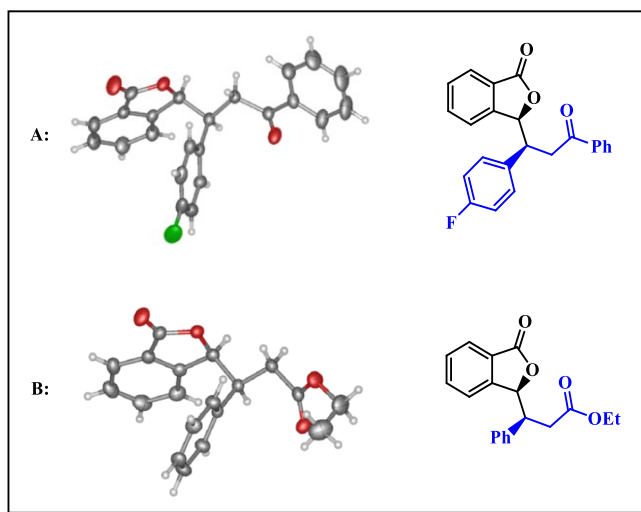
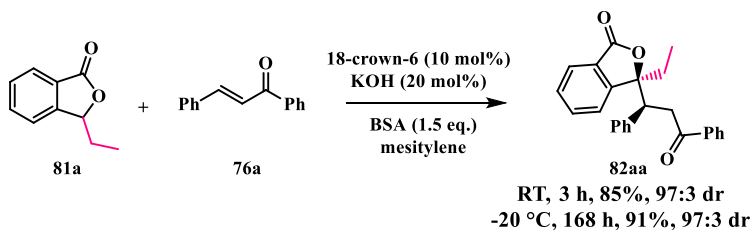


Figure 2.10 Single-crystal X-ray structure of **80ad** (A) and **80an** (B)

The relative *syn* configuration of the crystallized adducts **80ad** and **80an** was ulteriorly confirmed by X-ray diffraction analysis as shown in **Figure 2.10**. In order to deeply explore the potential of this phase transfer catalytic methodology, the AMR was also extended to unactivated 3-alkyl-phthalides, enabling the diastereoselective synthesis of the corresponding 3,3-dialkyl-phthalides. In particular, 3-ethyl-phthalide **81a** proved to be a suitable pro-nucleophile in the conjugate addition to *trans*-chalcones promoted by BSA and a catalytic amount of base and crown ether achieving the desired Michael adduct **82aa** with high yield and diastereomeric ratio at room temperature. As reported in **Scheme 2.25**, even higher yield was achieved at -20 °C, albeit with much longer reaction time. It is worth mentioning that 3-alkyl phthalides have never been employed in an arylogous Michael reaction prior to this example.



Scheme 2.25 Diastereoselective AMR of 3-ethylphthalide

2.5.3 Mechanistic insights and DFT calculations

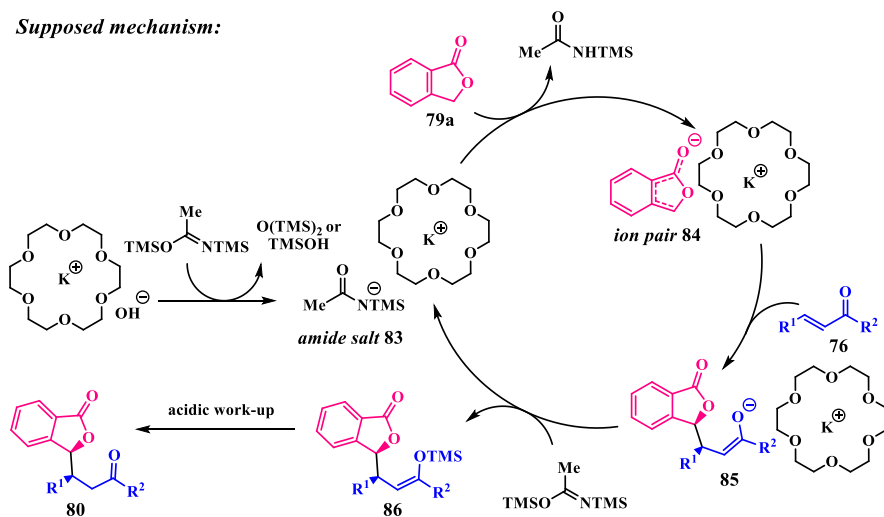
With the purpose to gain insights into the origin of the diastereocontrol in the AMR of unactivated phthalides, a plausible mechanism, shown in **Scheme 2.26**, was suggested.

It has been previously reported that BSA could be desilylated by a catalytic amount of Lewis bases generating the corresponding amide salt. This latter intermediate is an enough strong base to deprotonate acid sites of pro-

nucleophilic compounds and promote their reaction with various electrophiles.^{94,106}

Similarly, it was supposed that, under our developed conditions, BSA is desilylated by KOH/crown ether complex affording the corresponding K^+ -crown amide salt **83**. This species is basic enough to deprotonate the weakly acid α -site of phthalides giving rise to the nucleophilic K^+ -crown/phthalide anion ion pair **84**. The latter species would then undergo conjugate addition to the electrophilic unsaturated acceptor **76** forming the corresponding anionic Michael adduct **85**. The following silylation of the anion product by BSA would regenerate the amide salt **83** affording the silylated Michael adduct **86**. Finally, under simple acidic workup, the desired product **80** is released.

Supposed mechanism:



Scheme 2.26 Postulated mechanism of the AMR with BSA catalyzed by KOH/18-crown-6

¹⁰⁶ G. Haufe, S. Suzuki, H. Yasui, C. Terada, T. Kitayama, M. Shiron, N. Shibata, *Angew. Chem. Int. Ed.*, **2012**, *51*, 12275–12279; *Angew. Chem.*, **2012**, *124*, 12441–12445.

Evidence of the formation of the silylated Michael adduct **86** was achieved experimentally. In fact, performing the AMR of phthalide **79a** to *trans*-chalcone under the best reaction conditions but avoiding the final acidic workup, the silylated adduct **86** was isolated with 88% yield, in accordance with the proposed mechanism.

In line with this scenario, other phase transfer catalysts such as ammonium salts and cryptands should be able to promote the AMR through the involvement of a reactive ion pair similar to **84**. This was confirmed experimentally during the screening of the catalysts, since BTEAC, TBAC and [2,2,2]-cryptand provide to be suitable catalysts for this transformation. As depicted in **Scheme 2.26**, the major advantage of this methodology is the substantially full consumption of the catalytic amount of hydroxide ion in the early stages of the reaction mechanism preventing the development of side reactions as the lactone opening.

Furthermore, with the aim to establish whether the conjugate addition occurs under kinetic or thermodynamic control, a specific test was performed. In particular, an equimolar mixture of *syn/anti* diastereoisomers was subjected to the usual reaction conditions (BSA 1.5 eq., KOH 20 mol%, 18-crown-6 10 mol%, -40 °C) in toluene and, after 24 hours, the diastereomeric ratio was measured by ¹H NMR analysis of the crude reaction mixture. A negligible increase in the amount of *syn* product (53:47 *syn:anti*) was found. Considering that 99:1 diastereomeric ratio was achieved in the Michael reaction of phthalide **79a** with *trans*-chalcone after 15 hours under such conditions, the above reported result supports the hypothesis of *syn*-diastereopreference arising from the kinetic controlled irreversible pathway. Subsequently, in order to properly understand the origin of the diastereocontrol under different reaction conditions, DFT calculations of the transition states were carried out by Professor Luigi Cavallo of the University

of Science and Technology, Saudi Arabia, for the AMR of phthalide anion with *trans*-chalcone. Theoretical calculations¹⁰⁷ were performed considering that a suitable model must agree with the dependence of the observed *syn/anti* diastereoselectivity on both the solvent dielectric constant and the nature of phase transfer catalyst. In fact, from data reported in **section 2.7**, the diastereoselectivity of the arylogous Michael addition seems to strongly depend on the intimacy of the nucleophilic ion pair **84**. In particular, the high *syn*-diastereoselectivity appears to be favored under reaction conditions entailing the formation of a tight ion pair, such as apolar solvents and highly accessible cations. In this situation, the catalyst-derived cation can be involved in the transition state.

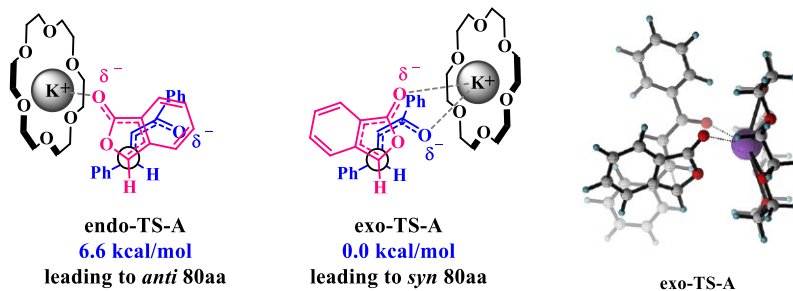
Two different Diels–Alder-like transition states, *exo*-TS-A and *endo*-TS-A, which lead to the *syn* and *anti* products respectively, were modeled in the presence of K⁺⊂18-crown-6 complex in toluene. As reported in **Figure 2.11 (A)**, the calculations of the relative energies of the transition states showed that *exo*-TS-A is more stable than *endo*-TS-A by 6.6 kcal mol⁻¹. This energy gap is completely in agreement with the experimental high *syn*-diastereoselectivity achieved under these conditions. The preference for the chelated *exo*-TS-A is due to the favorable simultaneous coordination of the two negatively charged oxygen atoms of the reactants with the K⁺ cation.

Moreover, DFT calculations with K⁺⊂DCH-18-crown-6 complex in toluene also were performed. As shown in **Figure 2.11 (B)**, *exo*-TS-B, which promotes the formation of the *syn* product, was favored over *endo*-TS-B also under these conditions, but with a lower difference of energy (3.6 kcal mol⁻¹) compared to K⁺⊂18-crown-6. This is in accordance with the lower *syn*-

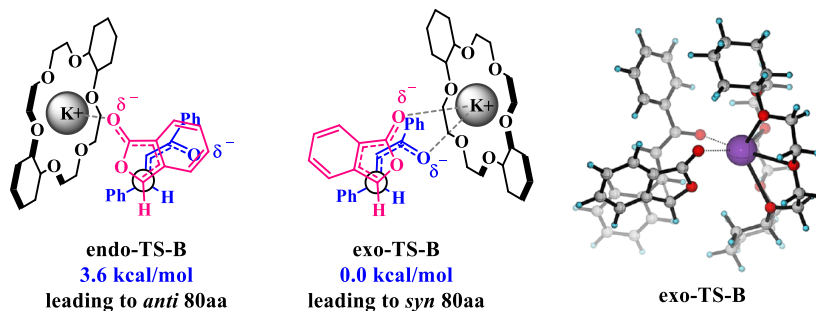
¹⁰⁷ DFT calculations were performed at M06-2X(SMD)/TZVPD//B3LYP/SVP level of theory for the reaction of phthalide anion with *trans*-chalcone.

diastereopreference experimentally observed with DCH-18-crown-6 than with 18-crown-6.

A) Attack of phthalide anion as a tight ion pair with K^+ /18-crown-6 in toluene



B) Attack of phthalide anion as a tight ion pair with K^+ /DCH-18-crown-6 in toluene



C) Attack of "naked" phthalide anion in DMF

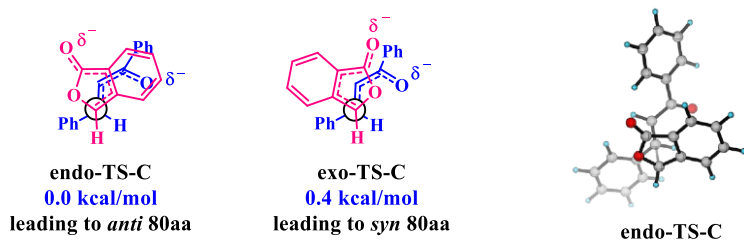


Figure 2.11 DFT calculations of *exo* and *endo* transition states for the AMR of the phthalide anion with *trans*-chalcone under cation-free or tight ion pair conditions. Values in parentheses represent Gibbs free energy at M06-2X(SMD)/TZVPD//B3LYP/SVP level of theory.

On the contrary, in polar media and with scarcely accessible cations, separated ion pairs are involved. In this case, the cation is far removed from the reactants and its participation in the transition state is no longer possible. On this basis, DFT calculations were performed considering the naked phthalide anion in DMF, giving the *exo*-TS-C and the *endo*-TS-C transition states, which lead to *syn* and *anti*-product respectively, characterized by similar energies (**Figure 2.11 (C)**). In fact, both of these transition states are governed by repulsive interaction so that neither of them is especially favored: *exo*-TS-C presents electrostatic repulsions between the two negatively charged oxygen atoms, whereas *endo*-TS-C is destabilized by repulsive interactions between aromatic phthalide π -electrons and the negatively charged *trans*-chalcone oxygen atom. Only a gap of 0.4 kcal mol⁻¹ was, therefore, found with a small preference for the *endo*-attack. This result explains the equimolar *syn/anti* mixture obtained experimentally both in ACN and with K⁺/15-crown-5, and the small preference for the *anti* product achieved in DMF and with K⁺⊂[2,2,2]-cryptand.

2.5.4 Conclusions

In conclusion, the first highly diastereoselective AMR of 3-unsubstituted phthalides under mild reaction conditions has been developed.¹⁰⁸ Good to high yields and good to excellent levels of *syn* diastereoselectivity were obtained with a large range of aliphatic and aromatic α,β -unsaturated carbonyl compounds and with variously functionalized unactivated phthalides. Thus, this method showed to be an efficient and original approach to give access to naturally occurring 3-alkylated phthalides. Interesting

¹⁰⁸ M. Sicignano, R. Schettini, L. Sica, G. Pierri, F. De Riccardis, I. Izzo, M. Bholanath, Y. Minenkov, L. Cavallo, G. Della Sala, *Chem. Eur. J.*, **2019**, *25*, 7131–7141. (Cover and Hot paper)

results were achieved also with 3-ethyl-phthalide exhibiting to be suitable for the synthesis of 3,3-dialkylphthalides too. Finally, the origin of the diastereoselectivity has been efficiently rationalized by mechanistic studies and DFT calculations of transition states. This method is, in addition, particularly suited for large-scale applications thank its low environmental impact, low cost, availability of reactants and simple operations.

2.6 Asymmetric Michael addition of weakly activated phthalides

2.6.1 Specific objectives

Having demonstrated that crown ethers efficiently catalyze the arylogous Michael additions of unsubstituted and 3-aryl or 3-alkyl substituted phthalides under mild reaction conditions affording 3- and 3,3-disubstituted products with high stereocontrol and yield, our interest moved to the asymmetric AMR of 3-aryl phthalides with α,β -unsaturated compounds containing chiral auxiliaries. The employment of enantiopure oxazolidinones as chiral auxiliaries allows their easy removal enabling access to the desired enantioenriched products.¹⁰⁹

2.6.2 Results and discussions

Preliminary run tests were carried out with the commercially available 3-phenylphthalide **75a** and the (*S*)-*N*-cynamoyl-4-phenyloxazolidin-2-one **87a** in the presence of different base/crown ether catalyst combinations. Depending on what diastereotopic face (*Re* or *Si*) of the chiral Michael acceptor **87a** is attacked by the phthalide anion, two *syn* products can be

¹⁰⁹ a) Z. Leitis, V. Lūsis, *Tetrahedron Asymmetry*, **2016**, *27*, 843-851; b) P. G. Andersson, H. E. Schink, K. Österlund, *J. Org. Chem.*, **1998**, *63*, 8067-8070.

obtained in principle, (3*R*,3'*S*) and (3*S*,3'*R*), along with two *anti* products, (3*S*,3'*S*) and (3*R*,3'*R*), as shown in **Figure 2.12**.

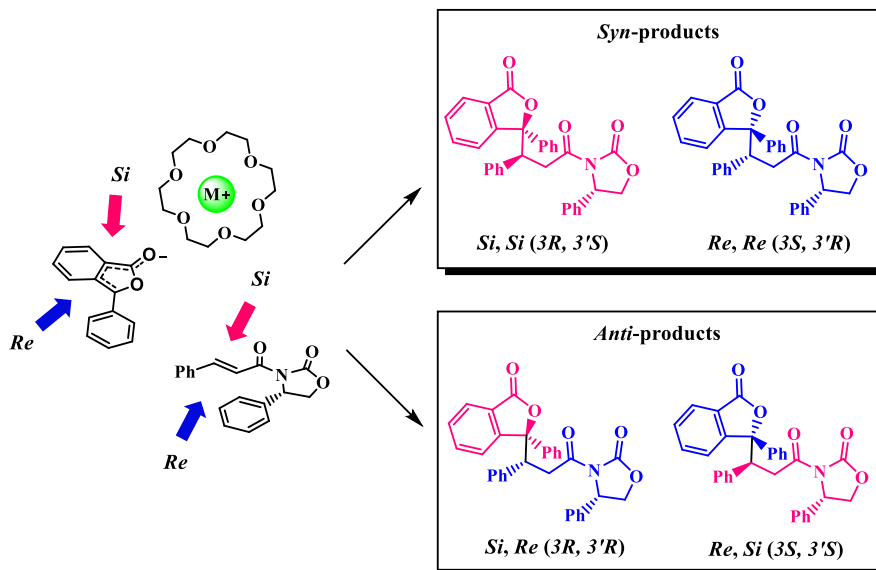
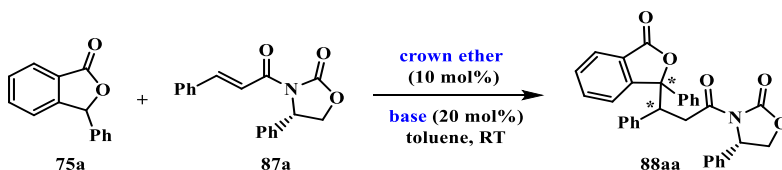


Figure 2.12 Representation of the possible *syn*- and *anti*-Michael products

In most of the experiments made, the corresponding *syn*-products were almost exclusively achieved; only traces of the respective *anti*-diastereoisomers could be detected by ¹H NMR analysis of the crude reaction mixture in < 2 % of the amount, unless otherwise noted. In fact, the diastereomeric ratios reported in **Table 2.8** refer to the amount of the two possible *syn*-products. Due to the difficulty of accurately measuring this ratio by ¹H NMR analysis of the crude mixture (the respective peaks of the two diastereomers turned up often partially overlapped) we followed a different procedure: the product was purified, submitted to erbium triflate catalyzed methanolysis, and the enantiomeric excess of the resulting *syn* enantiomer pair, (3*R*^{*},3'*S*^{*}) was measured by chiral HPLC.

The *syn* relative configuration of the major diastereomers obtained was, instead, assumed by analogy with the addition product to *N*-crotonoyloxazolidinone **78af** described in section 2.4.2.



entry	Base	catalyst	t (d)	yield (%) ^b	dr ^c
1	KOH	DCH-18C6	1	65	85:15
2	NaOH	DCH-18C6	1	74	86:14
3	LiOH•H ₂ O	DCH-18C6	3	12	72:28
4	Ba(OH) ₂ •8H ₂ O	DCH-18C6	3	<2 ^d	-
5	LiOH•H ₂ O	Benzo-15C5	3	<2 ^d	-
6	NaOH	Benzo-15C5	3	4 ^d	58:42
7	NaOH	dibenzo-18C6	3	79	32:68
8	NaOH	di <i>t</i> -BuDCH-18C6	3	57	82:18
9	NaOH	18C6	3	25	84:16
10	KOH	18C6	3	-	-

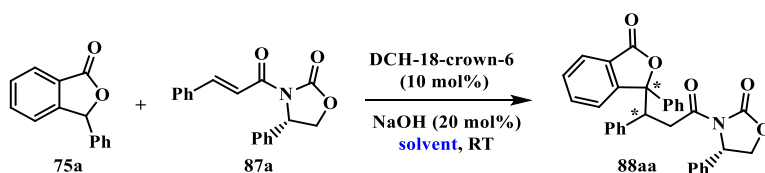
^aReaction conditions: **75a** (0.20 mmol), **87a** (0.20 mmol), base (0.040 mmol), cat (0.020 mmol), toluene (1.0 mL). ^bIsolated yields. ^cDiastereomeric ratios determined by chiral HPLC of the corresponding methyl ester obtained after methanolytic removal of the chiral auxiliary. ^dYield determined by ¹H NMR spectroscopy using 1,3,5-trimethoxybenzene as an internal standard.

Table 2.8 Asymmetric AMR of 3-*Ph*-phthalide under different base/crown ether systems^a

As described in **Table 2.8**, different bases and catalyst systems were tested. High yield and diastereoselectivity were achieved with KOH/DCH-18C6 (**entry 1**) and results were slightly improved using NaOH instead of KOH (**entry 2**). Other bases, such as LiOH•H₂O and Ba(OH)₂•8H₂O, provided disappointing conversions after prolonged reaction times (**entries 3, 4, 5**).

Other 18-crown-6 derivatives led to different outcomes. In fact, di-(*tert*-butylcyclohexyl)-18-crown-6 gave the Michael adduct with lower yield and similar diastereoselectivity compared to DCH-18C6. Whereas, 18-crown-6 afforded the product in very low yield after 3 days with NaOH, and failed to promote the reaction with KOH. Interestingly, the reaction promoted by dibenzo-18-crown-6 and NaOH provided the *syn*-product **88aa** with opposite facial selectivity (**entry 7**).

Next, with the best catalytic system (NaOH/DCH-18C6) in hands, the solvent effect was studied (**Table 2.9**).



entry	Solvent	t (d)	yield (%) ^b	dr ^c
1	Toluene	1	74	86:14
2	Mesitylene	1	74	80:20
3	Fluorobenzene	1	82	78:22
4	Chlorobenzene	1	75	75:25
5	Et ₂ O	4	46	68:32
6	CH ₂ Cl ₂	3	75	54:46
7	DMF	6	54	15:85
8	CH ₃ CN	6	34	11:89

^aReaction conditions: **75a** (0.20 mmol), **87a** (0.20 mmol), NaOH (0.040 mmol), DCH-18C6 (0.020 mmol), solvent (1.0 mL). ^bIsolated yields. ^cDiastereomeric ratios determined by HPLC analysis of the pure product.

Table 2.9 Screening of solvents

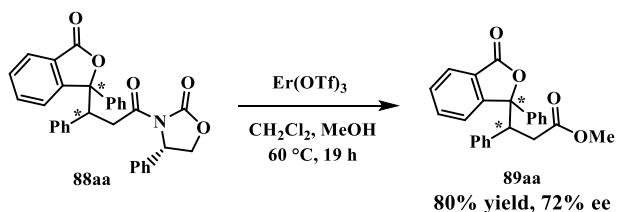
Other apolar aromatic solvents showed the same specificity for the *syn*-product as toluene. Very small amounts of *anti*-adduct could be, instead,

observed in other solvents such as Et₂O (5 %), CH₂Cl₂ (6 %), DMF (7 %) and CH₃CN (8 %) (**entries 5-8**).

Most importantly, a rough relationship between the solvent polarity and the diastereomeric ratio of the two possible *syn*-products was observed. As shown in **Table 2.9**, as the solvent dielectric constant increased, the amount of the minor diastereomer was progressively enhanced, until to obtain stereopreference inversion with highly polar solvents and DMF and CH₃CN (**entries 7, 8**). However, in these latter solvents conversions turned out to be slow and incomplete leading to disappointing yields.

Toluene turned out to be the best solvent for this reaction, yielding the *syn*-product with a high diastereomeric ratio of 86:14 (**entry 1**). Despite the higher d.r., CH₃CN is not a convenient solvent, since the inversion of stereocontrol of the newly generated chiral centers might be also achieved in toluene by using the chiral auxiliary with opposite configuration.

Finally, to completion of the asymmetric sequence, the removal of the chiral auxiliary was performed with Er(OTf)₃ in MeOH/CH₂Cl₂ (1:1) at 60 °C, leading to the desired enantioenriched ester **89aa** with 80 % of yield. This is the formal product of the asymmetric Michael addition to methyl cinnamate (**Scheme 2.24**).



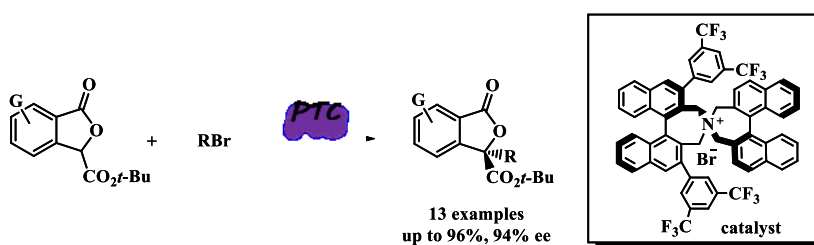
Scheme 2.24 Synthesis of chiral compound **89aa**

2.6.3 Conclusions

The asymmetric AMR of 3-phenyl-phthalide to (*S*)-1-cynamoyl-4-phenyloxazolidin-2-one catalyzed by dicyclohexane-18-crown-6 and NaOH under phase transfer reaction conditions, followed by removal of the oxazolidinone chiral auxiliary, has been described as an indirect and convenient strategy for the asymmetric conjugated addition to cynamate derivatives. It should be noted that enantioselective Michael addition at C-3 of phthalide core has been reported in literature only with activated 3-carboxy-derivatives, so this is the first example using unactivated Michael donor.

Chapter 3

Enantioselective alkylation of 3-substituted-phthalides



3. Enantioselective alkylation of 3-substituted-phthalides

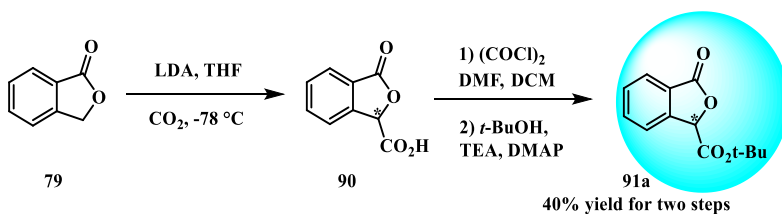
3.1 Enantioselective alkylation of 3-carboxylic-t-Bu-ester-phthalides

3.1.1 Specific objectives

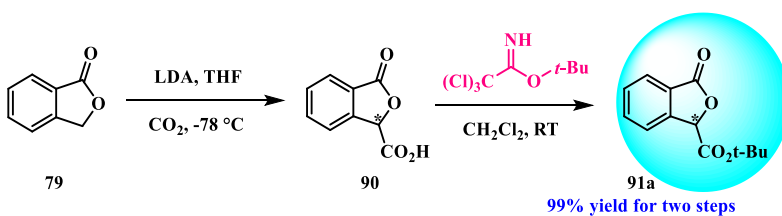
As reported in the literature, 3-carboxylic-ester-phthalides are sufficiently activated substrates to react with different electrophiles in the presence of chiral base organocatalysts enabling the asymmetric synthesis of diverse 3,3-disubstituted phthalides. High enantio- and diastereoselectivities have been achieved with Michael acceptors,^{94,95} imines⁹² and Morita-Baylis-Hillman (MBH) carbonates,⁹¹ but simple alkylating agents have never been investigated to date. The opportunity to introduce an alkyl moiety at C-3 site of the lactone ring in stereoselective manner is attracting and would broaden the range of structures accessible with the 3,3-disubstituted phthalide framework. Phase transfer catalysis conditions have shown to be well-suited in catalyzing asymmetric alkylation reactions and were therefore considered as optimal candidates for this transformation. In particular, chiral quaternary ammonium salts have been chosen as phase transfer catalysts thanks to their well-known efficiency, wide range of applications and commercial availability. The main objective of this research has been the screening of reaction conditions and their application to different alkylating agents and variously substituted phthalides in order to synthesize new interesting chiral enantioenriched 3-alkyl-substituted phthalides.

3.1.2 Results and Discussion

To begin the research study, 3-carboxylic-*t*-Bu-ester-phthalide was chosen as the pro-nucleophilic substrate and benzyl bromide as the alkylating agent. Although a two-steps strategy for the synthesis of 3-carboxylic-*t*-Bu-ester-phthalide has already been reported in the literature (**Scheme 3.1**),⁹¹ during this investigation a more efficient and reliable route for the synthesis of this substrate was developed (**Scheme 3.2**). In detail, in the first step the 3-carboxylic-phthalide acid **90** was synthesized, as previously reported, by carboxylation of phthalide anion, and then it was treated in presence of *tert*-Butyl 2,2,2-trichloroacetimidate obtaining the desired ester **91** with excellent yield (99% for two steps).



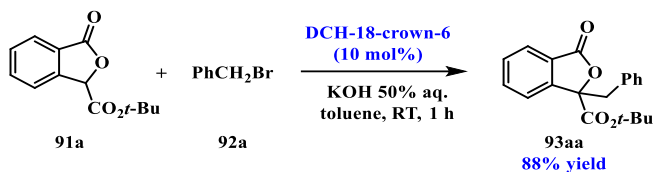
Scheme 3.1 Previously reported procedure for the synthesis of 3-carboxylic-*t*-Bu-ester-phthalide



Scheme 3.2 New strategy for the synthesis of 3-carboxylic-*t*-Bu-ester-phthalide

To assess the feasibility of the phase transfer alkylation, a preliminary test was carried out with 3-carboxylic-*t*-Bu-ester-phthalide **91** and benzyl

bromide **92a** in the presence of DCH-18-crown-6 **77a** and KOH 50% aqueous. The crown ether **77a** proved capable to effectively catalyze the reaction forming the racemic alkylated product **93aa** with 88% yield after 1 h at room temperature (**Scheme 3.3**).



Scheme 3.3 Racemic alkylation reaction of 3-carboxylic-*t*-Bu-ester-phthalide promoted by DCH-18-crown-6 and KOH 50% aq.

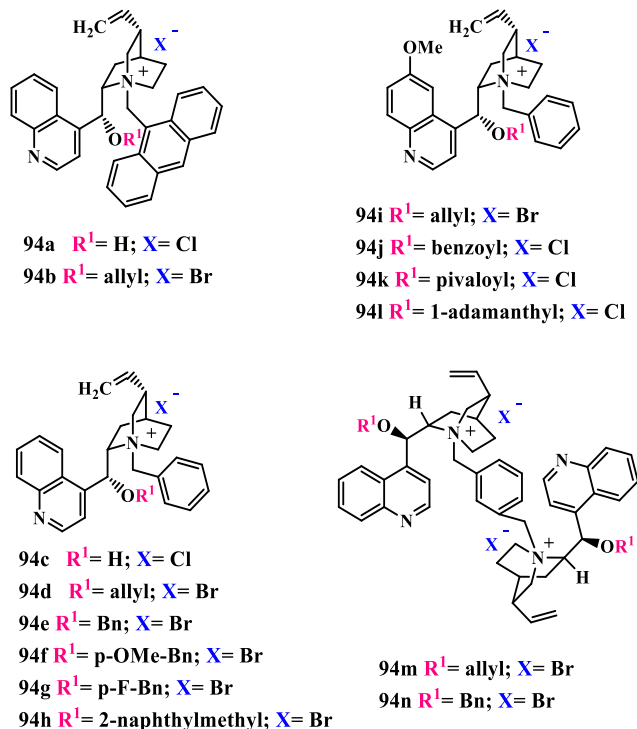
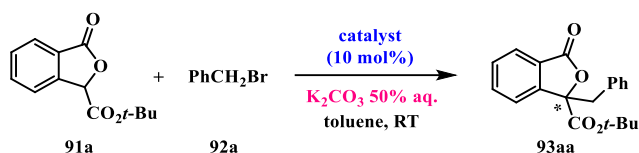


Figure 3.1 Investigated Cinchona alkaloid-derived quaternary ammonium salts **94**

The enantioselective version was thus investigated in the presence of K_2CO_3 50% aq. as the inorganic base and a wide variety of chiral Cinchona alkaloid-derived quaternary ammonium salts **94a-n** characterized by different groups both at quinuclidine nitrogen and on C9-hydroxyl functionality (**Figure 3.1**).



entry	catalyst	t (h)	ee ^b
1	94a	7	22 (S)
2	94b	18	2 (S)
3	94c	24	24 (R)
4	94d	24	16 (R)
5	94e	6	30 (R)
6	94f	24	18 (R)
7	94g	24	2 (R)
8	94h	24	14 (R)
9	94i	24	4 (R)
10	94j	24	6 (R)
11	19m	3	22 (S)
12	20n	3	26 (S)

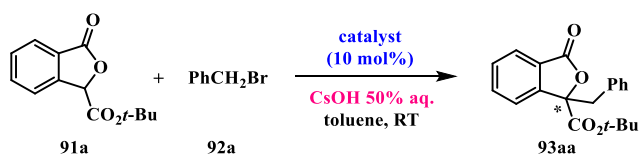
^aReactions were performed with **91a** (0.050 mmol), **92a** (0.060 mmol), catalyst (0.005 mmol), K_2CO_3 aqueous 50% (0.3 mL) in toluene (0.5 mL), unless otherwise noted. ^bDetermined by HPLC analysis of the pure product.

Table 3.1 Screening of phase transfer catalysts in the presence of K_2CO_3 aq. 50%^a

As reported in **Table 3.1**, only low enantiomeric excesses (up to 30%) were achieved in the preliminary tests performed in toluene at room temperature. In addition, even though full conversions were obtained in all cases, the formation of the desired product was always accompanied by a considerable

amount of an unidentified side-product. The further purifications by flash chromatography did not provide the product in pure form, and it was therefore not possible to determine the isolated yields.

To overcome this problem, aqueous CsOH 50% aqueous was used as the base in the following asymmetric alkylations tests. Under these conditions, the above mentioned by-product was not formed, allowing the isolation of the product in pure form with all the catalysts, in moderate to high yields (Table 3.2). However, the enantioselectivities achieved were still low: the best result (30% ee) was obtained with the *N*-benzyl-*O*-benzyl cinchonidinium salt **94e** in 4 hours (entry 5).



entry	catalyst	t (h)	yield (%) ^b	ee ^c
1	94a	5	63	22 (<i>S</i>)
2	94b	3	87	22 (<i>S</i>)
3	94c	5	25	20 (<i>R</i>)
4	94d	18	88	4 (<i>R</i>)
5	94e	4	45	30 (<i>R</i>)
6	94f	24	58	8 (<i>R</i>)
7	94g	2	40	14 (<i>R</i>)
8	94h	24	75	14 (<i>R</i>)
9	94m	24	88	24 (<i>S</i>)
10	94n	4	37	16 (<i>S</i>)

^aReactions were performed with **91a** (0.050 mmol), **92a** (0.060 mmol), catalyst (0.005 mmol), CsOH aqueous 50% (0.3 mL) in toluene (0.5 mL), unless otherwise noted. ^bYield of isolated product. ^cDetermined by HPLC analysis of the pure product.

Table 3.2 Screening of phase transfer catalysts in the presence of CsOH 50% aq. ^a

Since the presence of a 9-benzyloxy group induced an enantioselectivity improvement, novel Cinchonidinium salts **94o-s** with variously *N*-arylmethyl groups were synthesized and investigated in order to evaluate the steric and electronic effects on the stereocontrol (**Figure 3.2**).

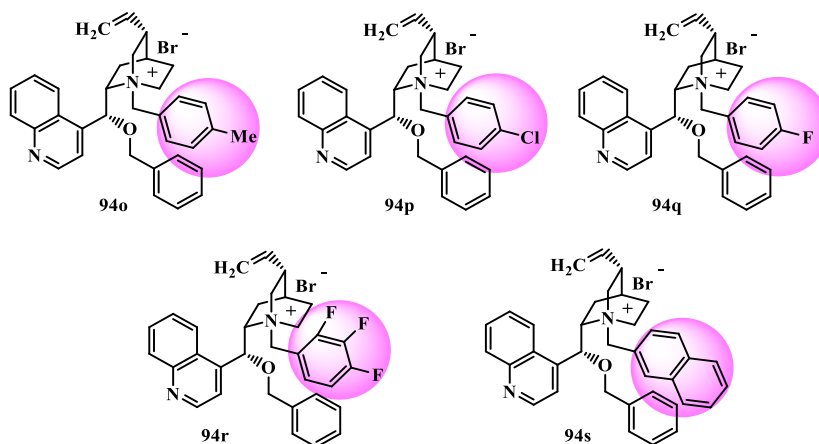
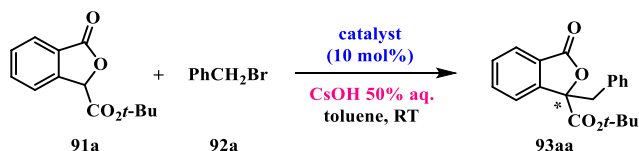


Figure 3.2 Novel Cinchonidinium salts variously substituted

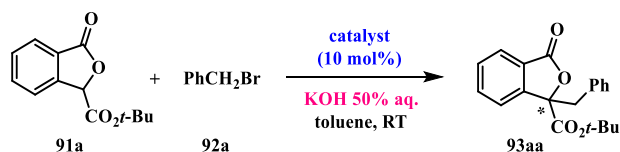


entry	catalyst	t (min)	yield (%) ^b	ee ^c
1	94o	30	60	18 (<i>R</i>)
2	94p	30	64	20 (<i>R</i>)
3	94q	30	58	20 (<i>R</i>)
4	94s	30	80	28 (<i>R</i>)

^aReactions were performed with **91a** (0.050 mmol), **92a** (0.060 mmol), catalyst (0.005 mmol), CsOH aqueous 50% (0.3 mL) in toluene (0.5 mL), unless otherwise noted. ^bYield of isolated product. ^cDetermined by HPLC analysis of the pure product.

Table 3.3 Alkylation of 3-carboxylic-*t*-Bu-ester-phthalide catalyzed by **94o-q,s**

As reported in **Table 3.3**, shorter reaction times were observed with all the new catalysts tested, but no increase of the enantioselectivity was achieved. Thus, further screening of phase transfer catalysts was conducted with 50% aqueous KOH as summarized in **Table 3.4**. The pure product was achieved with good to excellent yields in short times but, unfortunately, still low enantioselectivities were observed.



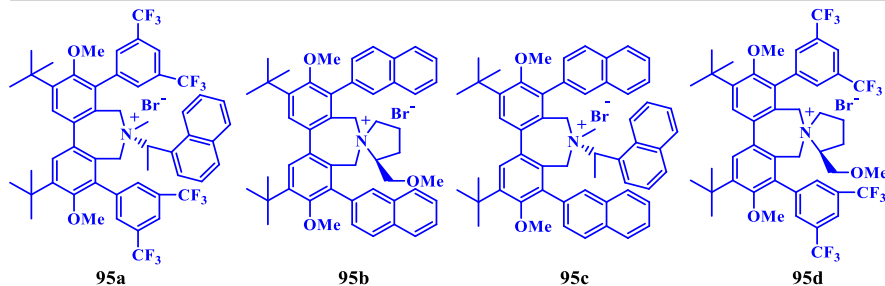
entry	catalyst	t (min)	yield (%) ^b	ee ^c
1	94a	30	99	20 (<i>S</i>)
2	94b	60	87	22 (<i>S</i>)
3	94c	180	41	2 (<i>S</i>)
4	94d	60	52	6 (<i>S</i>)
5	94e	30	50	18 (<i>R</i>)
6	95g	30	63	22 (<i>R</i>)
7	94r	60	70	24 (<i>S</i>)

^aReactions were performed with **91a** (0.005 mmol), **92a** (0.060 mmol), catalyst (0.005 mmol), KOH aqueous 50% (0.3 mL) in toluene (0.5 mL), unless otherwise noted. ^bYield of isolated product. ^cDetermined by HPLC analysis of the pure product.

Table 3.4 Screening of phase transfer catalysts in presence of KOH aq. 50%^a

The above experiments showed that chiral Cinchona alkaloid derivatives efficiently catalyze the alkylation reaction, but with poor asymmetric induction.

In this regard, more rigid ammonium salts characterized by biphenyl moieties with chiral exocyclic appendages, known as Lygo's phase transfer catalysts, were investigated under various base conditions (**Table 3.5**).



entry	catalyst	base aq. 50%	T (°C)	t (h)	yield (%) ^b	ee (%) ^c
1	95a	K ₂ CO ₃	RT	60	not determinate	46 (<i>S</i>)
2	95a	CsOH	RT	168	75	28 (<i>S</i>)
3	95b	CsOH	RT	32	67	20 (<i>S</i>)
4	95c	CsOH	RT	120	26	2 (<i>S</i>)
5	95d	CsOH	RT	36	64	18 (<i>S</i>)
6	95a	KOH	RT	1	70	34 (<i>S</i>)
7	95b	KOH	RT	1	64	16 (<i>S</i>)
8	95c	KOH	RT	19	70	4 (<i>S</i>)
9	95d	KOH	RT	1	50	12 (<i>S</i>)
10	95a	KOH	0	1	82	34 (<i>S</i>)
11	95a	KOH	-20	2	74	32 (<i>S</i>)

^aReactions were performed with **91a** (0.050 mmol), **92a** (0.060 mmol), catalyst (0.005 mmol), base aqueous 50% (0.3 mL) in toluene (0.5 mL), unless otherwise noted. ^bYield of isolated product. ^cDetermined by HPLC analysis of the pure product.

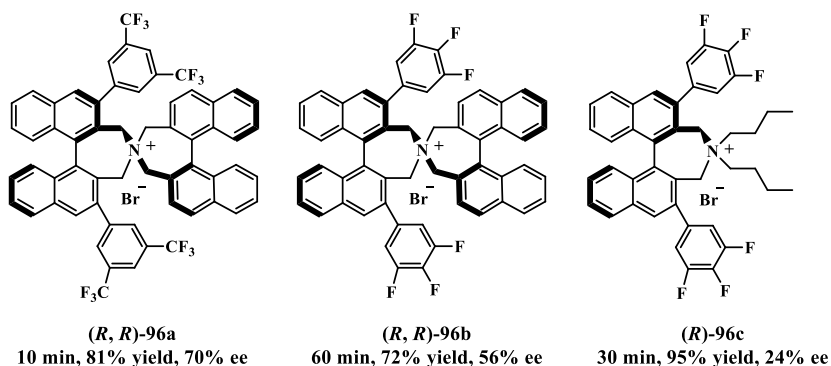
Table 3.5 Screening of Lygo's catalysts^a

As described in **Table 3.5**, the asymmetric alkylations promoted by Lygo's catalysts **95a-d** required long reaction times with both K₂CO₃ and CsOH aqueous 50%, allowing full conversions in 32-168 hours (**entries 1-5**). With KOH aq. 50%, faster conversions were achieved forming the product **93aa** with moderate to high yields after just 1 hour with **95a**, **95b** and **95d** catalysts

and after 19 hours with **95c**. However, the values of enantioselectivities were generally comparable to those obtained with cinchona alkaloid-derived salts; a slight increase up to 34% ee was reached with catalyst **95a** in KOH aq. 50% (**entry 6**). The best enantioselectivity was achieved with **95a** and K₂CO₃ 50% aq. (46 % ee, **entry 1**), but again the presence of the above mentioned inseparable by-product did not allow to obtain the pure isolated product.

The effect of temperature was thus investigated. The alkylation catalyzed by **95a** in the presence of KOH aq. 50% at 0 °C led to the product with a higher yield but without any improvement of the enantiomeric excess, whereas at -20 °C slightly lower enantioselectivity was detected.

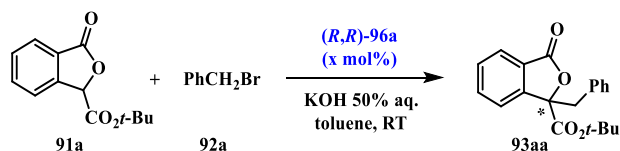
Finally, we moved to consider C₂-symmetric bis(binaphthyl)ammonium salts developed by Maruoka, which are well-known efficient phase transfer catalysts widely employed for enantioselective alkylation reactions and other transformation of pro-nucleophilic species. Since Maruoka's salts are more expensive than Cinchona alkaloid-derivatives but generally well-performing even in very low amounts, we decided to carry out experiments under the usual conditions (KOH aq. 50%, toluene, RT) but employing 5 mol % of catalyst loading. Pleasingly, as showed in **Scheme 3.4**, better enantiomeric excesses were achieved this time.



Scheme 3.4 Alkylation of 3-carboxylic-*t*-Bu-ester-phthalide catalyzed by Maruoka's catalysts

The Maruoka catalyst **96a** effectively promoted the benzylation of 3-carboxylic-*t*-Bu-ester-phthalide in only 10 minutes affording the desired product **93aa** with 70 % ee and high yield (81 %). Also the catalysts **96b** and **96c** led to the product in short time and good to excellent yields, but the enantiomeric excesses were lower compared to catalyst **96a**. For this reason, (*R,R*)-**96a** was chosen for further screening of the reaction conditions.

The alkylation was then performed using different catalyst loadings (Table 3.6). 2 mol % of (*R,R*)-**96a** was enough to catalyze the asymmetric alkylation, generating the 3,3-disubstituted phthalide **93aa** with good yield in short time, although with significantly lower enantioselectivity (entry 1). Using 10 mol%, an increase of the enantioselectivity up to 74 % was achieved (entry 3). However, considering the only slight improvement, 5 mol% was confirmed as the preferred catalyst loading. Moreover, an experiment was carried out using 5 mol % of catalyst at -20 °C (Table 3.6, entry 4), but the same enantioselectivity and a lower yield were observed.

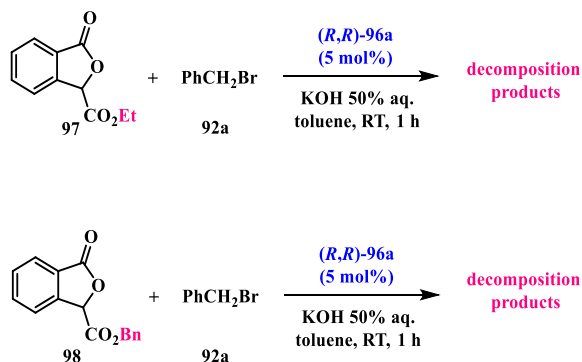


entry	Cat mol%	t (min)	yield (%) ^b	ee ^c
1	2	15	62	43 (<i>R</i>)
2	5	10	81	70 (<i>R</i>)
3	10	10	81	74 (<i>R</i>)
4 ^d	5	10	66	70 (<i>R</i>)

^aReactions were performed with **91a** (0.05 mmol), **92a** (0.06 mmol), Maruoka catalyst **96a** (*x* mmol), KOH aqueous 50% (0.3 mL) in toluene (0.5 mL), at room temperature, unless otherwise noted. ^bYield of isolated product. ^cDetermined by HPLC analysis of the pure product. ^dReaction performed at -20 °C.

Table 3.6 Screening of Maruoka's catalysts loading^a

Since the enantioselectivity of the reaction might in principle be affected by the type of activating ester group at C-3 site of the lactone ring, 3-carboxylic-ethyl-ester-phthalide **97** and 3-carboxylic-benzyl-ester-phthalide **98** were synthesized and investigated as pro-nucleophilic substrates. However, as reported in **Scheme 3.5**, carrying out the asymmetric alkylation with benzyl bromide at room temperature, in toluene, in the presence of KOH 50% aqueous and 5% mol of **96a**, only degradation side-products were detected after 1 hour with both phthalides. Probably, base-promoted hydrolysis takes place due to the increased susceptibility of the ethyl and benzyl ester groups.

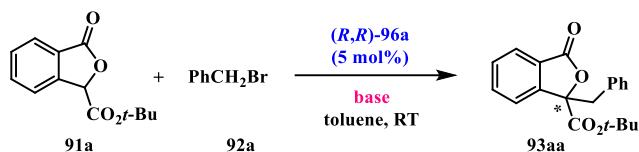


Scheme 3.5 *Asymmetric alkylation of 3-carboxylic-ethyl-ester-phthalide and 3-carboxylic-benzyl-ester-phthalide*

Therefore, holding 3-carboxylic-*t*-butyl-ester-phthalide **91a** as the model substrate, different bases were next screened as described in **Table 3.7**.

High enantiomeric ratios were achieved with all the aqueous bases investigated affording the desired product with enantiomeric excesses up to 80%. Cs_2CO_3 aq. 50% showed to be the best base screened, in fact, the product was obtained with the highest yield (82%) and enantioselectivity (80% ee) although with slightly longer reaction time compared to KOH aq. 50% (**entry 3**). Moderate and low yields were obtained with K_2CO_3 aq. 50% and K_3PO_4 aq. 50% respectively due to the formation of several side-

products in the reaction mixtures (**entries 4 and 5**). On the contrary, when solid bases were investigated, no traces of the desired alkyl-phthalide **93aa** were detected but only several decomposition products. An exception, solid CsOH (5.0 eq.) was able to promote the asymmetric benzylation of 3-carboxylic-*t*-Bu-ester-phthalide generating the product with high yield but with low enantioselectivity after very long reaction time (**entry 6**).



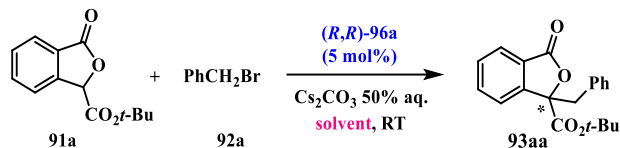
entry	base	t	yield (%) ^b	ee ^c
1	KOH aq. 50%	10 min	81	70 (<i>R</i>)
2	CsOH aq. 50%	1 h	65	78 (<i>R</i>)
3	Cs ₂ CO ₃ aq. 50%	4 h	82	80 (<i>R</i>)
4	K ₂ CO ₃ aq. 50%	78 h	40	78 (<i>R</i>)
5	K ₃ PO ₄ aq. 50%	78 h	15	70 (<i>R</i>)
6	CsOH (s)	168 h	82	26 (<i>R</i>)
7	KOH (s)	24 h	–	–
8 ^d	KOH (s)	24 h	–	–
9	Cs ₂ CO ₃ (s)	24 h	–	–

^aReactions were performed with **91a** (0.05 mmol), **92a** (0.06 mmol), Maruoka catalyst **96a** (5 mol%), base aqueous 50% (0.3 mL) or solid base (5 eq.) in toluene (0.5 mL), at room temperature, unless otherwise noted. ^bYield of isolated product. ^cDetermined by HPLC analysis of the pure product. ^dReaction performed at -20 °C. ^eReaction performed with 2.0 eq. of KOH solid.

Table 3.7 Screening of bases^a

Therefore, the subsequent solvent screening was carried out in the presence of Cs₂CO₃ aq. 50%, at room temperature, using 5 mol% of Maruoka catalyst **96a**. As reported in **Table 3.8**, good to high enantioselectivities and moderate

to high yields were achieved in short reaction times with all the solvents surveyed.



entry	solvent	t (h)	yield (%) ^b	ee ^c
1	CH_2Cl_2	72	73	60 (<i>R</i>)
2	Et_2O	3	78	73 (<i>R</i>)
3	MTBE	6	62	71 (<i>R</i>)
4	toluene	4	82	80 (<i>R</i>)
5	Mesitylene	4	73	76 (<i>R</i>)
6	<i>p</i> -xylene	4	83	80 (<i>R</i>)
7	<i>o</i> -xylene	4	80	80 (<i>R</i>)
8	chlorobenzene	20	75	72 (<i>R</i>)
9	fluorobenzene	4	63	60 (<i>R</i>)
10 ^d	toluene	20	88	78 (<i>R</i>)
11 ^e	toluene	20	–	–

^aReactions were performed with **1a** (0.05 mmol), **2a** (0.06 mmol), Maruoka catalyst **45** (5 mol%), Cs_2CO_3 aqueous 50% (0.3 mL) in the solvent (0.5 mL), at room temperature, unless otherwise noted. ^bYield of isolated product. ^cDetermined by HPLC analysis of the pure product. ^dReaction performed at 0 °C. ^eReaction performed at -20 °C.

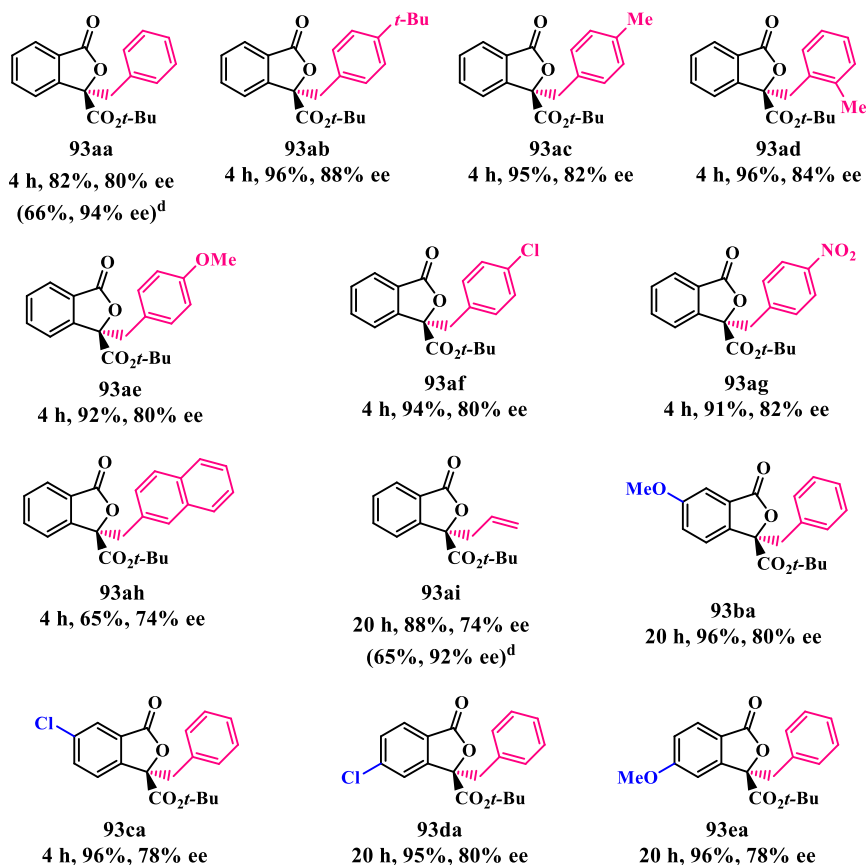
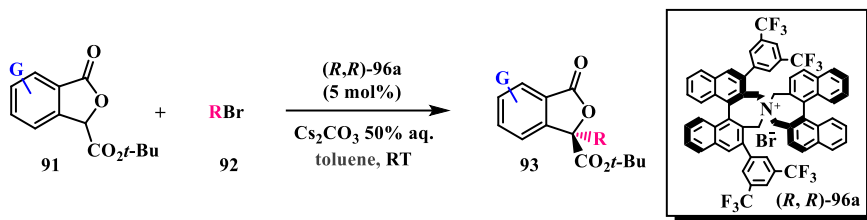
Table 3.8 Screening of solvents^a

In particular, with ethereal solvents such as Et_2O and MTBE (**entries 2** and **3**), the desired product was obtained with good enantiomeric ratios and yields after 3 and 6 hours respectively. Employing CH_2Cl_2 , longer reaction time was, instead, necessary to achieve full conversion, affording the 3,3-disubstituted-phthalide with 60% ee (**entry 1**). Aromatic solvents showed to be the most suitable reaction media to perform the asymmetric alkylation of 3-carboxylic-*t*-Bu-ester-phthalide, resulting in uniformly high yields and

enantioselectivities (**entries 4-8**). Although similar results were achieved with *p*-xylene, *o*-xylene and toluene, the latter was chosen as the best reaction solvent.

Next, the temperature effect was also investigated. Performing the asymmetric alkylation in toluene at 0 °C (**Table 3.8, entry 10**) a slight decrease of the enantioselectivity was observed although with a slightly higher yield, whereas only by-products were detected at -20 °C (**Table 3.8, entry 11**).

Thus, with the best reaction conditions in hand (5 mol % of catalyst **96a**, Cs₂CO₃ 50% aqueous, toluene, room temperature), the versatility of the phase transfer asymmetric alkylation was assessed with both different alkylating agents and variously functionalized 3-carboxylic-*t*-Bu-ester-phthalides. As it can be seen in **Scheme 3.6**, both electron-withdrawing and electron-donating *para*-substituents of benzyl bromide were well-tolerated in the asymmetric alkylation of 3-carboxylic-*t*-Bu-ester-phthalide affording the corresponding chiral products in high to excellent yields and high enantiomeric excesses after 4 hours. In particular, the product **93ab** arising from alkylation with *p*-*t*-Bu-benzyl bromide **92b** was obtained with the highest enantioselectivity (88% ee) and very high isolated yield. *o*-methyl substituted benzyl bromide was also used generating the 3,3-disubstituted phthalide **93ad** with excellent yield (96%) and high enantioselectivity (84% ee). A slight decrease of the enantiomeric excess was instead observed employing the more sterically hindered naphthylmethyl bromide, resulting in 74% ee and a moderate yield (65 %) due to the formation of several side-products. Longer reaction times (20 hours) were required to achieve full conversion with allyl bromide. The corresponding 3-allylated product **93ai** was however obtained with an interesting enantiomeric excess (74 % ee) and high yield (88%).



^aReactions were performed with **91a** (0.10 mmol), **92a** (0.12 mmol), Maruoka catalyst **96a** (5 mol%), Cs_2CO_3 aqueous 50% (0.6 mL) in toluene (1.0 mL), at room temperature, unless otherwise noted. ^bYield of isolated product. ^cEnantiomeric excesses were determined by HPLC analysis of the pure products. ^dYield and enantiomeric excess determined after crystallization.

Scheme 3.6 Scope of the asymmetric alkylation reaction^{a-c}

Finally, variously substituted phthalides **91b-e** with methoxy and chlorine groups in 5 or 6 positions were employed in order to examine the effect of both electron-releasing and electron-withdrawing functionalities on the course of the asymmetric alkylation. As expected, the 6-methoxy group (product **93ba**) induced a rate reduction likely because the phthalide anion formed under base conditions is poorly stabilized by the electronic effect. Compared to the phthalide **91a**, the benzylation required indeed longer reaction time (20 hours) to afford the product. However, high enantioselectivity and excellent yield were obtained. By introducing an electron-withdrawing group, such as chlorine, at C-6 of the phthalide aromatic ring (**91c**) full conversion was accomplished in 4 h. In this case, the corresponding chloro-substituted product (**93ca**) was isolated with 76% of yield and 72% of enantiomeric excess. High yields and enantioselectivities were also achieved with 5-chloro (**91d**) and 5-methoxy (**91e**) substrates. Moreover, it is important to note that the enantiomeric excesses of **93aa** and **93ai** were further improved after a facile crystallization process. In fact, an efficient gradual cooling crystallization in hexane led to a further enantioenrichment of the products **93aa** and **93ai** up to 94% and 92% ee respectively in good overall yields (**93aa**: 66%; **93ai**: 65%). The absolute (*R*) configuration of the chiral product **93aa** was, then, determined by X-ray diffraction analysis (**Figure 3.3**).

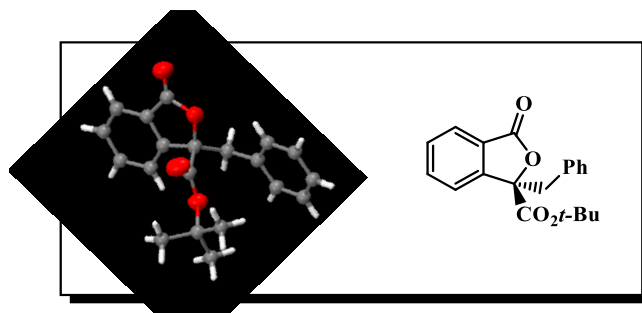


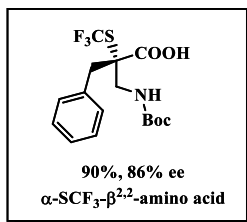
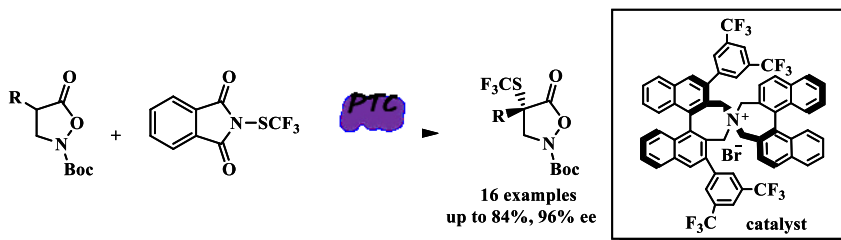
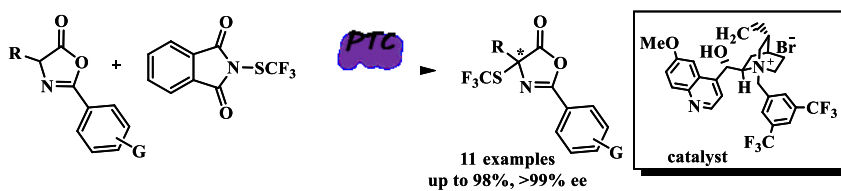
Figure 3.3 Single-crystal X-ray structure of (*R*)-**93aa**

3.1.3 Conclusions

In conclusion, the first asymmetric alkylation of activated phthalides has been developed. Maruoka's chiral quaternary ammonium salts have demonstrated to be highly efficient catalysts to promote the asymmetric alkylation of 3-carboxylic-*t*-Bu-ester-phthalides with benzyl and allyl bromides with good to high enantioselectivities and good to excellent yields. In addition, further enantioenrichment of the products has been easily obtained by a crystallization process. The absolute configuration of the chiral product was determined by X-ray diffraction analysis. This methodology opens up a new route to obtain previously undescribed 3,3-disubstituted alkyl phthalides in high enantiomeric excesses. It is important to emphasize the great synthetic value of these novel class of chiral products. It could be anticipated their facile conversion into chiral bioactive 3,3-dialkyl phthalides through the transformation of the ester functionality.

Chapter 4

Novel asymmetric trifluoromethylthiolation reactions



4. Novel asymmetric trifluoromethylthiolation reactions

4.1 Thiofluorinated compounds

Over the last recent years, the development of new strategies aimed at the incorporation of fluorine atoms and fluoroalkyl groups into organic molecules has emerged as one of the most trending topics in organic synthesis with important applications in the agrochemical, pharmaceutical and medicinal chemistry field.¹¹⁰

Thanks to their peculiar characteristics, fluorinated motifs strongly affect the biological and physicochemical properties of organic compounds. In particular, it has been demonstrated that molecules containing the trifluoromethylthio group (SCF₃) show a remarkably improved lipophilicity which led to the design of pharmaceuticals with outstanding bioavailability and transmembrane permeability.¹¹¹ The contribution of a given substituent to the molecule lipophilicity can be measured through the Hansch's hydrophobic parameter (π), defined by the following expression:¹¹²

$$\pi_S = \log P_{\text{substituted molecule}} - \log P_{\text{molecule}}$$

The π parameter of a substituent is defined by the difference between the lipophilicity of the substituted molecule and that of the unsubstituted

¹¹⁰ For selected examples see: a) Richardson, R.; Expert Opin. Drug Dis., 2016, 11, 983-999; b) R. Filler, R. Saha, *Future Med. Chem.*, **2009**, 1, 777-791; c) B. E. Smart, *J. Fluorine Chem.*, **2001**, 109, 3-11; d) M. Shimizu, T. Hiyama, *Angew. Chem. Int. Ed.*, **2005**, 44, 214-231.

¹¹¹ For selected examples see: a) M. A. Hardy, H. Chachignon, D. Cahard, *Asian J. Org. Chem.*, **2019**, 8, 591-609; b) X. Yang, T. Wu, R. J. Phipps, F. D. Toste, *Chem. Rev.*, **2015**, 115, 826-870; c) S. Rossi, A. Puglisi, L. Raimondi, M. Benaglia, *ChemCatChem*, **2018**, 10, 2717-2733; d) S. Barata-Vallejo, S. Bonesi, A. Postigo, *Org. Biomol. Chem.*, **2016**, 14, 7150-7182; e) X.-H. Xu, K. Matsuzaki, N. Shibata, *Chem. Rev.*, **2015**, 115, 731-764.

¹¹² a) A. Leo, C. Hansch, D. Elkins, *Chem. Rev.*, **1971**, 71, 525-616; b) C. Hansch, A. Leo, S. H. Unger, K. H. Kim, D. Nikaitani, E. J. Lien, *J. Med. Chem.*, **1973**, 16, 1207-1216; c) A. J. Leo, *Method. Enzymol.*, **1991**, 202, 544-591.

molecule, where P is the partition coefficient between two solvents (typically *n*-octanol/water). Greater is the π parameter and higher is the lipophilicity. The SCF₃ moiety provides the highest π value (1.44) among those reported in **Table 4.1**, confirming its strong influence on the lipophilic properties of organic molecules.

Substituent	π	Substituent	π
F	0.14	OCH ₃	-0.02
Cl	0.71	OCF ₃	1.04
NO ₂	-0.27	SCH ₃	0.61
CH ₃	0.56	SCF ₃	1.44
CF ₃	0.88	SO ₂ CH ₃	-1.63
OH	-0.67	SO ₃ CF ₃	0.55

Table 4.1 *Hansch's parameters of some substituents*

Several marketed drugs with potent pharmacological activity contain indeed the SCF₃ group. Examples are Toltrazuril and Monepantel used in veterinary medicine,¹¹³ Tiflorex¹¹⁴ sold as an anorectic agent and Cefazaflur¹¹⁵ a parenteral cephalosporin. In addition, Trifluoromethionine¹¹⁶ has emerged as a promising drug for amebiasis (**Figure 4.1**).

¹¹³ a) P. Laczay, G. Vörös, G. Semjén, *Int. J. Parasitol.*, **1995**, 25, 753-756; b) P. Pommier, A. Keïta, S. Wessel-Robert, B. Dellac, H. C. Mundt, *Rev. Med. Vet.*, **2003**, 154, 41-46.

¹¹⁴ T. Silverstone, J. Fincham, J. Br. Plumley, *J. Clin. Pharmacol.*, **1979**, 7, 353-356.

¹¹⁵ G. W. Counts, D. Gregory, D. Zeleznik, M. Turck, *Antimicrob. Agents Chemother.*, **1977**, 11, 708-711; b)

¹¹⁶ a) G. H. Coombs, J. C. Mottram, *Antimicrob. Agents Chemother.*, **2001**, 45, 1743-1745; b) M. Tokoro, T. Asai, S. Kobayashi, T. Takeuchi, T. Nozaki, *J. Biol. Chem.*, **2003**, 278, 42717-42727.

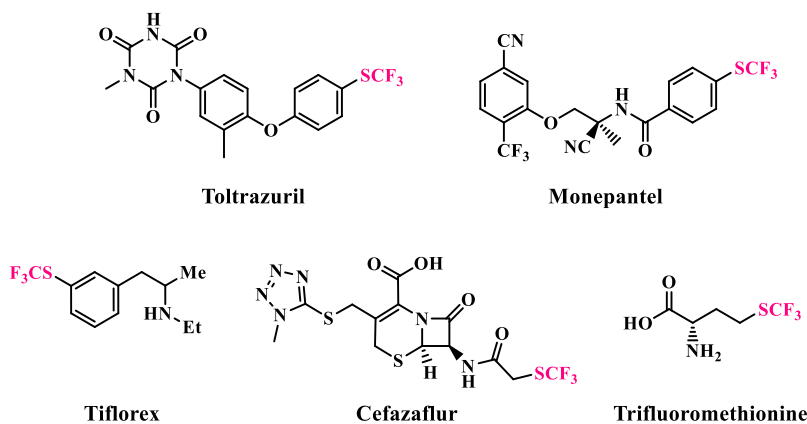
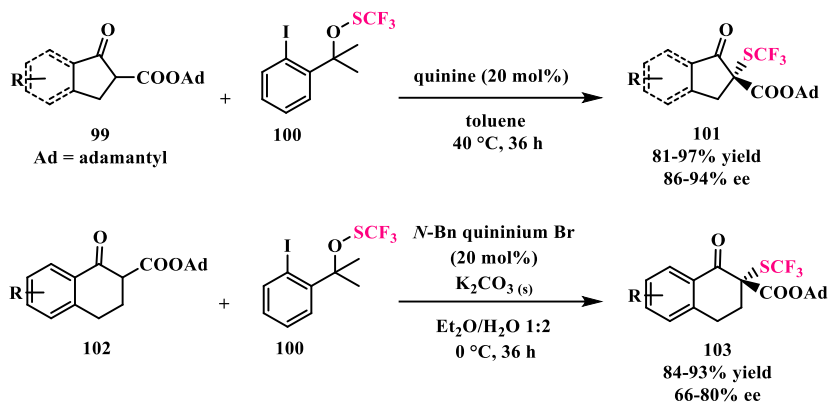


Figure 4.1 Medicinal compounds containing the SCF₃ functionality

However, despite the known great potential, the majority of the developed synthetic routes focus on the construction of aromatic and heteroaromatic fluorinated molecules. Therefore, in recent years, great interest has been addressed to the development of new synthetic methods for the direct installation of SCF₃ moiety on C(sp₃) centers. In particular, the asymmetric introduction of trifluoromethylthio group at the α -C(sp₃) of carbonyl compounds has attracted broad interest considered the widespread presence of carbonyl derivatives in biologically active molecules. Therefore, enantioenriched trifluoromethylthiolated carbonyl derivatives have high application potential in medicinal chemistry. To date, stereoselective methodologies fulfilling this objective cover the functionalization of highly activated carbonyl compounds such as β -keto esters under organocatalyzed reaction conditions.

The first stereoselective Cinchona alkaloid-catalyzed trifluoromethylthiolation of indanone **99** and tetralone **102** β -ketoesters was

reported, in 2013, by Shen's research group using a trifluoromethylthiolated hypervalent iodine reagent **100** as an electrophilic SCF₃ source.¹¹⁷



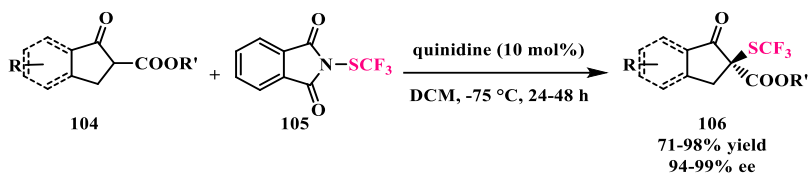
Scheme 4.1 Asymmetric trifluoromethylthiolation of indanone- and tetralone- β -ketoesters reported by Shen

As shown in **Scheme 4.1**, SCF₃-indanone derivatives **101** were obtained with good to high enantiomeric excesses in the presence of catalytic amounts of quinine, while better results in the synthesis of enantioenriched SCF₃-tetralone compounds **103** were obtained with the phase transfer catalyst *N*-Bn quinidinium bromide.

At the same time, Rueping and co-workers reported the highly enantioselective organocatalyzed trifluoromethylthiolation of indanone β -ketoester derivatives **104** using *N*-trifluoromethylthiophthalimide **105** as the electrophilic SCF₃-source (**Scheme 4.2**).¹¹⁸

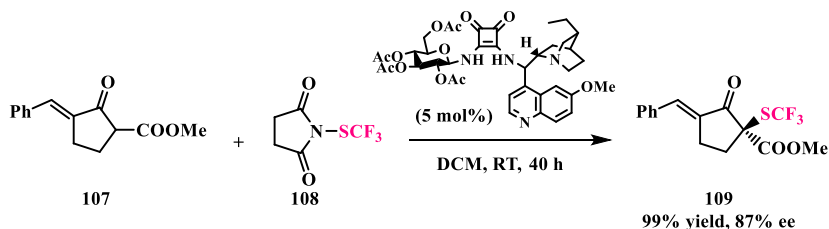
¹¹⁷ X. Wang, T. Yang, X. Cheng, Q. Shen, *Angew. Chem. Int. Ed.*, **2013**, *52*, 12860–12864; *Angew. Chem.*, **2013**, *125*, 13098–13102.

¹¹⁸ T. Bootwicha, X. Liu, R. Pluta, I. Atodiresei, M. Rueping, *Angew. Chem. Int. Ed.*, **2013**, *52*, 12856–12859; *Angew. Chem.*, **2013**, *125*, 13093–13097.



Scheme 4.2 Asymmetric trifluoromethylthiolation of indanone- β -ketoesters reported by Rueping

In 2017, the research group of Du developed the asymmetric trifluoromethylthiolation of cycloalkenone β -ketoesters **107** with *N*-trifluoromethylthiosuccinimide **108** as SCF_3 source. (**Scheme 4.3**).¹¹⁹



Scheme 4.3 Asymmetric trifluoromethylthiolation of cycloalkenone β -ketoester by Du

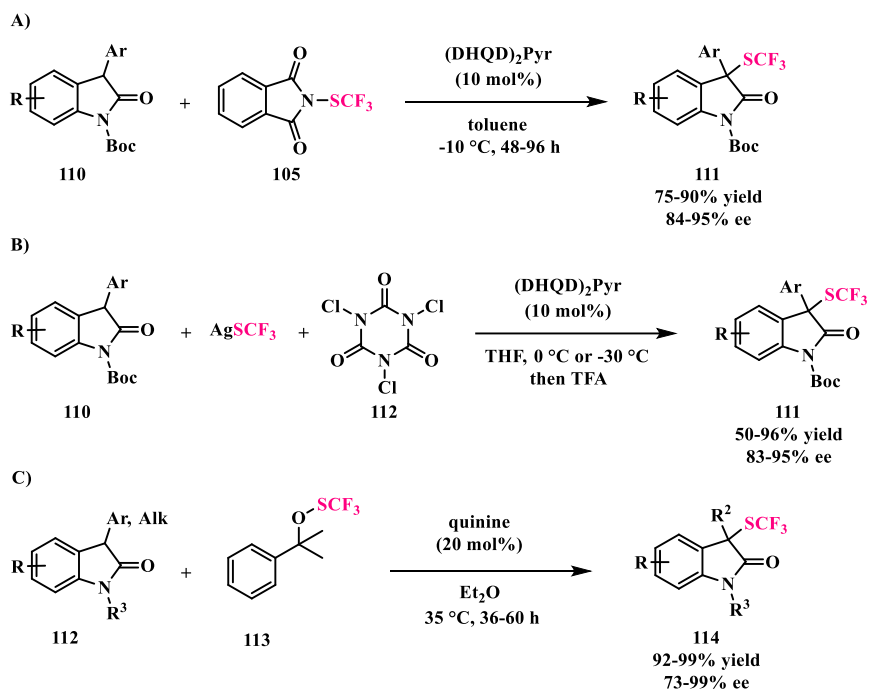
Moreover, oxindoles were also investigated in the organocatalyzed asymmetric trifluoromethylthiolation. The Rueping's research group reported the first example in 2014 using a dimeric Chineona alkaloid-derivative $(\text{DHQD})_2\text{Pyr}$ to catalyze the stereoselective introduction of SCF_3 group at the α -position of *N*-Boc protected 3-aryl-oxindoles **110** (**Scheme 4.4 A**).¹²⁰ Similar products were achieved in the same year by Tan and co-workers using a reactive electrophilic SCF_3 source generated *in situ* from AgSCF_3 and trichloroisocyanuric acid **112** (**Scheme 4.4 B**).¹²¹ In addition,

¹¹⁹ B.-L. Zhao, D.-M. Du, *Org. Lett.*, **2017**, *19*, 1036–1039.

¹²⁰ M. Rueping, X. Liu, T. Bootwicha, R. Pluta, C. Merckens, *Chem. Commun.*, **2014**, *50*, 2508–2511.

¹²¹ X. L. Zhu, J. H. Xu, D. J. Cheng, L. J. Zhao, X. Y. Liu, B. Tan, *Org. Lett.*, **2014**, *16*, 2192–2195.

the asymmetric trifluoromethylthiolation was extended for the first time to 3-alkyl-oxindoles by Shen's group affording the desired functionalized products **114** with excellent results (Scheme 4.4 C).¹²²

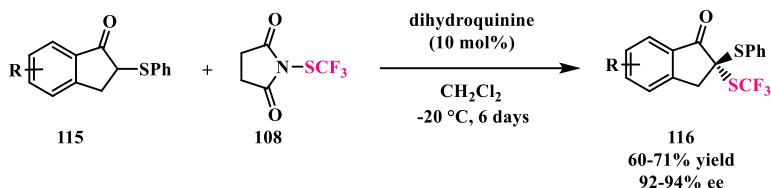


Scheme 4.4 Asymmetric trifluoromethylthiolation of oxindoles

Next, Zhou's research group studied the synthesis of SCF₃-thioketals through the asymmetric trifluoromethylthiolation of α -thioindanones **115** with *N*-SCF₃ succinimide, achieving high enantioselectivities, albeit with moderate yields after long reaction times (Scheme 4.5).¹²³

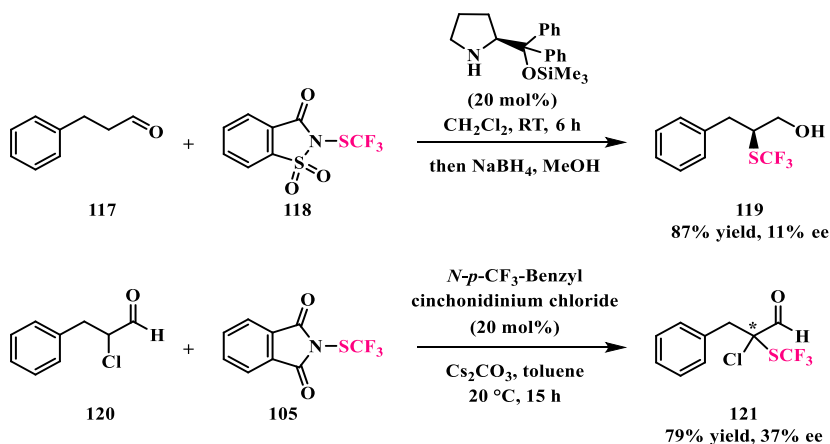
¹²² T. Yang, Q. Shen, L. Lu, *Chin. J. Chem.*, **2014**, *32*, 678–680.

¹²³ K. Liao, F. Zhou, J. S. Yu, W. M. Gao, J. Zhou, *Chem. Commun.*, **2015**, *51*, 16255–16258.



Scheme 4.5 Asymmetric trifluoromethylthiolation of indanone thioethers

Finally, the asymmetric trifluoromethylthiolation of aldehydes was also investigated but with poor results. As summarized in **Scheme 4.6**, in the first example, the Hayashi-Jørgensen catalyst was used to promote the reaction of the aldehyde **117** with *N*-SCF₃-saccharin obtaining the β-SCF₃ alcohol with high yield but only 11 % ee.¹²⁴ In the second example, phase transfer catalysis conditions were employed to catalyze the trifluoromethylthiolation of α-chloroaldehyde **120** yet with poor enantioselectivity.¹²⁵



Scheme 4.6 Asymmetric trifluoromethylthiolation of aldehydes

¹²⁴ L. Hu, M. Wu, H. Wan, J. Wang, G. Wang, H. Guo, S. Sun, *New J. Chem.*, **2016**, *40*, 6550–6553.

¹²⁵ F. Gelat, T. Poisson, A. T. Biju, X. Pannecoucke, T. Besset, *Eur. J. Org. Chem.*, **2018**, *2018*, 3693–3696.

4.2 Asymmetric trifluoromethylthiolation of azlactones

4.2.1 Specific objectives

As discussed above, in recent years considerable efforts have been directed toward the development of asymmetric trifluoromethylthiolation processes owing to the several advantages arising from the introduction of the SCF₃ group into organic molecules. However, up to date, such methods have a limited scope of substrates.

In this context, during my research stage at the Universidad Autonoma de Madrid under the supervision of Professor José Aléman, my interest focused on the development of new synthetic routes under phase transfer catalysis conditions leading to new enantioenriched SCF₃-derivatives.

With the challenging aim of expanding the direct asymmetric insertion of the SCF₃ group at α -C(sp₃) of carbonyl compounds, azlactones were chosen as interesting substrates.

Oxazolones or azlactones (**Figure 4.2**) are compounds widely used as versatile scaffolds for the synthesis of diverse heterocycles and natural products through different stereoselective approaches. For example, they are employed for the synthesis of quaternary natural and unnatural amino acids. The presence of numerous reactive sites in their ring system allows, in fact, a wide range of transformation.¹²⁶ In particular, the easy deprotonation of the acidic proton at the C-4 position (pka \approx 9) affords the nucleophilic azlactone enolate, which is able to react with a variety of electrophiles.

¹²⁶ For selected examples see: a) P. P. De Castro, A. G. Carpanez, G. W. Amarante, *Chem. Eur. J.*, **2016**, *22*, 10294-10318; b) R. A. Mosey, J. S. Fisk, J. J. Tepe, *Tetrahedron: Asymmetry.*, **2008**, *19*, 2755-2762; c) J. S. Fisk, R. A. Mosey, J. J. Tepe, *Chem. Soc. Rev.*, **2007**, *36*, 1432-1440. d) A.-N. R. Alba, R. Rios, *Chem. Asian J.*, **2011**, *6*, 720-734; e) L. N. Sharada, Y. Aparna, M. Saba, S. N. T. Sunitha, L. Viveka, *Int. J. Sci. Res. Pub.*, **2015**, *5*, 1-9.

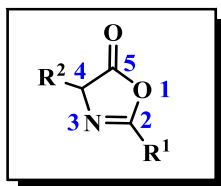


Figure 4.2 General structure of azlactone

Moreover, azlactones itself exhibit important biological activities such as analgesic, anti-inflammatory, antimicrobial, antifungal, anticancer, antibacterial, resulting in the increasing demand for their commercialization in enantiomerically pure forms and with modified properties.¹²⁷

N-(Trifluoromethylthio)phthalimide was chosen as the electrophilic trifluoromethylthiolating agent because it shows low toxicity and hazard, its preparation is very easy and it is stable under the usual reaction condition.¹²⁸

Indeed, it is moisture and air-stable as well as at light exposure, both in solution and at solid-state. Moreover, this electrophilic compound does not undergo decomposition under neutral and acidic aqueous conditions, even though it is sensitive to strong bases.

¹²⁷ For selected examples see: a) M. J. Aaglawe, S. S. Dhule, S. S. Bahekar, P. S. Wakte, D. B. Shinde, *J. Korean Chem. Soc.*, **2003**, *47*, 133-136; b) S. Nair, S. P. Garg, P. Sah, *J. Indian Chem. Soc.*, **2006**, *83*, 205-207; c) D. Benedlt, V. Daniel, *J. Med. Chem.*, **1994**, *37*, 710; d) L. R. Jat, R. Mishra, D. Pathak, *Int. J. Pharm. Pharm. Sci.*, **2012**, *4*, 378-380; e) C. Puig, M. I. Crespo, N. Godessart, J. Feixas, J. Ibarzo, J.-M. Jiménez, L. Soca, I. Cardelus, A. Heredia, M. Miralpeix, J. Puig, J. Beleta, J. M. Huerta, M. López, V. Segarra, H. Ryder, J. M. Palacios, *J. Med. Chem.*, **2000**, *43*, 214-223; f) M. A. Mesaik, S. Rahat, K. M. Khan, Z. Ullah, M. I. Choudhary, S. Murad, Z. Ismail, A.-u. Rahman, A. Ahmad, *Bioorg. Med. Chem.*, **2004**, *12*, 2049-2057.

¹²⁸ a) M. Li, H. Zheng, X.-s Xue, J.-p Cheng, *Tetrahedron Lett.*, **2018**, *59*, 1278-1285; b) X. Shao, C. Xu, L. Lu, Q. Shen, *Acc. Chem. Res.*, **2015**, *48*, 1227-1236; c) H. Chachignon, D. Cahard, *Chin. J. Chem.*, **2016**, *34*, 445-454.

4.2.2 Results and discussion

In order to assess the feasibility of the design asymmetric trifluoromethylthiolation, the azlactone **122a** was selected as model substrate and a large family of chiral phase transfer Chincona alkaloid-derived quaternary ammonium salts (**Figure 4.3**) was investigated under liquid-liquid (aqueous base-dichloromethane) conditions in presence of *N*-(trifluoromethylthio)phthalimide **105** as SCF_3 source.

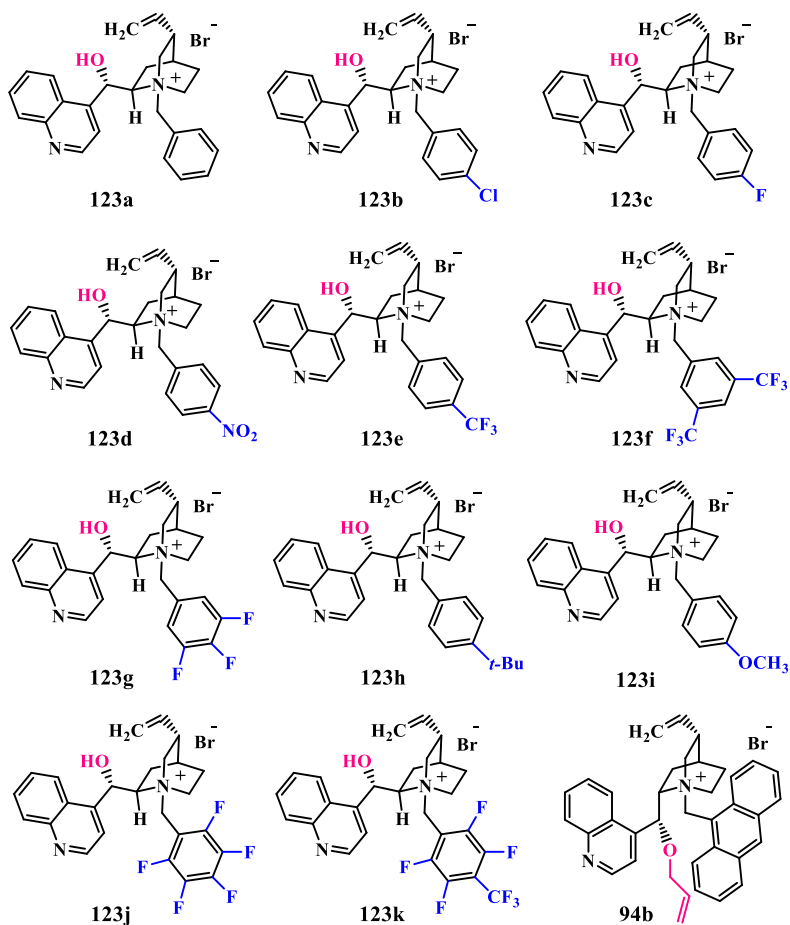
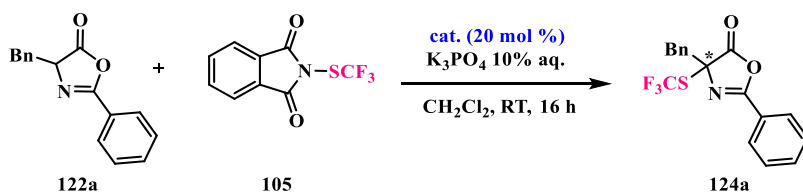


Figure 4.3 Chincona alkaloids-quaternary ammonium salts

As reported in **Table 4.2**, carrying out the first run in the absence of the catalyst (**entry 1**), no traces of the product were observed after 2 days proving that the reaction requires the presence of the quaternary ammonium salt to take place.



entry	catalyst	yield (%) ^b	ee (%) ^c
1 ^d	–	–	–
2	TBAB	44	–
3	123a	22	22
4	123b	33	23
5	123c	18	23
6	123d	33	25
7	123e	23	28
8	123f	28	28
9	123g	31	26
10	123h	42	19
11	123i	33	18
12	123j	18	14
13	123k	18	17
14	94b	29	–2
15 ^f	123f	28	28

^aReactions were performed with **122a** (0.10 mmol), **105** (0.12 mmol), catalyst (20 mol%), K₃PO₄ 10% aqueous (1.0 mL) in CH₂Cl₂ (1.0 mL), at room temperature, unless otherwise noted: ^bYield of product determined by ¹H NMR spectroscopy using 1,3,5-Trimethoxybenzene as an internal standard. ^cDetermined by HPLC on a chiral stationary phase (Chiralcel AS-H). ^dReaction time: 2 days. ^fReaction performed at 0 °C.

Table 4.2 Screening of catalysts under LL-PTC conditions^a

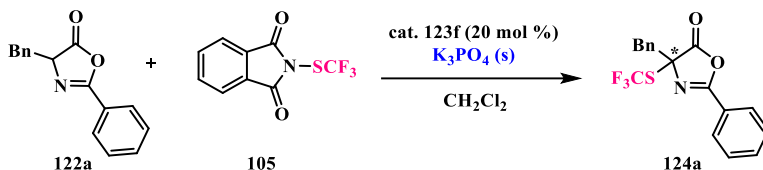
Catalyzing the reaction with phase transfer agents, the designed product **124a** was obtained in all the experiments under the mild reaction conditions selected. However, in all cases, disappointing results in terms of both yield and enantioselectivity were achieved after 16 hours, irrespective of the catalyst employed.

Searching for a rationale for the low yields observed, we first assessed the stability of the substrates under the reaction conditions adopted. To this end, the reaction was performed as usual but without the trifluoromethylthiolating agent. After 2 h, the azlactone turned out to be entirely consumed, presumably through hydrolysis of the labile azlactone ring. The reaction was conducted at 0 °C with catalyst **123f**, but no improvements were achieved (**entry 15**). Also in the presence of the racemic tetrabutylammonium bromide (TBAB) degradation processes took place affording the SCF₃-product with low yield (**entry 2**).

In order to avoid degradation pathways, solid-liquid phase transfer catalysis conditions were inspected with different amounts of solid K₃PO₄ and the chiral Chinconinium ammonium salt **123f** (**Table 4.3**).

The first asymmetric reaction conducted with the over-stoichiometric amount of K₃PO₄ at room temperature (**entry 1**) formed the product with slightly higher yield but with lower enantiomeric excess if compared with the reaction performed with the liquid-liquid system. Thus, the same amount of solid base was used at 0 °C achieving similar values of enantioselectivity and yield (**Table 4.3, entry 2**).

In both cases, considerable amounts of by-products due to the undesirable degradation of the azlactone were generated in the reaction mixtures.



entry	Base eq.	T (°C)	t (h)	yield (%) ^b	ee (%) ^c
1	5	RT	1	42	14
2	5	0	2	45	18
3	0.1	RT	5	64	31
4	0.1	-20	65	74	43
5	0.1	-40	65	35	24

^aReactions were performed with **122a** (0.10 mmol), **105** (0.12 mmol), catalyst **123f** (20 mol%), K₃PO₄ solid (x mmol) in CH₂Cl₂ (1.0 mL), unless otherwise noted ^bIsolated yield ^cDetermined by HPLC on a chiral stationary phase (Chiralcel AS-H).

Table 4.3 Asymmetric Trifluoromethylthiolation under SL-PTC conditions^a

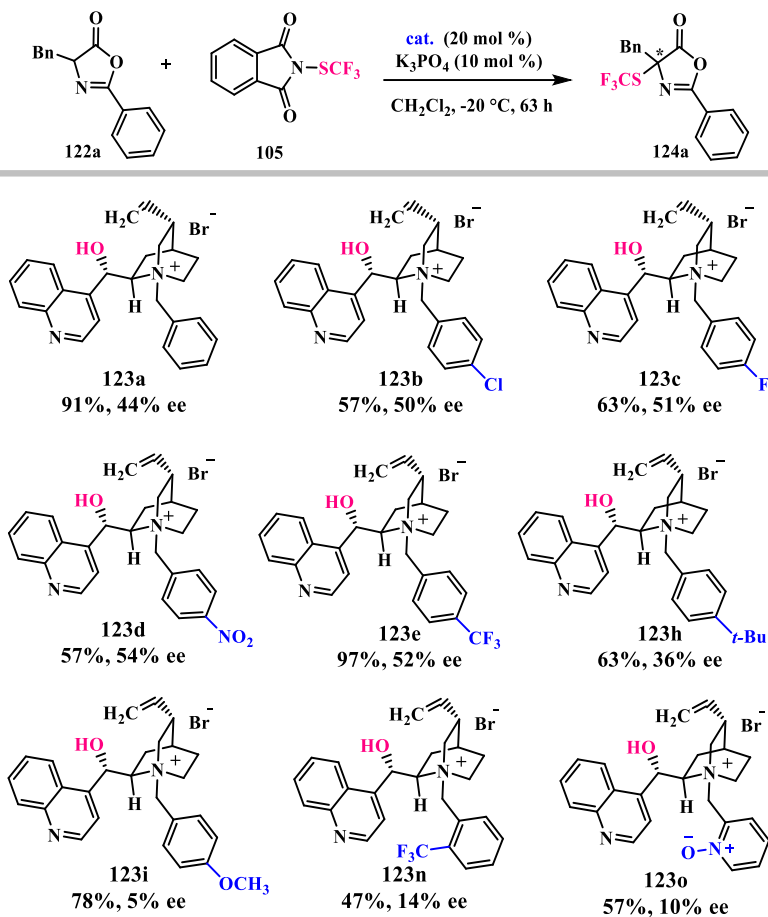
Surprisingly, a catalytic amount of solid base (10 % mol of K₃PO₄) proved to be sufficient to promote the asymmetric trifluoromethylthiolation reaction leading to the improvement of both enantioselectivity and yield and suppressing the formation of side-products. At room temperature, the desired product was, indeed, achieved with 64% of yield after only 5 hours (**entry 3**). This could be explained considering that the trifluoromethylation delivers the azlactone anion, which is basic enough to carry out the substrate's deprotonation.

Furthermore, lowering the temperature down to -20 °C, full conversion was obtained, albeit in longer reaction time, producing the desired SCF₃-azlactone **123a** with a promising 43% of enantiomeric excess and 74% of yield (**Table 4.3, entry 4**). Performing the reaction at -40 °C, only a low conversion of the substrate was, instead, observed after 65 hours.

Thus, given the encouraging results achieved using 10% mol of K₃PO₄ solid at -20 °C, such conditions were employed for the screening of a wide range

of chiral quaternary ammonium salts with the aim to further increase the enantioselectivity of the reaction.

Chiral cinchonine-derivatives substituted with both electron-donating and electron-withdrawing *p*-substituents of the *N*-benzyl group were used to promote the asymmetric trifluoromethylthiolation reaction. From reported data in **Scheme 4.7**, it is clear that the electronrich ammonium salts, including *p*-OMe and *p*-*t*-Bu benzyl derivatives (**123i**, **123h**), negatively affect the enantiocontrol of the nucleophilic attack affording the product with very low enantiomeric excesses, albeit with good yields.

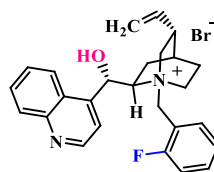




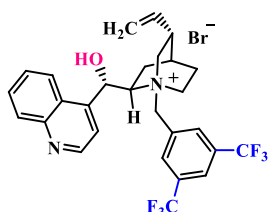
123p
94%, 26% ee



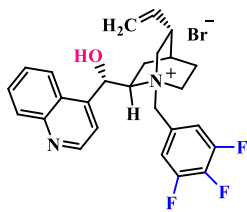
123q
69%, 12% ee



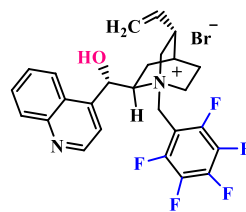
123r
59%, 41% ee



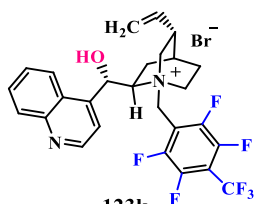
123f
74%, 43% ee



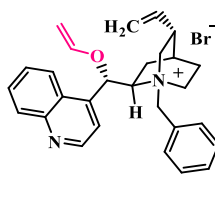
123g
63%, 55% ee



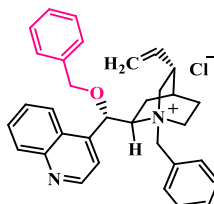
123j
80%, 44% ee



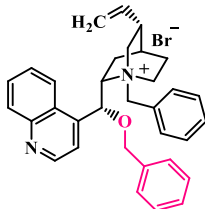
123k
80%, 46% ee



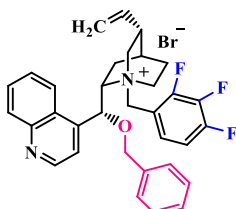
123l
80%, 2% ee



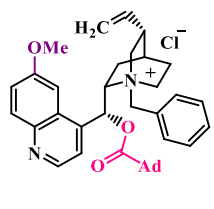
123m
78%, 8% ee



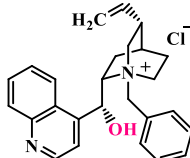
94e
72%, 1% ee



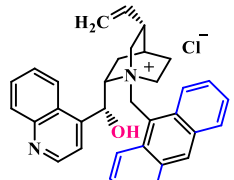
94r
88%, 9% ee



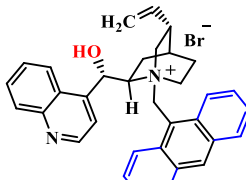
123s
86%, 2% ee



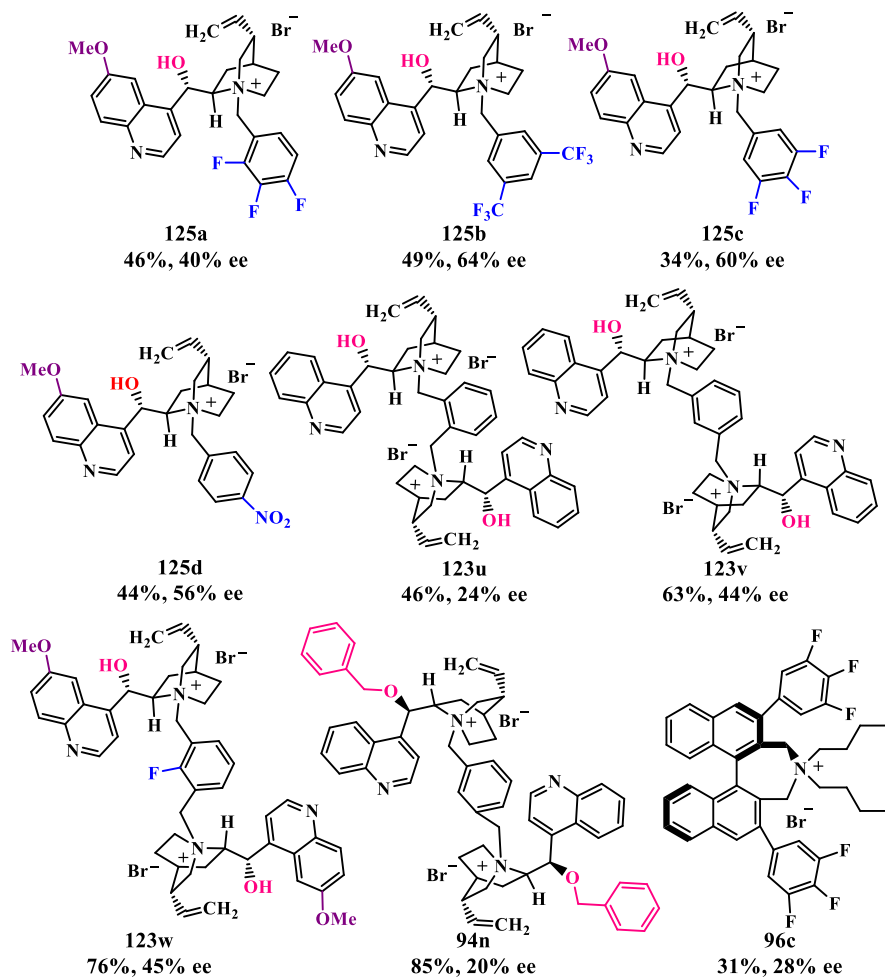
94c
70%, 16% ee



94a
69%, 29% ee



123t
27%, 52% ee



^aReactions were performed with **122a** (0.10 mmol), **105** (0.12 mmol), catalyst (20 mol%), K₃PO₄ solid (10 mol%) in CH₂Cl₂ (1.0 mL), unless otherwise noted; ^bIsolated yield; ^cDetermined by HPLC on a chiral stationary phase (Chiralcel AS-H).

Scheme 4.7 Screening of catalysts under SL-PTC conditions^{a-c}

On the contrary, improved enantiocontrol is achieved using electronpoor *p*-substituted *N*-benzyl-cinchoninium compounds containing groups such as *p*-Cl (**123b**), *p*-F (**123c**), *p*-CF₃ (**123e**) and *p*-NO₂ (**123d**), obtaining enantiomeric excesses up to 54%.

Then the nature, number, and position of electron-withdrawing substituents were varied on the *N*-benzyl group (**123f**, **123g**, **123j**, **123k**, **123r**). In all cases, the SCF₃-azlactone **124a** was produced with good to high yields and good enantioselectivities and a further slight increase up to 55 % of ee was obtained with the quaternary ammonium salt **123g**. Catalysts with fully substituted benzyl moieties afforded the product with 80% of yield but with slightly lower enantioselectivity compared to *p*-substituted derivatives. Subsequently, the effect of *o*-substituted-*N*-benzyl cinchoninium derivatives (**123n-q**) on the reaction stereocontrol was evaluated. Although it has been reported in the literature that hydrogen bond donor groups at the *ortho* position of *N*-benzyl-*Cinchona* alkaloids derivatives can improve the enantioselectivity of alkylation reactions thanks to their ability to form highly organized transition states¹²⁹, detrimental effect was observed in our process, maybe due to unfavorable steric effect. Moreover, protecting the C9-OH functionality of the catalyst with different groups, a drop of enantioselectivity was observed in all the cases (**123l**, **123m**, **123s**, **94e**, **94r**). This suggests the key role of the free hydroxyl group in the stabilization of the transition state through hydrogen bonds formation, as discussed below. Additionally, it was noted that the stereochemical features of the catalysts are very important. In fact, using the unsubstituted *N*-benzyl cinchonidinium derivative **94c** only a low 16% ee was achieved compared to 44% ee obtained with the pseudoenantiomeric *N*-benzyl cinchoninium compound **123a**. The same behavior was found comparing the more hindered pseudoenantiomers *N*-anthracenyl cinchonidinium and cinchoninium salts (cf **94a** with **123t**). In fact, the latter afforded product with 52 % of ee and low yield (27 %), whereas with the cinchonidinium-base catalyst lower enantioselectivity and

¹²⁹ a) S.-s. Jew, M.-S. Yoo, B.-S. Jeong, I. Y. Park and H.-g. Park, *Org. Lett.*, **2002**, *4*, 4245-4248; b) M.-S. Yoo, B.-S. Jeong, J.-H. Lee, H.-g. Park and S.-s. Jew, *Org. Lett.*, **2005**, *7*, 1129-1131.

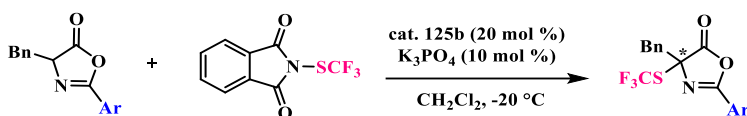
higher yield were achieved (69%, 29% ee). Different dimeric Cinchona alkaloids ammonium salts (**123u-w**, **94n**) were also investigated, but only low to moderate enantioselectivities were observed. Moreover, the more rigid Maruoka's ammonium salt **96c** proved to be ineffective, affording disappointing yield and enantioselectivity after 63 hours.

Interestingly, higher enantioselectivities were obtained with quinidinium derivatives. Switching the catalyst core from cinchonine to quinidine resulted in improved enantioselectivity in all cases. In detail, 3,4,5-trifluorobenzyl (**125c**), 3,5-bis(trifluoromethyl)benzyl (**125b**), 4-nitrobenzyl (**125d**) and 2,3,4-trifluorobenzyl (**125a**) substituted derivatives were tested, with the former three salts providing better enantioselectivities than their cinchonine counterparts. *N*-3,5-Bis(trifluoromethyl)benzyl quinidinium bromide (**125b**) afforded the chiral product with the best enantiomeric excess (64 % ee). On the contrary, yields obtained with cinchonine-derived catalysts were higher than those obtained with quinidine derivatives, as a result of the higher conversions of the starting material reached after 63 h.

Once identified the best phase transfer catalyst (**125b**), variously *p*-substituted 2-aryl-azlactones were screened.

As described in **Table 4.4**, the electronic nature of the C-2 aryl substituent of the azlactone was found to be crucial. In detail, the reaction did not take place when electron-poor aromatic rings, such as *p*-CF₃ (**126a**) and *p*-CN phenyl groups (**127a**), were present in the substrate, resulting only in incomplete degradation of the starting materials after long reaction times. Interestingly, when a chlorine atom was placed at the *p*-position of the phenyl moiety (**128a**), the reaction proceeded smoothly affording the product with higher yield compared to the unsubstituted 2-phenyl substrate **122a** in shorter reaction time. However, a drop in enantioselectivity was observed. Gratifyingly, upon introducing a *p*-methoxy electron-donating group on the

aromatic ring (**129a**), significant improvements of the rate reaction and the enantioselectivity were found. In fact, full conversion was reached in only 1 h affording the chiral product **130a** in pure form with 84% yield and with a marked improvement of the enantiomeric excess (88% ee).



entry	Ar ^d	t (h)	yield (%) ^b	ee(%) ^c
1	<i>p</i> -CF ₃ Ph	120	–	–
2	<i>p</i> -CNPh	120	–	–
3	<i>p</i> -ClPh	19	83	40
4	Ph	63	49	64
5	<i>p</i> -OMePh	1	84	88

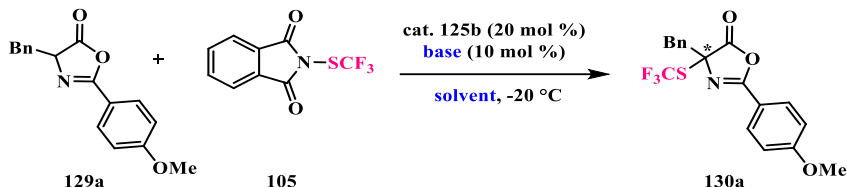
^aReactions were performed with azlactone (0.10 mmol), 105 (0.12 mmol), catalyst **125b** (20 mol%), K₃PO₄ solid (10 mol%) in CH₂Cl₂ (1.0 mL), at -20 °C, unless otherwise noted.
^bIsolated yield ^cDetermined by HPLC on a chiral stationary phase (Chiralcel AS-H). *p*-CF₃Ph-azlactone (**126a**), *p*-CNPh-azlactone (**127a**), *p*-ClPh-azlactone (**128a**), *p*-OMePh-azlactone (**129a**).

Table 4.4 Screening of different C-2 substituted azlactones^a

Optimization of base and solvent was then performed. The thorough screening (**Table 4.5**) revealed that the catalyst **125b** promotes the reaction with good results using a broad range of bases, providing the α -SCF₃-azlactone product **130a** with high yields and good to high enantioselectivities in only 1 hour. The best enantiomeric excess was obtained with potassium phosphate (**Table 4.5, entry 1**). Lowering the base amount down to 5 mol % (**entry 2**), a decrease of the enantioselectivity was found and slightly longer reaction time was needed.

A poor solvent effect was observed on the reactivity, in fact, full conversions were achieved in short reaction times in different reaction media (**entries 8-**

12). Nevertheless, lower enantioselectivity was observed in solvents other than dichloromethane.



entry	Base	solvent	t (h)	yield (%) ^b	ee (%) ^c
1	K ₃ PO ₄	CH ₂ Cl ₂	1	84	88
2 ^d	K ₃ PO ₄	CH ₂ Cl ₂	4	89	50
3	K ₂ CO ₃	CH ₂ Cl ₂	1	80	66
4	Cs ₂ CO ₃	CH ₂ Cl ₂	1	79	72
5	NaHCO ₃	CH ₂ Cl ₂	1	83	76
6	KF	CH ₂ Cl ₂	1	82	80
7	K-Phthalimide	CH ₂ Cl ₂	2	83	60
8	K ₃ PO ₄	CHCl ₃	6	83	66
9	K ₃ PO ₄	Et ₂ O	2	87	52
10	K ₃ PO ₄	THF	1	85	34
11	K ₃ PO ₄	DCE	3	88	44
12	K ₃ PO ₄	toluene	6	88	66

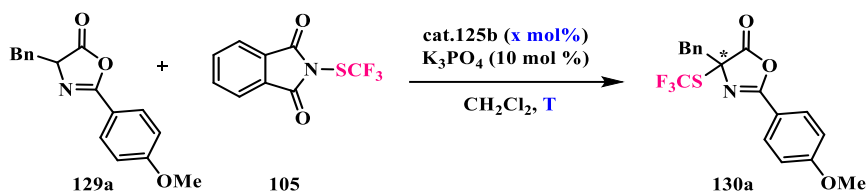
^aReactions were performed with **129a** (0.10 mmol), **105** (0.12 mmol), catalyst **125b** (20 mol%), base solid (10 mol%) in solvent (1.0 mL), at $-20\text{ }^{\circ}\text{C}$, unless otherwise noted. ^bIsolated yield. ^cDetermined by HPLC on a chiral stationary phase (Chiralcel AS-H). ^dReaction performed with 5 mol% of K₃PO₄.

Table 4.5 Screening of bases and solvents^a

Finally, a screening of temperature and catalyst loading was conducted as described in **Table 4.6**.

Lowering the catalyst from 20 to 2 mol%, a progressive decrease of the enantioselectivity was found, leaving the reactivity substantially unaffected

since full conversions were obtained after 1 hour in all the cases. The subsequent investigation of the temperature was, therefore, conducted using 20 mol% of catalyst amount. In particular, at lower temperatures (-40 °C and -70 °C) (**entries 5 and 6**) the pure product **130a** was afforded with very similar yield and slightly longer reaction times (3 h and 6 h respectively), but the enantioselectivity decreased progressively.



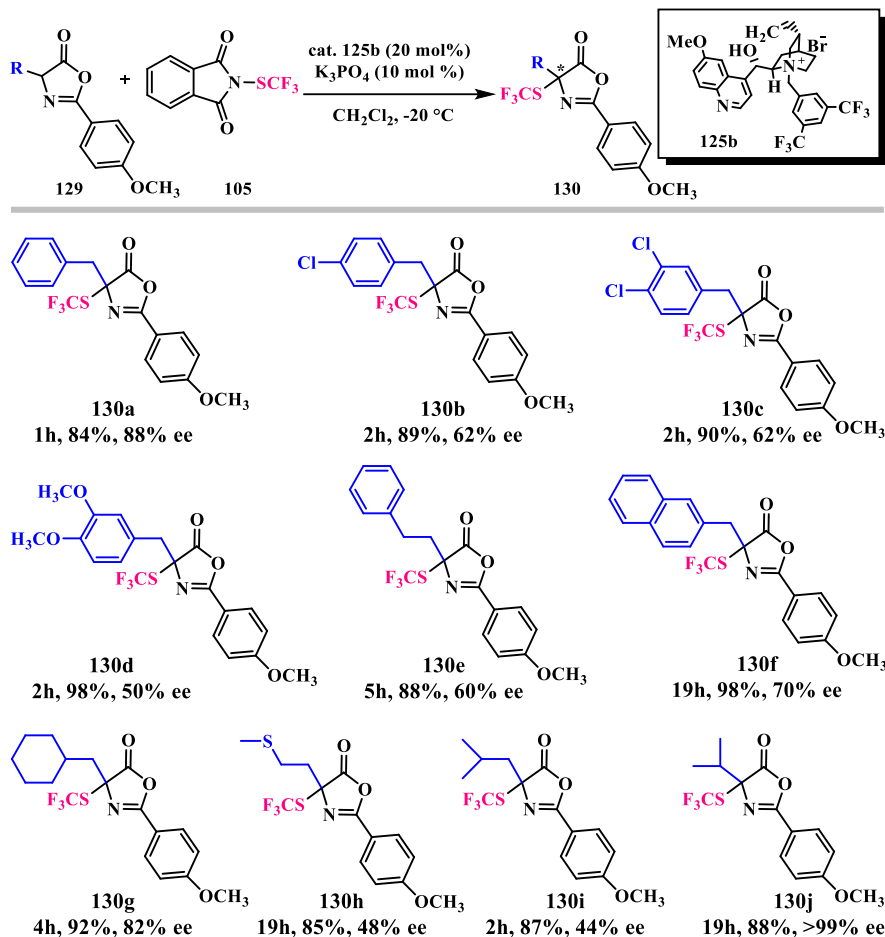
entry	(x mol%)	T (°C)	t (h)	yield (%) ^b	ee (%) ^c
1	20	-20	1	84	88
2	10	-20	1	86	80
3	5	-20	1	87	78
4	2	-20	1	89	72
5	20	-40	3	82	82
6	20	-70	6	85	74

^aReactions were performed with **1a** (0.10 mmol), **2a** (0.12 mmol), catalyst (x mol%), K_3PO_4 solid (10 mol%) in CH_2Cl_2 (1.0 mL), unless otherwise noted; ^bIsolated yield; ^cDetermined by HPLC on a chiral stationary phase (Chiralcel AS-H).

Table 4.6 Screening of catalyst's loading and temperature^a

Next, with the optimized conditions in hand, a wide set of 2-(*p*-methoxyphenyl)-azlactones were used as substrates with the aim to assess the versatility of this methodology.

As reported in **Scheme 4.8**, this method proved to be highly efficient with 4-substituted-azlactones allowing the enantiocontrolled installation of the SCF_3 group at C-4 position in high to excellent yields and with moderate to excellent stereocontrol of the novel chiral quaternary center.

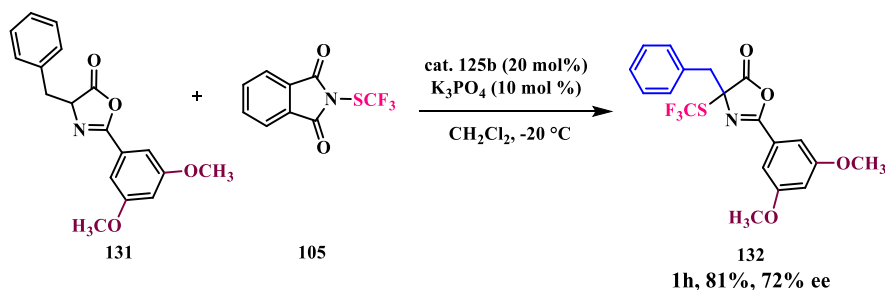


^aReactions were performed with **129** (0.10 mmol), **105** (0.12 mmol), catalyst **125b** (20 mol%), K_3PO_4 solid (10 mol%) in CH_2Cl_2 (1.0 mL), at $-20\text{ }^\circ\text{C}$, unless otherwise noted. ^bIsolated yield. ^cDetermined by HPLC on a chiral stationary phase.

Scheme 4.8 Scope of the asymmetric trifluoromethylthiolation reaction^a

Both electron-donating (**130d**) and electron-withdrawing *para* and *meta*-substituents of the 4-benzyl groups (**130b**, **130c**) were well-tolerated affording excellent yields after 2 hours, and good enantioselectivities. Slightly lower enantioselectivity was observed with electron-donating substituents.

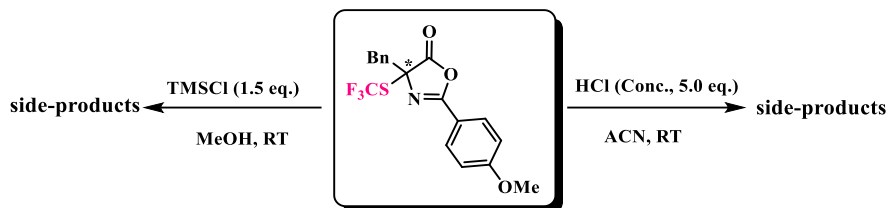
To our delight, this method proved to be also compatible with the presence of homobenzyl as well as more hindered naphthyl groups at C-4. In both cases, comparable enantiomeric excesses and very high yields were achieved. Finally, aliphatic 4-substituted azlactones were investigated giving very high yields and variable enantioselectivities. Excellent results of yield and enantioselectivity were found with the cyclohexylmethyl-substituted substrate **129g**. With the methionine and leucine-based azlactones the corresponding enantioenriched products (**130h**, **130i**) were synthesized with high yields but moderate enantiomeric excesses. Surprisingly, the isopropyl 2-substituted azlactone derived from valine showed to be an excellent substrate for this asymmetric trifluoromethylthiolation reaction affording the desired product **130j** in high yield and substantially enantiopure form. Replacing 2-*p*-methoxyphenyl 2-substituent with the 2-(3,5-dimethylphenyl) substituent, the thiofluorinated product **132** was generated also in this case with high enantiocontrol and yield in just 1 hour (**Scheme 4.9**).



Scheme 4.9 *Asymmetric trifluoromethylthiolation of azlactone 131*

Since azlactones are well-known precursor of amino acids, we decided to attempt the ring-opening of our products, with the aim to synthesize interesting chiral α -amino acids containing SCF₃ group. Unfortunately, from

the preliminary tests performed under widely described azlactone ring-opening conditions¹³⁰ (**Scheme 4.10**), only side-products were achieved.



Scheme 4.10 Attempts of ring-opening reactions

4.2.3 Mechanistic speculations

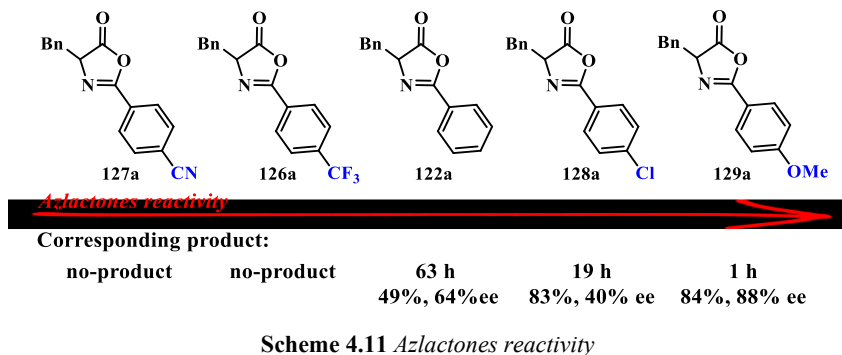
On the basis of the above described experimental data, some speculations on the origin of the stereoselectivity and on the more plausible mechanism could be advanced.

Taking inspiration from the proposed transition state of the closely related asymmetric trifluoromethylthiolation of β -keto esters with SCF_3 -phthalimide catalyzed by cinchona alkaloids, based on DFT calculations,¹³¹ it could be assumed that the stereocontrol of this azlactone trifluoromethylthiolation arises from the concerted action of multiple non-covalent substrate-electrophile-catalyst interactions (**Figure 4.4**).

In particular, a plausible mechanism should involve an electrostatic interaction between the azlactone enolate, which is generated upon deprotonation under base conditions, and the positively charged quaternary nitrogen of the catalyst. Electron-withdrawing substituents on the catalyst's *N*-benzyl moiety and electron-releasing substituents on the 2-aryl-azlactone likely enhance the π - π interactions between the two aromatic moieties.

¹³⁰ B. Qiao, X. Liu, S. Duan, L. Yan, Z. Jiang, *Org. Lett.*, **2014**, *16*, 672–675.

¹³¹ M. Li, X. S. Xue, J. P. Cheng, *ACS Catal.*, **2017**, *7*, 7977–7986.



This trend could be explained considering the higher stabilization of azlactone enolates containing electron-poor aromatic rings resulting in lower reactivity. An intermediate reactivity is, accordingly, exhibited by the unsubstituted 2-phenyl azlactone substrate **122a**. Whereas, the extraordinary reactivity showed by the *p*-OMe-functionalized compound **129a** could be ascribed to the absence of this stabilization effect. When the *p*-Cl-aryl-azlactone **128a** was investigated, a good reactivity was shown affording the product with high yield, but just moderate enantioselectivity after 19 hours. Apparently, this result could be puzzling, but it should be explained by the “double nature” of halogen atoms, behaving as inductive electron-withdrawing groups because of their marked electronegativity, but at the same time, acting as mesomeric donors of electron lone pair.

4.2.4 Conclusions

In conclusion, the first asymmetric trifluoromethylthiolation of azlactones under phase transfer catalysis conditions has been developed. A quinidinium-based ammonium salt in the presence of a catalytic amount of inorganic base efficiently promoted the enantioselective introduction of the SCF₃ group at C-4 position of the azlactone ring giving access to a novel

class of enantioenriched previously unreported compounds. High to excellent yields and moderate to high enantiocontrol of the quaternary chiral centers were achieved in short reaction times with a wide variety of 4-substituted azlactones. It is especially worth noting that the trifluoromethylthiolated product obtained from the valine-derived azlactone has been obtained in enantiopure form. Speculations on the plausible mechanism and on the origin of the enantioselectivity were also made. Considering the peculiar features of thiofluorinated products and the well-known bioactive properties of azlactone compounds, intriguing potential in the pharmaceutical and medical field could be expected from these chiral SCF₃-products. In this context, they could be investigated as synthons for the preparation of amino acids and/or proteins with attractive properties.

4.3 Asymmetric trifluoromethylthiolation of isoxazolidin-5-ones

4.3.1 Specific objectives

During my stage at the Universidad Autonoma de Madrid, with the aim to further expand the realm of the phase transfer catalyzed asymmetric trifluoromethylthiolations, isoxazolidin-5-ones (**Figure 4.5**) were also considered as potential substrates.

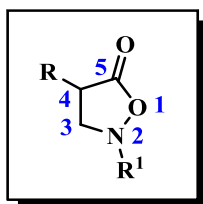
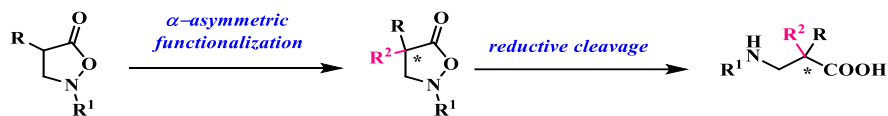


Figure 4.5 General structure of isoxazolidin-5-one

Isoxazolidin-5-ones have demonstrated to be suitable substrates for diverse enantioselective phase transfer catalyzed reactions, such as Michael addition,¹³² allylation reaction with Morita-Baylis-Hillman carbonates¹³³ and α -sulfonylation.¹³⁴ In addition, α -substituted isoxazolidin-5-ones have been recently reported to be ideal precursors of enantioenriched $\beta^{2,2}$ -amino acids containing α -chiral quaternary centers.



Scheme 4.12 General two-step approach for the synthesis of $\beta^{2,2}$ -amino acids

The two-steps synthetic sequence including the asymmetric C- α reaction with electrophiles followed by reductive N-O bond cleavage enables facile access to chiral $\beta^{2,2}$ -amino acids (**Scheme 4.12**). In this context, the development of the first asymmetric trifluoromethylthiolation of isoxazolidin-5-ones could be a reliable tool for the synthesis of enantioenriched thiofluorinated $\beta^{2,2}$ -amino acids. The great interest in this field arises from the relevance of β -amino acids in medical, biological and material chemistry. In addition to their use as pharmacophores, β -amino acids are used as building blocks for the synthesis of peptides and foldamers with unique well-defined secondary structures and enhanced metabolic stability.¹³⁵ The incorporation of fluorinated substituents into amino acid

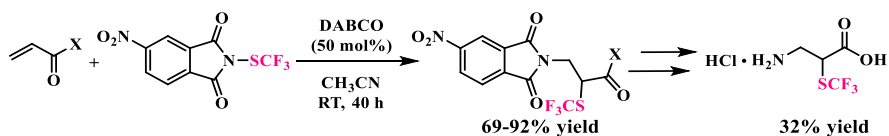
¹³² T. Cadart, V. Levacher, S. Perrio, J.-F. Brière, *Adv. Synth. Catal.*, **2018**, *360*, 1499-1509.

¹³³ V. Capaccio, K. Zielke, A. Eitzinger, A. Massa, L. Palombi, K. Faust, M. Waser, *Org. Chem. Front.*, **2018**, *5*, 3336-3340.

¹³⁴ T. Cadart, C. Berthonneau, V. Levacher, S. Perrio, J.-F. Brière, *Chem. Eur. J.*, **2016**, *22*, 15261-15264.

¹³⁵ For selected reviews see: a) L. Kiss, I. M. Mándity, F. Fülöp, *Amino Acids*, **2017**, *49*, 1441-1455; b) P. S. P. Wang, A. Schepartz, *Chem. Commun.*, **2016**, *52*, 7420-7432; c) H. M. Werner, W. S. Horne, *Curr. Opin. Chem. Biol.*, **2015**, *28*, 75-82; d) C. Cabrele, T. A. Martinek,

core strongly affects their physical and chemical properties, such as improvements in the proteolytic stability and modulation of their pharmacokinetic activity. Moreover, the presence of fluorine atoms into the amino acid structures allows the application of ^{19}F NMR and ^{18}F -based imaging techniques in medicinal chemistry.¹³⁶ However, although fluorinated amino acids are emerging as promising monomers in the development of new peptide-based drugs, only one example of achiral β -amino acid containing SCF_3 group in α -position has been reported in the literature (Scheme 4.13)¹³⁷ and examples of preparations of chiral derivatives are lacking to date.



Scheme 4.13 Example of racemic trifluoromethylthiolated β -amino acid

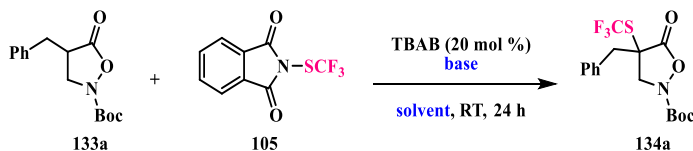
4.3.2 Results and discussion

O. Reiser, L. Berlicki, *J. Med. Chem.*, **2014**, *57*, 9718-9739; e) M.-I. Aguilar, A. W. Purcell, R. Devi, R. Lew, J. Rossjohn, A. I. Smith, P. Perlmutter, *Org. Biomol. Chem.*, **2007**, *5*, 2884-2890; f) F. Fülöp, *Chem. Rev.*, **2001**, *101*, 2181-2204; g) R. P. Cheng, S. H. Gellman, W. F. DeGrado, *Chem. Rev.*, **2001**, *101*, 3219-3232; h) W. F. DeGrado, J. P. Schneider, Y. Hamuro, *J. Peptide Res.*, **1999**, *54*, 206-217.

¹³⁶ For selected reviews see: a) S. J. M. Verhoorck, P. M. Killoran, C. M. Coxon, *Biochem.*, **2018**, *57*, 6132-6143; b) S. Huhmann, B. Kokschi, *Eur. J. Org. Chem.*, **2018**, 3667-3679; c) A. A. Berger, J.-S. Völler, N. Budisa, B. Kokschi, *Acc. Chem. Res.*, **2017**, *50*, 2093-2103; d) K. E. Arntson, W. C. K. Pomerantz, *J. Med. Chem.* **2016**, *59*, 5158-5171; e) E. N. G. Marsh, *Acc. Chem. Res.* **2014**, *47*, 2878-2886; f) M. Salwiczek, E. K. Nyakatura, U. I. M. Gerling, S. Ye, B. Kokschi, *Chem. Soc. Rev.*, **2012**, *41*, 2135-2171; g) N. C. Yoder, K. Kumar, *Chem. Soc. Rev.* **2002**, *31*, 335-341.

¹³⁷ Q. Xiao, Q. He, J. Li, J. Wang, *Org. Lett.*, **2015**, *17*, 6090-6093.

With the aim to develop the first asymmetric trifluoromethylthiolation of isoxazolidin-5-ones, the feasibility of this transformation under phase transfer catalysis conditions was first investigated using TBAB and *N*-(trifluoromethylthio)phthalimide as SCF₃-donor in the presence of diverse bases and solvents.



entry	base	solvent	yield (%) ^b
1	Na ₂ CO ₃ (2.0 eq.)	Et ₂ O	< 2
2	K ₂ CO ₃ (2.0 eq.)	Et ₂ O	36
3	Cs ₂ CO ₃ (2.0 eq.)	Et ₂ O	< 2
4	K ₃ PO ₄ (2.0 eq.)	Et ₂ O	15
5	NaH ₂ PO ₄ (2.0 eq.)	Et ₂ O	< 2
6	KF (2.0 eq.)	Et ₂ O	8
7	NaOH (2.0 eq.)	Et ₂ O	< 2
8	KOH (2.0 eq.)	Et ₂ O	< 2
9	K ₂ CO ₃ (20% aq.)	Et ₂ O	< 2
10	K ₂ CO ₃ (2.0 eq.)	toluene	9
11	K ₂ CO ₃ (2.0 eq.)	CH ₂ Cl ₂	< 2
12	K ₂ CO ₃ (2.0 eq.)	THF	8
13	K ₂ CO ₃ (0.5 eq.)	Et ₂ O	24
14	K ₂ CO ₃ (1.0 eq.)	Et ₂ O	30
15	K ₂ CO ₃ (5.0 eq.)	Et ₂ O	37

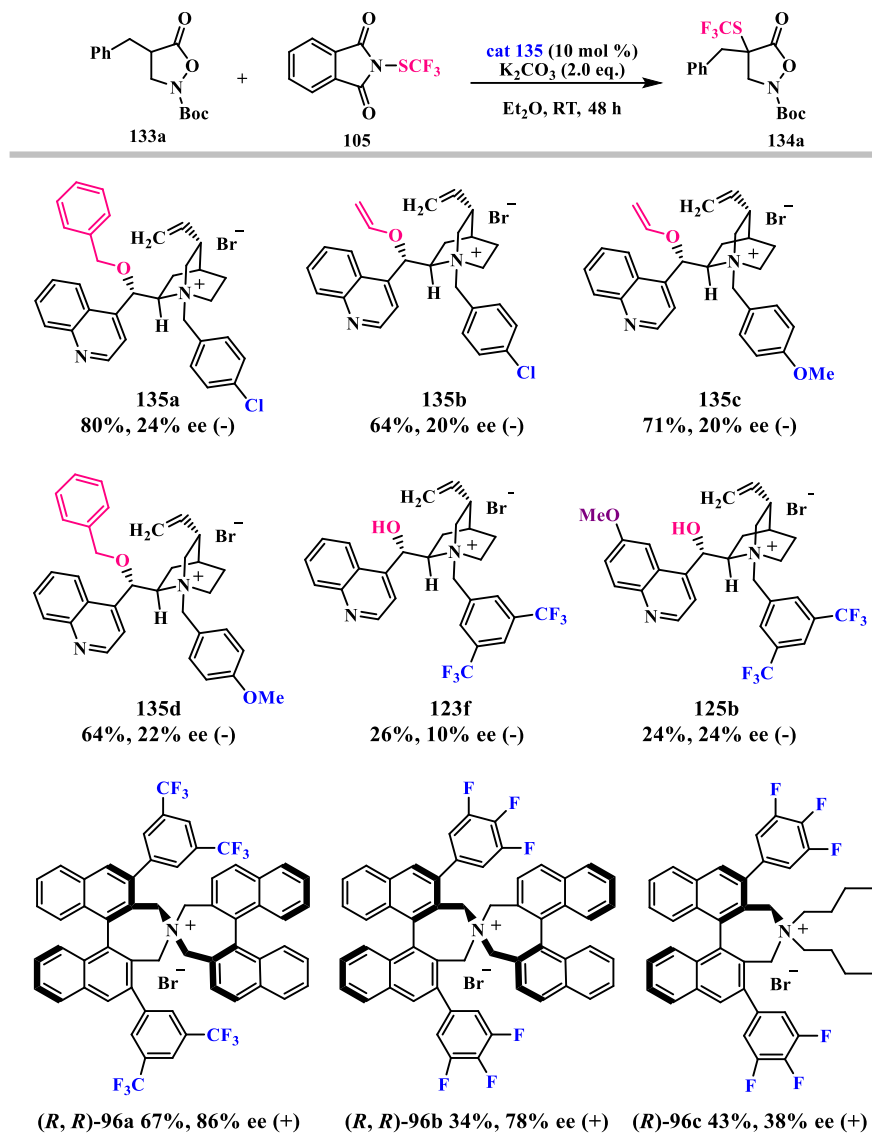
^aReactions were performed with **133a** (0.10 mmol), **105** (0.20 mmol), TBAB (20 mol%), base solid (x mmol) or aqueous (0.4 mL) in the solvent (1.0 mL), at room temperature. ^bYield of product determined by ¹H NMR spectroscopy using Terephthalaldehyde as an internal standard.

Table 4.7 Screening of bases and solvents in the presence of TBAB as the catalyst

As reported in **Table 4.7**, all the experiments were carried out at room temperature and stopped after 24 hours. Among the several bases and solvent used, only solid K_2CO_3 in diethyl ether furnished the racemic product with promising yield (**entry 2**). Very low conversions were achieved in other cases. In particular, in presence of strong bases, such as NaOH, KOH (**entries 7 and 8**) and aqueous K_2CO_3 (**entry 9**), rapid decomposition of the electrophile took place. Also the use of sub-stoichiometric or over-stoichiometric amount of K_2CO_3 solid (**entries 13-15**) did not provide a decisive impact on the conversion. Therefore, 2.0 eq. of K_2CO_3 solid and Et_2O as solvent were selected as the best conditions for the screening of chiral phase transfer catalysts (**Scheme 4.14**).

Various substituted cinchoninium and quinidinium quaternary ammonium salts were first tested to promote the asymmetric trifluoromethylthiolation. *O*-Protected derivatives (**135a-d**) afforded the desired product **134a** with good to high yields leading to some asymmetric induction albeit poor. Using catalysts containing free OH groups (**123f** and **125b**), disappointing results in terms both of yield and enantioselectivity were, instead, obtained. With great delight, Maruoka's ammonium salts **96a** and **96b** provided pretty good enantioselectivities. In particular, the best yield and enantioselectivity were afforded with the chiral 3,5-bis-(trifluoromethyl)phenyl substituted *N*-spiro quaternary ammonium salt **96a**, which furnished the enantioenriched product **134a** with 67 % yield and 86 % ee.

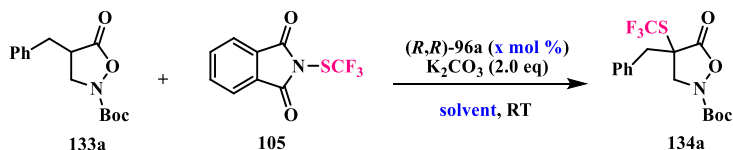
Subsequently, the effect of catalyst loading was studied (**Table 4.8**). A reduction of the amount of Maruoka catalyst to 2% mol (**entry 4**) led to a significant drop in the conversion, as well as a small decrease of the enantioselectivity.



^aReactions were performed with **133a** (0.10 mmol), **105** (0.20 mmol), cat (10 mol%), K₂CO₃ (0.20 mmol) in Et₂O (1.0 mL), at room temperature. ^bYield of product determined by ¹H NMR spectroscopy using terephthalaldehyde as internal standard. ^cEnantiomeric excesses determined by HPLC on a chiral stationary phase. ^d(+) or (-) are optical rotations.

Scheme 4.14 Screening of chiral catalysts^{a-d}

Using 5 mol% of catalyst amount (**entry 2**), instead, only a slight decrease in the yield resulted and the enantioselectivity was completely retained. Therefore, 5 % of catalyst loading was preferred for the following runs. No yield improvement was achieved by prolonging reaction time up to 72 h (**entry 3**).



entry	(x mol%)	solvent	t (h)	yield (%) ^b	ee (%) ^c
1	10	Et ₂ O	48	67	86
2	5	Et ₂ O	48	60	86
3	5	Et ₂ O	72	63	86
4	2	Et ₂ O	48	33	80
5	5	THF	72	21	56
6	5	Toluene	72	29	90
7	5	CH ₂ Cl ₂	72	–	–
8 ^d	5	Et ₂ O	48	–	–
9 ^e	5	Et ₂ O	96	55	84

^aReactions were performed with **133a** (0.10 mmol), **105** (0.20 mmol), **96a** (x mol%), K₂CO₃ (0.20 mmol) in solvent (1.0 mL), at room temperature. ^bYield of product determined by ¹H NMR spectroscopy using Terephthalaldehyde as internal standard. ^c Enantiomeric excess determined by HPLC on a chiral stationary phase. ^d Reaction performed with K₂CO₃ 20% aq. ^eReaction performed at 4 °C.

Table 4.8 Screening of solvents and catalyst loading^a

Next, the solvent (**entries 5-7**) and the temperature (**entry 9**) effects were investigated. Good to high enantiomeric excesses were achieved in most cases, but the conversions were moderate. In particular, in toluene, an improvement of the enantiomeric excess was achieved, but with a dramatic erosion of the yield. Dichloromethane turned out to be unsuitable solvent for

this transformation, since no traces of product were detected after 48 hours. A test was also carried out under liquid-liquid phase transfer conditions and, as noted with TBAB, degradations of both the starting material and the electrophile took place (**entry 8**).

Finally, the effect of diverse electrophilic SCF_3 sources (**Figure 4.6**) was evaluated. In particular, 5-nitro-phthalimide-, saccharine- and succinimide-derived trifluoromethylthio compounds were tested under the selected reaction conditions. The substituted-phthalimide **136** proved to be less reactive than the parent compound, affording only traces of products after 48 hours. Whereas the compounds **118** and **108** showed to be unstable under the reaction conditions.

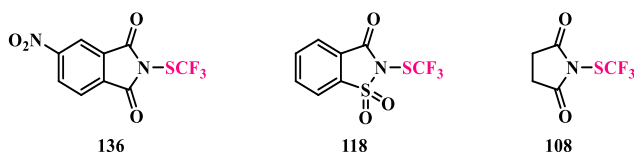
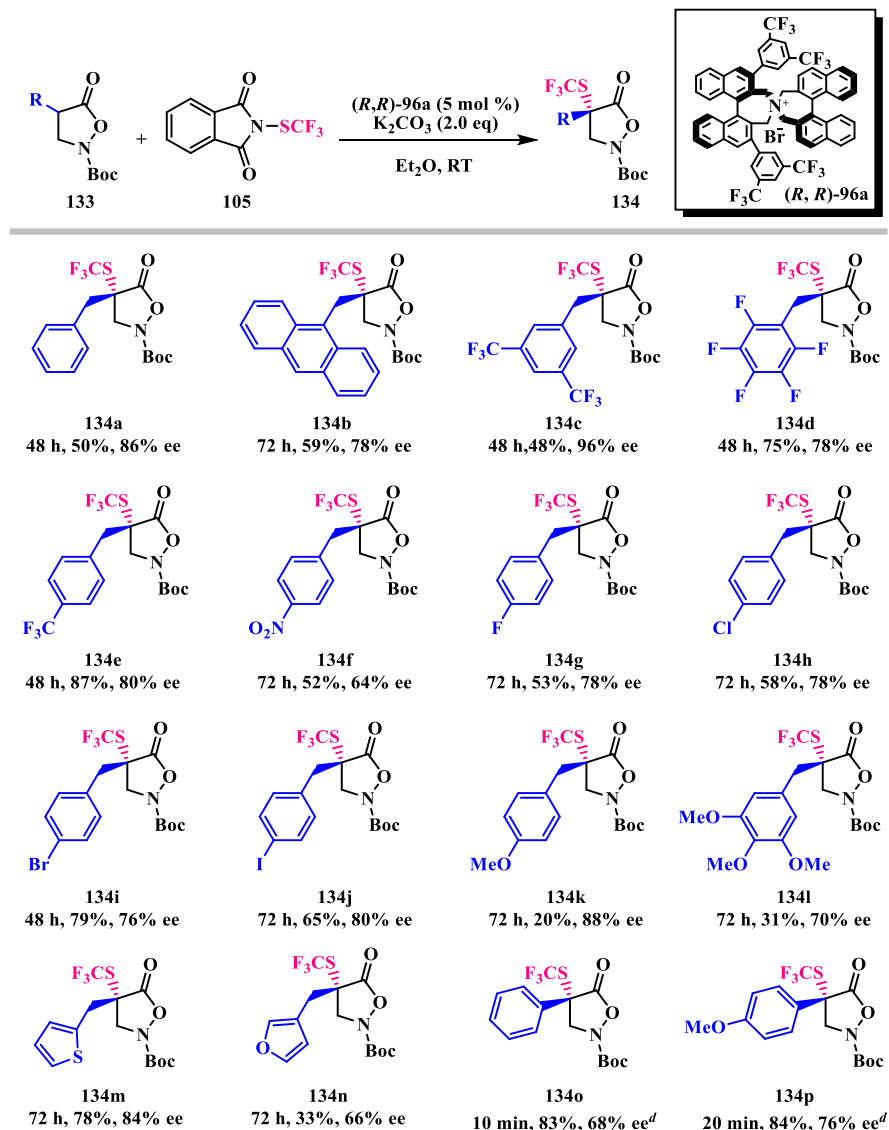


Figure 4.6 Others electrophilic compounds as a source of SCF_3 group

Having selected the optimal reaction conditions, the versatility of this methodology was, thus, assessed. A large variety of diversely functionalized 4-arylmethyl-isoxazolidin-5-ones and 4-heteroarylmethyl-isoxazolidin-5-ones was subjected to the usual reaction conditions. As reported in **Scheme 4.15**, good to excellent enantiomeric excesses (from 64% to 96%) were achieved in all the cases regardless of the number and type of the functional groups on the aromatic ring. The reactivity of substrates was, instead, distinctly affected by the electronic properties of the aryl or heteroaryl group. Indeed, the corresponding chiral thiofluorinated products (**134e-j**) were isolated in good to high yields (48-87%) starting from isooxazolidin-5-ones bearing one or more electron-withdrawing groups on the aromatic moiety.



^aReactions were performed with **131** (0.10 mmol), **105** (0.20 mmol), cat **96a** (5 mol %), K_2CO_3 (0.20 mmol) in Et_2O (1.0 mL), at room temperature. ^bIsolated yield. ^cEnantiomeric excess determined by HPLC on a chiral stationary phase. ^dCatalyst **10** (2 mol %) was used.

Scheme 4.15 Scope of the trifluoromethylthiolation of isoxazolidin-2-ones

Good reactivities were also observed with methylphenyl- and methylantraceny-substituted compounds (**134a**, **134b**), whereas variable

yields were achieved with heteroaromatic substrates (**134m**, **134n**). Only poor yields were, on the contrary, obtained with electron-rich starting materials containing one or more electron-donating substituents (**133k**, **133l**). A tentative explanation of such results could be the poor acidity at the C-4 site of the electron-rich substrates which hampers the generation of the enolate intermediate. Thus, as a proof of concept, the more acidic 4-aryl-isoxazolidin-5-ones **134o** and **134p** were used as substrates under the above described reaction conditions in order to verify whether they were more reactive. High yields in very short time were obtained with both the unsubstituted and the electron-rich derivatives, confirming our assumption. In addition, good enantiomeric excesses were achieved with these substrates too.

Finally, the facial selectivity of the developed asymmetric trifluoromethylthiolation reaction of isoxazolid-5-ones was revealed by X-ray crystal analysis of product **134d**. The (*S*) absolute configuration was determined, as represented in **Figure 4.7**, and the same enantioselectivity was assumed for the other substrates investigated.

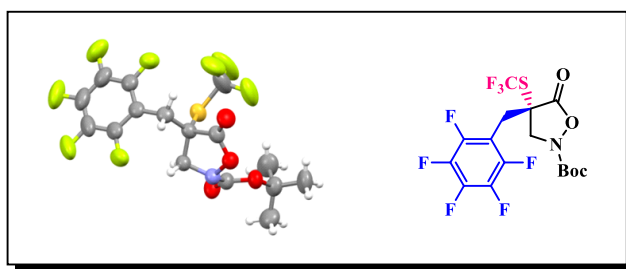
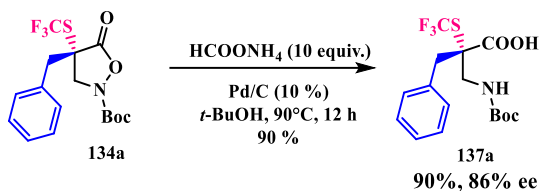


Figure 4.7 *Single-crystal X-ray structure of (S)- 134d*

At this point, the synthesis of the enantioenriched α -SCF₃- $\beta^{2,2}$ -amino acids was pursued. To our great satisfaction, smooth *N-O* cleavage was easily realized by hydrogenolysis with ammonium formate and Pd/C, affording the

first example of a valuable enantioenriched α -trifluoromethylthio- $\beta^{2,2}$ -amino acid (Scheme 4.16).



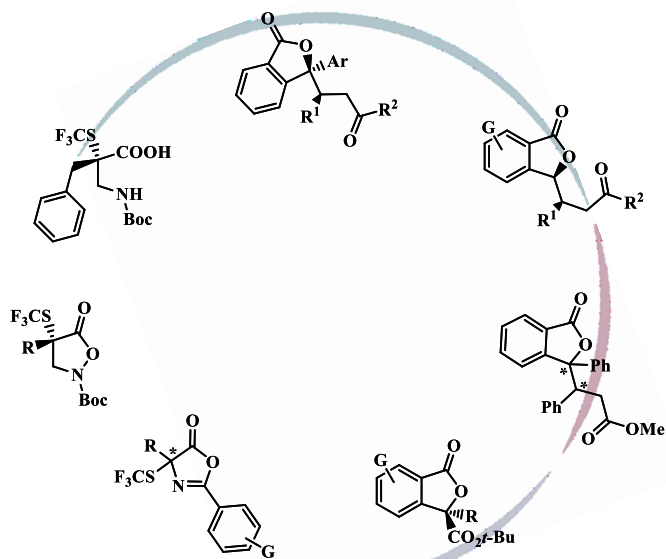
Scheme 4.16 Synthesis of 2-trifluoromethylthio- $\beta^{2,2}$ -amino acid **137a**

4.3.3 Conclusions

In conclusion, the first asymmetric phase transfer catalyzed α -trifluoromethylthiolation of 4-benzyl- and 4-aryl-isooxazolidin-5-ones has been developed. Unreported enantioenriched thiofluorinated compounds were produced with moderate to high yields and with good to excellent enantiocontrol, regardless of the steric and electronic properties of the substrates. *N*-SCF₃-phthalimide showed to be the best source of trifluoromethylthio group among those investigated. Finally, this new class of chiral products demonstrated to be valuable precursors of potentially useful enantioenriched α -trifluoromethylthio- $\beta^{2,2}$ -amino acids.

Chapter 5

Summary

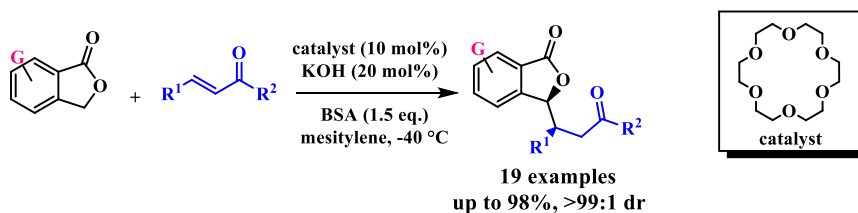
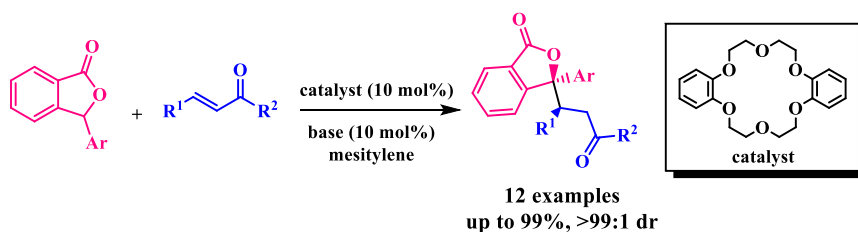


5. Summary

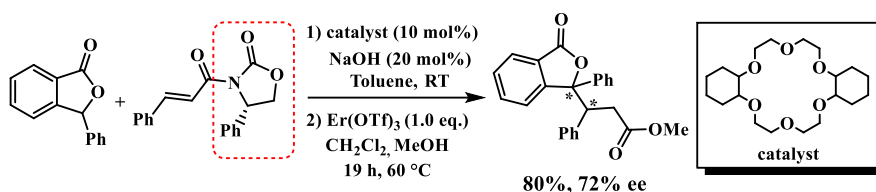
5.1 Final conclusions

In this doctoral project, the phase transfer catalysis has proved to be a powerful tool for the development of new stereoselective routes. Novel elegant diastereo- and enantio-selective methodologies for the synthesis of potentially bioactive products have been successfully advanced.

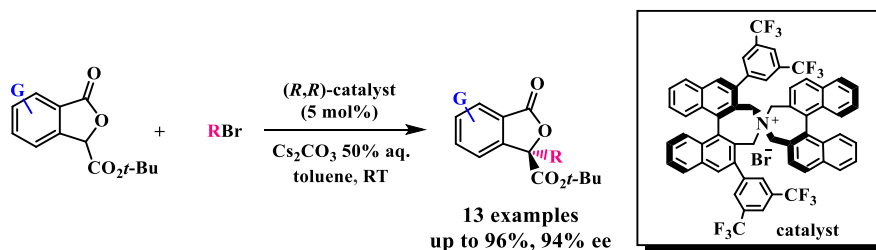
Since Phthalides are widespread in naturally occurring compounds and important scaffolds in medicinal chemistry, significant efforts have been addressed to produce novel phthalides products in a stereocontrolled manner. Two highly diastereoselective crown ether-catalyzed arylogous Michael reactions of weakly activated and unactivated Phthalides have been reported giving the easy access to new 3,3-disubstituted and 3-monosubstituted products. Both methodologies have shown to be efficient and original approaches affording high selectivities and yields with variously substituted substrates and diverse Michael acceptors.



The first example of asymmetric conjugated addition using an unactivated Michael donor and a chiral α,β -unsaturated carbonyl compound has been also studied, producing the enantioenriched 3,3-disubstituted adduct with high yield and enantiomeric excess under mild reaction conditions.

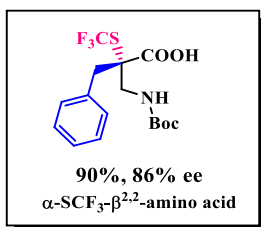
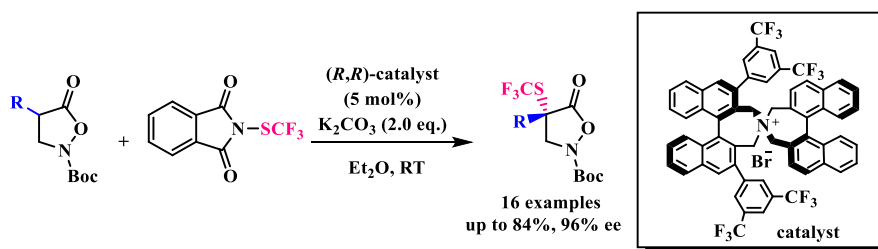
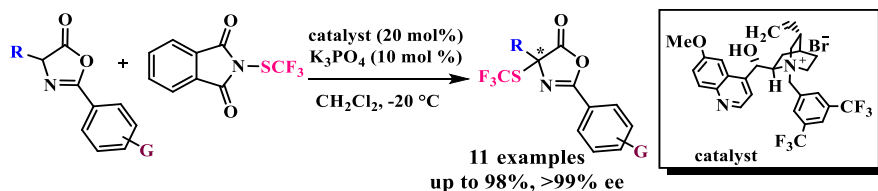


Moreover, previously undescribed chiral 3,3-disubstituted alkyl phthalides were prepared with high yields and enantiomeric ratios by the first asymmetric alkylation of 3-carboxylic-*t*-Bu-ester-phthalides with benzyl and allyl bromides. This is a novel class of powerful chiral products since they could be easily converted into chiral bioactive 3,3-dialkyl phthalides through the facile transformation of the ester group.



Finally, the development of two asymmetric trifluoromethylthiolation methodologies under phase transfer catalysis conditions was realized. Chiral quaternary ammonium salts have efficiently promoted the asymmetric introduction of the SCF₃ group at C-4 position of both azlactone and isoxazolidin-5-one substrates affording novel enantioenriched

thiofluorinated compounds with high to excellent enantiocontrol of the quaternary chiral centers and with good to excellent yields. Considering the well-known peculiar features of fluoro-containing molecules, significant pharmaceutical and medical applications of these new chiral compounds could be expected. Additionally, the first example of the valuable enantioenriched α -SCF₃- $\beta^{2,2}$ -amino acid was reported.



Chapter 6

Experimental section

6. Experimental section

6.1 General procedures

Reactions were performed using commercially available compounds without further purification and analytical grade solvents. All reactions requiring dry or inert conditions were conducted in flame dried glassware under a positive pressure of nitrogen. Molecular sieves (Aldrich Molecular Sieves 4 Å) were activated under vacuum at 200 °C overnight. All the reactions were monitored by thin layer chromatography (TLC) on precoated silica gel plates (0.25 mm) and visualized by fluorescence quenching at 254 nm. Flash chromatography was carried out using silica gel 60 (70–230 mesh, Merck). The ¹H-, ¹³C- and ¹⁹F-NMR spectra were recorded on Bruker Avance 600, 400, 300 spectrometers (600 MHz, 400 MHz, 300 MHz, ¹H; 150 MHz, 100 MHz, 75 MHz, ¹³C) at room temperature in CDCl₃, CD₃OD and CD₃CN as solvents. Spectra were referenced to residual CHCl₃ (7.26 ppm, ¹H; 77.00 ppm, ¹³C), CD₃OD (3.33 ppm, ¹H; 49.0 ppm, ¹³C) or CH₃CN (1.94 ppm, ¹H; 1.32 ppm, 118.26 ppm ¹³C) when indicated. The following abbreviations are used to indicate the multiplicity in NMR spectra: s - singlet; d - doublet; t - triplet; q - quartet; dd – double doublet; m - multiplet; bs - broad signal; hept – heptet. Coupling constants (*J*) are quoted in hertz. Yields are given for isolated products showing one spot on a TLC plate and no impurities detectable in the NMR spectrum. High-resolution mass spectra (HRMS) were acquired using a Bruker solariX XR Fourier transform ion cyclotron resonance mass spectrometer (Bruker Daltonik GmbH, Bremen, Germany) equipped with a 7 T refrigerated actively-shielded superconducting magnet or using an *Agilent Technologies 6120 Quadrupole LC/MS*. In this latter case, *MassWorks software ver. 4.0.0.0 (Cerno Bioscience)* was used for the formula identification. *MassWorks* is a MS calibration software which

calibrates for isotope profile as well as for mass accuracy allowing highly accurate comparisons between calibrated and theoretical spectra.¹³⁸ The samples were ionized in positive ion mode using electrospray ionization (ESI) or matrix-assisted laser desorption/ionization (MALDI). The optical rotation of compounds was performed on a Jasco P-2000 digital polarimeter and a Schmidt + Haensch Polarimeter Model UniPol L 1000 in cells with 10 cm path length and are reported as follows: $[\alpha]_D^T$ (c in g/100 mL, solvent). Enantiomeric excesses were determined by chiral HPLC or by Supercritical Fluid Chromatography (SFC) using CHIRALPAK® AS-H (250 x 4.6 mm, 5 μm), ID (250 x 4.6 mm, 5 μm) and IB (250 x 4.6 mm, 5 μm) columns with UV detector set at 260 nm. All ultraviolet (UV) measurements were made at 24–26 °C, using spectrophotometric grade solvents.

6.2 Diastereoselective Michael addition of weakly activated phthalides

The α,β-unsaturated carbonyl compounds were commercially available, except for **76c**,¹³⁹ **76e**¹⁴⁰ and **76f**¹⁴¹ that were prepared by methods reported in the literature.

¹³⁸ a) Y. Wang, M. Gu, *Anal. Chem.*, **2010**, 82, 7055-7062; b) Y. Wang, Methods for Operating MS Instrument Systems, United States Patent No. 6, 983, 213, **2006**; c) N. Ochiaiaia, K. Sasamoto, K. MacNamara *Journal of Chromatography A*, **2012**, 1270, 296-304; d) H.-P. Ho, R.-Y. Lee, C.-Y. Chen, S.-R. Wang, Z.-G. Li and M.-R. Lee, *Rapid Commun. Mass Spectrom.*, **2011**, 25, 25-32.

¹³⁹ C. Ni, L. Zhang, J. Hu, *J. Org. Chem.*, **2008**, 73, 5699-5713.

¹⁴⁰ S. S. Bhella, M. Elango, M. P. S. Ishar, *Tetrahedron*, **2009**, 65, 240-246.

¹⁴¹ D. A. Evans, K. T. Chapman, J. Bisaha, *J. Am. Chem. Soc.*, **1988**, 110, 1238-1256.

6.2.1 Synthesis of 3-aryl phthalides **75b-f**

Magnesium turnings (214 mg, 8.80 mmol) were introduced in a Schlenk round bottom flask fitted with a reflux condenser under nitrogen atmosphere and few crystals of iodine were added. The mixture was heated thoroughly with a heat gun until iodine vapors evolved. Then anhydrous THF (4.0 mL) was added, and the suspension was heated to reflux. A solution of 2-bromonaphthalene (1.66 g, 8.00 mmol) in anhydrous THF (4.0 mL) was added dropwise, and the resulting solution was stirred at reflux for 2 h to ensure complete formation of the Grignard reagent. The Grignard solution was slowly added to a solution of 2-formylbenzoic acid (600 mg, 4.00 mmol) in anhydrous THF (10 mL) under nitrogen at room temperature and the mixture was stirred overnight. After that, the reaction mixture was treated with 2 M HCl (10 mL) and then stirred at room temperature for 30 minutes. The resulting mixture was extracted with ethyl acetate (3 x 30 mL), dried over Na₂SO₄, filtered and concentrated in vacuo. The crude residue was purified by *flash* chromatography (silica gel, petroleum ether-ethyl acetate, 9:1 to 6:4) affording **75e** (1.03 g, 99% yield) as a white solid. The characterization data of **75e** matched those previously reported.¹⁴²

3-(4-Methoxyphenyl)isobenzofuran-1(3H)one (75b)

The same procedure as described for **75e** was employed, using 4-bromoanisole (0.500 mL, 4.00 mmol). The crude residue was purified by flash chromatography (silica gel, petroleum ether-ethyl acetate, 9:1 to 6:4) affording **75b** (321 mg, 40% yield) as a white solid. The characterization data of **75b** matched those previously reported.¹⁴³

¹⁴² Z. Ye, G. Lv, W. Wang, M. Zhang, J. Cheng, *Angew. Chem. Int. Ed.*, **2010**, *49*, 3671-3674.

¹⁴³ P. Amaladass, J. A. Clement, A. K. Mohanakrishnan, *Eur. J. Org. Chem.*, **2008**, 3798-3810.

3-(4-Methylphenyl)isobenzofuran-1(3H)one (75c)

The same procedure as described for **75e** was employed, using 4-bromotoluene (0.980 mL, 8.00 mmol). The crude residue was purified by flash chromatography (silica gel, petroleum ether to petroleum ether-ethyl acetate 7:3) affording **75c** (718 mg, 80% yield) as a white solid. The characterization data of **75c** matched those previously reported.¹⁴³

3-(4-(Trifluoromethyl)phenyl)isobenzofuran-1(3H)one (75d)

The same procedure as described for **75e** was employed, using 4-bromobenzotrifluoride (1.12 mL, 8.00 mmol). The crude residue was purified by flash chromatography (silica gel, petroleum ether to petroleum ether-ethyl acetate 1:1) affording **75d** (440 mg, 40% yield) as a white solid. The characterization data of **75d** matched those previously reported.¹⁴⁴

3-(2-Methylphenyl)isobenzofuran-1(3H)one (75f)

The same procedure as described for **75e** was employed, using 2-bromotoluene (0.960 mL, 8.00 mmol). The crude residue was purified by flash chromatography (silica gel, petroleum ether-ethyl acetate, 9:1 to 6:4) affording **175f** (802 mg, 94% yield) as a white solid. The characterization data of **175f** matched those previously reported.¹⁴²

6.2.2 General Procedure for the arylogous Michael reaction of 3-aryl phthalides

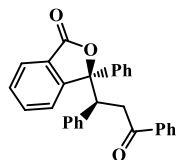
To a stirred solution of *trans*-chalcone (**76a**, 41.6 mg, 0.20 mmol) and dibenzo-18-crown-6 (**77c**, 7.2 mg, 0.020 mmol) in mesitylene (1.0 mL) were added KOH (1.1 mg, 0.020 mmol, method A) or K₃PO₄ (4.2 mg, 0.020 mmol,

¹⁴⁴ H.-T. Chang, M. Jegannmohan, C.-H. Cheng, *Chem. Eur. J.*, **2007**, 13, 4356-4363.

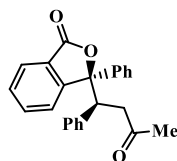
method B) and 3-phenylphthalide (**75a**, 42.0 mg, 0.20 mmol). The resulting solution was stirred at the appropriate temperature (Table 3) until the disappearance of the starting material and then brought to room temperature. The mixture was diluted with 1 M HCl (3.0 mL) and then extracted with CH₂Cl₂ (3 x 4 mL). The combined organic phases were washed with H₂O (4.0 mL), dried over Na₂SO₄, filtered and concentrated in vacuo. The crude residue was purified by *flash* chromatography (silica gel, hexane-ethyl acetate, 98:2 to 50:50) to afford **78aa** (method A: 69.5 mg, 83% yield; method B: 76.2 mg, 91% yield) as a white solid.

The reaction between **75a** and **76a** was also performed at the 1 mmol scale: To a stirred solution of *trans*-chalcone (**76a**, 208 mg, 1.00 mmol) and dibenzo-18-crown-6 (**77c**, 36.0 mg, 0.10 mmol) in mesitylene (5.0 mL) were added KOH (5.6 mg, 0.10 mmol, at 0 °C, method A) or K₃PO₄ (21.2 mg, 0.10 mmol, room temperature, method B) and 3-phenylphthalide (**75a**, 210 mg, 1.00 mmol). The resulting solution was stirred at the appropriate temperature (0 °C for the reaction with KOH, method A; room temperature for the reaction with K₃PO₄, method B) until the disappearance of the starting material (20 h for method A and 44 h for method B) and then brought to room temperature. The mixture was diluted with 1 M HCl (15 mL) and then extracted with CH₂Cl₂ (3 x 20 mL). The combined organic phases were washed with H₂O (20 mL), dried over Na₂SO₄, filtered and concentrated in vacuo. The crude residue was purified by *flash* chromatography (silica gel, hexane-ethyl acetate, 98:2 to 50:50) to afford **78aa** (method A: 377 mg, 90% yield; method B: 385 mg, 92% yield) as a white solid in >98:2 dr.

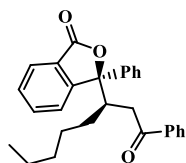
6.2.3 Analytical data of products 78aa-fd



(*R,*S**)-3-(3-Oxo-1,3-diphenylpropyl)-3-phenylisobenzofuran-1(3*H*)one (78aa):** Obtained as a white solid (method A: 69.5 mg, 83% yield; method B: 76.2 mg, 91% yield), mp 214-215 °C; ¹H NMR (400 MHz, CDCl₃) δ 7.83- 7.76 (m, 4H), 7.66 (d, *J* = 8.1 Hz, 1H), 7.56-7.26 (m, 8H), 7.24-7.18 (m, 3H), 7.01 (m, 2H), 6.95 (m, 1H), 4.73 (dd, *J* = 10.4, 2.7 Hz, 1H), 4.03 (dd, *J* = 18.0, 10.4 Hz, 1H), 3.22 (dd, *J* = 18.0, 2.7 Hz, 1H). ¹³C NMR (100 MHz, CDCl₃) δ 197.5, 169.9, 152.3, 139.8, 137.3, 136.6, 133.9, 133.0, 129.2, 129.1, 128.7, 128.4, 128.2, 127.9 (2 C), 127.0, 125.2, 124.8, 124.5, 122.2, 91.7, 48.8, 39.7. HRMS (MALDI) [*M* + Na⁺] calcd for C₂₉H₂₂NaO₃⁺ 441.1461, found 441.1460.

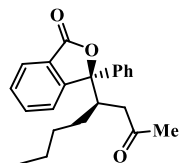


(*R,*S**)-3-(3-Oxo-1-phenylbutyl)-3-phenylisobenzofuran-1(3*H*)one (78ab):** Obtained as a white solid (method A 60.6, 85% yield; method B 61.3 mg, 86% yield), mp 181-182 °C; ¹H NMR (400 MHz, CDCl₃) δ 7.72 (d, *J* = 7.8 Hz, 2H), 7.60 (d, *J* = 7.8 Hz, 1H), 7.54-7.36 (m, 4H), 7.32 (m, 1H), 7.22 (m, 1H), 7.11 (m, 2H), 7.05-6.95 (m, 3H), 4.43 (dd, *J* = 10.2, 3.1 Hz, 1H), 3.30 (dd, *J* = 17.7, 10.2 Hz, 1H), 2.75 (dd, *J* = 17.7, 3.1 Hz, 1H), 1.89 (s, 3H). ¹³C NMR (100 MHz, CDCl₃) δ 206.4, 169.9, 152.1, 139.7, 137.1, 133.9, 129.3, 129.1, 128.7, 128.3, 128.0, 127.1, 125.3, 124.8, 124.6, 122.2, 91.4, 48.8, 44.6, 30.7. HRMS (MALDI) [*M* + Na⁺] calcd for, C₂₄H₂₀NaO₃⁺ 379.1305, found 379.1305.

**(*R*^{*},*R*^{*})-3-(1-Oxo-1-phenyloctan-3-yl)-3-****phenylisobenzofuran-1(3H)one (78ac):** Obtained as a

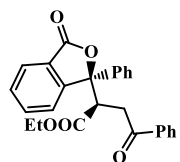
white solid (method A 73.4 mg, 89% yield; method B 76.7 mg, 93% yield), mp 65-65 °C; ¹H NMR (400 MHz, CDCl₃)

δ 7.87 (d, $J = 7.7$ Hz, 1H), 7.82 (d, $J = 7.7$ Hz, 2H), 7.67-7.55 (m, 4H), 7.53-7.44 (m, 2H), 7.38 (m, 2H), 7.27 (m, 2H), 7.17 (m, 1H), 3.65 (m, 1H), 3.15 (dd, $J = 18.2, 7.4$ Hz, 1H), 3.04 (dd, $J = 18.2, 2.4$ Hz, 1H), 1.22-0.87 (m, 8H), 0.69 (m, 3H). ¹³C NMR (100 MHz, CDCl₃) δ 198.6, 170.4, 153.0, 140.4, 136.7, 134.5, 133.0, 129.1, 128.9, 128.4, 128.0, 127.9, 125.8, 125.1, 124.6, 122.1, 93.3, 40.8, 40.3, 31.7, 30.2, 27.1, 22.2, 13.8. HRMS (MALDI) [$M + H^+$] calcd for C₂₈H₂₉O₃⁺ 413.2111, found 413.2111.

**(*R*^{*},*R*^{*})-3-(2-Oxo-octan-4-yl)-3-phenylisobenzofuran-****1(3H)one (78ad):** Obtained as a white solid (method A

53.2 mg, 79% yield; method B 58.5 mg, 87% yield), mp 65-65 °C; ¹H NMR (400 MHz, CDCl₃) δ 7.83 (m, 1H), 7.61

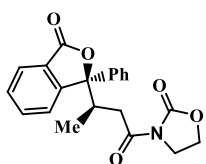
(m, 1H), 7.60-7.49 (m, 3H), 7.45 (m, 1H), 7.30 (m, 2H), 7.24 (m, 1H), 3.34 (m, 1H), 2.59 (dd, $J = 18.5, 3.3$ Hz, 1H), 2.45 (dd, $J = 18.5, 6.4$ Hz, 1H), 1.89 (s, 3H), 1.16-0.77 (m, 6H), 0.67 (m, 3H). ¹³C NMR (100 MHz, CDCl₃) δ 207.1, 170.3, 152.7, 140.4, 134.5, 129.1, 128.9, 128.1, 125.8, 125.1, 124.7, 122.0, 93.0, 45.0, 40.5, 30.1, 29.5, 29.5, 22.6, 13.7. HRMS (MALDI) [$M + Na^+$] calcd for C₂₂H₂₄NaO₃⁺ 359.1618, found 359.1618.

**(*R*^{*},*R*^{*})-Ethyl 4-oxo-2-(1,3-dihydro-1-oxo-3-****phenylisobenzofuran-3-yl)-4-phenylbutanoate (78ae):**

Obtained as a white solid (method A 35.6 mg, 43% yield; method B 53.9 mg, 65% yield), mp 33-34 °C; ¹H NMR (400

MHz, CDCl₃, major diastereomer) δ 7.89-7.82 (m, 3H), 7.79 (d, $J = 7.9$ Hz,

1H), 7.72-7.60 (m, 3H), 7.56-7.47 (m, 2H), 7.45-7.35 (m, 4H), 7.31 (m, 1H), 4.27 (dd, $J = 11.1, 2.4$ Hz, 1H), 3.94 (dd, $J = 18.3, 11.1$ Hz, 1H), 3.82-3.63 (m, 2H), 2.95 (dd, $J = 18.3, 2.4$ Hz, 1H), 0.76 (t, $J = 7.1$ Hz, 3H). ^{13}C NMR (100 MHz, CDCl_3 , major diastereomer) δ 197.6, 170.0, 169.1, 151.0, 138.9, 136.1, 134.1, 133.4, 129.5, 129.2, 128.6, 128.5, 128.1, 125.6, 124.6, 123.7, 88.9, 60.9, 49.5, 37.4, 13.5. HRMS (MALDI) $[\text{M} + \text{Na}^+]$ calcd for $\text{C}_{26}\text{H}_{22}\text{NaO}_5^+$ 437.1359, found 437.1361.

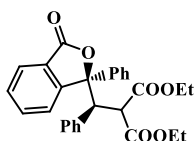


(R^*,R^*)-3-(1,3-dihydro-1-oxo-3-

phenylisobenzofuran-3-yl)butanoyl- 1,3-oxazolidin-

2-one (78af): Obtained as a white solid (method A 52.6 mg, 72% yield; method B 29.2 mg, 40% yield), mp 217-

218 °C; ^1H NMR (400 MHz, CDCl_3) δ 7.84 (d, $J = 7.6$ Hz, 1H), 7.68-7.52 (m, 4H), 7.47 (m, 1H), 7.33 (m, 2H), 7.25 (m, 1H), 4.31 (m, 2H), 3.89 (m, 2H), 3.41 (m, 1H), 3.03 (dd, $J = 17.8, 9.2$ Hz, 1H), 2.91 (dd, $J = 17.8, 3.2$ Hz, 1H), 0.73 (d, $J = 6.6$ Hz, 3H). ^{13}C NMR (100 MHz, CDCl_3) δ 172.1, 170.0, 153.1, 152.1, 139.9, 134.5, 129.2, 128.9, 128.1, 125.9, 125.4, 124.8, 122.1, 92.1, 62.0, 42.5, 37.6, 37.5, 14.4. HRMS (MALDI) $[\text{M} + \text{Na}^+]$ calcd for $\text{C}_{21}\text{H}_{19}\text{NNaO}_5^+$ 388.1155, found 388.1150.



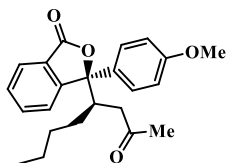
(R^*,S^*)-Diethyl2-((1,3-dihydro-1-oxo-3-

phenylisobenzofuran-3-

yl)phenylmethyl)propandioate (78ag): Obtained as a

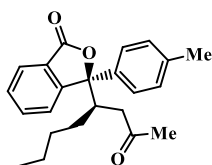
white solid (method A 77.9 mg, 85% yield; method B 80.7 mg, 88% yield), mp 33-34 °C; ^1H NMR (400 MHz, CDCl_3 , major diastereomer) δ 7.76 (d, $J = 7.7$ Hz, 2H), 7.64 (d, $J = 7.7$ Hz, 1H), 7.48 (m, 2H), 7.34 (m, 2H), 7.25 (m, 2H), 7.07 (m, 2H), 6.99 (m, 3H), 4.69 (d, $J = 10.6$ Hz, 1H), 4.34 (d, $J = 10.6$ Hz, 1H), 3.80-3.62 (m, 3H), 3.43 (m, 1H), 1.04 (t, $J = 7.1$ Hz, 3H), 0.80 (t, J

= 7.1 Hz, 3H). ^{13}C NMR (100 MHz, CDCl_3 , major diastereomer) δ 169.2, 167.7, 167.1, 151.7, 138.1, 135.5, 133.7, 129.8, 128.9, 128.4, 128.3, 127.7, 127.4, 126.1, 125.4, 125.1, 123.0, 90.1, 61.6, 61.4, 54.2, 53.4, 13.6, 13.4. HRMS (MALDI) $[\text{M} + \text{Na}^+]$ calcd for $\text{C}_{28}\text{H}_{26}\text{NaO}_6^+$ 481.1622, found 481.1614.



(*R,*R**)-3-(2-Oxo-octan-4-yl)-3-(4-methoxyphenyl)isobenzofuran- 1(3*H*)one (78bd):**

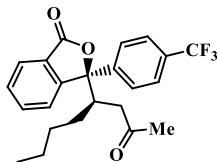
Obtained as a white solid (method A 58.6 mg, 80% yield; method B 68.9 mg, 94% yield), mp 88-89 °C; ^1H NMR (400 MHz, CDCl_3) δ 7.84 (d, $J = 7.7$ Hz, 1H), 7.62 (m, 1H), 7.52 (d, $J = 7.7$ Hz, 1H), 7.49-7.40 (m, 3H), 6.84 (d, $J = 8.9$ Hz, 2H), 3.75 (s, 3H), 3.31 (m, 1H), 2.62 (dd, $J = 18.5, 3.4$ Hz, 1H), 2.45 (dd, $J = 18.5, 6.6$ Hz, 1H), 1.94 (s, 3H), 1.14-0.82 (m, 6H), 0.69 (m, 3H). ^{13}C NMR (100 MHz, CDCl_3) δ 207.2, 170.3, 159.3, 153.0, 134.4, 132.3, 129.0, 126.0, 125.8, 125.2, 121.9, 114.2, 92.9, 55.2, 45.1, 40.5, 30.1, 29.6, 29.5, 22.6, 13.7. HRMS (MALDI) $[\text{M} + \text{Na}^+]$ calcd for $\text{C}_{23}\text{H}_{26}\text{NaO}_4^+$ 389.1723, found 389.1723.



(*R,*R**)-3-(2-Oxo-octan-4-yl)-3-(4-methylphenyl)isobenzofuran- 1(3*H*)one (78cd):**

Obtained as a white solid (method A 54.7 mg, 78% yield; method B 23.8 mg, 34% yield), mp 98-99 °C; ^1H NMR (400 MHz, CDCl_3) δ 7.83 (d, $J = 7.6$ Hz, 1H), 7.61 (m, 1H), 7.54 (d, $J = 7.6$ Hz, 1H), 7.45 (m, 1H), 7.40 (d, $J = 8.2$ Hz, 2H), 7.12 (d, $J = 8.2$ Hz, 2H), 3.33 (m, 1H), 2.61 (dd, $J = 18.5, 3.3$ Hz, 1H), 2.46 (dd, $J = 18.5, 6.7$ Hz, 1H), 2.27 (s, 3H), 1.92 (s, 3H), 1.14-0.80 (m, 6H), 0.68 (m, 3H). ^{13}C NMR (100 MHz, CDCl_3) δ 207.1, 170.3, 152.9, 137.8, 137.4, 134.4, 129.5, 128.9, 125.7, 125.1, 124.5, 121.9, 93.0, 45.0, 40.4, 30.1, 29.5, 29.5, 22.5,

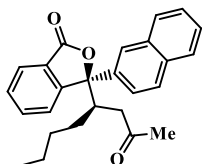
20.8, 13.7. HRMS (MALDI) $[M + H^+]$ calcd for $C_{23}H_{27}O_3^+$ 351.1955, found 351.1955.



(*R*,R)-3-(2-Oxo-octan-4-yl)-3-(4-(trifluoromethyl)phenyl)isobenzofuran-1(3*H*)one**

(78dd): Obtained as a white solid (method A 55.4 mg, 99% yield), mp 73-74 °C; 1H NMR (400 MHz, $CDCl_3$)

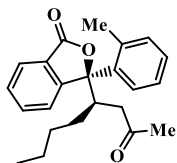
δ 7.87 (d, $J = 7.6$ Hz, 1H), 7.72-7.64 (m, 3H), 7.61- 7.54 (m, 3H), 7.50 (t, $J = 7.6$ Hz, 1H), 3.39 (m, 1H), 2.59-2.46 (m, 2H), 1.95 (s, 3H), 1.14-0.81 (m, 6H), 0.69 (m, 3H). ^{13}C NMR (100 MHz, $CDCl_3$) δ 206.7, 169.8, 151.9, 144.5, 134.8, 130.4 (q, $J = 32.7$ Hz), 129.5, 126.0, 125.9 (q, $J = 3.1$ Hz), 125.2, 125.1, 123.7 (q, $J = 272.2$ Hz), 121.9, 92.4, 45.0, 40.2, 30.0, 29.5, 29.4, 22.5, 13.7. HRMS (MALDI) $[M + Na^+]$ calcd for $C_{23}H_{23}F_3NaO_3^+$ 427.1492, found 427.1492.



(*R*,R)-3-(2-Oxo-octan-4-yl)-3-(2-naphthyl)isobenzofuran-1(3*H*)one (78ed):** Obtained as

a white solid (method A 58.7 mg, 76% yield; method B 41.0 mg, 53% yield), mp 116-117 °C; 1H NMR (400

MHz, $CDCl_3$) δ 8.00 (m, 1H), 7.89-7.73 (m, 4H), 7.67-7.58 (m, 3H), 7.50-7.41 (m, 3H), 3.50 (m, 1H), 2.65 (dd, $J = 18.6, 3.2$ Hz, 1H), 2.53 (dd, $J = 18.6, 6.8$ Hz, 1H), 1.87 (s, 3H), 1.19-0.-91 (m, 6H), 0.70 (m, 3H). ^{13}C NMR (100 MHz, $CDCl_3$) δ 207.0, 170.3, 152.6, 137.6, 134.5, 133.0, 132.6, 129.1, 128.9, 128.2, 127.4, 126.6, 126.5, 125.8, 125.1, 123.6, 122.4, 122.0, 93.1, 45.1, 40.2, 30.0, 29.6, 29.5, 22.6, 13.7. HRMS (MALDI) $[M + Na^+]$ calcd for $C_{26}H_{26}NaO_3^+$ 409.1774, found 409.1776.

**(*R*^{*},*R*^{*})-3-(2-Oxo-octan-4-yl)-3-(2-****methylphenyl)isobenzofuran-1(3*H*)one (78fd):** Obtained

as a white solid (method A 55.4 mg, 79% yield), mp 92-93 °C; ¹H NMR (400 MHz, CDCl₃) δ 7.90 (d, *J* = 7.6 Hz, 1H), 7.64 (m, 1H), 7.57-7.42 (m, 3H), 7.22-7.07 (m, 3H), 3.51 (m, 1H), 2.58 (dd, *J* = 18.5, 2.8 Hz, 1H), 2.44 (m, dd, *J* = 18.5, 7.1 Hz, 1H), 2.34 (s, 3H), 2.04 (s, 3H), 1.11-0.80 (m, 6H), 0.67 (m, 3H). ¹³C NMR (100 MHz, CDCl₃) δ 207.0, 170.4, 151.3, 136.9, 136.8, 134.2, 133.6, 129.1, 128.2, 126.7, 126.6, 126.2, 125.3, 123.1, 94.8, 46.0, 40.4, 30.2, 29.9, 29.6, 22.6 (2 C), 13.7. HRMS (MALDI) [*M* + Na⁺] calcd for C₂₃H₂₆NaO₃⁺ 373.1774, found 373.1774.

6.2.4 Procedure for the reaction of **75a** with **76a** catalyzed by **TBAB** and **KOH**

To a stirred solution of *trans*-chalcone (**76a**, 41.6 mg, 0.20 mmol) and tetrabutylammonium bromide (TBAB, 6.4 mg, 0.020 mmol) in mesitylene (1.0 mL) were added KOH (1.1 mg, 0.020 mmol) and 3-phenylphthalide (**75a**, 42.0 mg, 0.20 mmol). The resulting solution was stirred at room temperature for 68 h. After that time the reaction mixture was diluted with 1 M HCl (3.0 mL) and extracted with CH₂Cl₂ (3 x 4 mL). The combined organic phases were washed with H₂O (4.0 mL), dried over Na₂SO₄, filtered and concentrated in vacuo. The crude residue was purified by *flash* chromatography (silica gel, hexane-ethyl acetate, 98:2 to 50:50) to afford **3aa** (58.5 mg, 70% yield) as a white solid in 92:8 dr.

6.2.5 X-ray crystallography

Colorless needle-like single crystals of compound **78aa** suitable for X-ray diffraction analysis were obtained by slow evaporation of a solution of chloroform/toluene (2:1) dissolving 5 mg of the compound in 0.8 ml of chloroform and adding 0.4 ml of toluene. A crystal of 0.43 mm x 0.24 mm x 0.18 mm was selected and mounted on a cryoloop with paratone oil and measured at 100 K. Colorless needle-like single crystals of compound **78ag** suitable for X-ray diffraction analysis were obtained by slow evaporation of a solution obtained by dissolving 4 mg of the compound in 1.5 ml of hot methanol. A crystal of 0.37 mm x 0.24 mm x 0.16 mm was selected and mounted on a cryoloop with paratone oil and measured at 100 K. In both cases X-ray diffraction measurements were performed with a Rigaku AFC7S diffractometer equipped with a Mercury CCD detector using graphite monochromated MoK α radiation ($\lambda = 0.71069 \text{ \AA}$). Data reduction was performed with the crystallographic package CrystalClear. Data were corrected for Lorentz, polarization and absorption. The structure was solved by direct methods using the program SIR2014¹⁴⁵ and refined by means of full matrix least-squares based on F2 using the program SHELXL.¹⁴⁶ Non-hydrogen atoms were refined anisotropically, hydrogen atoms were positioned geometrically and included in structure factors calculations but not refined. ORTEP diagrams were drawn using OLEX2 (Fig. S1).¹⁴⁷

¹⁴⁵ M. C. Burla, R. Caliendo, B. Carrozzini, G. L. Cascarano, C. Cuocci, C. Giacovazzo, M. Mallamo, A. Mazzone, G. J. Polidori, *Appl. Cryst.*, **2015**, *48*, 306-309.

¹⁴⁶ G. M. Sheldrick, *Acta Cryst. C*, **2015**, *71*, 3-8.

¹⁴⁷ O. V. Dolomanov, L. J. Bourhis, R. J. Gildea, J. A. K. Howard, H. Puschmann, *J. Appl. Cryst.*, **2009**, *42*, 339-341.

	78aa	78ag
T (K)	100	100
Formula	C ₂₉ H ₂₂ O ₃	C ₂₈ H ₂₆ O ₆
Formula weight	418.46	458.49
System	Triclinic	Triclinic
Space group	<i>P</i>	<i>P</i>
<i>a</i> (Å)	9.229(7)	11.5473(19)
<i>b</i> (Å)	11.780(9)	11.750(2)
<i>c</i> (Å)	11.881(8)	18.402(3)
α (°)	116.064(7)	78.259(9)
β (°)	93.344(8)	74.402(8)
γ (°)	103.846(15)	88.332(10)
<i>V</i> (Å ³)	1106.6(14)	2353.8(7)
<i>Z</i>	2	4
<i>D_x</i> (g cm ⁻³)	1.256	1.294
λ (Å)	0.71073	0.71073
μ (mm ⁻¹)	0.080	0.091
<i>F</i> 000	440	968
R1 (<i>I</i> > 2 σ <i>I</i>)	0.0639 (2768)	0.0919 (4117)
wR2 (all)	0.1732 (4974)	0.2825 (10619)
N. of param.	290	618
GooF	0.991	0.955
ρ_{min} , ρ_{max} (eÅ ⁻³)	0.29, -0.25	0.58, -0.41

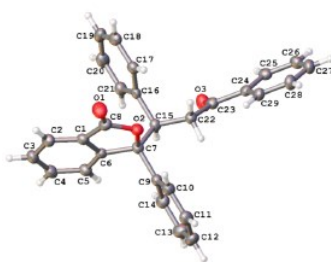
Table S1 Crystallographic data for compounds **3aa** and **3ag**

Fig. S1. ORTEP diagram for compound **3aa**. Atom types: C grey, O red, S red, H white. Ellipsoids are drawn at 50% probability level.

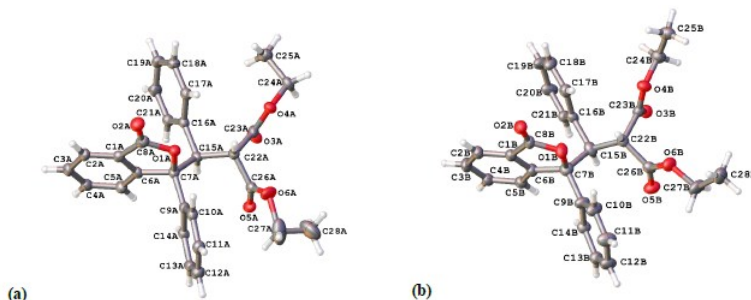


Fig. S2. ORTEP diagrams for compound **3ag**: (a) conformer A and (b) conformer B. Atom types: C grey, O red, H white. Ellipsoids are drawn at 50% probability level.

6.3 Diastereoselective Michael addition of unactivated phthalides

6.3.1 Synthesis of substrates

Phthalide **79a** and α,β -unsaturated carbonyl compounds **76a**, **76b**, **76d**, **76l-n** were commercially available. Phthalides **79b**,¹⁴⁸ **79c**,¹⁴⁹ **79d**,¹⁵⁰ **79e**,¹⁵⁰ and α,β -unsaturated ketone **76k**,¹⁵¹ were prepared by methods reported in the literature. The other substrates were prepared as follows.

Trans-chalcones **76c** and **76e-j**

Trans-chalcones were obtained by aldol reaction of the corresponding acetophenone and aromatic or heteroaromatic aldehyde.¹⁵²

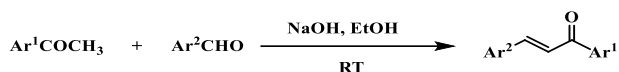
¹⁴⁸ J. Wang, D. M. Johnson, *Polym. Int.*, **2009**, *58*, 1234-1245.

¹⁴⁹ S. C. Koeberle, S. Fischer, D. Schollmeyer, V. Schattel, C. Grütter, D. Rauh, S. A. Laufer, *J. Med. Chem.*, **2012**, *55*, 5868-5877.

¹⁵⁰ Y.-H. Zhang, B.-F. Shi, J.-Q. Yu, *Angew. Chem.*, **2009**, *121*, 6213-6216; *Angew. Chem. Int. Ed.*, **2009**, *48*, 6097-6100.

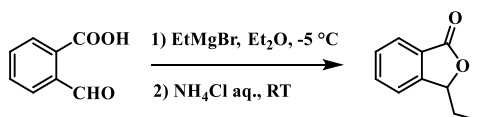
¹⁵¹ a) C. Ni, L. Zhang, J. Hu, *J. Org. Chem.*, **2008**, *73*, 5699-5713; b) H.-Y. Bi, F.-P. Liu, C. Liang, G.-F. Su, D.-L. Moa, *Adv. Synth. Catal.*, **2018**, *360*, 1510-1516.

¹⁵² E. P. Kohler, H. M. Chadwell, *Organic Synthesis*; Wiley, **1941**; Collect., Vol. 1, pp 78-79.



The appropriate acetophenone (8.3 mmol) and aromatic aldehyde (8.3 mmol) were sequentially added to a solution of sodium hydroxide (10.8 mmol) in 70:30 H₂O-EtOH mixture (7.2 mL) at room temperature. The resulting mixture was stirred at room temperature for 3 h, then kept at 0 °C overnight. The white precipitate formed was filtered on a large Büchner funnel, washed with water and cold ethanol, and dried under vacuum. The crude residue was purified by flash chromatography (silica gel, hexane-diethyl ether, 95-5 to 90-10) affording products **76c** (81% yield), **76e** (85% yield), **76f** (91% yield), **76g** (83% yield), **76h** (77% yield), **76i** (70% yield), **76j** (79% yield) as white solids. The characterization data of **76c**,¹⁵³ **76e**,¹⁵⁴ **76f**,¹⁵⁵ **76g**,¹⁵⁴ **76h-j**,¹⁵⁶ matched those reported in the literature.

3-Ethylphthalide **81a**



In a Schlenk round bottom flask, a solution of 2-carboxybenzaldehyde (1.00 g, 6.67 mmol) in anhydrous diethyl ether (20 mL) was added dropwise to ethylmagnesium bromide solution 3.0 M in diethyl ether (33.3 mmol, 3.7 mL) at -5 °C. After completing the addition, the reaction mixture was allowed to warm to room temperature and stirred for 20 h. Then the reaction was treated with a saturated NH₄Cl aqueous solution (40 mL), acidified with

¹⁵³ J.-L. Zuo, J.-X. Yanga, F.-Z. Wang, X.-N. Dang, J.-L. Sun, D.-C. Zoub, Y.-P. Tian, N. Lin, X.-T. Tao, M.-H. Jiang, *J. Photochem. Photobiol. A: Chem.*, **2008**, *199*, 322-329.

¹⁵⁴ C. Downey, H. M. Glist, A. Takashima, S. R. Bottum, G. J. Dixon, *Tetrahedron Lett.*, **2018**, *59*, 3080-3083.

¹⁵⁵ H. Lebel, M. Davi, *Adv. Synth. Catal.*, **2008**, *350*, 2352-2358.

¹⁵⁶ J. R. Schmink, J. L. Holcomb, N. E. Leadbeater, *Org. Lett.*, **2009**, *11*, 365-368.

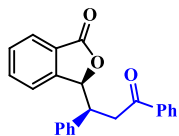
1 M HCl to pH 2 and stirred at room temperature for 1 h. The resulting mixture was extracted with diethyl ether (3 x 50 mL), dried over anhydrous Na₂SO₄ and evaporated in vacuo. The crude residue was purified by flash chromatography (silica gel, hexane-ethyl acetate, 90-10 to 85-15) affording **81a** (0.81 g, 77% yield) as a white solid. The characterization data of **81a** matched those previously reported.¹⁵⁷

6.3.2 General Procedure for the arylogous Michael reaction of unactivated phthalides

To a stirred solution of *trans*-chalcone **76a** (41.6 mg, 0.20 mmol), 18-crown-6 (18C6, 5.3 mg, 0.02 mmol) and KOH (2.2 mg, 0.04 mmol) in mesitylene (1.0 mL) at -40 °C, phthalide **79a** (26.8 mg, 0.20 mmol) and *N,O*-Bis(trimethylsilyl)acetamide (BSA, 61.0 mg, 0.30 mmol) were added. The mixture was stirred at -40 °C and monitored by TLC until the disappearance of the starting material. Then the solution was treated with 1 M HCl (1.0 mL) and THF (3.0 mL) and stirred at room temperature for 2 h. The resulting mixture was diluted with H₂O (1.0 mL) and extracted with CH₂Cl₂ (3 x 3 mL). The combined organic phases were dried over Na₂SO₄ and concentrated in vacuo. The crude residue was purified by flash chromatography (silica gel, toluene) affording **80aa** (61.6 mg, 96% yield) as a white solid.

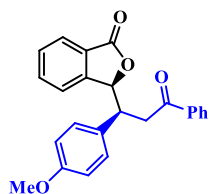
6.3.3 Analytical data of arylogous Michael adducts of phthalides

¹⁵⁷ K. Knepper, R. E. Ziegert, S. Bräse, *Tetrahedron*, **2004**, *60*, 8591-8603.



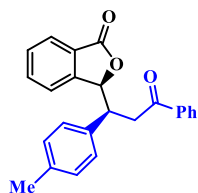
(*S*^{*})-3-((*S*^{*})-3-oxo-1,3-diphenylpropyl)isobenzofuran-1(3*H*)-one (80aa):

Obtained as a white solid (61.6 mg, 96% yield), mp 147-148 °C. ¹H NMR (400 MHz, CDCl₃) δ 8.00 (d, *J* = 7.5 Hz, 2H), 7.64-7.50 (m, 4H), 7.46 (t, *J* = 7.5 Hz, 2H), 7.32 (t, *J* = 7.5 Hz, 1H), 7.12-6.97 (m, 5H), 5.87 (bs, 1H), 4.16 (m, 1H), 3.94 (dd, *J* = 18.0, 8.3 Hz, 1H), 3.56 (dd, *J* = 18.0, 5.5 Hz, 1H). ¹³C NMR (100 MHz, CDCl₃) δ 197.9, 170.2, 148.2, 136.6, 136.4, 133.5, 133.3, 128.8 (2 C), 128.6, 128.0, 127.9, 127.0, 126.2, 125.2, 122.2, 82.4, 43.8, 40.4. HRMS (MALDI) [*M* + *H*⁺] calcd for C₂₃H₁₉O₃⁺ 343.1329, found 343.1318.



(*S*^{*})-3-((*S*^{*})-1-(4-methoxyphenyl)-3-oxo-3-phenylpropyl)isobenzofuran-1(3*H*)-one (80ab):

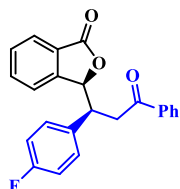
Obtained as a white solid (71.4 mg, 96% yield), mp 210-211 °C. ¹H NMR (400 MHz, CDCl₃) δ 7.99 (d, *J* = 7.8 Hz, 2H), 7.65-7.49 (m, 4H), 7.45 (t, *J* = 7.6 Hz, 2H), 7.33 (t, *J* = 7.5 Hz, 1H), 6.97 (d, *J* = 8.5 Hz, 2H), 6.58 (d, *J* = 8.5 Hz, 2H), 5.82 (d, *J* = 1.9 Hz, 1H), 4.10 (m, 1H), 3.88 (dd, *J* = 18.0, 8.3 Hz, 1H), 3.61 (s, 3H), 3.52 (dd, *J* = 18.0, 5.7 Hz, 1H). ¹³C NMR (100 MHz, CDCl₃) δ 198.0, 170.3, 158.3, 148.4, 136.7, 133.6, 133.3, 129.8, 128.7, 128.6, 128.4, 127.9, 126.2, 125.2, 122.1, 113.3, 82.7, 54.8, 43.1, 40.6. HRMS (MALDI) [*M* + Na⁺] calcd for C₂₄H₂₀NaO₄⁺ 395.1254, found 395.1240.



(*S*^{*})-3-((*S*^{*})-3-oxo-3-phenyl-1-(p-tolyl)propyl)isobenzofuran-1(3*H*)-one (80ac):

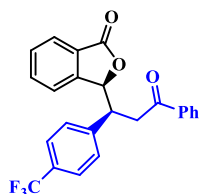
Obtained as a white solid (69.8 mg, 98% yield), mp 260-261 °C. ¹H NMR (600 MHz, CDCl₃) δ 8.01 (m, 2H), 7.65-7.56 (m, 3H), 7.53 (d, *J* = 7.6 Hz, 1H), 7.48 (t, *J* = 7.6 Hz, 2H), 7.35 (t, *J* =

7.6 Hz, 1H), 6.95 (d, $J = 8.0$ Hz, 2H), 6.87 (d, $J = 8.0$ Hz, 2H), 5.85 (d, $J = 2.5$ Hz, 1H), 4.13 (m, 1H), 3.92 (dd, $J = 18.0, 8.4$ Hz, 1H), 3.52 (dd, $J = 18.0, 5.5$ Hz, 1H), 2.14 (s, 3H). ^{13}C NMR (150 MHz, CDCl_3) δ 198.2, 170.4, 148.4, 136.8, 136.7, 133.6, 133.4, 128.8, 128.8, 128.7, 128.7, 128.0, 126.4, 125.3, 122.3, 82.7, 43.6, 40.6, 20.8. HRMS (MALDI) $[\text{M} + \text{H}^+]$ calcd for $\text{C}_{24}\text{H}_{21}\text{O}_3^+$ 357.1485, found 357.1473.



(*S*^{*})-3-((*S*^{*})-1-(4-fluorophenyl)-3-oxo-3-phenylpropyl)isobenzofuran-1(3*H*)-one (80ad):

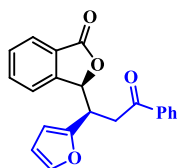
Obtained as a white solid (64.1 mg, 89% yield), mp 166–167 °C. ^1H NMR (400 MHz, CDCl_3) δ 8.01 (d, $J = 8.2$ Hz, 2H), 7.67–7.52 (m, 4H), 7.49 (t, $J = 7.5$ Hz, 2H), 7.37 (t, $J = 7.5$ Hz, 1H), 7.03 (m, 2H), 6.75 (m, 2H), 5.84 (bs, 1H), 4.15 (m, 1H), 3.93 (dd, $J = 18.0, 8.1$ Hz, 1H), 3.56 (dd, $J = 18.0, 5.5$ Hz, 1H). ^{13}C NMR (100 MHz, CDCl_3) δ 197.7, 170.2, 161.8 (d, $J_{\text{CF}} = 246$ Hz), 148.2, 136.6, 133.8, 133.6, 132.2, 130.4 (d, $J_{\text{CF}} = 8$ Hz), 129.0, 128.8, 128.1, 126.2, 125.5, 122.1, 115.0 (d, $J_{\text{CF}} = 21$ Hz), 82.5, 43.4, 40.8. HRMS (MALDI) $[\text{M} + \text{Na}^+]$ calcd for $\text{C}_{23}\text{H}_{17}\text{FNaO}_3^+$ 383.1054, found 383.1040.



(*S*^{*})-3-((*S*^{*})-3-oxo-3-phenyl-1-(4-(trifluoromethyl)phenyl)propyl)isobenzofuran-1(3*H*)-one (80ae):

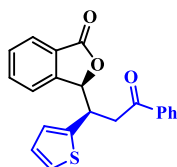
Obtained as a white solid (31.2 mg, 38% yield), mp 160–161 °C. ^1H NMR (400 MHz, CDCl_3) δ 8.02 (m, 2H), 7.66–7.56 (m, 4H), 7.50 (t, $J = 7.7$ Hz, 2H), 7.39 (t, $J = 7.5$ Hz, 1H), 7.33 (d, $J = 8.2$ Hz, 2H), 7.21 (d, $J = 8.2$ Hz, 2H), 5.88 (d, $J = 2.5$ Hz, 1H), 4.23 (m, 1H), 3.97 (dd, $J = 18.1, 8.0$ Hz, 1H), 3.62 (dd, $J = 18.1, 5.8$ Hz, 1H). ^{13}C NMR (100 MHz, CDCl_3) δ 197.5, 170.0, 147.9, 140.8, 136.5, 134.0, 133.7, 129.5 (q, $J_{\text{CF}} = 32$ Hz), 129.3,

129.3, 128.8, 128.1, 126.2, 125.7, 125.1 (m), 123.9 (q, $J_{CF} = 273$ Hz), 122.1, 82.2, 43.9, 40.6. HRMS (MALDI) $[M + H^+]$ calcd for $C_{24}H_{18}F_3O_3^+$ 411.1203, found 411.1209.



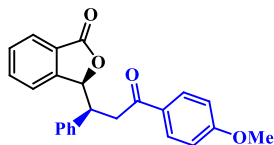
(*S*^{*})-3-((*R*^{*})-1-(furan-2-yl)-3-oxo-3-phenylpropyl)isobenzofuran-1(3*H*)-one (80af):

Obtained as a white solid (65.1 mg, 98% yield), mp 203-204 °C. 1H NMR (600 MHz, $CDCl_3$) δ 7.99 (m, 2H), 7.77 (d, $J = 7.6$ Hz, 1H), 7.64 (t, $J = 7.6$ Hz, 1H), 7.59 (t, $J = 7.6$ Hz, 1H), 7.51-7.44 (m, 3H), 7.41 (d, $J = 7.6$ Hz, 1H), 7.11 (d, $J = 1.8$ Hz, 1H), 6.10 (dd, $J = 3.2, 1.8$ Hz, 1H), 5.93 (d, $J = 3.2$ Hz, 1H), 5.84 (d, $J = 2.9$ Hz, 1H), 4.36 (m, 1H), 3.68 (dd, $J = 17.9, 7.3$ Hz, 1H), 3.45 (dd, $J = 17.9, 6.6$ Hz, 1H). ^{13}C NMR (150 MHz, $CDCl_3$) δ 197.5, 170.2, 151.1, 147.8, 141.7, 136.5, 133.8, 133.5, 129.2, 128.7, 128.1, 126.4, 125.4, 122.5, 110.2, 107.8, 81.4, 38.3, 38.1. HRMS (MALDI) $[M + H^+]$ calcd for $C_{21}H_{17}O_4^+$ 333.1121, found 333.1126.



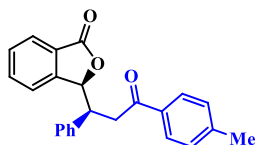
(*S*^{*})-3-((*R*^{*})-3-oxo-3-phenyl-1-(thiophen-2-yl)propyl)isobenzofuran-1(3*H*)-one (80ag):

Obtained as a white solid (53.0 mg, 76% yield), mp 237-238 °C. 1H NMR (600 MHz, $CDCl_3$) δ 8.01 (m, 2H), 7.69 (d, $J = 7.7$ Hz, 1H), 7.66-7.57 (m, 2H), 7.54 (d, $J = 7.7$ Hz, 1H), 7.49 (t, $J = 7.7$ Hz, 2H), 7.41 (t, $J = 7.5$ Hz, 1H), 6.96 (dd, $J = 4.6, 1.7$ Hz, 1H), 6.73-6.69 (m, 2H), 5.85 (d, $J = 2.5$ Hz, 1H), 4.50 (m, 1H), 3.91 (dd, $J = 18.0, 8.4$ Hz, 1H), 3.57 (dd, $J = 18.0, 5.4$ Hz, 1H). ^{13}C NMR (150 MHz, $CDCl_3$) δ 197.6, 170.3, 148.1, 138.7, 136.6, 133.8, 133.6, 129.1, 128.8, 128.1, 126.5, 126.4, 126.3, 125.4, 124.6, 122.2, 81.9, 42.1, 39.6. HRMS (MALDI) $[M + Na^+]$ calcd for $C_{21}H_{16}NaO_3S^+$ 371.0712, found 371.0702.



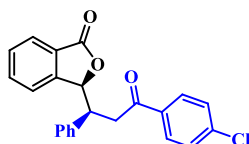
(S*)-3-((S*)-3-(4-methoxyphenyl)-3-oxo-1-phenylpropyl)isobenzofuran-1(3H)-one (80ah):

Obtained as a white solid (72.2 mg, 97% yield), mp 208-209 °C. ¹H NMR (600 MHz, CDCl₃) δ 8.01 (d, *J* = 8.7 Hz, 2H), 7.63-7.57 (m, 2H), 7.54 (d, *J* = 7.7 Hz, 1H), 7.34 (t, *J* = 7.5 Hz, 1H), 7.09-7.00 (m, 5H), 6.95 (d, *J* = 8.7 Hz, 2H), 5.87 (d, *J* = 2.5 Hz, 1H), 4.15 (m, 1H), 3.91 (dd, *J* = 17.7, 8.5 Hz, 1H), 3.88 (s, 3H), 3.49 (dd, *J* = 17.7, 5.3 Hz, 1H). ¹³C NMR (150 MHz, CDCl₃) δ 196.6, 170.4, 163.8, 148.4, 136.7, 133.6, 130.4, 129.9, 128.9, 128.8, 128.1, 127.1, 126.3, 125.3, 122.3, 113.9, 82.6, 55.5, 44.2, 40.1. HRMS (MALDI) [M + Na⁺] calcd for C₂₄H₂₀NaO₄⁺ 395.1254, found 395.1239.



(S*)-3-((S*)-3-oxo-1-phenyl-3-(p-tolyl)propyl)isobenzofuran-1(3H)-one (80ai):

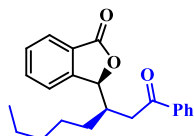
Obtained as a white solid (69.1 mg, 97% yield), mp 239-240 °C. ¹H NMR (600 MHz, CDCl₃) δ 7.92 (d, *J* = 8.2 Hz, 2H), 7.63-7.57 (m, 2H), 7.54 (m, 1H), 7.34 (t, *J* = 7.5 Hz, 1H), 7.28 (d, *J* = 7.9 Hz, 2H), 7.09-7.00 (m, 5H), 5.87 (d, *J* = 2.6 Hz, 1H), 4.16 (m, 1H), 3.94 (dd, *J* = 17.9, 8.5 Hz, 1H), 3.52 (dd, *J* = 17.9, 5.4 Hz, 1H), 2.42 (s, 3H). ¹³C NMR (150 MHz, CDCl₃) δ 197.7, 170.4, 148.4, 144.4, 136.6, 134.3, 133.6, 129.4, 129.0, 128.9, 128.2, 128.1, 127.2, 126.4, 125.3, 122.3, 82.6, 44.1, 40.4, 21.6. HRMS (MALDI) [M + H⁺] calcd for C₂₄H₂₁O₃⁺ 357.1485, found 357.1474.



(S*)-3-((S*)-3-(4-chlorophenyl)-3-oxo-1-phenylpropyl)isobenzofuran-1(3H)-one (80aj):

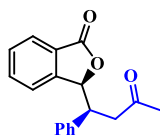
Obtained as a white solid (70.8 mg, 94% yield), mp 135-136 °C. ¹H NMR (400 MHz, CDCl₃) δ 7.94 (d, *J* = 8.5 Hz, 2H), 7.59 (t, *J* = 7.6 Hz, 1H), 7.52 (d, *J* = 7.6 Hz, 1H), 7.44 (d, *J* = 8.4 Hz, 2H), 7.34 (d, *J*

= 7.6 Hz, 2H), 7.10-6.94 (m, 5H), 5.85 (s, 1H), 4.14 (m, 1H), 3.89 (dd, $J = 18.1, 8.3$ Hz, 1H), 3.53 (dd, $J = 18.1, 5.6$ Hz, 1H). ^{13}C NMR (100 MHz, CDCl_3) δ 196.8, 170.2, 148.2, 139.9, 136.3, 134.9, 133.6, 129.4, 129.0, 128.9, 128.8, 128.1, 127.2, 126.2, 125.3, 122.2, 82.4, 43.9, 40.4. HRMS (MALDI) $[\text{M} + \text{H}^+]$ calcd for $\text{C}_{23}\text{H}_{18}\text{ClO}_3^+$ 377.0939, found 377.0927.



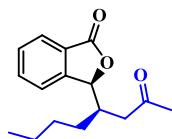
(*S)-3-((*R**)-1-oxo-1-phenyloctan-3-yl)isobenzofuran-1(3*H*)-one (80ak):**

Obtained as a white solid (65.9 mg, 98% yield), mp 201-202 °C. ^1H NMR (600 MHz, CDCl_3) δ 8.02 (m, 2H), 7.90 (d, $J = 7.6$ Hz, 1H), 7.71 (t, $J = 7.5$ Hz, 1H), 7.62-7.52 (m, 3H), 7.49 (m, 2H), 5.67 (d, $J = 2.2$ Hz, 1H), 3.44 (dd, $J = 17.9, 8.8$ Hz, 1H), 3.07 (dd, $J = 17.9, 4.3$ Hz, 1H), 2.88 (m, 1H), 1.24-0.99 (m, 6H), 0.96-0.80 (m, 2H), 0.77 (t, $J = 7.1$, 3H). ^{13}C NMR (100 MHz, CDCl_3) δ 199.4, 170.7, 148.9, 137.0, 134.1, 133.4, 129.2, 128.7, 128.1, 126.8, 125.6, 122.1, 83.3, 39.5, 37.4, 31.6, 26.9, 26.8, 22.3, 13.8. HRMS (MALDI) $[\text{M} + \text{H}^+]$ calcd for $\text{C}_{22}\text{H}_{25}\text{O}_3^+$ 337.1798, found 337.1789.



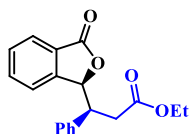
(*S)-3-((*S**)-3-oxo-1-phenylbutyl)isobenzofuran-1(3*H*)-one (80al):**

Obtained as a white solid (40.9 mg, 73% yield), mp 195-196 °C. ^1H NMR (600 MHz, CDCl_3) δ 7.62-7.55 (m, 2H), 7.45 (d, $J = 7.6$ Hz, 1H), 7.33 (t, $J = 7.6$ Hz, 1H), 7.09-7.01 (m, 3H), 6.98 (m, 2H), 5.76 (d, $J = 2.7$ Hz, 1H), 3.92 (m, 1H), 3.36 (dd, $J = 18.1, 8.4$ Hz, 1H), 3.01 (dd, $J = 18.1, 5.8$ Hz, 1H), 2.20 (s, 3H). ^{13}C NMR (150 MHz, CDCl_3) δ 206.7, 170.2, 148.2, 136.3, 133.6, 128.9, 128.8, 128.1, 127.2, 126.3, 125.3, 122.3, 82.4, 45.2, 43.7, 30.6. HRMS (MALDI) $[\text{M} + \text{Na}^+]$ calcd for $\text{C}_{18}\text{H}_{16}\text{NaO}_3^+$ 303.0992, found 303.0983.



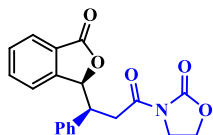
(*S*^{*})-3-((*R*^{*})-2-oxooctan-4-yl)isobenzofuran-1(3*H*)-one (80am):

Obtained as a white solid (46.8 mg, 90% yield), mp 128-129 °C. ¹H NMR (600 MHz, CDCl₃) δ 7.89 (d, *J* = 7.6 Hz, 1H), 7.68 (dt, *J* = 7.6, 1.1 Hz, 1H), 7.55-7.48 (m, 2H), 5.59 (d, *J* = 2.4 Hz, 1H), 2.82 (dd, *J* = 18.1, 8.8 Hz, 1H), 2.65 (m, 1H), 2.57 (dd, *J* = 18.1, 4.4 Hz, 1H), 2.22 (s, 3H), 1.21-0.98 (m, 5H), 0.85 (m, 1H), 0.74 (t, *J* = 7.1 Hz, 3H). ¹³C NMR (150 MHz, CDCl₃) δ 207.8, 170.6, 148.7, 134.1, 129.1, 126.7, 125.6, 122.0, 82.9, 44.3, 36.7, 30.6, 29.2, 26.4, 22.4, 13.7. HRMS (MALDI) [*M* + Na⁺] calcd for C₁₆H₂₀NaO₃⁺ 283.1305, found 283.1300.



ethyl(*S*^{*})-3-((*S*^{*})-3-oxo-1,3-dihydroisobenzofuran-1-yl)-3-phenylpropanoate (80an):

Obtained as a white solid (48.4 mg, 78% yield), mp 135-136 °C. ¹H NMR (400 MHz, CDCl₃) δ 7.63 (d, *J* = 7.6 Hz, 1H), 7.58 (t, *J* = 7.6 Hz, 1H), 7.41-7.33 (m, 2H), 7.13-6.98 (m, 5H), 5.81 (d, *J* = 2.1 Hz, 1H), 4.12 (q, *J* = 7.1 Hz, 2H), 3.88 (m, 1H), 3.13 (dd, *J* = 16.6, 8.0 Hz, 1H), 2.87 (dd, *J* = 16.6, 7.2 Hz, 1H), 1.20 (t, *J* = 7.1 Hz, 3H). ¹³C NMR (150 MHz, CDCl₃) δ 171.8, 170.1, 147.9, 135.9, 133.6, 129.0, 128.8, 128.1, 127.4, 126.4, 125.4, 122.3, 82.4, 60.8, 45.2, 36.2, 14.1. HRMS (MALDI) [*M* + Na⁺] calcd for C₁₉H₁₈NaO₄⁺ 333.1097, found 333.1086.



(*S*^{*})-3-((*S*^{*})-3-(oxazolidin-2-one)-3-oxo-1-phenylpropyl)isobenzofuran-1(3*H*)-one (80ao):

Obtained as a white solid (29.4 mg, 42% yield), mp 158-160 °C. ¹H NMR (600 MHz, CDCl₃) δ 7.64 (d, *J* = 7.7 Hz, 1H), 7.58 (t, *J* = 7.6 Hz, 1H), 7.40 (d, *J* = 7.7 Hz, 1H), 7.36 (t, *J* = 7.6 Hz, 1H), 7.15-7.03 (m, 5H), 5.84 (d, *J* = 2.8 Hz, 1H), 4.47-4.36 (m, 2H), 4.06-3.95 (m, 3H), 3.73

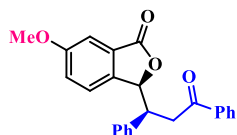
(dd, $J = 18.0, 7.9$ Hz, 1H), 3.59 (dd, $J = 18.0, 6.5$ Hz, 1H). ^{13}C NMR (150 MHz, CDCl_3) δ 171.5, 170.1, 153.3, 147.9, 136.0, 133.6, 129.0, 128.9, 128.2, 127.4, 126.5, 125.5, 122.3, 82.5, 62.2, 44.4, 42.5, 37.0. HRMS (MALDI) [$\text{M} + \text{Na}^+$] calcd for $\text{C}_{20}\text{H}_{17}\text{NNaO}_5^+$ 374.0999, found 374.0996.



(*S*^{*})-6-nitro-3-((*S*^{*})-3-oxo-1,3-

diphenylpropyl)isobenzofuran-1(3*H*)-one (80ba):

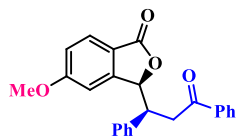
Obtained as a white solid (67.4 mg, 87% yield), mp 193-194 °C. ^1H NMR (400 MHz, CDCl_3) δ 8.47 (m, 1H), 8.41 (bs, 1H), 8.02 (d, $J = 7.6$ Hz, 2H), 7.78 (d, $J = 8.3$ Hz, 1H), 7.61 (t, $J = 7.6$ Hz, 1H), 7.49 (t, $J = 7.6$ Hz, 2H), 7.12-7.01 (m, 5H), 6.03 (d, $J = 2.0$ Hz, 1H), 4.19 (m, 1H), 4.01 (dd, $J = 18.2, 9.1$ Hz, 1H), 3.56 (dd, $J = 18.2, 4.7$ Hz, 1H). ^{13}C NMR (100 MHz, CDCl_3) δ 197.8, 167.7, 153.8, 148.7, 136.4, 135.7, 133.7, 128.8 (2 C), 128.4 (2 C), 128.0, 127.9, 127.7, 123.6, 120.9, 82.5, 43.9, 40.4. HRMS (MALDI) [$\text{M} + \text{Na}^+$] calcd for $\text{C}_{23}\text{H}_{17}\text{NNaO}_5^+$ 410.0999, found 410.0987.



(*S*^{*})-6-methoxy-3-((*S*^{*})-3-oxo-1,3-

diphenylpropyl)isobenzofuran-1(3*H*)-one (80ca):

Obtained as a white solid (36.5 mg, 49% yield), mp 216-217 °C. ^1H NMR (400 MHz, CDCl_3) δ 8.01 (d, $J = 7.6$ Hz, 1H), 7.59 (t, $J = 7.6$ Hz, 1H), 7.48 (t, $J = 7.6$ Hz, 2H), 7.39 (d, $J = 8.4$ Hz, 1H), 7.15 (dd, $J = 8.4, 2.3$ Hz, 1H), 7.12-7.03 (m, 6H), 5.80 (d, $J = 2.6$ Hz, 1H), 4.13 (m, 1H), 3.91 (dd, $J = 17.9, 8.2$ Hz, 1H), 3.76 (s, 3H), 3.54 (dd, $J = 17.9, 5.6$ Hz, 1H). ^{13}C NMR (150 MHz, CDCl_3) δ 198.2, 170.4, 160.4, 140.8, 136.8, 136.7, 133.5, 129.0, 128.7, 128.2, 128.1, 127.7, 127.2, 123.1, 122.7, 107.2, 82.5, 55.6, 44.1, 40.5. HRMS (MALDI) [$\text{M} + \text{Na}^+$] calcd for $\text{C}_{24}\text{H}_{20}\text{NaO}_4^+$ 395.1254, found 395.1240.



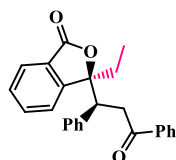
(*S*^{*})-5-methoxy-3-((*S*^{*})-3-oxo-1,3-diphenylpropyl)isobenzofuran-1(3*H*)-one (80da):

Obtained as a white solid (69.2 mg, 93% yield), mp 196-197 °C. ¹H NMR (400 MHz, CDCl₃) δ 8.01 (d, *J* = 7.5 Hz, 1H), 7.59 (t, *J* = 7.5 Hz, 1H), 7.54-7.44 (m, 3H), 7.15-7.02 (m, 5H), 6.94 (d, *J* = 2.1 Hz, 1H), 6.85 (dd, *J* = 8.5, 2.1 Hz, 1H), 5.77 (d, *J* = 2.5 Hz, 1H), 4.13 (m, 1H), 3.94 (dd, *J* = 18.1, 8.4 Hz, 1H), 3.88 (s, 3H), 3.52 (dd, *J* = 18.1, 5.3 Hz, 1H). ¹³C NMR (100 MHz, CDCl₃) δ 198.2, 170.1, 164.4, 151.1, 136.7, 136.6, 133.5, 128.9, 128.7, 128.1, 128.1, 127.2, 126.8, 118.7, 116.4, 106.1, 81.8, 55.8, 43.9, 40.4. HRMS (MALDI) [*M* + Na⁺] calcd for C₂₄H₂₀NaO₄⁺ 395.1254, found 395.1240.



(*S*^{*})-3-((*S*^{*})-3-oxo-1,3-diphenylpropyl)-5-(trifluoromethyl)isobenzofuran-1(3*H*)-one (80ea):

Obtained as a white solid (72.2 mg, 88% yield), mp 216-217 °C. ¹H NMR (400 MHz, CDCl₃) δ 8.03 (d, *J* = 7.7 Hz, 1H), 7.84 (bs, 1H), 7.72 (d, *J* = 8.0 Hz, 1H), 7.64-7.57 (m, 2H), 7.50 (t, *J* = 7.6 Hz, 2H), 7.13-6.98 (m, 5H), 5.97 (bs, 1H), 4.18 (m, 1H), 4.00 (dd, *J* = 18.1, 9.0 Hz, 1H), 3.56 (dd, *J* = 18.1, 4.8 Hz, 1H). ¹³C NMR (100 MHz, CDCl₃) δ 197.9, 168.8, 148.8, 136.5, 135.9, 135.4 (q, *J*_{CF} = 33 Hz), 133.6, 129.4, 128.8, 128.7, 128.3, 128.0, 127.5, 126.1 (q, *J*_{CF} = 3 Hz), 126.0, 123.3 (q, *J*_{CF} = 274 Hz), 119.7 (q, *J*_{CF} = 3 Hz), 82.4, 44.0, 40.3. HRMS (MALDI) [*M* + Na⁺] calcd for C₂₄H₁₇F₃NaO₃⁺ 433.1022, found 433.1018.



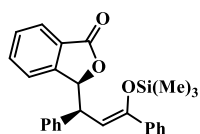
(*S*^{*})-3-ethyl-3-((*S*^{*})-3-oxo-1,3-diphenylpropyl)isobenzofuran-1(3*H*)-one (82aa):

Obtained as a white solid (69.2 mg, 91% yield), mp 149-150 °C. ¹H NMR (400 MHz, CDCl₃) δ 7.93 (d, *J* = 7.4 Hz,

2H), 7.60-7.50 (m, 3H), 7.43 (t, $J = 7.4$ Hz, 2H), 7.37-7.27 (m, 2H), 7.08-6.92 (m, 5H), 4.16 (m, 1H), 3.76 (dd, $J = 17.8, 4.4$ Hz, 1H), 3.64 (dd, $J = 17.8, 8.0$ Hz, 1H), 2.25 (m, 1H), 2.06 (m, 1H), 0.59 (t, $J = 7.3$ Hz, 3H). ^{13}C NMR (100 MHz, CDCl_3) δ 197.8, 170.2, 150.7, 138.7, 136.6, 133.5, 133.2, 129.0, 128.6, 128.6, 128.0, 127.8, 127.1, 126.8, 125.1, 122.0, 91.9, 47.5, 39.6, 29.7, 7.5. HRMS (MALDI) $[\text{M} + \text{Na}^+]$ calcd for $\text{C}_{25}\text{H}_{22}\text{NaO}_3^+$ 393.1461, found 393.1470.

6.3.4 Arylogous Michael reaction of **79a** and **76a** with neutral work-up

To a stirred solution of *trans*-chalcone **76a** (41.6 mg, 0.20 mmol), dicyclohexane-18-crown-6 (DCH18C6, 7.4 mg, 0.02 mmol) and KOH (2.2 mg, 0.04 mmol) in toluene (1.0 mL) at room temperature, phthalide **79a** (26.8 mg, 0.20 mmol) and *N,O*-Bis(trimethylsilyl)acetamide (BSA, 61.0 mg, 0.30 mmol) were added. The mixture was stirred at room temperature for 1 h, and then it was diluted with H_2O (1.0 mL) and extracted with CH_2Cl_2 (3 x 3 mL). The combined organic phases were dried over Na_2SO_4 and concentrated *in vacuo*. The crude residue was purified by *flash* chromatography (silica gel, toluene) affording the silylated Michael product **86aa** (73.0 mg, 88% yield) as a white solid, along with small amounts of **80aa** (8.2 mg, 12% yield).

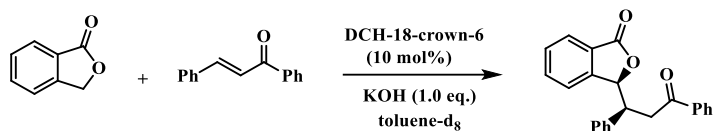


(*S)-3-((*S,Z*)-1,3-diphenyl-3-**

((trimethylsilyl)oxy)allyl)isobenzofuran-1(3*H*)-one

(6aa): ^1H NMR (400 MHz, CDCl_3) δ 7.76 (d, $J = 7.6$ Hz, 1H), 7.62-7.53 (m, 1H), 7.48-7.38 (m, 3H), 7.37-7.13 (m, 10H), 5.78 (d, $J = 4.7$ Hz, 1H), 5.51 (d, $J = 9.8$ Hz, 1H), 3.94 (dd, $J = 9.8, 4.7$ Hz, 1H), 0.02 (s, 9H).

6.3.5 ¹H NMR monitoring of arylogous Michael reaction of **79a** and **76a** in the absence of BSA



The conversion of **79a** to **80aa** over time, in the presence of 1 mol equiv. of KOH was studied by ¹H NMR. To a stirred solution of trans-chalcone **76a** (124.8 mg, 0.60 mmol), dicyclohexane-18-crown-6 (DCH18C6, 22.2 mg, 0.06 mmol) and KOH (33.0 mg, 0.60 mmol) in toluene-d₈ (3.0 mL), at room temperature, phthalide **1a** (80.4 mg, 0.60 mmol) was added. Aliquots of 0.14 mL were taken at time intervals reported in **Figure S3**. Each aliquot was diluted to 0.4 mL with toluene-d₈ and, after addition of 1,3,5-trimethoxybenzene (1.6 mg, 0.0095 mmol) as internal standard, submitted to ¹H NMR quantitative analysis (400 MHz). As the reaction proceeded a white precipitate separated and the red reaction mixture turned to brown and then pale yellow.

The % amounts of product **80aa** and residual **79a** and **76a**, determined using the following formula, are reported in **Figure S3**.

$$\% y = \frac{n}{0.60 \times \frac{0.14}{3.0}} \times 100$$

% y = % amount of **80aa**, **79a** and **76a**

n = mmol of **80aa**, **79a** and **76a** measured in the aliquot

After 168 h, the reaction mixture remaining in the flask was treated with 1 M HCl (3.0 mL). The white precipitate totally dissolved. The resulting mixture was extracted with CH₂Cl₂ (3 x 9 mL). The combined organic phases were dried over Na₂SO₄ and concentrated in vacuo. Quantitative ¹H NMR

analysis (400 MHz) of the crude mixture, after addition of 1,3,5-trimethoxybenzene (1.6 mg, 0.0095 mmol) as internal standard, furnished the following % amounts: **80aa** (45 %), **79a** (35 %), **76a** (20 %). The amount of **1a** recovered is presumably the result of re-lactonization of the ring-opening insoluble product during acidic workup.

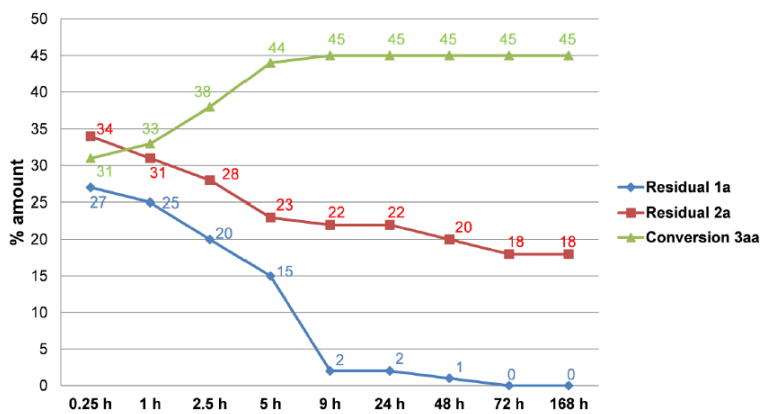


Figure S3. % Amounts of product **3aa**, and residual **1a** and **2a**, measured at time intervals up to 168 h in the arylogous Michael reaction promoted by stoichiometric KOH and catalytic DCH18C6.

6.3.6 Study of degradation of *trans*-chalcone under the reaction conditions at different temperatures

In order to assess the extent of decomposition of *trans*-chalcone **75a** at different temperatures, it was submitted to the reaction conditions, in the absence of phthalide **79a**, both at room temperature and at -40 °C. To a solution of *trans*-chalcone **75a** (41.6 mg, 0.20 mmol), dicyclohexane-18-crown-6 (DCH18C6, 7.4 mg, 0.02 mmol) and KOH (2.2 mg, 0.04 mmol) in toluene (1.0 mL), stirred at room temperature, *N,O*-Bis(trimethylsilyl)acetamide (BSA, 61.0 mg, 0.30 mmol) was added. After 1 h stirring at room temperature, TLC monitoring revealed complete

disappearance of **75a**. The reaction mixture was diluted with H₂O (1.0 mL) and extracted with CH₂Cl₂ (3 x 3 mL). The combined organic phases were dried over Na₂SO₄ and concentrated *in vacuo*. ¹H NMR analysis of the crude residue showed a complex mixture of products and no traces of **75a**. In another experiment, **75a** was submitted to the same reaction conditions at –40 °C. After 48 h stirring at –40 °C, the reaction mixture was subjected to the same work-up as described above. The ¹H NMR analysis of the crude residue showed the presence of **75a**, DCH18C6 and signals attributable to decomposition products of BSA. No traces of decomposition products of **75a** could be detected in the mixture.

6.3.7 Study of possible *anti* to *syn* conversion under reaction conditions

In order to ascertain whether the diastereomeric *syn/anti* ratio is due to thermodynamic or kinetic control, we set up an experiment to rule out a possible *anti* to *syn* conversion under reaction conditions. To this end, to a stirred solution of a 50:50 *syn/anti* mixture of adduct **80aa** (34.2 mg, 0.10 mmol) in toluene (0.5 mL) at –40 °C, 18-crown-6 (18C6, 2.6 mg, 0.01 mmol), KOH (1.1 mg, 0.02 mmol) and *N,O*-Bis(trimethylsilyl)acetamide (BSA, 30.5 mg, 0.15 mmol) were added. After 24 h stirring at –40 °C, the reaction mixture was treated with 1 M HCl (0.5 mL) and THF (1.5 mL) and stirred at room temperature for 2 h. Then the mixture was diluted with H₂O (0.5 mL) and extracted with CH₂Cl₂ (3 x 2 mL). The combined organic phases were dried over Na₂SO₄ and concentrated *in vacuo*. ¹H NMR analysis of the crude residue showed **80aa** as a 53:47 *syn/anti* ratio. This small d.r. change proves the negligible *anti* to *syn* conversion during addition reaction.

6.3.8 X-ray crystallography

Colorless prismatic single crystal of compound **80aa** suitable for X-ray diffraction analysis was obtained by slow evaporation of a solution of acetonitrile/hexane (2:1) dissolving 4 mg of the compound in 0.4 ml of acetonitrile and adding 0.2 ml of hexane. A crystal of 0.51 mm x 0.24 mm x 0.19 mm was selected and mounted on a cryoloop with paratone oil and measured at room temperature. Colorless prismatic single crystals of compound **80ad** suitable for X-ray diffraction analysis were obtained by slow evaporation of a solution of methanol dissolving 5 mg of the compound in 1.6 ml of hot methanol. A crystal of 0.67 mm x 0.40 mm x 0.22 mm was selected and mounted on a cryoloop with paratone oil and measured at room temperature. Colorless prismatic single crystal of compound **80an** suitable for X-ray diffraction analysis was obtained by slow evaporation of a solution of methanol dissolving 4 mg of the compound in 1.4 ml of hot methanol. A crystal of 0.42 mm x 0.24 mm x 0.17 mm was selected and mounted on a cryoloop with paratone oil and measured at room temperature. The crystals were mounted on cryoloop with paratone oil and measured at room temperature with a Bruker D8 QUEST diffractometer equipped with a PHOTON II detector using CuK α radiation ($\lambda=1.54178$ Å). Data Indexing was performed using APEX3.¹⁵⁸ Data integration and reduction were performed using SAINT1. Absorption correction was performed by multi-scan method in SADABS1. The structures were solved using SHELXS-97¹⁵⁹ and refined by means of full matrix least-squares based on F^2 using the program SHELXL.¹⁴⁶ Non-hydrogen atoms were refined anisotropically, hydrogen atoms were positioned geometrically and included in structure

¹⁵⁸ Bruker. APEX3, SAINT and SADABS. Bruker AXS Inc, Madison, Wisconsin, USA, **2015**.

¹⁵⁹ G. M. Sheldrick, *Acta Cryst.* **2008**, *A64*, 112-122.

factors calculations but not refined. ORTEP diagrams were drawn using OLEX2¹⁴⁷ (Figures S4-S6). Interestingly compounds **80aa** and **80ad** crystallize with two crystallographically independent molecules in the unit cell, which differ in the molecular conformation (conformer A and conformer B in Figures S4 and S5).

	3aa	3ad	3an
T (K)	296	296	296
Formula	C23H18O3	C23H17FO3	C19H18O4
Formula weight	342.37	360.36	310.33
System	Monoclinic	Monoclinic	Monoclinic
Space group	<i>P</i> 21/n	<i>P</i> 21/n	<i>P</i> 21/c
<i>a</i> (Å)	12.7819(16)	12.7968(19)	9.275(4)
<i>b</i> (Å)	14.9238(19)	15.412(4)	9.8596(18)
<i>c</i> (Å)	18.950(4)	18.886(3)	17.882(6)
α (°)	90	90	90
β (°)	99.297(12)	100.188(12)	100.700(16)
γ (°)	90	90	90
<i>V</i> (Å ³)	3567.2(10)	3666.1(13)	1606.9(9)
<i>Z</i>	8	8	4
<i>D_x</i> (g cm ⁻³)	1.275	1.306	1.283
λ (Å)	1.54178	1.54178	1.54178
μ (mm ⁻¹)	0.671	0.761	0.731
<i>F</i> 000	1440	1504	656
R1 (I > 2 σ I)	0.0473(5216)	0.0647 (4652)	0.0394 (2846)
wR ₂ (all)	0.1359(6952)	0.1854 (6582)	0.0997 (2981)
N. of param.	470	487	210
GooF	1.026	1.037	1.050
ρ_{min}, ρ_{max} (eÅ ⁻³)	-0.17, 0.19	-0.24, 0.32	-0.13, 0.14

Table S2. Crystallographic data for compounds **80aa**, **80ad** and **80an**.

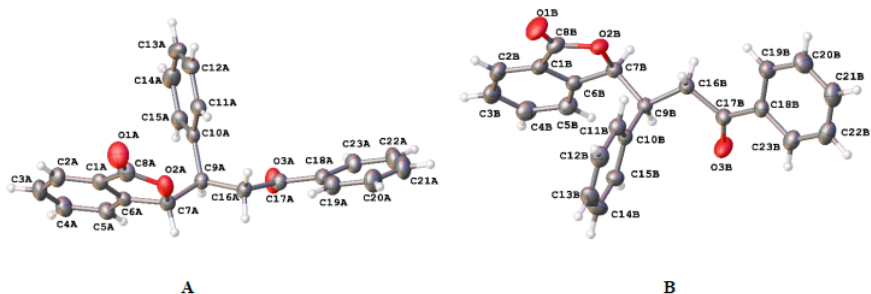


Figure S3. ORTEP diagrams for compound **3aa**: conformer A and conformer B. Atom types: C grey, O red, H white. Ellipsoids are drawn at 30% probability level.

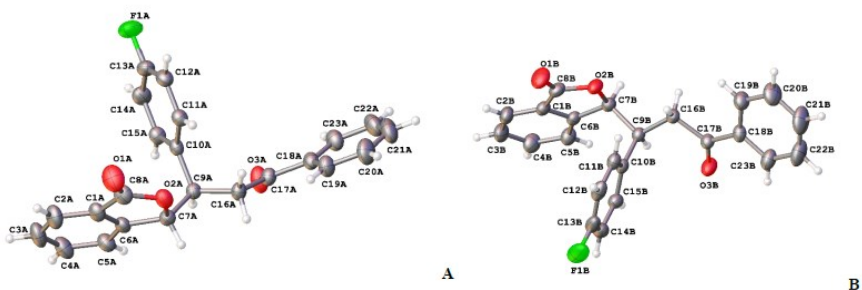


Figure S4. ORTEP diagrams for compound **3ad**: conformer A and conformer B. Atom types: C grey, O red, H white, F green. Ellipsoids are drawn at 30% probability level.

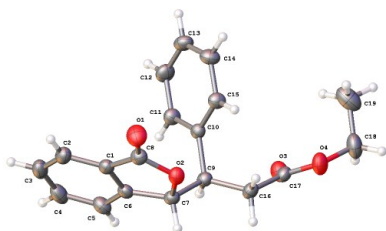


Figure S5. ORTEP diagrams for compound **3an**. Atom types: C grey, O red, H white. Ellipsoids are drawn at 30% probability level.

6.3.9 Computational data

Cartesian coordinates of the optimized structures of transition states

exo-TS-A

86

$E_s = -2635.35557383$
(toluene solvent)

C 2.731649 0.549660 1.476045
 O 1.347523 0.695604 1.514284
 C 0.797518 -0.173556 2.447991
 H 3.274425 1.362060 0.998348
 O -0.420592 -0.243668 2.577603
 C -2.089476 -4.466757 1.288677
 C -1.408277 -3.352051 0.796690
 C -1.429157 -5.692205 1.428733
 H -1.915002 -2.393478 0.677360
 H -1.963896 -6.566944 1.808851
 C -0.047129 -3.435014 0.450726
 C -0.079723 -5.791300 1.075739
 H 0.442738 -6.747052 1.171240
 C 0.605703 -4.671867 0.597420
 H 1.655161 -4.770978 0.313976
 H -3.144164 -4.382028 1.566410
 C 0.631718 -2.194948 -0.078562
 O -0.083603 -1.315977 -0.612606
 C 2.056976 -2.087822 0.066365
 H 2.577701 -2.899514 0.573622
 C 2.775473 -0.990466 -0.386426
 H 2.200118 -0.242386 -0.938946
 C 4.229887 -0.943562 -0.586270
 C 4.790215 0.093304 -1.364797
 C 5.114264 -1.902838 -0.047493
 C 6.163101 0.173618 -1.593862
 C 6.489395 -1.821918 -0.275575
 C 7.024297 -0.785816 -1.048087
 H 4.123373 0.843961 -1.799908
 H 4.721038 -2.721634 0.556557
 H 6.565702 0.985925 -2.205546
 H 7.151168 -2.579197 0.153924
 H 8.101082 -0.728033 -1.226627

C 3.116375 -0.278179 2.545543
 C 1.916060 -0.810252 3.110008
 C 4.369078 -0.709330 3.055588
 C 1.945057 -1.736021 4.166333

C 4.378710 -1.624238 4.096436
 H 5.303626 -0.321641 2.644749
 C 3.178376 -2.141492 4.656112
 H 1.010124 -2.120793 4.581553
 H 5.337276 -1.956376 4.506026
 H 3.235126 -2.860665 5.476938
 K -1.157419 1.055052 0.174842
 O -1.245677 3.238494 2.206034
 O 0.118531 3.840355 -0.207269
 O -0.020105 1.993243 -2.358445
 O -2.313519 0.248037 -2.469631
 C -0.640392 4.483290 1.960898
 H -1.356150 5.184778 1.484803
 H -0.296761 4.947370 2.908540
 C 0.557402 4.286199 1.058726
 H 1.243600 3.547399 1.515477
 H 1.098731 5.250153 0.965682
 C 1.152043 3.686164 -1.152369
 H 1.882309 2.923549 -0.815949
 H 1.702622 4.639560 -1.291449
 C 0.556818 3.271246 -2.479408
 H -0.203607 4.015938 -2.791116
 H 1.358515 3.270392 -3.246711
 C -0.596295 1.509177 -3.554225
 C -1.190716 0.138789 -3.322880
 H -1.383672 2.203941 -3.910490
 H -1.491529 -0.280519 -4.305569
 H 0.172746 1.434817 -4.350002
 H -0.434076 -0.529009 -2.872219
 O -3.588438 -0.447108 0.011004
 O -3.413528 1.379199 2.196962
 C -2.942304 -0.995838 -2.225796
 H -2.212664 -1.710776 -1.805722
 H -3.346081 -1.415357 -3.170948
 C -4.090083 -0.806653 -1.258876
 H -4.780231 -0.024848 -1.636316
 H -4.658929 -1.756479 -1.195845
 C -4.567549 -0.340834 1.020254
 C -3.909215 0.063031 2.321489
 H -5.331402 0.413282 0.742316
 H -4.666552 0.006945 3.131175
 H -5.086975 -1.310618 1.162376
 H -3.089725 -0.637469 2.570479
 C -2.811472 1.871849 3.377855

C -2.310917 3.276585 3.128903
 H -3.550445 1.900794 4.205643
 H -1.967895 1.223801 3.676924
 H -3.137341 3.909353 2.745217
 H -1.973936 3.710834 4.092579

endo-TS-A

86

$E_s = -2635.34222805$
 (toluene solvent)

C 9.932834 1.751628 3.985697
 C 8.926824 2.712126 4.095424
 C 9.603341 0.418542 3.713652
 H 9.156744 3.762396 4.285942
 H 10.389895 -0.336161 3.623518
 C 7.573493 2.360029 3.956716
 C 8.261877 0.060297 3.547932
 H 7.998022 -0.975593 3.314985
 C 7.253614 1.021693 3.670761
 H 6.214566 0.733018 3.501958
 H 10.980550 2.041417 4.108193
 C 6.542972 3.465420 4.087505
 O 6.920413 4.636993 3.954599
 C 5.179512 3.101349 4.398277
 H 4.946297 2.056527 4.598148
 C 4.199700 4.092933 4.546336
 H 4.591688 5.114299 4.554706
 C 2.964517 3.901873 5.342230
 C 2.266194 5.026957 5.827515
 C 2.445381 2.630586 5.661704
 C 1.109138 4.894870 6.597731
 C 1.292537 2.495839 6.439282
 C 0.613287 3.625208 6.911498
 H 2.654504 6.024435 5.601408
 H 2.963449 1.737055 5.308889
 H 0.598532 5.788913 6.966853
 H 0.929824 1.496123 6.697377
 H -0.282783 3.516614 7.528454
 C 3.285562 4.261175 2.599791
 O 3.107401 2.890443 2.367043
 C 4.232785 2.375805 1.738684
 H 2.357353 4.797480 2.798727

O 4.311344 1.163548 1.529854
 C 4.357256 4.689887 1.764100
 C 4.882328 5.958566 1.427609
 C 5.023524 3.513897 1.321618
 C 6.036447 6.014883 0.664715
 H 4.393090 6.875609 1.766756
 C 6.210751 3.584337 0.569877
 C 6.709716 4.836343 0.246720
 H 6.454102 6.988069 0.392169
 H 6.722556 2.669685 0.261185
 H 7.632093 4.924546 -0.332763
 K 1.555158 0.833910 1.225182
 O -0.803039 2.299215 2.044444
 O 0.377656 2.990490 -0.441380
 O 2.516454 1.420867 -1.389607
 O 2.978642 -1.200415 -0.340975
 C -1.344342 3.276646 1.181911
 H -2.065141 2.815573 0.476731
 H -1.887261 4.049734 1.762128
 C -0.230346 3.942063 0.405049
 H 0.511040 4.373818 1.105316
 H -0.660497 4.775462 -0.186972
 C 1.400942 3.519225 -1.263845
 H 2.230676 3.917350 -0.648185
 H 1.009482 4.348878 -1.886485
 C 1.918526 2.426517 -2.172928
 H 1.084210 2.012400 -2.775535
 H 2.654755 2.868087 -2.874395
 C 3.141727 0.389069 -2.123820
 C 3.897099 -0.516095 -1.176722
 H 2.389128 -0.193405 -2.693840
 H 4.486553 -1.241537 -1.774311
 H 3.861032 0.814295 -2.852086
 H 4.587208 0.088622 -0.562265
 O 1.836910 -1.796946 2.226310
 O -0.417463 -0.318946 3.077531
 C 3.611402 -2.008092 0.632530
 H 4.243216 -1.386994 1.293946
 H 4.258061 -2.767544 0.146988
 C 2.560343 -2.729358 1.446720
 H 1.875677 -3.279621 0.770473
 H 3.059544 -3.472168 2.100904
 C 0.818843 -2.364032 3.017490
 C 0.206254 -1.290908 3.890822

H 0.035223 -2.820917 2.379337
 H -0.531003 -1.762112 4.572075
 H 1.225747 -3.161864 3.671443
 H 0.994231 -0.827947 4.517494
 C -1.062649 0.708276 3.806384
 C -1.760928 1.646219 2.848156
 H -1.817787 0.279343 4.495778
 H -0.332084 1.276002 4.413875
 H -2.475775 1.078747 2.218168
 H -2.342398 2.382455 3.438617

exo-TS-B

106

 $E_s = -2947.44224710$

(toluene solvent)

K -1.315728 0.946186 0.034550
 O -0.573862 3.565148 1.087623
 O 0.238960 3.146291 -1.524779
 O -1.618537 1.303594 -2.846996
 O -3.699858 -0.391468 -1.621312
 O -3.935237 0.163567 1.089669
 O -2.549490 2.145126 2.540811
 C 0.375420 4.435447 0.487315
 C 1.812351 4.025865 0.834205
 H 1.949846 2.983421 0.510259
 H 1.943503 4.034137 1.928618
 C 2.841105 4.946824 0.165129
 H 3.861632 4.592286 0.383976
 H 2.767451 5.961788 0.598975
 C 2.615590 5.031449 -1.349291
 H 3.316590 5.749444 -1.806120
 H 2.828900 4.048728 -1.804313
 C 1.170490 5.433949 -1.668730
 H 1.006735 5.493849 -2.756152
 H 0.970306 6.448337 -1.280400
 C 0.147571 4.477250 -1.028370
 C 0.059280 3.006892 -2.919885
 H -0.753432 3.671050 -3.275223
 H 0.981859 3.279153 -3.467925
 C -0.295258 1.579309 -3.269524
 H 0.411458 0.867692 -2.803655
 H -0.219266 1.469119 -4.370639
 C -2.132344 0.097316 -3.376809

H -1.541146 -0.763606 -3.015853
 H -2.072182 0.117279 -4.484777
 C -3.586365 -0.053590 -2.989018
 H -4.114336 0.897868 -3.200346
 H -4.034133 -0.836829 -3.630294
 C -4.992626 -0.217615 -1.052575
 C -6.080957 -1.056169 -1.748572
 H -7.050986 -0.792176 -1.291212
 H -6.164221 -0.769176 -2.808635
 C -5.830653 -2.562455 -1.602720
 H -4.897953 -2.828856 -2.129078
 H -6.640782 -3.127683 -2.092532
 C -5.712043 -2.962784 -0.126677
 H -6.695259 -2.832829 0.363229
 H -5.461878 -4.032471 -0.036030
 C -4.659192 -2.117491 0.602783
 H -4.645992 -2.363764 1.677094
 H -3.652975 -2.338725 0.214871
 C -4.919672 -0.616668 0.426480
 C -4.252622 0.481040 2.431574
 H -4.637952 -0.405890 2.969922
 H -5.038210 1.262883 2.460751
 C -3.019063 0.963553 3.158923
 H -3.293683 1.160598 4.216679
 H -2.234971 0.184642 3.145019
 C -1.406556 2.689107 3.163611
 H -0.591539 1.942326 3.187963
 H -1.635220 2.985027 4.209521
 C -0.955767 3.916853 2.404347
 H -1.772893 4.665264 2.375926
 H -0.108906 4.361854 2.959003
 H -5.260357 0.857373 -1.111634
 H -5.915291 -0.371676 0.847876
 H -0.878976 4.852696 -1.217812
 H 0.194094 5.469274 0.844583
 C 3.096690 0.217729 1.282727
 O 1.745096 0.532748 1.355194
 C 1.061077 -0.441556 2.051846
 H 3.754222 1.040123 1.012860
 O -0.160081 -0.367729 2.176329
 C -1.898719 -4.635526 -0.890066
 C -1.205470 -3.435807 -1.059936
 C -1.292497 -5.711952 -0.233872
 H -1.678753 -2.581834 -1.545982

H-1.834262	-6.651746	-0.096894	H 9.289699	-8.027328	4.695914
C 0.115841	-3.289027	-0.600917	C 8.378321	-4.281888	5.372133
C 0.010495	-5.571796	0.253789	C 7.864697	-6.432603	4.351773
H 0.488511	-6.399315	0.784975	H 7.207784	-7.048708	3.730654
C 0.707687	-4.375264	0.070742	C 7.534184	-5.095170	4.596744
H 1.714371	-4.283868	0.480191	H 6.637703	-4.670747	4.139509
H-2.919824	-4.732664	-1.269776	H 10.813513	-6.591110	6.056747
C 0.818017	-1.972111	-0.845125	C 8.106304	-2.817378	5.657259
O 0.122081	-0.984511	-1.183581	O 9.069048	-2.085830	5.920525
C 2.248101	-1.941568	-0.731261	C 6.735532	-2.358304	5.653606
H 2.757953	-2.880000	-0.518948	H 5.936506	-3.086053	5.515841
C 3.003660	-0.791352	-0.905219	C 6.446128	-1.015619	5.921083
H 2.453770	0.106032	-1.198916	H 7.303842	-0.427995	6.260864
C 4.451674	-0.754933	-1.153145	C 5.132218	-0.536897	6.403625
C 5.039873	0.426190	-1.657116	C 5.041379	0.686740	7.098625
C 5.302091	-1.857832	-0.922454	C 3.935162	-1.252920	6.199117
C 6.407396	0.506391	-1.917241	C 3.818709	1.172372	7.566716
C 6.671882	-1.776620	-1.179755	C 2.710988	-0.770424	6.666176
C 7.234842	-0.597071	-1.678333	C 2.641716	0.446956	7.353040
H 4.400274	1.293035	-1.849229	H 5.955903	1.259500	7.278007
H 4.887049	-2.789323	-0.534854	H 3.965989	-2.208646	5.676174
H 6.831759	1.433777	-2.312024	H 3.785502	2.121435	8.109308
H 7.307108	-2.646630	-0.991382	H 1.807291	-1.363600	6.499546
H 8.307178	-0.538879	-1.881746	H 1.684607	0.821575	7.725779
C 3.336094	-0.895328	2.106741	C 6.342634	-0.063343	3.951613
C 2.057708	-1.377599	2.527775	O 5.493312	-1.009792	3.361572
C 4.501683	-1.615208	2.478033	C 6.244662	-1.985443	2.729993
C 1.928067	-2.533277	3.316233	H 5.859121	0.889007	4.165514
C 4.355064	-2.757016	3.249682	O 5.676430	-2.960708	2.229009
H 5.492098	-1.273133	2.169867	C 7.636453	-0.260682	3.396313
C 3.079023	-3.222119	3.672733	C 8.849164	0.463787	3.470939
H 0.938068	-2.872431	3.631600	C 7.610549	-1.514738	2.724938
H 5.246071	-3.315716	3.551146	C 9.977711	-0.074378	2.877621
H 3.013040	-4.124943	4.285019	H 8.896358	1.424802	3.989700
			C 8.770175	-2.061414	2.143564
			C 9.947937	-1.336703	2.225197
			H 10.922256	0.474826	2.923089
			H 8.730878	-3.033522	1.646254
			H 10.866836	-1.733813	1.786739
			K 3.009894	-2.265609	2.555150
			O 1.812237	0.338009	1.876665
			O 3.393163	-0.849650	-0.099137
			O 3.330201	-3.774832	0.107613
			O 2.794722	-5.303290	2.557333

endo-TS-B

106

 $E_s = -2947.43611522$

(toluene solvent)

C 9.889473	-6.173683	5.646282
C 9.567545	-4.835418	5.875543
C 9.036259	-6.980135	4.884038
H 10.229502	-4.178480	6.443508

O 1.357948 -3.837416 4.463487
 O 0.150113 -1.656499 3.059781
 C 2.537934 1.123626 0.937777
 C 3.858195 1.542623 1.582583
 H 4.414022 0.637687 1.869161
 H 3.635142 2.088648 2.512804
 C 4.707810 2.396120 0.632227
 H 5.675787 2.621794 1.106943
 H 4.209087 3.368399 0.459759
 C 4.924008 1.693880 -0.713739
 H 5.478225 2.348331 -1.406235
 H 5.546516 0.796261 -0.560765
 C 3.586255 1.282851 -1.340365
 H 3.738027 0.780495 -2.309027
 H 2.983082 2.181232 -1.563457
 C 2.759532 0.389312 -0.397801
 C 3.506960 -1.749677 -1.182661
 H 2.505073 -1.982507 -1.598236
 H 4.115142 -1.317158 -1.998567
 C 4.184590 -3.024961 -0.736850
 H 5.128660 -2.791047 -0.211452
 H 4.429945 -3.615500 -1.643475
 C 3.884719 -5.036241 0.438606
 H 4.827021 -4.902579 0.999758
 H 4.106747 -5.602242 -0.489491
 C 2.907839 -5.847796 1.258429
 H 1.917926 -5.866724 0.757930
 H 3.285221 -6.886255 1.292894
 C 1.950759 -6.010748 3.457664
 C 2.485614 -7.405233 3.831551
 H 1.735425 -7.884697 4.485658
 H 2.548419 -8.044681 2.936645
 C 3.836215 -7.326398 4.552359
 H 4.594400 -6.921052 3.861796
 H 4.174366 -8.337346 4.832114
 C 3.752157 -6.428217 5.792015
 H 3.109596 -6.911619 6.551290
 H 4.747107 -6.314694 6.249666
 C 3.183264 -5.044346 5.450180
 H 3.054467 -4.437226 6.359066
 H 3.889960 -4.508503 4.796242
 C 1.838883 -5.151710 4.731241
 C -0.027489 -3.745020 4.213981
 H -0.601223 -4.251149 5.016194

H -0.300314 -4.224807 3.254074
 C -0.444796 -2.292851 4.170577
 H -1.550645 -2.245381 4.096762
 H -0.150373 -1.787785 5.111331
 C -0.230862 -0.302996 2.920851
 H 0.074835 0.278863 3.812369
 H -1.332511 -0.220767 2.821032
 C 0.416970 0.286120 1.688345
 H 0.144793 -0.326274 0.805971
 H 0.006460 1.303449 1.529547
 H 0.949414 -6.124306 2.993635
 H 1.115621 -5.661487 5.399983
 H 1.777847 0.178851 -0.870717
 H 1.946449 2.032838 0.704908

exo-TS-C

43

 $E_s = -1112.44099217$

(DMF solvent)

C 5.032604 -0.458688 0.171282
 C 3.853332 -0.488597 -0.573676
 C 4.984848 -0.228795 1.551697
 H 3.856062 -0.688595 -1.647393
 H 5.906714 -0.212151 2.141221
 C 2.605160 -0.272163 0.034924
 C 3.747336 -0.035940 2.173801
 H 3.697361 0.120098 3.255678
 C 2.568252 -0.057107 1.422551
 H 1.606794 0.062669 1.924866
 H 5.995881 -0.621888 -0.322563
 C 1.371149 -0.320366 -0.848581
 O 1.470685 -0.879380 -1.950877
 C 0.176359 0.345111 -0.384045
 H 0.226109 0.948383 0.523290
 C -1.002157 0.260364 -1.123224
 H -0.899588 -0.312059 -2.049998
 C -2.096733 1.241505 -1.121001
 C -3.063295 1.213774 -2.151799
 C -2.234941 2.244743 -0.137085
 C -4.109718 2.134366 -2.201043
 C -3.280290 3.169616 -0.187106
 C -4.226380 3.124096 -1.216255
 H -2.975108 0.450264 -2.930678
 H -1.506386 2.302301 0.673055

H -4.836811 2.085728 -3.017687
H -3.357100 3.935394 0.590883
H -5.043040 3.850808 -1.253073
C -2.155280 -1.506341 -0.207789
O -1.101781 -2.396318 -0.079548
C -0.590821 -2.365567 1.211493
H -2.825537 -1.707624 -1.042887
O 0.360166 -3.035901 1.552446
C -1.475823 -1.472420 1.964078
C -2.502605 -1.031600 1.081646
C -1.468382 -1.127359 3.319818
C -3.536629 -0.206724 1.590296
C -2.493739 -0.320963 3.809511
H -0.670410 -1.499577 3.969034
C -3.518570 0.128566 2.938553
H -4.336982 0.154082 0.940033
H -2.516591 -0.034730 4.864859
H -4.318727 0.758043 3.341479

endo-TS-C

43

 $E_s = -1112.44164787$

(DMF solvent)

C 0.611252 -1.987861 -4.938707
C -0.054264 -1.159411 -4.034340
C 1.556791 -2.912078 -4.477497
H -0.816265 -0.448305 -4.361004
H 2.076655 -3.568421 -5.182388
C 0.225035 -1.216863 -2.657838
C 1.819797 -3.000623 -3.106615
H 2.534893 -3.739561 -2.732685
C 1.163359 -2.159644 -2.201376
H 1.348630 -2.278091 -1.131558

H 0.389121 -1.920158 -6.008618
C -0.544181 -0.278759 -1.743740
O -1.619159 0.183064 -2.155837
C 0.055140 0.071557 -0.478406
H 1.060911 -0.286256 -0.259701
C -0.604350 0.911982 0.418084
H -1.537831 1.342174 0.043423
C 0.065208 1.684283 1.478854
C -0.515687 2.882507 1.948066
C 1.287170 1.284474 2.063985
C 0.091698 3.649414 2.944081
C 1.892425 2.049484 3.061204
C 1.304246 3.239116 3.508777
H -1.462048 3.213291 1.509479
H 1.747989 0.348253 1.746484
H -0.383577 4.576614 3.279665
H 2.836187 1.710221 3.499362
H 1.784028 3.836459 4.289510
C -1.589127 -0.552848 1.884106
O -0.469647 -1.356903 2.045942
C -0.496100 -2.405540 1.136536
H -1.810125 0.094472 2.731854
O 0.433261 -3.186481 1.031950
C -2.509307 -1.233357 1.049149
C -3.845186 -0.987948 0.647264
C -1.807322 -2.340128 0.495662
C -4.427640 -1.841228 -0.275461
H -4.405741 -0.141067 1.054138
C -2.404277 -3.189030 -0.447724
C -3.714161 -2.934998 -0.834275
H -5.460213 -1.664540 -0.593191
H -1.837113 -4.026810 -0.862124
H -4.204406 -3.575907 -1.572343

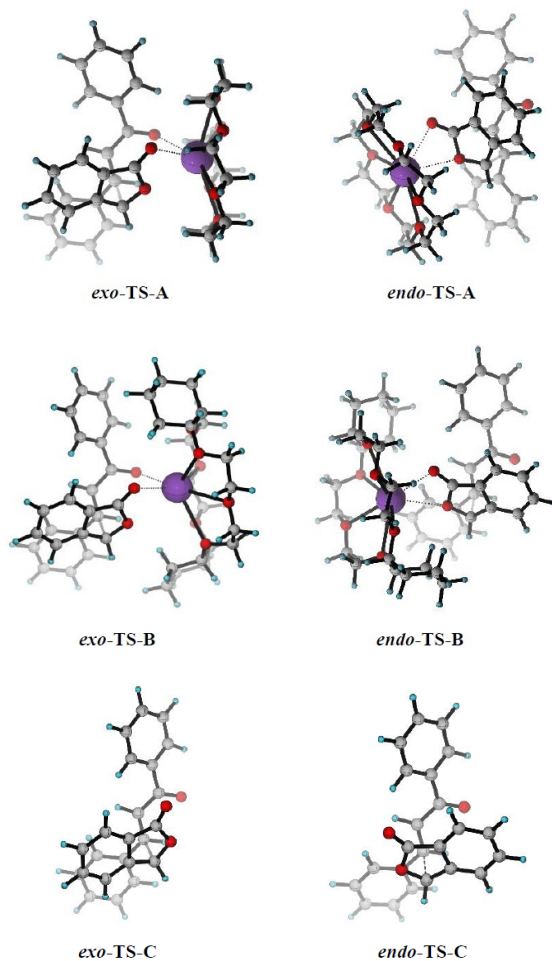


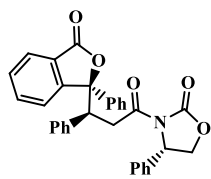
Figure S7 Optimized Structures of *exo*- and *endo*-transition states of Michael reaction of phthalide with *trans*-chalcone calculated at B3LYP/SVP level.

6.4 Asymmetric Michael addition of weakly activated phthalides

3-Phenyl-phthalide **75a** was commercially available, whereas the Michael acceptor **87a** was prepared according the reported procedure.^{109a}

6.4.1 General procedure for the asymmetric AMR of 3-Ph-phthalide

In a 4 mL vial, to a mixture of 3-Ph-phthalide **75a** (1.0 eq., 0.20 mmol, 42.0 mg), Michael acceptor **87a** (1.0 eq., 0.20 mmol, 58.7 mg), DCH-18-crown-6 (0.1 eq., 0.02 mmol, 7.4 mg) and NaOH (0.2 eq., 0.04 mmol, 1.6 mg), toluene (1.0 mL) was added and the reaction mixture was stirred at room temperature for 1 day. Next, the mixture was diluted with H₂O (2.0 mL) and extracted with CH₂Cl₂ (3 x 5 mL). The combined organic phases were dried over Na₂SO₄ and concentrated in vacuo. The crude residue was purified by *flash* chromatography (silica gel, petroleum ether-ethyl acetate 90/10 to 70/30) affording the chiral Michael product **88aa** (74.5 mg, 74% yield) as a white solid.

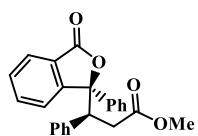


(S)-3-((S)-3-((R)-3-oxo-1-phenyl-1,3-dihydroisobenzofuran-1-yl)-3-phenylpropanoyl)-4-phenyloxazolidin-2-one (88aa**):** mp 119-120 °C. ¹H

NMR (600 MHz, CDCl₃) δ 7.70 (d, *J* = 7.9 Hz, 2H), 7.56 (d, *J* = 7.6 Hz, 1H), 7.52-7.44 (m, 2H), 7.39-7.33 (m, 2H), 7.32-7.25 (m, 4H), 7.22 (m, 1H), 7.15-7.08 (m, 2H), 7.05-6.96 (m, 5H), 5.10 (m, 1H), 4.50 (dd, *J* = 11.0, 2.7 Hz, 1H), 4.45 (m, 1H), 4.11-4.03 (m, 2H), 3.05 (dd, *J* = 17.8, 2.7 Hz, 1H). ¹³C NMR (150 MHz, CDCl₃) δ 170.7, 169.7, 153.4, 152.1, 139.5, 138.7, 136.6, 133.8, 129.6, 129.1, 128.9, 128.7, 128.5, 128.3, 127.9, 127.2, 125.6, 125.3, 125.0, 124.7, 122.2, 91.2, 69.9, 49.2, 37.0, 22.6. HRMS (MALDI) [M + Na⁺] calcd for C₃₂H₂₅NaNO₅⁺ 526.1625, found 526.1630.

6.4.2 General procedure for the synthesis of compound 89aa

The removal of (*S*)-4-phenyloxazolidin-2-one was performed according to the literature.¹⁶⁰



methyl (S)-3-((R)-3-oxo-1-phenyl-1,3-dihydroisobenzofuran-1-yl)-3-phenylpropanoate

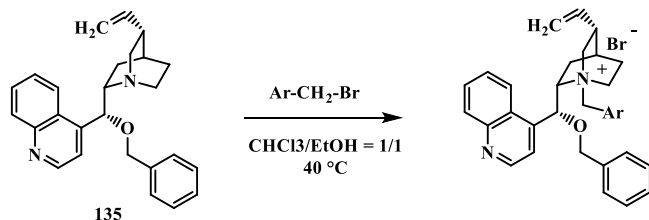
(89aa): Obtained as a white solid (59.6 mg, 80% yield), mp 117-118 °C. ¹H NMR (600 MHz, CDCl₃) δ 7.74 (d, *J* = 7.8 Hz, 2H), 7.62 (d, *J* = 7.6 Hz, 2H), 7.54-7.47 (m, 2H), 7.45-7.41 (m, 2H), 7.33 (m, 1H), 7.25 (m, 1H), 7.12-7.07 (m, 2H), 7.06-6.99 (m, 3H), 4.32 (dd, *J* = 10.9, 3.5 Hz), 3.43 (s, 3H), 3.06 (dd, *J* = 16.4, 10.9 Hz), 2.73 (dd, *J* = 16.4, 3.5 Hz). ¹³C NMR (150 MHz, CDCl₃) δ 172.2, 169.7, 152.0, 139.5, 136.4, 133.8, 129.3, 129.1, 128.8, 128.3, 127.9, 127.3, 125.4, 124.7, 122.2, 91.1, 51.6, 50.4, 35.6. HRMS (MALDI) [*M* + *H*⁺] calcd for C₂₄H₂₁O₄⁺ 373.1440, found 373.1446. [*α*]_D²⁰ = -141.2° (c = 0.1, CHCl₃).

6.5 Enantioselective alkylation of 3-substituted-Phthalides

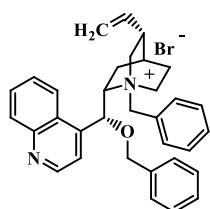
Phase transfer catalysts **94a-d** and **96a-c** were commercially available, phase transfer catalysts **94e-n** and **95a-d** were provided by Professor Luca Bernardi of the University of Bologna, whereas phase transfer catalysts **94e**, **94o-s** were prepared by the procedure detailed below.¹⁶¹

¹⁶⁰ W. Zhang, D. Tan, R. Lee, G. Tong, W. Chen, B. Qi, K.-W. Huang, C.-H. Tan, Z. Jiang, *Angew. Chem. Int. Ed.*, **2012**, *51*, 10069–10073.

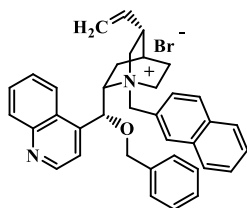
¹⁶¹ Y. Liu, B. A. Provencher, K. J. Bartelson, L. Deng, *Chem. Sci.*, **2011**, *2*, 1301-1304.

6.5.1 Synthesis of phase transfer catalysts **94e**, **94o-s**

In a reacti-vial of 2.5 mL, to a solution of **135** (1.0 eq., 0.14 mmol, 52.8 mg) in $\text{CHCl}_3/\text{EtOH} = 1/1$ (0.52 mL), arylmethyl bromide or substituted benzyl bromide (1.2 eq., 0.16 mmol) was added. The reaction mixture was stirred for 48 hours at $40\text{ }^\circ\text{C}$. Next, the reaction mixture was cooled to room temperature and slowly added to ethyl ether (25 mL) with stirring. The precipitated was filtered and washed with ethyl ether (20 mL). The solid was collected and purified by flash chromatography (silica gel: AcOEt-MeOH 99-1 to 80-20) affording the pure desired product.



(8S, 9R)-1-(benzyl)-9-(phenylmethoxy)-Cinchonanium bromide (94e): Obtained as a white solid (52.9 mg, 68% yield). The characterization data matched those previously reported.¹⁶²

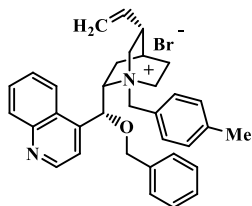


(8S, 9R)-1-(2-naphthalenylmethyl)-9-(phenylmethoxy)-Cinchonanium bromide (94s): Obtained as a white solid (43.4 mg, 62% yield). The characterization data matched those previously

reported.¹⁶³

¹⁶² T. Tozawa, H. Nagao, Y. Yamane, T. Mukaiyama, *Chem. Asian J.*, **2007**, 2, 123 -134.

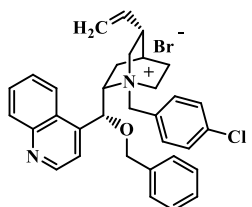
¹⁶³ S. E. Denmark, R. C. Weintraub, *HETEROCYCLES*, **2011**, 82, 2, 1527-1540.

**(8*S*, 9*R*)-1-(4-methylbenzyl)-9-(phenylmethoxy)-****Cinchonanum bromide (94o):** Obtained as a whitesolid (34.4 mg, 45% yield), 167 °C decomp. ¹H NMRNMR (400 MHz, CDCl₃) δ 8.99 (d, *J* = 4.5 Hz, 1H),8.72 (d, *J* = 8.4 Hz, 1H), 8.14 (d, *J* = 8.4 Hz, 1H),7.93 (m, 1H), 7.78 (t, *J* = 7.7 Hz, 1H), 7.68 (m, 1H), 7.54-7.28 (m, 7H), 7.18(d, *J* = 7.8 Hz, 2H), 6.22 (m, 1H), 5.27 (d, *J* = 17.1 Hz, 1H), 4.96 (d, *J* = 10.5Hz, 1H), 4.83 (d, *J* = 11.3 Hz, 1H), 4.60 (m, 1H), 4.36 (d, *J* = 11.3 Hz, 1H),

4.19-3.97 (m, 2H), 3.28-3.06 (m, 2H), 2.52 (m, 1H), 2.35 (s, 3H), 2.23-2.04

(m, 2H), 2.01 (m, 1H), 1.73 (m, 1H), 1.45 (m, 1H), 1.33-1.13 (m, 1H). ¹³CNMR (100 MHz, CDCl₃) δ 149.3, 148.5, 139.8, 136.2, 135.5, 130.4, 129.8,

129.6, 129.3, 129.2, 129.1, 125.2, 124.6, 123.8, 119.2, 118.3, 72.6, 71.4,

65.6, 61.6, 59.4, 50.8, 37.7, 26.9, 25.2, 22.5, 21.2. HRMS (MALDI) [*M* –Br]⁺ calcd for C₃₄H₃₇N₂O⁺ 489.2900, found 489.2900. [α]_D²⁰ = -75.3° (c = 0.2,CHCl₃).**(8*S*, 9*R*)-1-(4-chlorobenzyl)-9-(phenylmethoxy)-****Cinchonanum bromide (94p):** Obtained as a whitesolid (58.1 mg, 68% yield), 169 °C decomp. ¹H NMR(400 MHz, CDCl₃) δ 8.97 (d, *J* = 4.4 Hz, 1H), 8.70 (d,*J* = 8.4 Hz, 1H), 8.12 (d, *J* = 8.4 Hz, 1H), 7.89 (m, 1H),7.74 (t, *J* = 7.6 Hz, 1H), 7.66 (m, 1H), 7.58 (d, *J* = 7.6 Hz, 1H), 7.48-7.27(m, 8H), 6.31-6.10 (m, 2H), 5.62 (m, 1H), 5.27 (d, *J* = 17.2 Hz, 1H), 4.93 (d,*J* = 10.7 Hz, 1H), 4.83 (d, *J* = 11.5 Hz, 1H), 4.57 (m, 1H), 4.38 (d, *J* = 11.5

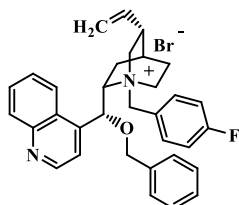
Hz, 1H), 4.22-3.94 (m, 2H), 3.20-2.97 (m, 2H), 2.52 (m, 1H), 2.33-1.94 (m,

3H), 1.75 (m, 1H), 1.44 (m, 1H), 1.21 (m, 1H). ¹³C NMR (150 MHz, CDCl₃)

δ 149.3, 148.4, 139.6, 136.8, 135.9, 135.5, 135.3, 135.2, 130.4, 129.9, 129.4,

129.3, 129.2, 129.1, 125.4, 124.5, 119.2, 118.4, 72.4, 71.3, 65.9, 60.6, 59.3,

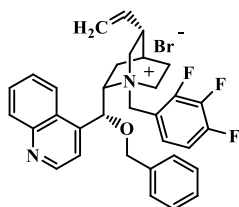
51.0, 37.6, 26.8, 25.1, 22.4. HRMS (MALDI) $[M - Br]^+$ calcd for $C_{33}H_{34}ClN_2O^+$ 509.2394, found 509.2394. $[\alpha]_D^{20} = -114.8^\circ$ ($c = 1.0$, $CHCl_3$).



(8*S*, 9*R*)-1-(4-fluorobenzyl)-9-(phenylmethoxy)-Cinchonanium bromide (94q): Obtained as a white

solid (68.1 mg, 86% yield), mp 78-79 °C. 1H NMR NMR (400 MHz, $CDCl_3$) δ 8.99 (d, $J = 4.5$ Hz, 1H), 8.74 (d, $J = 8.4$ Hz, 1H), 8.14 (d, $J = 8.4$ Hz, 1H), 7.93

(m, 1H), 7.77 (t, $J = 7.6$ Hz, 1H), 7.72-7.60 (m, 2H), 7.49-7.34 (m, 6H), 7.07 (t, $J = 8.39$ Hz, 2H), 6.38-6.13 (m, 2H), 5.65 (m, 1H), 5.31 (d, $J = 17.2$ Hz, 1H), 4.97 (d, $J = 10.53$ Hz, 1H), 4.85 (d, $J = 11.8$ Hz, 1H), 4.20-3.95 (m, 2H), 3.23-2.98 (m, 2H), 2.54 (m, 1H), 2.27-1.94 (m, 3H), 1.76 (m, 1H), 1.46 (m, 1H), 1.21 (m, 1H). ^{13}C NMR (100 MHz, $CDCl_3$) δ 164.9, 162.4, 149.3, 148.4, 139.6, 135.9, 135.4, 134.3, 133.5, 132.6, 130.2, 129.8, 129.3, 129.2, 129.1, 128.6, 128.4, 128.0, 127.6, 125.2, 122.8, 118.4, 116.0 (d, $J = 21.3$ Hz), 72.4, 71.3, 65.8, 60.6, 59.2, 50.8, 37.6, 26.8, 25.0, 22.4. HRMS (MALDI) $[M - Br]^+$ calcd for $C_{33}H_{34}FN_2O^+$ 493.2650, found 493.2651. $[\alpha]_D^{20} = -77.1^\circ$ ($c = 0.2$, $CHCl_3$).



(8*S*, 9*R*)-1-(2,3,4-trifluorobenzyl)-9-(phenylmethoxy)-Cinchonanium bromide (94r):

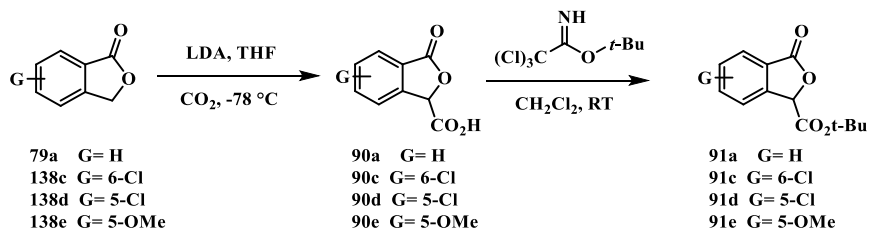
Obtained as a white solid (74.0 mg, 88% yield), mp 87-88 °C. 1H NMR NMR (400 MHz, $CDCl_3$) δ 8.98 (d, $J = 4.9$ Hz, 1H), 8.77 (d, $J = 8.3$ Hz, 1H), 8.52 (m,

1H), 8.13 (d, $J = 8.3$ Hz, 1H), 7.91 (m, 1H), 7.77 (t, $J = 7.4$ Hz, 1H), 7.65 (m, 1H), 7.50-7.23 (m, 5H), 7.11 (m, 1H), 6.46 (d, $J = 11.2$ Hz, 1H), 6.23 (m, 1H), 5.64 (m, 1H), 5.35 (d, $J = 17.2$ Hz, 1H), 5.10-4.90 (m, 2H), 4.72 (d,

$J = 11.2$ Hz, 1H), 4.64 (m, 1H), 4.58-4.41 (m, 2H), 4.35 (m, 1H), 3.21-2.94 (m, 2H), 2.60 (m, 1H), 2.29-1.96 (m, 2H), 1.81 (m, 1H), 1.42 (m, 1H), 1.22 (m, 1H). ^{13}C NMR (100 MHz, CDCl_3) δ 153.8 (d, $J = 8.7$ Hz), 152.2 (d, $J = 9.4$ Hz), 151.3 (d, $J = 8.0$ Hz), 149.7 (d, $J = 8.1$ Hz), 149.2, 148.5, 139.2, 135.7, 134.9, 130.9, 130.3, 129.8, 129.1, 129.0, 128.1, 127.6, 125.0, 124.5, 119.1, 118.5, 113.5 (d, $J = 17.5$), 112.3 (d, $J = 9.4$), 72.8, 71.5, 66.2, 59.5, 53.9, 51.9, 37.6, 26.4, 25.1, 22.6. HRMS (MALDI) $[\text{M} - \text{Br}]^+$ calcd for $\text{C}_{33}\text{H}_{32}\text{F}_3\text{N}_2\text{O}^+$ 529.2461, found 529.2461. $[\alpha]_D^{20} = -109.3^\circ$ ($c = 1.0$, CHCl_3).

6.5.2 Synthesis of 3-carboxylic-*t*-butyl-ester-phthalides 91a, 91c-e

3-carboxylic-*t*-Bu-ester-phthalides **91a**, **91c-e** were prepared in two steps. Isobenzofuran-1(3*H*)-one **79a** is commercially available, whereas 6-chloroisobenzofuran-1(3*H*)-one **138c**, 5-chloroisobenzofuran-1(3*H*)-one **136d** and 5-methoxyisobenzofuran-1(3*H*)-one **138e** were prepared according to the literature.¹⁶⁴

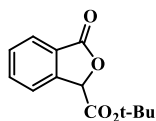


First step:⁹¹ To a solution of isopropylamine 0.5 M (1.5 equiv. 28.0 mmol) in anhydrous THF (55 mL) was added BuLi (1.5 equiv. 28 mmol) at -78°C under nitrogen atmosphere. The mixture was stirred for 30 minutes at -78°C . Next, a solution of phthalide **79a** or **138c-e**, (1 equiv. 18.6 mmol) in anhydrous THF (3.8 ml) was added slowly to the previous solution

¹⁶⁴ Y.-H. Zhang, B.-F. Shi, J.-Q. Yu, *Angew. Chem. Int. Ed.*, **2009**, 48, 6097–610.

containing fresh LDA. The resulting mixture was stirred for 50 minutes at -78°C under nitrogen atmosphere. Subsequently, 5 freeze-pump-thaw cycles were performed and carbon dioxide was bubbled into the solution using a balloon for about 2 hours at -78°C . To stop the reaction, sat. aqueous NH_4Cl solution (15 mL) was added dropwise and THF was removed under reduced pressure. The mixture was basified with sat. Na_2CO_3 aqueous solution until $\text{pH} = 9$ and washed with AcOEt (2 x 20 mL). The aqueous phase was acidified with conc. HCl solution until $\text{pH} = 1$ and the product was extracted with AcOEt (3 x 50 mL). The combined organic phase was dried over Na_2SO_4 and concentrated under reduced pressure. The resulting phthalide 3-carboxylic acid **90** was used in the next step without further purification.

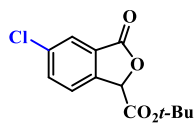
Second step: To a solution of synthesized phthalide 3-carboxylic acid **90** (1.0 eq., 18.6 mmol) in anhydrous CH_2Cl_2 (70 mL) was added *tert*-Butyl 2,2,2-trichloroacetimidate (1.0 eq., 18.6 mmol, 3.3 mL). The resulting reaction mixture was stirred for 48 hours under nitrogen atmosphere. Next, the reaction mixture was diluted with CH_2Cl_2 and centrifuged. The supernatant solution was concentrated under reduced pressure and the crude residue was purified by flash chromatography (silica gel, petroleum ether-ethyl acetate 95-5 to 80-20) affording the desired product **91**.



tert-butyl 3-oxo-1,3-dihydroisobenzofuran-1-carboxylate

3-carboxylic-*t*-butyl-ester-phthalide (91a): Obtained as a white solid (4.36 g, 99% yield). The characterization data

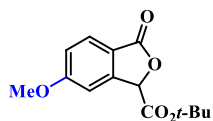
matched those previously reported.⁹¹



tert-butyl 5-chloro-3-oxo-1,3-dihydroisobenzofuran-1-carboxylate (91c): Obtained as a white solid (2.78 g, 37% yield), mp 87-88 °C. $^1\text{H NMR}$ (400 MHz, CDCl_3) δ 7.80 (d, $J = 1.4$ Hz, 1H), 7.64 (dd, $J = 8.2, 1.9$ Hz, 1H) 7.57, (d, $J = 8.2$ Hz, 1H), 5.73 (s, 1H), 1.45 (s, 9H). $^{13}\text{C NMR}$ (100 MHz, CDCl_3) δ 168.2, 164.9, 142.7, 136.4, 134.8, 125.7, 123.9, 84.4, 77.5, 27.8. HRMS (MALDI) $[\text{M} + \text{H}^+]$ calcd for $\text{C}_{13}\text{H}_{14}\text{ClO}_4^+$ 269.0581, found 269.0586.



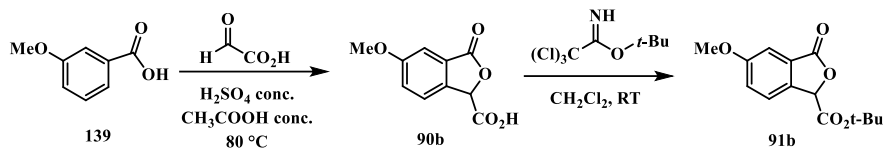
tert-butyl 6-chloro-3-oxo-1,3-dihydroisobenzofuran-1-carboxylate (91d): Obtained as a white solid (2.71 g, 36% yield), mp 94-95 °C. $^1\text{H NMR}$ (400 MHz, CDCl_3) δ 7.83 (d, $J = 8.2$ Hz, 1H), 7.62 (d, $J = 1.2$ Hz, 1H), 7.55 (dd, $J = 8.2, 1.2$ Hz, 1H), 5.72 (s, 1H), 1.49 (s, 9H). $^{13}\text{C NMR}$ (100 MHz, CDCl_3) δ 168.4, 164.8, 146.1, 141.1, 130.8, 127.0, 123.6, 123.0, 84.5, 77.1, 27.9. HRMS (MALDI) $[\text{M} + \text{H}^+]$ calcd for $\text{C}_{13}\text{H}_{14}\text{ClO}_4^+$ 269.0581, found 269.0582.



tert-butyl 6-methoxy-3-oxo-1,3-dihydroisobenzofuran-1-carboxylate (91e): Obtained as a white solid (3.55 g, 48% yield), mp 82-81 °C. $^1\text{H NMR}$ (600 MHz, CDCl_3) δ 7.81 (d, $J = 8.6$ Hz, 1H), 7.09 – 7.06 (m, 2H), 5.68 (s, 1H), 3.92 (s, 3H), 1.49 (s, 9H). $^{13}\text{C NMR}$ (150 MHz, CDCl_3) δ 169.4, 165.6, 164.9, 163.6, 147.3, 127.4, 117.3, 106.6, 84.0, 77.2, 55.9, 27.9. HRMS (MALDI) $[\text{M} + \text{H}^+]$ calcd for $\text{C}_{14}\text{H}_{17}\text{O}_5^+$ 265.1072, found 265.1076.

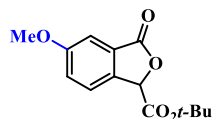
6.5.3 Synthesis of compound 91b

The compound **91b**, unreported in literature, was prepared in two steps.



First step:¹⁶⁵ To a mixture of 3-methoxybenzoic acid **139** (5.0 mmol), glyoxylic acid monohydrate (2.0 eq., 10 mmol), and H₂SO₄ (2.0 eq., 10 mmol, 0.55 mL), glacial acetic acid (20.0 mL) was added and the reaction mixture was stirred at 80 °C for 48 hours. Then, the mixture was cooled to room temperature and extracted with AcOEt (3 x 50 mL). The combined organic phase was dried over Na₂SO₄ and concentrated under reduced pressure. The phthalide-3-carboxylic acid **90b** was achieved as a white solid (0.56 g, 54% yield) and used in the next step without further purification.

Second step: To a solution of phthalide 3-carboxylic acid **90b** (1.0 eq., 2.7 mmol, 3.3 g) in anhydrous CH₂Cl₂ (10 mL) was added *tert*-Butyl 2,2,2-trichloroacetimidate (1.0 eq., 2.7 mmol, 0.5 mL). The resulting reaction mixture was stirred for 48 hours under nitrogen atmosphere. Next, the reaction mixture was diluted with CH₂Cl₂ and centrifuged. The supernatant solution was concentrated under reduced pressure and the crude residue was purified by flash chromatography (silica gel, petroleum ether-ethyl acetate 95-5 to 80-20) affording the desired product **91b** as a white solid (0.30 g, 43% yield).



tert-butyl

5-methoxy-3-oxo-1,3-

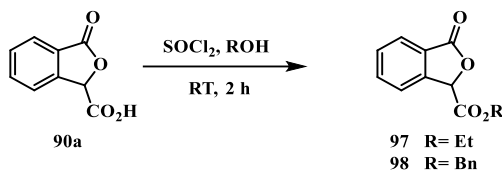
dihydroisobenzofuran-1-carboxylate (91b): Obtained as a white solid (0.30 g, 43% yield), mp 89-90 °C. ¹H

NMR (400 MHz, CDCl₃) δ 7.47 (d, *J* = 8.4 Hz, 1H), 7.27 (d, *J* = 1.9 Hz, 1H),

¹⁶⁵ J. Ni, H. Xiao, L. Weng, X. Wei, Y. Xu, *Tetrahedron*, **2011**, 67, 5162-5167.

7.21 (dd, $J = 8.4, 1.9$ Hz, 1H), 5.66 (s, 1H), 3.83 (s, 3H), 1.44 (s, 9H). ^{13}C NMR (100 MHz, CDCl_3) δ 169.6, 165.6, 161.3, 136.7, 126.3, 123.3, 123.1, 107.7, 83.7, 77.4, 55.7, 27.8. HRMS (MALDI) $[\text{M} + \text{Na}^+]$ calcd for $\text{C}_{14}\text{H}_{16}\text{NaO}_5^+$ 287.0890, found 287.0892.

6.5.4 Synthesis of compounds **97** and **98**



To a solution of phthalide 3-carboxylic acid **90a** (1.0 eq., 1.1 mmol, 0.2 g) in anhydrous ROH (1.3 eq., 1.4 mmol) was added thionyl chloride (1.2 eq., 1.3 mmol, 96 μL). The resulting solution was stirred for 2 hours at room temperature under nitrogen atmosphere. Next, the ROH was evaporated and water (10 mL) was added to the crude reaction. The mixture was extracted with AcOEt (3 x 20 mL) and the combined organic phases were dried over Na_2SO_4 , filtered and concentrated in vacuo. The products **97** (0.22 g, 96% yield) and **98** (0.26 g, 90% yield) were obtained in a form suitable for use without further purification.

The characterization data of compounds **97**¹⁶⁶ and **98**¹⁶⁷ matched those previously reported.

6.5.5 Typical procedure for the synthesis of racemic compound **93a**

¹⁶⁶ J. Tatsugi, T. Hara, Y. Izawa, Chem. Lett., 1997, 177-178.

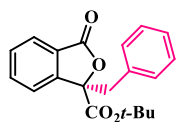
¹⁶⁷ M. Ishibashi, A. Wagner, C. Mioskowski, C. Sylvain, *PCT Int. Appl.*, **2001**, WO 2001072730 A1 20011004.

In a 4 ml vial, to a mixture of 3-carboxylic-*t*-butyl-ester-phthalide **91a** (1.0 eq., 0.1 mmol), DCH-18-crown-6 (0.10 eq., 0.010 mmol) and benzylbromide **92a** (1.2 eq., 0.12 mmol) in toluene (1 mL), was added KOH aqueous 50% (0.6 mL). The reaction mixture was stirred for 1 hour at room temperature. Then, the mixture was diluted with HCl 1 M (1 mL) and extracted with CH₂Cl₂ (3 x 5 mL). The combined organic phases were dried over Na₂SO₄ and concentrated under reduced pressure. The crude residue was purified by flash chromatography (silica gel, petroleum ether-ethyl acetate 98-2 to 80-20) affording the racemic product **93aa** as a white solid (28.5 mg, 88% yield).

6.5.6 General procedure for the enantioselective alkylation of 3-carboxylic-*t*-butyl-ester-phthalide

In a 4 ml vial, to a mixture of 3-carboxylic-*t*-butyl-ester-phthalide **91** (1.0 eq., 0.1 mmol), (*R,R*)-**x** (0.05 eq., 0.005 mmol) and alkylbromide **92** (1.2 eq., 0.12 mmol) in toluene (1 mL), was added Cs₂CO₃ aqueous 50% (0.6 mL). The reaction mixture was stirred for the indicated time at room temperature. Then, the mixture was diluted with HCl 1 M (1 mL) and extracted with CH₂Cl₂ (3 x 5 mL). The combined organic phases were dried over Na₂SO₄ and concentrated under reduced pressure. The crude residue was purified by flash chromatography (silica gel, petroleum ether-ethyl acetate 98-2 to 80-20) affording the desired product **93** as a white solid.

6.5.7 Analytical data of asymmetric 3,3-disubstituted phthalides



tert-butyl

(*R*)-1-benzyl-3-oxo-1,3-

dihydroisobenzofuran-1-carboxylate (**93aa**): Obtained as a white solid (21.4 mg, 66% yield), mp 88-89 °C. ¹H NMR

(400 MHz, CDCl₃) δ 7,78–7,66 (3H, m), 7.50 (1H, m), 7,20–7.12 (5H, m),

3.64 (1H, d, $J = 14.3$), 3.35 (1H, d, $J = 14.3$), 1.37 (9H, s). ^{13}C NMR (100 MHz, CDCl_3) δ 169.0, 167.2, 147.6, 134.1, 133.4, 130.4, 129.9, 128.1, 127.2, 124.7, 125.6, 122.6, 87.7, 83.8, 43.2, 27.8. HRMS (MALDI) $[\text{M} + \text{H}^+]$ calcd for $\text{C}_{20}\text{H}_{21}\text{O}_4^+$ 325.1434, found 325.1437. $[\alpha]_D^{20} = +37.2^\circ$ ($c = 0.20$, CHCl_3). Enantiomeric excess = 94% determined by HPLC analysis (CHIRALPAK[®] AS-H column ($\phi 0.46$ cm x 25 cm), n -hexane: i -PrOH = 90:10, 0.5 mL/min, $t_{\text{minor}} = 16.4$ min, $t_{\text{major}} = 21.4$ min).



tert-butyl (R)-1-(4-(*tert*-butyl)benzyl)-3-oxo-1,3-dihydroisobenzofuran-1-carboxylate (93ab):

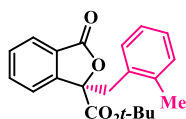
Obtained as a white solid (36.5 mg, 96% yield), mp 99–100 °C. ^1H NMR (400 MHz, CDCl_3) δ 7.78 (d, $J = 7.6$ Hz, 1H), 7.75–7.65 (m, 2H), 7.56–7.47 (m, 1H), 7.20 (d, $J = 8.2$ Hz, 2H), 7.11 (d, $J = 8.2$ Hz, 2H), 3.62 (d, $J = 14.3$ Hz, 1H), 3.28 (d, $J = 14.3$ Hz, 1H), 1.35 (s, 9H), 1.24 (s, 9H). ^{13}C NMR (100 MHz, CDCl_3) δ 169.1, 167.1, 150.0, 147.8, 134.1, 130.4, 130.0, 129.8, 125.7, 125.6, 124.9, 122.5, 87.8, 83.6, 42.8, 34.3, 31.2, 27.6. HRMS (MALDI) $[\text{M} + \text{Na}^+]$ calcd for $\text{C}_{24}\text{H}_{28}\text{NaO}_4^+$ 403.1880, found 403.1882. $[\alpha]_D^{20} = +63.5^\circ$ ($c = 0.20$, CHCl_3). Enantiomeric excess = 88% determined by HPLC analysis (CHIRALPAK[®] AS-H column ($\phi 0.46$ cm x 25 cm), n -hexane: i -PrOH = 90:10, 0.3 mL/min, $t_{\text{minor}} = 28.1$ min, $t_{\text{major}} = 31.4$ min).



tert-butyl (R)-1-(4-methylbenzyl)-3-oxo-1,3-dihydroisobenzofuran-1-carboxylate (93ac):

Obtained as a white solid (32.1 mg, 95% yield), mp 93–94 °C. ^1H NMR (400 MHz, CDCl_3) δ 7.75 (d, $J = 7.6$ Hz, 1H), 7.72–7.64 (m, 2H), 7.56–7.45 (m, 1H), 7.01 (d, $J = 7.9$ Hz, 2H), 6.96 (d, $J = 7.9$ Hz, 2H), 3.60 (d, $J = 14.3$ Hz, 1H), 3.32 (d, $J = 14.3$ Hz, 1H), 2.23 (s, 3H), 1.39 (s, 9H). ^{13}C

NMR (100 MHz, CDCl₃) δ 169.1, 167.2, 147.6, 136.7, 134.0, 130.2, 130.1, 129.8, 128.7, 125.7, 125.6, 122.5, 87.7, 83.7, 42.6, 27.7, 21.0. HRMS (MALDI) [M + K⁺] calcd for C₂₁H₂₂KO₄⁺ 377.1150, found 377.1163. $[\alpha]_D^{20} = +24.4^\circ$ (c = 0.20, CHCl₃). Enantiomeric excess = 82% determined by HPLC analysis (CHIRALPAK[®] AS-H column (ϕ 0.46 cm x 25 cm), *n*-hexane:*i*-PrOH = 90:10, 0.5 mL/min, $t_{\text{minor}} = 22.3$ min, $t_{\text{major}} = 32.0$ min).



tert-butyl (R)-1-(2-methylbenzyl)-3-oxo-1,3-dihydroisobenzofuran-1-carboxylate (**93ad**): Obtained as a white solid (32.5 mg, 96% yield), mp 90-91 °C. ¹H

NMR (400 MHz, CDCl₃) δ 7.81 – 7.66 (m, 3H), 7.57– .49 (m, 1H), 7.11– 7.01 (m, 3H), 6.99– 6.91 (m, 1H), 3.75 (d, *J* = 14.7 Hz, 1H), 3.35 (d, *J* = 14.7 Hz, 1H), 2.33 (s, 3H), 1.38 (s, 9H). ¹³C NMR (100 MHz, CDCl₃) δ 168.9, 167.4, 147.9, 137.6, 134.0, 131.9, 130.4, 129.9, 127.2, 125.6, 125.4, 122.6, 88.1, 83.6, 39.4, 27.7, 20.1. HRMS (MALDI) [M + K⁺] calcd for C₂₁H₂₂NaO₄⁺ 361.1410, found 361.1421. $[\alpha]_D^{20} = +40.8^\circ$ (c = 0.40, CHCl₃). Enantiomeric excess = 84% determined by HPLC analysis (CHIRALPAK[®] AS-H column (ϕ 0.46 cm x 25 cm), *n*-hexane:*i*-PrOH = 90:10, 0.5 mL/min, $t_{\text{minor}} = 15.0$ min, $t_{\text{major}} = 17.8$ min).



tert-butyl (R)-1-(4-methoxybenzyl)-3-oxo-1,3-dihydroisobenzofuran-1-carboxylate (**93ae**): Obtained as a white solid (32.6 mg, 92% yield), mp 97-

98 °C. ¹H NMR (600 MHz, CDCl₃) δ 7.75 (m, 1H), 7.71–7.67 (m, 2H), 7.50 (m, 1H), 7.05 (d, *J* = 8.2 Hz), 6.69 (d, *J* = 8.2 Hz), 3.73 (s, 3H), 3.58 (d, *J* = 14.3 Hz), 3.30 (d, *J* = 14.3 Hz), 1.41 (s, 9H). ¹³C NMR (150 MHz, CDCl₃) δ 169.1, 167.3, 158.7, 147.7, 134.1, 131.5, 129.8, 125.9, 125.6, 125.3, 122.5, 113.5, 87.8, 83.7, 55.1, 42.3, 27.8. Enantiomeric excess = 80% determined by HPLC analysis (CHIRALPAK[®] AS-H column (ϕ 0.46 cm x 25 cm), *n*-

hexane:*i*-PrOH = 90:10, 0.5 mL/min, $t_{\text{minor}} = 16.2$ min, $t_{\text{major}} = 21.3$ min. HRMS (ESI) $[M + Na^+]$ calcd for $C_{21}H_{22}NaO_5^+$ 377.1358, found 377.1359. $[\alpha]_D^{20} = +11.9^\circ$ ($c = 0.80$, $CHCl_3$). Enantiomeric excess = 84% determined by HPLC analysis (CHIRALPAK[®] AS-H column ($\phi 0.46$ cm x 25 cm), *n*-hexane:*i*-PrOH = 90:10, 0.5 mL/min, $t_{\text{minor}} = 26.8$ min, $t_{\text{major}} = 42.9$ min).



***tert*-butyl (R)-1-(4-chlorobenzyl)-3-oxo-1,3-dihydroisobenzofuran-1-carboxylate (93af):** Obtained as a white solid (33.7 mg, 94% yield), mp 110-111 °C. ¹H

NMR (400 MHz, $CDCl_3$) δ 7.82–7.74 (m, 1H), 7.74–7.66 (m, 2H), 7.57–7.48 (m, 1H), 7.15 (d, $J = 8.3$ Hz, 2H), 7.09 (d, $J = 8.3$ Hz, 2H), 3.62 (d, $J = 14.3$ Hz, 1H), 3.31 (d, $J = 14.3$ Hz, 1H), 1.38 (s, 9H). ¹³C NMR (100 MHz, $CDCl_3$) δ 168.8, 167.0, 147.3, 134.2, 133.2, 131.8, 131.7, 130.0, 128.2, 125.8, 125.6, 122.3, 87.3, 83.9, 42.2, 27.7. HRMS (MALDI) $[M + K^+]$ calcd for $C_{20}H_{19}ClKO_4^+$ 397.0603, found 397.0609. $[\alpha]_D^{20} = +14.4^\circ$ ($c = 0.20$, $CHCl_3$). Enantiomeric excess = 80% determined by HPLC analysis (CHIRALPAK[®] AS-H column ($\phi 0.46$ cm x 25 cm), *n*-hexane:*i*-PrOH = 90:10, 0.5 mL/min, $t_{\text{minor}} = 21.3$ min, $t_{\text{major}} = 28.8$ min).



***tert*-butyl (R)-1-(4-nitrobenzyl)-3-oxo-1,3-dihydroisobenzofuran-1-carboxylate (93ag):** Obtained as a white solid (33.6 mg, 91% yield), mp 96-

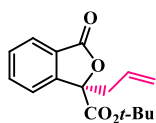
97 °C. ¹H NMR (400 MHz, $CDCl_3$) δ 8.05 (d, $J = 8.6$ Hz, 2H), 7.82–7.75 (m, 1H), 7.73 (s, 2H), 7.60–7.49 (m, 1H), 7.36 (d, $J = 8.6$ Hz, 2H), 3.79 (d, $J = 14.2$ Hz, 1H), 3.43 (d, $J = 14.2$ Hz, 1H), 1.37 (s, 9H). ¹³C NMR (100 MHz, $CDCl_3$) δ 168.6, 166.6, 147.1, 147.0, 141.1, 134.5, 131.3, 130.32, 126.0, 125.4, 123.2, 122.1, 86.7, 84.3, 42.4, 27.6. HRMS (MALDI) $[M + K^+]$ calcd for $C_{20}H_{19}NKO_6^+$ 408.0844, found 408.0844. $[\alpha]_D^{20} = +37.4^\circ$ ($c = 0.80$,

CHCl₃). Enantiomeric excess = 82% determined by HPLC analysis (CHIRALPAK[®] AS-H column (ϕ0.46 cm x 25 cm), *n*-hexane:*i*-PrOH = 80:20, 0.5 mL/min, *t*_{minor} = 35.2 min, *t*_{major} = 45.7 min).



***tert*-butyl (*R*)-1-(naphthalen-2-ylmethyl)-3-oxo-1,3-dihydroisobenzofuran-1-carboxylate (93ah):**

Obtained as a white solid (24.3 mg, 65% yield), mp 128–129 °C. ¹H NMR (400 MHz, CDCl₃) δ 7.80–7.68 (m, 5H), 7.66 (d, *J* = 8.4 Hz, 1H), 7.63 (s, 1H), 7.53–7.46 (m, 1H), 7.44 – 7.38 (m, 2H), 7.30 (d, *J* = 8.4 Hz, 1H), 3.82 (d, *J* = 14.3 Hz, 1H), 3.51 (d, *J* = 14.3 Hz, 1H), 1.36 (s, 9H). ¹³C NMR (100 MHz, CDCl₃) δ 169.0, 167.1, 147.6, 134.1, 133.0, 132.4, 131.0, 129.9, 129.3, 128.3, 127.6, 127.4, 125.9, 125.7, 125.7, 122.5, 87.7, 83.8, 43.2, 27.7. HRMS (MALDI) [*M* + *K*⁺] calcd for C₂₄H₂₂KO₄⁺ 413.1150, found 413.1157. [*α*]_D²⁰ = +37.1° (*c* = 0.20, CHCl₃). Enantiomeric excess = 74% determined by HPLC analysis (CHIRALPAK[®] AS-H column (ϕ0.46 cm x 25 cm), *n*-hexane:*i*-PrOH = 90:10, 0.5 mL/min, *t*_{minor} = 26.2 min, *t*_{major} = 36.7 min).



***tert*-butyl (*R*)-1-allyl-3-oxo-1,3-dihydroisobenzofuran-1-carboxylate (93ai):** Obtained as a white solid (17.8 mg, 65% yield), mp 90–91 °C. ¹H NMR (400 MHz, CDCl₃) δ 7.88 (d,

J = 7.6 Hz, 1H), 7.73–7.66 (m, 1H), 7.64–7.52 (m, 2H), 5.62 (m, 1H), 5.20–5.05 (m, 2H), 3.10 (dd, *J* = 14.4, 7.7 Hz, 1H), 2.77 (dd, *J* = 14.4, 6.5 Hz, 1H), 1.43 (s, 9H). ¹³C NMR (100 MHz, CDCl₃) δ 169.2, 167.0, 147.7, 134.3, 129.9, 129.8, 125.7, 125.6, 122.3, 120.7, 87.1, 83.7, 41.3, 27.7. HRMS (MALDI) [*M* + *K*⁺] calcd for C₁₆H₁₈KO₄⁺ 313.0837, found 313.0842. [*α*]_D²⁰ = -29.8° (*c* = 0.80, CHCl₃). Enantiomeric excess = 92% determined by HPLC

analysis (CHIRALPAK[®] AS-H column (ϕ 0.46 cm x 25 cm), *n*-hexane:*i*-PrOH = 90:10, 0.5 mL/min, $t_{\text{minor}} = 18.2$ min, $t_{\text{major}} = 23.5$ min).



tert-butyl (R)-1-benzyl-5-methoxy-3-oxo-1,3-dihydroisobenzofuran-1-carboxylate (93ba):

Obtained as a white solid (34.0 mg, 96% yield), mp 109-110 °C. ¹H NMR (400 MHz, CDCl₃) δ 7.57 (d, $J = 8.4$ Hz, 1H), 7.23 (dd, $J = 8.4, 2.3$ Hz, 1H), 7.20–7.10 (m, 7H), 3.83 (s, 3H), 3.60 (d, $J = 14.3$ Hz, 1H), 3.33 (d, $J = 14.3$ Hz, 1H), 1.37 (s, 9H). ¹³C NMR (100 MHz, CDCl₃) δ 169.0, 167.3, 161.1, 140.0, 133.4, 130.4, 128.01, 127.2, 127.1, 123.4, 122.9, 107.3, 87.4, 83.6, 55.7, 43.0, 27.7. HRMS (MALDI) [M + K⁺] calcd for C₂₁H₂₂KO₅⁺ 393.1099, found 393.1110. $[\alpha]_D^{20} = +70.4^\circ$ (c = 0.80, CHCl₃). Enantiomeric excess = 80% determined by HPLC analysis (CHIRALPAK[®] AS-H column (ϕ 0.46 cm x 25 cm), *n*-hexane:*i*-PrOH = 98:2, 1.0 mL/min, $t_{\text{minor}} = 29.1$ min, $t_{\text{major}} = 32.3$ min).



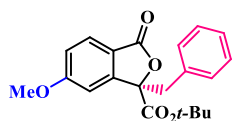
tert-butyl (R)-1-benzyl-5-chloro-3-oxo-1,3-dihydroisobenzofuran-1-carboxylate (93ca):

Obtained as a white solid (34.43 mg, 96% yield), mp 98-99 °C. ¹H NMR (600 MHz, CDCl₃) δ 7.72 – 7.32 (m, 3H), 7.16 – 7.11 (m, 5H), 3.62 (d, $J = 14.4$ Hz, 1H), 3.36 (d, $J = 14.4$ Hz, 1H), 1.39 (s, 9H). ¹³C NMR (150 MHz, CDCl₃) δ 167.5, 166.8, 145.8, 136.3, 134.4, 133.0, 130.4, 128.2, 127.6, 127.4, 125.5, 123.9, 87.6, 84.1, 43.0, 27.7. HRMS (MALDI) [M + K⁺] calcd for C₂₀H₁₉ClKO₄⁺ 397.0603, found 397.0604. $[\alpha]_D^{20} = +16.7^\circ$ (c = 0.68, CHCl₃). Enantiomeric excess = 78% determined by HPLC analysis (CHIRALPAK[®] AS-H column (ϕ 0.46 cm x 25 cm), *n*-hexane:*i*-PrOH = 90:10, 0.5 mL/min, $t_{\text{major}} = 12.1$ min, $t_{\text{minor}} = 14.1$ min).



tert-butyl (R)-1-benzyl-6-chloro-3-oxo-1,3-dihydroisobenzofuran-1-carboxylate (93da):

Obtained as a white solid (34.1 mg, 95% yield), mp 95–96 °C. ¹H NMR (600 MHz, CDCl₃) δ 7.70 (d, *J* = 1.6 Hz, 1H), 7.67 (d, *J* = 8.0 Hz, 1H), 7.48 (dd, *J* = 8.0, 1.6 Hz, 1H), 7.21–7.17 (m, 3H), 7.16–7.13 (m, 2H), 3.62 (d, *J* = 13.6 Hz, 1H), 3.33 (d, *J* = 13.6 Hz, 1H), 1.41 (s, 9H). ¹³C NMR (150 MHz, CDCl₃) δ 167.8, 166.7, 149.3, 140.8, 132.9, 130.7, 130.4, 128.2, 127.4, 126.7, 124.3, 123.1, 87.2, 84.3, 43.2, 27.7. HRMS (MALDI) [M + K⁺] calcd for C₂₀H₁₉ClKO₄⁺ 397.0603, found 397.0603. [α]_D²⁰ = +32.2° (c = 0.85, CHCl₃). Enantiomeric excess = 80% determined by HPLC analysis (CHIRALPAK[®] AS-H column (φ0.46 cm x 25 cm), *n*-hexane:*i*-PrOH = 90:10, 0.5 mL/min, *t*_{minor} = 13.2 min, *t*_{major} = 18.4 min).



tert-butyl (R)-1-benzyl-6-methoxy-3-oxo-1,3-dihydroisobenzofuran-1-carboxylate (83ea):

Obtained as a white solid (34.0 mg, 96% yield), mp 88–89 °C. ¹H NMR (600 MHz, CDCl₃) δ 7.66 (d, *J* = 8.5 Hz, 1H), 7.17–7.13 (m, 5H), 7.02 (m, 1H), 7.00 (dd, *J* = 8.5, 2.0 Hz, 1H), 73.93 (s, 3H), 3.60 (d, *J* = 13.8 Hz, 1H), 3.31 (d, *J* = 13.8 Hz, 1H), 1.37 (s, 9H). ¹³C NMR (150 MHz, CDCl₃) δ 167.3, 164.6, 133.5, 130.4, 128.0, 127.2, 127.1, 118.0, 117.1, 106.7, 86.9, 83.7, 55.9, 43.4, 27.7. HRMS (MALDI) [M + H⁺] calcd for C₂₁H₂₃O₅⁺ 355.1545, found 355.1543. [α]_D²⁰ = +5.6° (c = 0.80, CHCl₃). Enantiomeric excess = 78% determined by HPLC analysis (CHIRALPAK[®] AS-H column (φ0.46 cm x 25 cm), *n*-hexane:*i*-PrOH = 90:10, 0.5 mL/min, *t*_{minor} = 29.9 min, *t*_{major} = 61.4 min).

6.5.8 X-ray crystallography

The compound **93aa** (9 mg) was dissolved in hot hexane (1.0 mL) and the resulting solution was cooled down at 4° C. After 19 hours, chiral crystals suitable for X-ray diffraction analysis were obtained. A colorless prismatic single crystal of 0.56 mm x 0.38 mm x 0.27 mm was selected and mounted on a cryoloop with paratone oil and measured at room temperature with a Bruker D8 QUEST diffractometer equipped with a PHOTON II detector using CuK α radiation ($\lambda = 1.54178$ Å). Data Indexing was performed using APEX3. Data integration and reduction were performed using SAINT. Absorption correction was performed by multi-scan method in SADABS. The structures were solved using SHELXS-97 and refined by means of full matrix least-squares based on F^2 using the program SHELXL.¹⁴⁶ Non-hydrogen atoms were refined anisotropically, hydrogen atoms were positioned geometrically and included in structure factors calculations but not refined. ORTEP diagrams were drawn using OLEX2.⁴

	93aa
T (K)	296
Formula	C ₂₀ H ₂₀ O ₄
Formula weight	324.36
System	Orthorhombic
Space group	<i>P</i> 2 ₁ 2 ₁ 2 ₁
<i>a</i> (Å)	6.0173(2)
<i>b</i> (Å)	16.8850(5)
<i>c</i> (Å)	17.2658(5)
α (°)	90
β (°)	90
γ (°)	90
<i>V</i> (Å ³)	1754.24(9)

Z	4
D_x (g cm ⁻³)	1.228
λ (Å)	1.54178
μ (mm ⁻¹)	0.690
F_{000}	688
R1 ($I > 2\sigma I$)	0.338 (3157)
wR ₂	0.0892 (3280)
N. of param.	221
Goof	1.053
ρ_{min}, ρ_{max} (eÅ ⁻³)	-0.11, 0.12

Table S3. Crystallographic data for compound

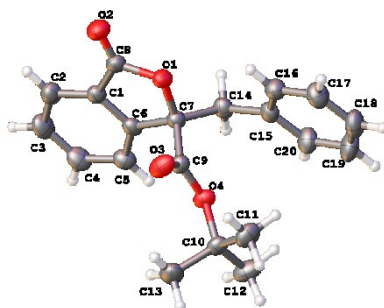


Figure S8 ORTEP diagrams for compound **93aa**. Atom types: C grey, O red, H white. Ellipsoids are drawn at 30% probability level.

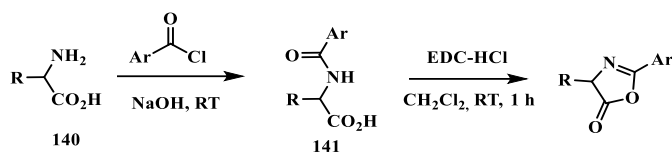
6.6 Asymmetric trifluoromethylthiolation of azlactones

Phase transfer catalysts **94a**, **94c**, **96c** and **123t** were commercially available, phase transfer catalysts **123l-s**, **123u-w** and **94n** were provided by Professor Luca Bernardi of the University of Bologna, whereas phase transfer catalysts **123a-k** were prepared according to the procedure reported in the literature.¹⁶⁸

¹⁶⁸ M. Lian, Z. Li, J. Du, Q. Meng, Z. Gao, *Eur. J. Org. Chem.*, **2010**, 34, 6525-6530.

6.6.1 Synthesis of azlactones substrates

Azlactones **122a**, **126a**, **127a**, **128a**, **129a-j**, **131a** were prepared in two steps starting from racemic amino acids, slightly modifying synthetic procedures reported in the literature.



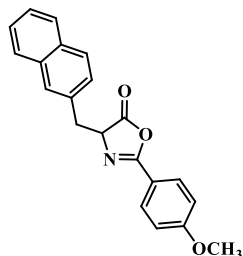
First step:¹⁶⁹ To a solution of amino acid **140** (1.0 eq., 15.0 mmol) in 2 M NaOH aqueous solution (18 ml), aroylchloride was added (1.0 eq., 15.0 mmol). The resulting reaction mixture was stirred at room temperature until complete homogenization and then acidified to pH 2 by adding 1 M HCl aqueous solution. After 2 hours, the mixture was extracted with EtOAc (2 x 50 ml) and the combined organic phases were dried over Na₂SO₄ and concentrated under reduced pressure. The crude residue **141** was used in the next step without further purification.

Second step:¹⁷⁰ *N*-aroyl amino acid **141** (1 eq., 15 mmol) and EDC-HCl (1.3 eq., 19.5 mmol) were dissolved in CH₂Cl₂ anhydrous (50 ml) under nitrogen atmosphere. The resulting reaction mixture was stirred at room temperature for 1 hour. The mixture was diluted with an equal volume of CH₂Cl₂ and washed with water (2 x 50 ml) and a brine solution (30 ml). Then, the organic phase was dried over Na₂SO₄ and concentrated under reduced pressure. In all cases products were obtained in a form suitable for use without further purification.

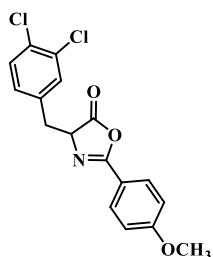
¹⁶⁹ C. Macovei, P. Vicennati, J. Quinton, M. C. Nevers, H. Volland, C. Creminon, F. Taran, *Chem. Commun.*, **2012**, 48, 4411-4413.

¹⁷⁰ A. D. Melhado, M. Luparia, F. D. Toste, *J. AM. CHEM. SOC.*, **2007**, 129, 12638-12639.

The characterization data of the compound **122a**, **126a**, **127a**, **128a**, **129a**, **129d**, **129e**, **129g-j**, **131a** matched those previously reported.¹⁷¹

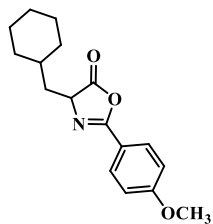


2-(4-methoxyphenyl)-4-(naphthalen-2-ylmethyl)oxazol-5(4H)-one (129f): Obtained as a yellow solid (4.6 g, 92% yield), mp 116-117 °C. ¹H NMR (300 MHz, CDCl₃) δ 7.87 (d, *J* = 8.8 Hz, 2H), 7.83–7.71 (m, 4H), 7.51–7.37 (m, 3H), 6.90 (d, *J* = 8.8 Hz, 2H), 4.75 (dd, *J* = 6.8, 4.9 Hz, 1H), 3.78 (s, 3H), 3.53 (dd, *J* = 14.0, 4.9 Hz, 1H), 3.33 (dd, *J* = 14.0, 6.8 Hz, 1H). ¹³C NMR (75 MHz, CDCl₃) δ 177.9, 163.2, 161.5, 133.4, 133.3, 132.6, 129.8, 128.4, 128.0, 127.8, 127.8, 127.7, 126.1, 125.8, 118.1, 114.2, 66.6, 55.4, 37.6. HRMS (ESI) [*M* + *H*⁺] calcd for C₂₁H₁₈NO₃⁺ 332.1281, found 332.1286.



4-(3,4-dichlorobenzyl)-2-(4-methoxyphenyl)oxazol-5(4H)-one (129c): Obtained as a yellow solid (4.6 g, 90% yield), mp 108-109 °C. ¹H NMR (300 MHz, CDCl₃) δ 7.84 (d, *J* = 8.8 Hz, 2H), 7.36 (d, *J* = 1.7 Hz, 1H), 7.30 (d, *J* = 8.2 Hz, 1H), 7.09 (dd, *J* = 8.2, 1.7 Hz, 1H), 6.92 (d, *J* = 8.8 Hz, 2H), 4.60 (dd, *J* = 6.8, 5.0 Hz, 1H), 3.83 (s, 3H), 3.28 (dd, *J* = 14.1, 5.0 Hz, 1H), 3.07 (dd, *J* = 14.1, 6.8 Hz, 1H). ¹³C NMR (75 MHz, CDCl₃) δ 177.3, 163.4, 161.8, 135.8, 132.3, 131.6, 131.3, 130.3, 129.8, 129.0, 117.7, 114.3, 65.9, 55.5, 36.4. HRMS (ESI) [*M* + *H*⁺] calcd for C₁₇H₁₄Cl₂NO₃⁺ 350.0345, found 350.0349.

¹⁷¹ a) S. K. Nimmagadda, M. Liu, M. K. Karunananda, D.-W. Gao, Omar Apolinar, J. S. Chen, P. Liu, Keary M. Engle, *Angew. Chem. Int. Ed.*, **2019**, *58*, 3923–3927; b) Y. Wang, Y. Chen, X. Li, Y. Mao, W. Chen, R. Zhan, H. Huang, *Org. Biomol. Chem.*, **2019**, *17*, 3945–3950; c) D. Uraguchi, Y. Ueki, A. Sugiyama, T. Ooi, *Chem. Sci.*, **2013**, *4*, 1308–1311; d) H. Hu, Y. Liu, J. Guo, L. Lin, Y. Xu, X. Liua, X. Feng, *Chem. Commun.*, **2015**, *51*, 3835–383; e) T. Takafumi, T. Tsukushi, T. Taro, Y. Ryo, O. Takashi, *Org. Lett.*, 2018, *21*, 3541–3544; f) T. Wang, Z. Yu, D. L. Hoon, C. Y. Phee, Y. Lan, Y. Lu, *J. Am. Chem. Soc.*, **2016**, *138*, 265–271.



4-(cyclohexylmethyl)-2-(4-methoxyphenyl)oxazol-

5(4H)-one (129g): Obtained as a white solid (3.6 g, 84%

yield), mp 115-114 °C. ¹H NMR (300 MHz, CDCl₃) δ

7.92 (d, *J* = 8.9 Hz, 2H), 6.96 (d, *J* = 8.9 Hz, 2H), 4.41

(dd, *J* = 8.6, 5.5 Hz, 1H), 3.86 (s, 3H), 1.93 – 1.54 (m,

8H), 1.39–1.10 (m, 3H), 1.07–0.85 (m, 2H). ¹³C NMR (75 MHz, CDCl₃) δ

179.3, 163.1, 161.2, 129.8, 118.3, 114.2, 63.2, 55.5, 39.6, 34.3, 33.5, 32.7,
26.4, 26.1, 26.0. HRMS (ESI) [M + H⁺] calcd for C₁₇H₁₂NO₃⁺ 288.1594,
found 288.1591.

6.6.2 Typical procedure for the synthesis of racemic compound **130a**

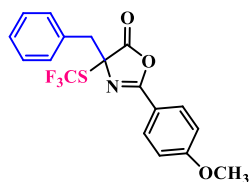
In a 4 ml vial, to a mixture of azlactone **129a** (1.0 eq., 0.10 mmol, 28.1 mg), *N*-(trifluoromethylthio)phthalimide **105** (1.2 eq., 0.12 mmol, 29.7 mg), TBAB (0.20 eq., 0.02 mmol, 6.4 mg), and K₃PO₄ (0.1 eq., 0.01 mmol, 2.1 mg) was added dichloromethane (1.0 mL) and the reaction mixture was stirred for 15 hours at -20 °C. Then, the mixture was filtered and concentrated in vacuo. The crude residue was purified by chromatography (10 g silica gel cyclohexane-ethyl acetate, 99/1 to 80/20) to afford the desired product **130a** (30.5 mg, 80 % yield) as a white solid.

6.6.3 General procedure for the enantioselective trifluoromethylthiolation of azlactones

In a 4 ml vial, to a mixture of the selected azlactone (1.0 eq., 0.10 mmol), *N*-(trifluoromethylthio)phthalimide **105** (1.2 eq., 0.12 mmol, 29.7 mg), catalyst **11** (0.20 eq., 0.02 mmol, 12.6 mg), and K₃PO₄ (0.1 eq., 0.01 mmol, 2.1 mg) was added dichloromethane (1.0 mL) and the reaction mixture was stirred

for the indicated time at $-20\text{ }^{\circ}\text{C}$. Then, the mixture was filtered and concentrated in vacuo. The crude residue was purified by chromatography (10 g silica gel cyclohexane-ethyl acetate, 99/1 to 80/20) to afford the corresponding product.

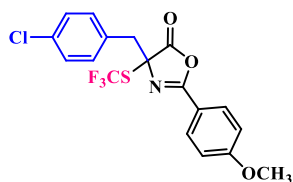
6.6.4 Analytical data of asymmetric trifluoromethylthiolated compounds



4-benzyl-2-(4-methoxyphenyl)-4-

(trifluoromethylthio)oxazol-5(4H)-one (130a):

Obtained after 1 h as a yellow solid (32.0 mg, 84% yield), mp $115\text{--}116\text{ }^{\circ}\text{C}$. ^1H NMR (300 MHz, CDCl_3) δ 7.85 (d, $J = 8.9$ Hz, 2H), 7.21 (m, 5H), 6.94 (d, $J = 8.9$ Hz, 2H), 3.86 (s, 3H), 3.47 (d, $J = 13.1$ Hz, 1H), 3.32 (d, $J = 13.1$ Hz, 1H). ^{13}C NMR (75 MHz, CDCl_3) δ 174.6, 163.9, 162.1, 131.3, 130.5, 130.3, 128.7 (q, $J = 311.1$ Hz), 128.4, 128.1, 116.7, 114.3, 76.7, 55.4, 42.4. ^{19}F NMR (282 MHz, CDCl_3) δ -37.5. $[\alpha]_D^{20} = -65.5^{\circ}$ ($c = 0.80$, CHCl_3). Enantiomeric excess = 88% determined by SFC analysis (CHIRALPAK[®] AS-H column ($\phi 0.46$ cm x 25 cm), n -hexane: i -PrOH = 95:5, 0.5 mL/min, $t_{\text{minor}} = 7.2$ min, $t_{\text{major}} = 8.1$ min). HRMS (ESI) $[\text{M} + \text{H}^+]$ calcd for $\text{C}_{18}\text{H}_{15}\text{F}_3\text{NO}_3\text{S}^+$ 382.0719, found 382.0710.

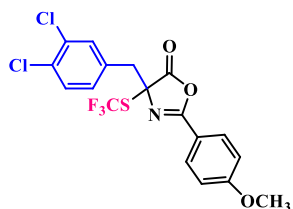


4-(4-chlorobenzyl)-2-(4-methoxyphenyl)-4-

(trifluoromethylthio)oxazol-5(4H)-one (130b):

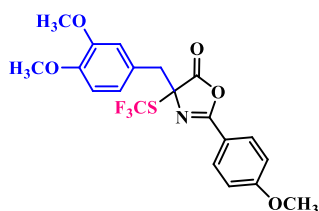
Obtained after 2 h as a yellow solid (37.0 mg, 89% yield), mp $100\text{--}101\text{ }^{\circ}\text{C}$. ^1H NMR (300 MHz, CDCl_3) δ 7.87 (d, $J = 8.9$ Hz, 2H), 7.19 (d, $J = 8.6$ Hz, 2H), 7.14 (d, $J = 8.6$ Hz, 2H), 6.96 (d, $J = 8.9$ Hz, 2H), 3.87 (s, 3H), 3.44 (d, $J = 13.3$ Hz,

1H), 3.30 (d, $J = 13.3$ Hz, 1H). ^{13}C NMR (75 MHz, CDCl_3) δ 174.6, 164.2, 162.4, 134.3, 131.9, 130.5, 130.0, 128.7, 128.7 (q, $J = 310.0$ Hz), 116.6, 114.5, 76.5, 55.6, 41.7 (q, 1.1 Hz). ^{19}F NMR (282 MHz, CDCl_3) δ -37.4. $[\alpha]_D^{20} = -52.0^\circ$ ($c = 0.80$, CHCl_3). Enantiomeric excess 62% determined by HPLC analysis (CHIRALPAK[®] IB column ($\phi 0.46$ cm x 25 cm), *n*-hexane:*i*-PrOH = 99:1, 0.5 mL/min, $t_{\text{major}} = 15.1$ min, $t_{\text{minor}} = 16.2$ min). HRMS (ESI) $[\text{M} + \text{H}^+]$ calcd for $\text{C}_{18}\text{H}_{14}\text{ClF}_3\text{NO}_3\text{S}^+$ 416.0330, found 416.0335.



4-(3,4-dichlorobenzyl)-2-(4-methoxyphenyl)-4-(trifluoromethyl)-thioxazol-5(4H)-one

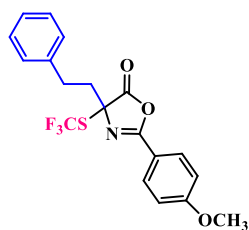
(130c): Obtained after 2 h as a yellow solid (40.5 mg, 90% yield), mp 109-110 °C. ^1H NMR (300 MHz, CDCl_3) δ 7.89 (d, $J = 8.9$ Hz, 1H), 7.33 (d, $J = 2.0$ Hz, 1H), 7.30 (d, $J = 8.2$ Hz, 1H), 7.06 (dd, $J = 8.2, 2.0$ Hz, 1H), 6.97 (d, $J = 8.9$ Hz, 1H), 3.88 (s, 3H), 3.43 (d, $J = 13.4$ Hz, 1H), 3.28 (d, $J = 13.4$ Hz, 1H). ^{13}C NMR (75 MHz, CDCl_3) δ 174.3, 164.3, 162.7, 132.6, 132.6, 132.5, 131.8, 130.5, 130.4, 129.8, 128.6 (q, $J = 310.0$ Hz), 116.4, 114.5, 76.2, 55.6, 41.5 (q, 1.1 Hz). ^{19}F NMR (282 MHz, CDCl_3) δ -37.3. $[\alpha]_D^{20} = -53.8^\circ$ ($c = 0.80$, CHCl_3). Enantiomeric excess 62% determined by HPLC analysis (CHIRALPAK[®] IB column ($\phi 0.46$ cm x 25 cm), *n*-hexane:*i*-PrOH = 99:1, 0.5 mL/min, $t_{\text{major}} = 17.9$ min, $t_{\text{minor}} = 20.9$ min). HRMS (ESI) $[\text{M} + \text{H}^+]$ calcd for $\text{C}_{18}\text{H}_{13}\text{Cl}_2\text{F}_3\text{NO}_3\text{S}^+$ 449.9940, found 449.4942.



4-(3,4-dimethoxybenzyl)-2-(4-methoxyphenyl)-4-(trifluoromethyl)-thioxazol-5(4H)-one

(130d): Obtained after 2 h as a yellow solid

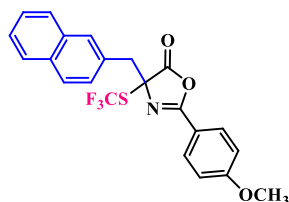
(43.2 mg, 98% yield), mp 107-108 °C. ^1H NMR (300 MHz, CDCl_3) δ 7.87 (d, $J = 9.0$ Hz, 2H), 6.94 (d, $J = 9.0$ Hz, 2H), 6.77–6.67 (m, 3H), 3.86 (m, 3H), 3.79 (s, 3H), 3.68 (s, 3H), 3.42 (d, $J = 13.2$ Hz, 1H), 3.26 (d, $J = 13.2$ Hz, 1H). ^{13}C NMR (75 MHz, CDCl_3) δ 174.7, 164.1, 162.3, 148.9, 148.5, 130.3, 128.8 (q, $J = 310.1$ Hz), 123.7, 122.6, 116.8, 114.4, 113.5, 111.0, 76.8, 55.7, 55.7, 55.6, 42.1. ^{19}F NMR (282 MHz, CDCl_3) δ -37.5. $[\alpha]_D^{20} = -40.2^\circ$ ($c = 0.80$, CHCl_3). Enantiomeric excess 50% determined by HPLC analysis (CHIRALPAK[®] AS-H column ($\phi 0.46$ cm x 25 cm), n -hexane: i -PrOH = 80:20, 0.5 mL/min, $t_{\text{minor}} = 11.1$ min, $t_{\text{major}} = 12.1$ min). HRMS (ESI) $[\text{M} + \text{H}^+]$ calcd for $\text{C}_{20}\text{H}_{19}\text{F}_3\text{NO}_5\text{S}^+$ 442.0931, found 442.0930.



2-(4-methoxyphenyl)-4-phenethyl-4-

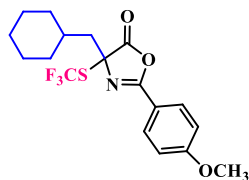
((trifluoromethyl)thio)oxazol-5(4H)-one (130e):

Obtained after 5 h as a white solid (34.8 mg, 88% yield), mp 103-104 °C. ^1H NMR (300 MHz, CDCl_3) δ 8.05 (d, $J = 8.8$ Hz, 2H), 7.34-7.13 (m, 5H), 7.05 (d, $J = 8.8$ Hz, 2H), 3.93 (s, 3H), 2.78 (m, 1H), 2.65 (m, 1H), 2.56-2.33 (m, 2H). ^{13}C NMR (75 MHz, CDCl_3) δ 175.2, 164.2, 162.7, 138.9, 130.6, 128.8 (q, $J = 309.5$ Hz), 128.7, 128.4, 126.7, 116.9, 114.5, 75.9, 55.6, 38.4, 30.1. ^{19}F NMR (282 MHz, CDCl_3) δ -37.6. $[\alpha]_D^{20} = -58.8^\circ$ ($c = 0.80$, CHCl_3). Enantiomeric excess 60% determined by HPLC analysis (CHIRALPAK[®] AS-H column ($\phi 0.46$ cm x 25 cm), n -hexane: i -PrOH = 98:2, 0.5 mL/min, $t_{\text{minor}} = 13.2$ min, $t_{\text{major}} = 16.2$ min). HRMS (ESI) $[\text{M} + \text{H}^+]$ calcd for $\text{C}_{19}\text{H}_{17}\text{F}_3\text{NO}_3\text{S}^+$ 396.0876, found 396.0870.



2-(4-methoxyphenyl)-4-(naphthalen-2-ylmethyl)-4-((trifluoromethyl)thio)oxazol-5(4H)-one (130f):

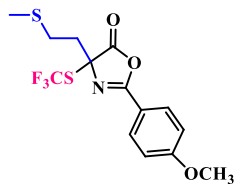
Obtained after 19 h as a yellow solid (42.3 mg, 98% yield), mp 119-120 °C. ¹H NMR (300 MHz, CDCl₃) δ 7.87–7.81 (m, 2H), 7.77–7.71 (m, 2H), 7.71–7.65 (m, 2H), 7.49–7.37 (m, 2H), 7.35 (dd, *J* = 8.6, 1.7 Hz, 1H), 6.94–6.87 (m, 2H), 3.83 (s, 3H), 3.65 (d, *J* = 13.1 Hz, 1H), 3.51 (d, *J* = 13.1 Hz, 1H). ¹³C NMR (75 MHz, CDCl₃) δ 174.7, 164.0, 162.4, 133.1, 132.8, 130.4, 129.9, 129.1, 128.8 (q, *J* = 309.8 Hz), 128.1, 128.0, 127.6, 126.3, 126.2, 116.8, 114.4, 76.9, 55.5, 42.7. ¹⁹F NMR (282 MHz, CDCl₃) δ -37.5. [α]_D²⁰ = -47.6° (c = 0.80, CHCl₃). Enantiomeric excess 70% determined by HPLC analysis (CHIRALPAK[®] AS-H column (ϕ 0.46 cm x 25 cm), *n*-hexane:*i*-PrOH = 98:2, 0.5 mL/min, *t*_{minor} = 14.7 min, *t*_{major} = 17.2 min). HRMS (ESI) [M + H⁺] calcd for C₂₂H₁₇F₃NO₃S⁺ 432.0876, found 432.0873.



4-(cyclohexylmethyl)-2-(4-methoxyphenyl)-4-((trifluoromethyl)thio)oxazol-5(4H)-one (130g):

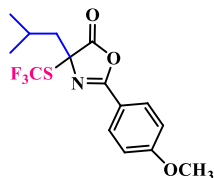
Obtained after 4 h as a white solid (35.6 mg, 92% yield), mp 114-115 °C. ¹H NMR (300 MHz, CDCl₃) δ 8.00 (d, *J* = 8.9 Hz, 2H), 7.01 (d, *J* = 8.9 Hz, 2H), 3.90 (s, 3H), 2.10 (dd, *J* = 14.0, 5.3 Hz, 1H), 1.96 (dd, *J* = 14.0, 6.6 Hz, 1H), 1.78–1.52 (m, 5H), 1.50–1.38 (m, 1H), 1.29–1.08 (m, 3H), 1.08–0.87 (m, 2H). ¹³C NMR (75 MHz, CDCl₃) δ 176.0, 164.1, 162.1, 130.5, 128.8 (q, *J* = 310.1 Hz), 117.1, 114.5, 76.1, 76.1, 55.6, 43.8, 34.4, 34.2, 33.6, 26.0, 25.9. ¹⁹F NMR (282 MHz, CDCl₃) δ -37.9. [α]_D²⁰ = -43.3° (c = 0.60, CHCl₃). Enantiomeric excess 82% determined by HPLC analysis (CHIRALPAK[®] AS-H column (ϕ 0.46 cm x 25 cm), *n*-hexane:*i*-PrOH = 99.5:0.5, 0.3 mL/min, *t*_{minor} = 17.3 min, *t*_{major} =

18.8 min). HRMS (ESI) $[M + H]^+$ calcd for $C_{18}H_{21}F_3NO_3S^+$ 388.1189, found 388.1193.



2-(4-methoxyphenyl)-4-(2-(methylthio)ethyl)-4-((trifluoromethyl)thio)oxazol-5(4H)-one (130h):

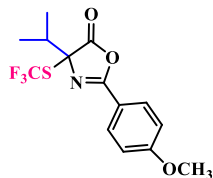
Obtained after 19 h as a pink solid (31.0 mg, 85% yield), mp 97-98 °C. 1H NMR (300 MHz, $CDCl_3$) δ 8.00 (d, $J = 9.0$ Hz, 2H), 7.00 (d, $J = 9.0$ Hz, 2H), 3.90 (s, 3H), 2.67-2.39 (m, 4H), 2.07 (s, 3H). ^{13}C NMR (75 MHz, $CDCl_3$) δ 175.4, 164.6, 159.9, 130.4, 129.3, 128.8 (q, $J = 310.0$ Hz), 114.5, 75.3, 55.8, 29.7, 28.3, 15.1. ^{19}F NMR (282 MHz, $CDCl_3$) δ -37.5. $[\alpha]_D^{20} = -29.4^\circ$ ($c = 0.50$, $CHCl_3$). Enantiomeric excess 48% determined by HPLC analysis (CHIRALPAK[®] AS-H column ($\phi 0.46$ cm x 25 cm), n -hexane: i -PrOH = 98:2, 0.5 mL/min, $t_{minor} = 15.5$ min, $t_{major} = 18.0$ min). HRMS (ESI) $[M + H]^+$ calcd for $C_{14}H_{15}F_3NO_3S_2^+$ 366.0440, found 366.0447.



4-isobutyl-2-(4-methoxyphenyl)-4-((trifluoromethyl)thio)oxazol-5(4H)-one (130i):

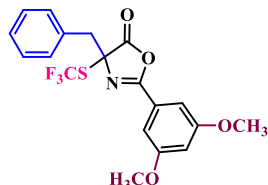
Obtained after 2 h as a white solid (30.2 mg, 87% yield), mp 102-103 °C. 1H NMR (300 MHz, $CDCl_3$) δ 8.07–7.93 (m, 2H), 7.07–6.95 (m, 2H), 3.90 (s, 3H), 2.14 (dd, $J = 13.8, 5.6$ Hz, 1H), 1.98 (dd, $J = 13.8, 6.9$ Hz, 1H), 1.88–1.68 (m, 1H), 1.00–0.86 (m, 6H). ^{13}C NMR (75 MHz, $CDCl_3$) δ 175.9, 164.1, 162.1, 130.5, 128.8 (q, $J = 309.7$ Hz), 117.1, 114.5, 76.1, 55.6, 45.0, 25.4, 23.8, 23.0. ^{19}F NMR (282 MHz, $CDCl_3$) δ -37.9. $[\alpha]_D^{20} = -39.9^\circ$ ($c = 0.80$, $CHCl_3$). Enantiomeric excess 44% determined by HPLC analysis (CHIRALPAK[®] IB column ($\phi 0.46$ cm x 25 cm), n -hexane: i -PrOH = 99.2:0.8, 0.35 mL/min, $t_{major} = 17.8$ min, $t_{minor} = 19.1$

min). HRMS (ESI) $[M + H^+]$ calcd for $C_{15}H_{17}F_3NO_3S^+$ 347.0803, found 347.0800.



4-isopropyl-2-(4-methoxyphenyl)-4-((trifluoromethyl)thio)oxazol-5(4H)-one (130j):

Obtained after 19 h as a white solid (29.3 mg, 88% yield), mp 98-99 °C. 1H NMR (300 MHz, $CDCl_3$) δ 8.06–7.96 (m, 2H), 7.04–6.96 (m, 2H), 3.89 (s, 3H), 2.39 (hept, $J = 6.5$ Hz, 1H), 1.20 (d, $J = 6.8$ Hz, 3H), 1.03 (d, $J = 6.7$ Hz, 3H). ^{13}C NMR (75 MHz, $CDCl_3$) δ 174.4, 163.0, 161.2, 129.5, 128.0 (q, 309.7 Hz), 116.0, 113.4, 79.1, 54.6, 34.8, 16.2, 15.8. ^{19}F NMR (282 MHz, $CDCl_3$) δ -37.5. $[\alpha]_D^{20} = -61.3^\circ$ ($c = 0.80$, $CHCl_3$). Enantiomeric excess >99% determined by HPLC analysis (CHIRALPAK[®] AS-H column ($\phi 0.46$ cm x 25 cm), *n*-hexane:*i*-PrOH = 99.5:0.5, 0.3 mL/min, $t_{major} = 16.8$ min. HRMS (ESI) $[M + H^+]$ calcd for $C_{14}H_{15}F_3NO_3S^+$ 334.0719, found 334.0714.



4-benzyl-2-(3,5-dimethoxyphenyl)-4-((trifluoromethyl)thio)oxazol-5(4H)-one (132a):

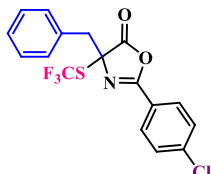
Obtained after 1 h as a white solid (33.3 mg, 81% yield), mp 117-118 °C. 1H NMR (300 MHz, $CDCl_3$) δ 7.22 (m, 5H), 7.02 (d, $J = 2.3$ Hz, 2H), 6.65 (t, $J = 2.3$ Hz, 1H), 3.81 (s, 6H), 3.48 (d, $J = 13.2$ Hz, 1H), 3.33 (d, $J = 13.2$ Hz, 1H). ^{13}C NMR (75 MHz, $CDCl_3$) δ 174.4, 162.4, 161.0, 131.2, 130.5, 128.7 (q, 310.2 Hz), 128.6, 128.3, 126.2, 106.6, 105.9, 76.7, 55.7, 42.4. ^{19}F NMR (282 MHz, $CDCl_3$) δ -37.5. $[\alpha]_D^{20} = -51.0^\circ$ ($c = 0.80$, $CHCl_3$). Enantiomeric excess 72% determined by HPLC analysis (CHIRALPAK[®] AS-H column ($\phi 0.46$ cm x 25 cm), *n*-hexane:*i*-PrOH = 99:1, 0.5 mL/min, $t_{minor} = 21.4$ min, $t_{major} = 22.2$

min). HRMS (ESI) $[M + H^+]$ calcd for $C_{19}H_{17}F_3NO_4S^+$ 412.0825, found 412.0826.



4-benzyl-2-phenyl-4-((trifluoromethyl)thio)oxazol-5(4H)-one (122a): Obtained after 19 h as a white solid

(17.2 mg, 49% yield), mp 104-105 °C. 1H NMR (300 MHz, $CDCl_3$) δ = 7.90 (dd, J = 8.4 Hz, 1.4 Hz, 2H), 7.59 (t, J = 7.4 Hz, 1.5 Hz, 1H), 7.46 (t, J = 7.7 Hz, 2H), 7.24-7.18 (m, 5H), 3.49 (d, J = 13.2 Hz, 1H), 3.35 (d, J = 13.2 Hz, 1H). ^{13}C NMR (300 MHz, $CDCl_3$) δ = 174.5, 162.5, 133.7, 131.3, 130.6, 129.2 (q, J = 298 Hz), 128.9, 128.5, 128.34, 128.27, 124.7, 42.5. ^{19}F NMR (300 MHz, $CDCl_3$): δ = -37.51 (s, 3 F). $[\alpha]_D^{20}$ = -41.1° (c = 0.80, $CHCl_3$). Enantiomeric excess 64% determined by HPLC analysis (CHIRALPAK® AS-H column (ϕ 0.46 cm x 25 cm), *n*-hexane:*i*-PrOH = 90:10, 0.5 mL/min, t_{major} = 9.9 min, t_{minor} = 10.5 min). HRMS (ESI) $[M + H^+]$ calcd for $C_{17}H_{13}F_3NO_2S^+$ 352.3174, found 352.3170.



4-benzyl-2-(4-chlorophenyl)-4-((trifluoromethyl)thio)oxazol-5(4H)-one (128a'):

Obtained after 19 h as a white solid (32.0 mg, 83% yield), mp 118-119 °C. 1H NMR (300 MHz, $CDCl_3$) δ 7.83 (d, J = 6.9 Hz, 2H), 7.44 (d, J = 6.9 Hz, 2H), 7.21 (s, 5H), 3.48 (d, J = 13.2 Hz, 1H), 3.34 (d, J = 13.2 Hz, 1H). ^{13}C NMR (75 MHz, $CDCl_3$) δ 174.18, 161.67, 140.29, 131.14, 130.51, 129.56, 129.38, 128.7 (q, J = 309.9 Hz), 128.54, 128.33, 123.04, 77.21, 42.4. ^{19}F NMR (282 MHz, $CDCl_3$) δ -37.5. $[\alpha]_D^{20}$ = -38.2° (c = 0.80, $CHCl_3$). Enantiomeric excess 40% determined by HPLC analysis (CHIRALPAK® AS-H column (ϕ 0.46 cm x 25 cm), *n*-hexane:*i*-PrOH = 99:1, 0.5 mL/min, t_{minor} = 13.3 min, t_{major} = 17.5 min).

HRMS (ESI) $[M + H^+]$ calcd for $C_{17}H_{12}ClF_3NO_2S^+$ 386.0224, found 386.0228.

6.7 Asymmetric trifluoromethylthiolation of isoxazolidin-5-ones

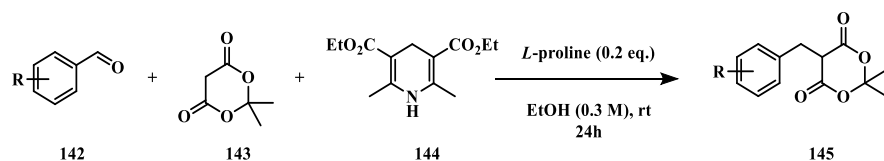
Substrates *N*-Boc α -substituted isoxazolidin-5-one **133a-p** and *N*-(trifluoromethylthio)phthalimide **105** were prepared according to the reported procedures.¹⁷² Catalysts **96a-c** were commercially available, whereas catalysts **135a-d**, **123f** and **125b** were prepared following the general procedure described in the literature.¹⁶¹

6.7.1 Synthesis of *N*-Boc α -substituted isoxazolidin-5-one **133a-p**

The *N*-Boc α -substituted isoxazolidin-5-one **133a-p** were prepared following the general procedure A, for the synthesis of benzyl-substituted isoxazolidin-5-one **133a-n**, and general procedure B, for the synthesis of phenyl-substituted isoxazolidin-5-one **133o-p**, according to literature.

Procedure A:^{172a}

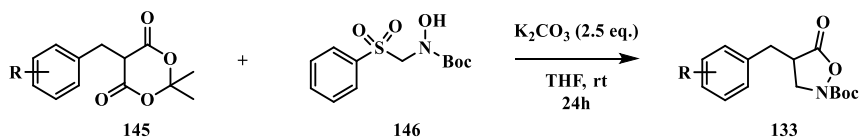
STEP 1



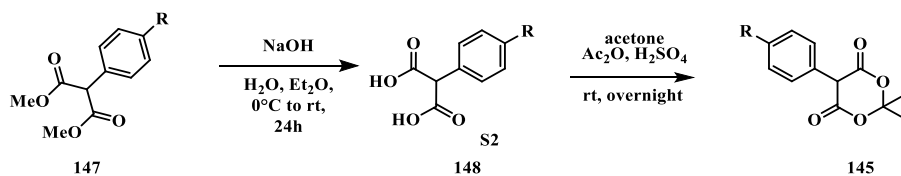
STEP 1. Meldrum's acid **143** (1.0 eq., 2.0 mmol), corresponding aldehyde **142** (1.0 eq., 2.0 mmol), L-proline (0.2 eq., 0.4 mmol) and diethyl 2,6-dimethyl-1,4-dihydropyridine-3,5-dicarboxylate **144** (1.0 eq., 2.0 mmol)

¹⁷² a) J.-S. Yu, H. Noda, M. Shibasaki, *Angew. Chem. Int. Ed.*, **2018**, *57*, 818-822; b) M. Nascimento de Oliveira, S. Arseniyadis, J. Cossy, *Chem. Eur. J.*, **2018**, *24*, 4810-4814; c) K. Kang, C. Xu, Q. Shen, *Org. Chem. Front.* **2014**, *1*, 294-297.

were dissolved in EtOH (0.3 M) and the mixture was stirred for 24 h at room temperature. Then, the solvent was removed in vacuum and the residue dissolved in DCM and washed with H₂O. The organic layer was dried over MgSO₄, filtered and concentrated in vacuo to yield crude **145**, which was used without further purification.

STEP 2

STEP 2. To a solution of crude **145** (1.0 eq., 1.8 mmol) in THF (0.1 M), tert-butyl hydroxy((phenylsulfonyl)methyl)carbamate **146** (1.0 eq., 1.8 mmol) and K₂CO₃ (2.5 eq., 4.5 mmol) were added and the reaction mixture was stirred for 24 hours at room temperature. Next, the reaction mixture was filtered through a plug of Celite®, washed with DCM and the filtrate evaporated under reduced pressure to give the crude residue that was purified by chromatography (silica gel, cyclohexane-ethyl acetate, 25/1 to 15/1) to yield benzyl-substituted isoxazolidin-5-one **133a-p** as oil or a white/yellow solid.

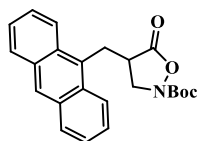
Procedure B:^{172b}

The arylated dimethyl malonate **147** (1.0 eq., 2.0 mmol) was dissolved in Et₂O (2.0 ml) and then this solution added to a solution of NaOH (4.00 eq., 8.0 mmol) in H₂O (7 ml) at 0 °C for 10 min. The resulting mixture was stirred

at room temperature for 24 h. Next, the aqueous phase was separated and washed with ethyl acetate (2 x 15 mL), acidified to pH 2 with an aqueous solution of HCl (6 M), and extracted with EtOAc (2 x 30 mL). The combined organic phase was washed with brine (50 mL), dried over anhydrous MgSO₄. The solvent was vacuum at rotavapor affording the corresponding arylated malonic acid **148**, which was used without further purification.

To a suspension of arylmalonic acid **148** (1.00 eq., 3.90 mmol) in Ac₂O (5.0 eq., 19.5 mmol) concentrated H₂SO₄ (0.40 eq., 1.56 mmol) was added dropwise. After the complete dissolution of the arylmalonic acid, acetone (1.60 eq., 6.24 mmol) was added and the reaction mixture stirred for the indicated time. Then, the crude dissolved in DCM and washed with saturated aqueous NaHCO₃. Afterward, 1 M aqueous HCl was added drop by drop to the aqueous phase until the pH value to 4-5. Next, the aqueous phase was extracted three times with DCM, the organic phases collected and washed with brine, dried on magnesium sulfate and evaporated under vacuum. Then the solid product was washed several times with cyclohexane, affording crude **145**, which was used without further purification.

Compound **133a**,¹⁷³ **133e**,¹³³ **133h**,^{172a} **133i**,^{172a} **133k**,¹⁷³ **133m**,¹⁷³ **133o**,^{172b} **133p**^{172b} were synthesized according the general procedures A and B and the characterization data matched those previously reported.

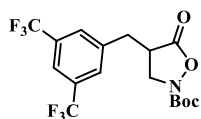


tert-butyl 4-(anthracen-9-ylmethyl)-5-oxisoxazolidine-2-carboxylate (133b): Obtained as a

yellow solid (0.6 g, 82% yield). ¹H NMR (300 MHz, CDCl₃) δ 8.44 (s, 1H), 8.24 (d, *J* = 8.9 Hz, 2H), 8.05 (d, *J* = 8.9 Hz, 2H), 7.62–7.45 (m, 4H), 4.23 (dd, *J* = 14.8, 4.1 Hz, 1H), 3.94 (dd, *J* = 14.8, 10.6

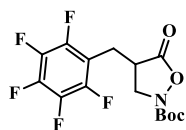
¹⁷³ T. Tite, M. Sabbah, V. Levacher, J. F. Brière, *Chem. Commun.*, **2013**, 49, 11569-11571.

Hz, 1H), 3.91–3.81 (m, 2H), 3.41 (m, 1H), 1.49 (s, 9H). ^{13}C NMR (75 MHz, CDCl_3) δ 174.4, 155.7, 131.6, 129.8, 129.6, 129.0, 127.5, 126.7, 125.2, 123.4, 84.2, 53.5, 42.5, 28.0, 26.1. HRMS (MALDI) $[\text{M}+\text{Na}^+]$ calcd for $\text{C}_{23}\text{H}_{23}\text{NNaO}_4$ 400.1519, found 400.1505.



tert-butyl 4-(3,5-bis(trifluoromethyl)benzyl)-5-

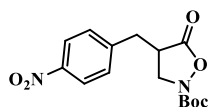
oxoisoxazolidine-2-carboxylate (133c): Obtained as a white solid (0.6 g, 75% yield). ^1H NMR (300 MHz, CDCl_3) δ 7.83 (s, 1H), 7.71 (s, 2H), 4.27 (dd, $J = 11.0, 8.4$ Hz, 1H), 3.71 (dd, $J = 11.0, 9.5$ Hz, 1H), 3.39 (dd, $J = 14.2, 5.1$ Hz, 1H), 3.32–3.18 (m, 1H), 3.00 (dd, $J = 14.2, 8.9$ Hz, 1H), 1.54 (s, 9H). ^{13}C NMR (75 MHz, CDCl_3) δ 172.2, 154.7, 138.4, 131.3 (q, $J = 33.4$ Hz), 128.0 (q, $J = 4.0$ Hz), 122.0 (q, $J = 273.0$ Hz), 120.5 (hept, $J = 3.8$ Hz), 83.6, 51.8, 40.6, 33.0, 27.0. ^{19}F NMR (282 MHz, CDCl_3) δ -62.9. HRMS (MALDI) $[\text{M}+\text{Na}^+]$ calcd for $\text{C}_{17}\text{H}_{17}\text{F}_6\text{NNaO}_4$ 436.0954, found 436.0969.



tert-butyl 5-oxo-4-

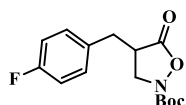
((perfluorophenyl)methyl)isoxazolidine-2-carboxylate

(133d): Obtained as a white solid (0.5 g, 78% yield). ^1H NMR (300 MHz, CDCl_3) δ 4.29 (dd, $J = 11.2, 8.3$ Hz, 1H), 3.81–3.70 (m, 1H), 3.36–3.11 (m, 2H), 2.98 (dd, $J = 13.8, 8.9$ Hz, 1H), 1.54 (s, 9H). ^{13}C NMR (75 MHz, CDCl_3) δ 171.8, 154.7, 83.6, 52.3, 38.9, 26.9, 20.5. ^{19}F NMR (282 MHz, CDCl_3) δ -142.2 – -142.6 (m), -154.6 (m), -161.2 – -161.4 (m). HRMS (MALDI) $[\text{M}+\text{Na}^+]$ calcd for $\text{C}_{15}\text{H}_{14}\text{F}_5\text{NNaO}_4$ 390.0736, found 390.390.0731.



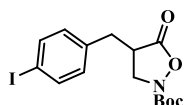
tert-butyl 4-(4-nitrobenzyl)-5-oxoisoxazolidine-2-carboxylate (133f): Obtained as a white solid (0.4 g, 65% yield).

^1H NMR (300 MHz, CDCl_3) δ 8.17 (d, $J = 8.8$ Hz, 2H), 7.41 (d, $J = 8.8$ Hz, 2H), 4.22 (dd, $J = 11.1, 8.5$ Hz, 1H), 3.70 (dd, $J = 11.1, 9.4$ Hz, 1H), 3.37–3.19 (m, 2H), 2.97 (dd, $J = 13.3, 8.5$ Hz, 1H), 1.49 (s, 9H). ^{13}C NMR (75 MHz, CDCl_3) δ 172.6, 154.7, 146.2, 143.5, 128.8, 123.1, 83.4, 51.8, 40.5, 33.0, 27.0. HRMS (MALDI) $[\text{M}+\text{Na}^+]$ calcd for $\text{C}_{15}\text{H}_{18}\text{N}_2\text{NaO}_6$ 345.1057, found 345.1049.



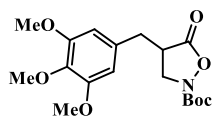
tert-butyl 4-(4-fluorobenzyl)-5-oxoisoxazolidine-2-carboxylate (133g): Obtained as a white solid (0.4 g, 77% yield).

^1H NMR (300 MHz, CDCl_3) δ 7.23–7.12 (m, 2H), 7.07–6.97 (m, 2H), 4.16 (dd, $J = 11.0, 8.4$ Hz, 1H), 3.70 (dd, $J = 11.0, 9.2$ Hz, 1H), 3.27–3.08 (m, 2H), 2.89–2.74 (m, 1H), 1.51 (s, 9H). ^{13}C NMR (75 MHz, CDCl_3) δ 173.0, 161.0 (d, $J = 245.7$ Hz), 154.8, 131.6 (d, $J = 3.3$ Hz), 129.3 (d, $J = 8.0$ Hz), 114.8 (d, $J = 21.5$ Hz), 83.2, 51.7, 41.1, 32.5, 27.0. ^{19}F NMR (282 MHz, CDCl_3) δ -115.3. HRMS (MALDI) $[\text{M}+\text{Na}^+]$ calcd for $\text{C}_{15}\text{H}_{18}\text{FNNaO}_4$ 318.1112, found 318.1118.



tert-butyl 4-(4-iodobenzyl)-5-oxoisoxazolidine-2-carboxylate (133j): Obtained as a white solid (0.6 g, 81% yield).

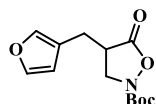
^1H NMR (300 MHz, CDCl_3) δ 7.67 (d, $J = 8.4$ Hz, 2H), 6.97 (d, $J = 8.4$ Hz, 2H), 4.16 (dd, $J = 11.1, 8.3$ Hz, 1H), 3.69 (dd, $J = 11.1, 9.1$ Hz, 1H), 3.23–3.10 (m, 2H), 2.78 (dd, $J = 15.3, 10.5$ Hz, 1H), 1.52 (s, 9H). ^{13}C NMR (75 MHz, CDCl_3) δ 172.9, 154.8, 137.0, 135.5, 129.8, 91.7, 83.2, 51.8, 40.9, 32.9, 27.0. HRMS (MALDI) $[\text{M}+\text{Na}^+]$ calcd for $\text{C}_{15}\text{H}_{18}\text{INNaO}_4$ 426.0173, found 426.0182.



tert-butyl 5-oxo-4-(3,4,5-trimethoxybenzyl)isoxazolidine-2-carboxylate

(133i): Obtained as a yellow solid (0.5 g, 74% yield).

^1H NMR (300 MHz, CDCl_3) δ 6.39 (s, 2H), 4.26–4.04 (m, 1H), 3.85 (s, 6H), 3.83 (s, 3H), 3.74 (dd, $J = 11.3, 8.9$ Hz, 1H), 3.24–3.07 (m, 2H), 2.76 (dd, $J = 15.1, 10.4$ Hz, 1H), 1.51 (s, 9H). ^{13}C NMR (75 MHz, CDCl_3) δ 174.2, 155.9, 153.6, 137.2, 132.4, 105.8, 84.2, 60.8, 56.2, 52.7, 42.3, 34.8, 28.0. HRMS (MALDI) $[\text{M}+\text{Na}^+]$ calcd for $\text{C}_{18}\text{H}_{25}\text{NNaO}_7$: 390.1524, found 390.1518.



tert-butyl 4-(furan-3-ylmethyl)-5-oxoisoxazolidine-2-carboxylate (133n): Obtained as a white solid (0.3 g, 70%

yield).

^1H NMR (300 MHz, CDCl_3) δ 7.38–7.33 (m, 1H), 7.30–7.27 (m, 1H), 6.29–6.23 (m, 1H), 4.20 (dd, $J = 11.0, 8.7$ Hz, 1H), 3.66 (dd, $J = 11.0, 9.4$ Hz, 1H), 3.11 (qd, $J = 9.4, 8.7, 4.6$ Hz, 1H), 2.95 (dd, $J = 14.9, 4.6$ Hz, 1H), 2.72 (dd, $J = 14.9, 8.7$ Hz, 1H), 1.48 (s, 9H). ^{13}C NMR (75 MHz, CDCl_3) δ 174.2, 155.8, 143.6, 140.2, 119.9, 110.7, 84.1, 52.7, 41.1, 28.0, 23.7. HRMS (MALDI) $[\text{M}+\text{Na}^+]$ calcd for $\text{C}_{13}\text{H}_{17}\text{NNaO}_5$ 290.0099, found 290.0108.

6.7.2 General procedure for the synthesis of compounds 105, 108, 118 and 136

According to reference.^{172c} In a 100 ml round bottom flask, *N*-bromophthalimide (1.0 eq., 23.0 mmol, 5.20 g), AgSCF_3 (1.1 eq., 25.3 mmol, 5.28 g) and dried CH_3CN (40 mL) were added under inert atmosphere and the mixture stirred at room temperature for 3 h. Next, the solvent was vacuum at rotavapor and the residue dissolved in DCM (20 ml), filtered through a

short plug of Celite® and the filter was evacuated again at rotavapor to yield the title compound **105** as a white solid (5.11 g, 90%).

The same procedure was used for the synthesis of 5-nitro-trifluoromethylthio phthalimide¹⁷⁴ (**136**, 5.84g, 87%), trifluoromethylthio saccharine¹⁷⁵ (**118**, 6.12g, 94%) and trifluoromethylthio succinimide^{170c} (**108**, 4.26g, 93%). The characterization data matched those previously reported.

6.7.3 Typical procedure for the synthesis of racemic compounds **134a**

In a 4 ml vial, to a mixture of isoxazolidinone **133a** (1.0 eq., 0.20 mmol), *N*-(trifluoromethylthio)phthalimide **105** (2.0 eq., 0.40 mmol, 99.0 mg), TBAB (0.2 eq., 0.040 mmol, 12.9 mg) and K₂CO₃ (2.0 eq., 0.40 mmol, 55.3 mg) was added diethyl ether (2.0 mL) and the reaction mixture was stirred for 24-72 hours. Then, the mixture was filtered over a pad of Na₂SO₄, the solvent evaporated and the residue dried under reduced pressure. The resulting crude product was purified by chromatography (minimum amount of silica gel, cyclohexane-ethyl acetate, 20/1 to 10/1) to afford racemic products **134a**.

6.7.4 General procedure for the asymmetric Trifluoromethylthiolation of Isoxazolidin-5-ones

¹⁷⁴ Q. Xiao, Q. He, J. Li, J. Wang, *Org. Lett.*, **2015**, *17*, 6090–6093.

¹⁷⁵ C. Xu, B. Ma, Q. Shen, *Angew. Chem. Int. Ed.*, **2014**, *53*, 9316–9320.

In a 4 ml vial, to a mixture of isoxazolidinone **133** (1.0 eq., 0.10 mmol), *N*-(trifluoromethylthio)phthalimide **105** (2.0 eq., 0.20 mmol, 49.4 mg), catalyst **96a** (0.05 eq., 0.005 mmol, 5.4 mg) or **96b** (0.02 eq., 0.002 mmol, 1.8 mg) where indicated), K₂CO₃ (2.0 eq., 0.20 mmol, 27.6 mg) was added diethyl ether (1.0 mL) and the reaction mixture was stirred for the indicated time. Then, the mixture was filtered over a pad of Na₂SO₄, the solvent evaporated and the residue dried under reduced pressure. The resulting crude product was purified by chromatography (minimum amount of silica gel, cyclohexane-ethyl acetate, 20/1 to 10/1 (or cyclohexane/DCM 1/3 where indicated) to yield the desired products **134a-p**.



tert-butyl

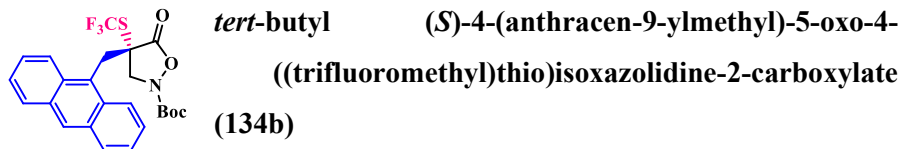
(*S*)-4-benzyl-5-oxo-4-

((trifluoromethyl)thio)isoxazolidine-2-carboxylate (**134a**)

Following the general procedure with *tert*-butyl 4-benzyl-5-oxoisoxazolidine-2-carboxylate **133a** (27.7 mg, 0.10 mmol, 1.0 eq.), *N*-(trifluoromethylthio)phthalimide **105** (2.0 eq., 0.20 mmol, 49.4 mg) and catalyst **96a** (0.05 eq., 0.005 mmol, 5.4 mg) for 48 hours, the title compound **134a** (18.9 mg, 50%) was obtained as a colorless oil after column chromatography (minimum amount of silica gel, cyclohexane-ethyl acetate, 20/1 to 10/1).

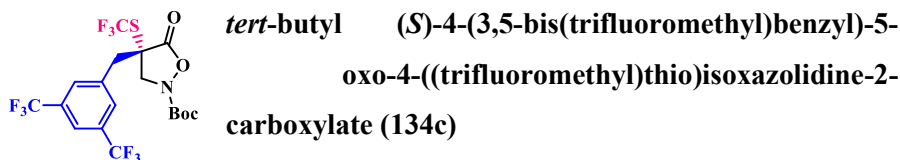
¹H NMR (300 MHz, CDCl₃) δ 7.42–7.30 (m, 3H), 7.25–7.17 (m, 2H), 4.24 (d, *J* = 13.1 Hz, 1H), 4.11 (d, *J* = 13.1 Hz, 1H), 3.48 (d, *J* = 14.4 Hz, 1H), 3.35 (d, *J* = 14.4 Hz, 1H), 1.51 (s, 9H). ¹³C NMR (75 MHz, CDCl₃) δ 169.5, 154.6, 131.9, 129.4, 128.0, 127.8 (q, *J* = 310.6 Hz), 127.3, 84.0, 55.9, 53.3, 39.6 (q, *J* = 1.1 Hz), 26.9. ¹⁹F NMR (282 MHz, CDCl₃) δ -35.6. HRMS (MALDI) [M+Na⁺] calcd for C₁₆H₁₈F₃NNaO₄S 400.0801, found 400.0801. [α]_D²⁰ = +55.8° (c = 0.80, CHCl₃). Enantiomeric excess = 86% determined by

HPLC analysis (CHIRALPAK® AS-H column (ϕ 0.46 cm x 25 cm), *n*-hexane:*i*-PrOH = 99:1, 0.5 mL/min, $t_{\text{major}} = 12.9$ min, $t_{\text{minor}} = 14.6$ min).



Following the general procedure with *tert*-butyl 4-(anthracen-9-ylmethyl)-5-oxoisoxazolidine-2-carboxylate **133b** (37.7 mg, 0.10 mmol, 1.0 eq.), *N*-(trifluoromethylthio)phthalimide **105** (2.0 eq., 0.20 mmol, 49.4 mg) and catalyst **96a** (0.05 eq., 0.005 mmol, 5.4 mg) for 72 hours, the title compound **134b** (28.2 mg, 59%) was obtained as a pale yellow oil after column chromatography (minimum amount of silica gel, cyclohexane-ethyl acetate, 20/1 to 10/1).

^1H NMR (300 MHz, CDCl_3) δ 8.51 (s, 1H), 8.24 (bs, 2H), 8.12–8.02 (m, 2H), 7.69–7.57 (m, 2H), 7.59–7.49 (m, 2H), 5.00 (d, $J = 15.8$ Hz, 1H), 4.49 (d, $J = 15.8$ Hz, 1H), 4.19 (d, $J = 13.5$ Hz, 1H), 3.42 (d, $J = 13.5$ Hz, 1H), 1.47 (s, 9H). ^{13}C NMR (75 MHz, CDCl_3) δ 170.2, 154.5, 130.5, 130.0, 128.5, 128.0 (q, 311.0 Hz), 127.8, 126.2, 124.5, 124.3, 123.0, 83.8, 55.2, 52.6, 32.3, 26.8. ^{19}F NMR (282 MHz, CDCl_3) δ -35.5. HRMS (MALDI) $[\text{M}+\text{H}^+]$ calcd for $\text{C}_{24}\text{H}_{23}\text{F}_3\text{NO}_4\text{S}$ 478.1294, found 478.1299. $[\alpha]_D^{20} = +50.0^\circ$ ($c = 0.80$, CHCl_3). Enantiomeric excess = 78% determined by HPLC analysis (CHIRALPAK® AS-H column (ϕ 0.46 cm x 25 cm), *n*-hexane:*i*-PrOH = 95:5, 0.5 mL/min, $t_{\text{major}} = 9.9$ min, $t_{\text{minor}} = 10.9$ min).



Following the general procedure with *tert*-butyl 4-(3,5-bis(trifluoromethyl)benzyl)-5-oxoisoxazolidine-2-carboxylate **133c** (41.3 mg, 0.10 mmol, 1.0 eq.), *N*-(trifluoromethylthio)phthalimide **105** (2.0 eq., 0.20 mmol, 49.4 mg) and catalyst **96a** (0.05 eq., 0.005 mmol, 5.4 mg) for 48 hours, the title compound **134c** (24.6 mg, 48%) was obtained as a colorless oil after column chromatography (minimum amount of silica gel, cyclohexane-ethyl acetate, 20/1 to 10/1).

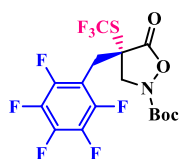
^1H NMR (300 MHz, CDCl_3) δ 7.89 (s, 1H), 7.70 (s, 2H), 4.29 (d, $J = 12.9$ Hz, 1H), 4.07 (d, $J = 12.9$ Hz, 1H), 3.55 (s, 2H), 1.53 (s, 9H). ^{13}C NMR (75 MHz, CDCl_3) δ 169.6, 155.4, 135.4, 132.4 (q, $J = 33.7$ Hz), 130.6 (q, $J = 4.0$ Hz), 128.6 (q, $J = 310.0$ Hz), 122.9 (q, $J = 273.0$ Hz), 122.5 (hept, $J = 3.8$ Hz), 85.56, 57.4, 53.87, 39.98, 27.89. ^{19}F NMR (282 MHz, CDCl_3) δ -35.5, -63.0. HRMS (MALDI) $[\text{M}+\text{H}^+]$ calcd for $\text{C}_{18}\text{H}_{17}\text{F}_9\text{NO}_4\text{S}$ 514.0729, found 514.0734. $[\alpha]_D^{20} = +68.1^\circ$ ($c = 0.50$, CHCl_3). Enantiomeric excess = 96% determined by HPLC analysis (CHIRALPAK[®] AS-H column ($\phi 0.46$ cm x 25 cm), *n*-hexane:*i*-PrOH = 98:2, 0.5 mL/min, $t_{\text{minor}} = 8.6$ min, $t_{\text{major}} = 12.4$ min).



tert-butyl (S)-5-oxo-4-(4-(trifluoromethyl)benzyl)-4-((trifluoromethyl)thio)isoxazolidine-2-carboxylate (**134e**)

Following the general procedure with *tert*-butyl 5-oxo-4-(4-(trifluoromethyl)benzyl)isoxazolidine-2-carboxylate **133e** (34.5 mg, 0.10 mmol, 1.0 eq.), *N*-(trifluoromethylthio)phthalimide **2** (2.0 eq., 0.20 mmol, 49.4 mg) and catalyst **96a** (0.05 eq., 0.005 mmol, 5.4 mg) for 48 hours, the title compound **134e** (38.7 mg, 87%) was obtained as a colorless oil after column chromatography (minimum amount of silica gel, cyclohexane-ethyl acetate, 20/1 to 10/1).

^1H NMR (300 MHz, CDCl_3) δ 7.63 (d, $J = 8.0$ Hz, 1H), 7.36 (d, $J = 8.0$ Hz, 1H), 4.26 (d, $J = 13.0$ Hz, 1H), 4.07 (d, $J = 13.0$ Hz, 1H), 3.52 (d, $J = 14.4$ Hz, 1H), 3.43 (d, $J = 14.4$ Hz, 1H), 1.51 (s, 9H). ^{13}C NMR (75 MHz, CDCl_3) δ 170.1, 155.6, 136.9 (q, $J = 1.4$ Hz), 130.8, 130.7 (q, $J = 32.0$ Hz), 128.6 (q, $J = 310.0$ Hz), 126.0 (q, $J = 3.8$ Hz), 123.8 (q, $J = 272.1$ Hz), 85.3, 57.1, 54.1, 40.2, 27.9. ^{19}F NMR (376 MHz, CDCl_3) δ -35.7, -62.9. HRMS (MALDI) $[\text{M}+\text{K}^+]$ calcd for $\text{C}_{17}\text{H}_{17}\text{F}_6\text{KNO}_4\text{S}$ 484.0414, found 484.0404. $[\alpha]_D^{20} = +48.0^\circ$ ($c = 0.50$, CHCl_3). Enantiomeric excess = 80% determined by HPLC analysis (CHIRALPAK[®] ID column ($\phi 0.46$ cm x 25 cm), *n*-hexane:*i*-PrOH = 98:2, 1.0 mL/min, $t_{\text{minor}} = 4.7$ min, $t_{\text{major}} = 6.3$ min).



tert-butyl ((*S*)-5-oxo-4-((perfluorophenyl)methyl)-4-((trifluoromethyl)thio)isoxazolidine-2-carboxylate (**134d**)

Following the general procedure with *tert*-butyl 5-oxo-4-((perfluorophenyl)methyl)isoxazolidine-2-carboxylate **133d** (36.7 mg, 0.10 mmol, 1.0 eq.), *N*-(trifluoromethylthio)phthalimide **105** (2.0 eq., 0.20 mmol, 49.4 mg) and catalyst **96a** (0.05 eq., 0.005 mmol, 5.4 mg) for 48 hours, the title compound **134d** (35.0 mg, 75%) was obtained as a waxy white solid after column chromatography (minimum amount of silica gel, cyclohexane-ethyl acetate, 20/1 to 10/1).

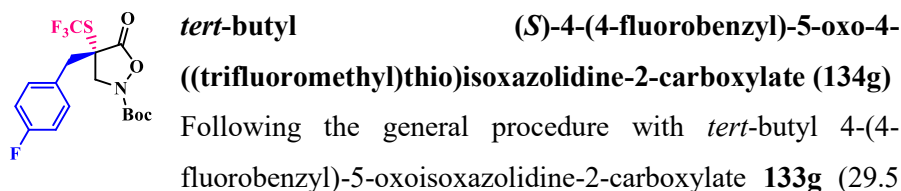
^1H NMR (300 MHz, CDCl_3) δ 4.37 (d, $J = 13.1$ Hz, 1H), 4.25 (d, $J = 13.1$ Hz, 1H), 3.72 (d, $J = 15.0$ Hz, 1H), 3.38 (d, $J = 15.0$ Hz, 1H), 1.56 (s, 9H). ^{13}C NMR (75 MHz, CDCl_3) δ 168.5, 154.6, 146.6–146.1 (m), 143.3–142.8 (m), 138.7–138.1 (m), 135.4–134.7 (m), 127.4 (q, $J = 311.2$ Hz), 106.3, 84.4, 57.8, 52.3, 27.3, 26.8. ^{19}F NMR (282 MHz, CDCl_3) δ -36.3 (m), -138.5 – -138.8 (m), -152.0 (m), -160.3 – -160.5 (m). HRMS (MALDI) $[\text{M}+\text{H}^+]$ calcd for $\text{C}_{16}\text{H}_{14}\text{F}_8\text{NO}_4\text{S}$ 468.0510, found 468.0511. $[\alpha]_D^{20} = +86.6^\circ$ ($c = 0.50$,

CHCl₃). Enantiomeric excess = 78% determined by HPLC analysis (CHIRALPAK[®] AS-H column (ϕ 0.46 cm x 25 cm), *n*-hexane:*i*-PrOH = 95:5, 0.5 mL/min, t_{major} = 9.3 min, t_{minor} = 10.1 min).



Following the general procedure with *tert*-butyl 4-(4-nitrobenzyl)-5-oxoisoxazolidine-2-carboxylate **133f** (32.2 mg, 0.10 mmol, 1.0 eq.), *N*-(trifluoromethylthio)phthalimide **105** (2.0 eq., 0.20 mmol, 49.4 mg) and catalyst **96a** (0.05 eq., 0.005 mmol, 5.4 mg) for 72 hours, the title compound **134f** (22.0 mg, 52%) was obtained as a colorless oil solid after column chromatography (minimum amount of silica gel, cyclohexane-ethyl acetate, 20/1 to 10/1).

¹H NMR (300 MHz, CDCl₃) δ 8.23 (d, J = 8.8 Hz, 2H), 7.42 (d, J = 8.8 Hz, 2H), 4.28 (d, J = 13.0 Hz, 1H), 4.07 (d, J = 13.0 Hz, 1H), 3.65–3.40 (m, 2H), 1.52 (s, 9H). ¹³C NMR (75 MHz, CDCl₃) δ 169.8, 155.5, 148.0, 140.2, 131.4, 128.6 (q, J = 310.7 Hz), 124.1, 85.4, 57.3, 54.0, 40.2, 27.9. ¹⁹F NMR (282 MHz, CDCl₃) δ -35.5. HRMS (MALDI) [M+H⁺] calcd for C₁₆H₁₈F₃N₂O₆S 423.0832, found 423.0834. $[\alpha]_D^{20}$ = +30.0° (c = 0.50, CHCl₃). Enantiomeric excess = 64% determined by HPLC analysis (CHIRALPAK[®] AS-H column (ϕ 0.46 cm x 25 cm), *n*-hexane:*i*-PrOH = 70/30, 1.0 mL/min, t_{major} = 7.0 min, t_{minor} = 7.8 min).



mg, 0.10 mmol, 1.0 eq.), *N*-(trifluoromethylthio)phthalimide **105** (2.0 eq., 0.20 mmol, 49.4 mg) and catalyst **96a** (0.05 eq., 0.005 mmol, 5.4 mg) for 72 hours, the title compound **134g** (21.0 mg, 53%) was obtained as a colorless oil after column chromatography (minimum amount of silica gel, cyclohexane-ethyl acetate, 20/1 to 10/1).

^1H NMR (300 MHz, CDCl_3) δ 7.24–7.12 (m, 2H), 7.12–6.94 (m, 2H), 4.24 (d, $J = 13.0$ Hz, 1H), 4.09 (d, $J = 13.0$ Hz, 1H), 3.45 (d, $J = 14.4$ Hz, 1H), 3.32 (d, $J = 14.4$ Hz, 1H), 1.51 (s, 9H). ^{13}C NMR (75 MHz, CDCl_3) δ 170.3, 162.7 (d, $J = 248.1$ Hz), 155.6, 132.1 (d, $J = 8.2$ Hz), 128.8 (q, $J = 310.8$ Hz), 128.6 (d, $J = 3.6$ Hz), 116.0 (d, $J = 21.7$ Hz), 85.1, 56.9, 54.4, 39.8, 27.9. ^{19}F NMR (282 MHz, CDCl_3) δ -35.6, -113.4. HRMS (MALDI) $[\text{M}^+]$ calcd for $\text{C}_{16}\text{H}_{17}\text{F}_4\text{NO}_4\text{S}$ 395.0809, found 395.0818. $[\alpha]_D^{20} = +57.0^\circ$ ($c = 0.50$, CHCl_3). Enantiomeric excess = 78% determined by HPLC analysis (CHIRALPAK[®] AS-H column ($\phi 0.46$ cm x 25 cm), *n*-hexane:*i*-PrOH = 96/4, 0.5 mL/min, $t_{\text{major}} = 10.5$ min, $t_{\text{minor}} = 11.1$ min).



tert-butyl

(*S*)-4-(4-chlorobenzyl)-5-oxo-4-

((trifluoromethylthio)isoxazolidine-2-carboxylate

(**134h**)

Following the general procedure with *tert*-butyl 4-(4-chlorobenzyl)-5-oxoisoxazolidine-2-carboxylate **133h** (31.2 mg, 0.10 mmol, 1.0 eq.), *N*-(trifluoromethylthio)phthalimide **105** (2.0 eq., 0.20 mmol, 49.4 mg) and catalyst **96a** (0.05 eq., 0.005 mmol, 5.4 mg) for 72 hours, the title compound **134h** (23.9 mg, 58%) was obtained as a colorless oil after column chromatography (minimum amount of silica gel, cyclohexane-ethyl acetate, 20/1 to 10/1).

^1H NMR (300 MHz, CDCl_3) δ 7.36 (d, $J = 8.7$ Hz, 2H), 7.18 (d, $J = 8.7$ Hz, 2H), 4.27 (d, $J = 13.0$ Hz, 1H), 4.10 (d, $J = 13.0$ Hz, 1H), 3.47 (d, $J = 14.5$

Hz, 1H), 3.35 (d, $J = 14.5$ Hz, 1H), 1.54 (s, 9H). ^{13}C NMR (75 MHz, CDCl_3) δ 169.7, 155.0, 134.0, 131.2, 130.8, 128.7, 128.2 (q, $J = 310.7$ Hz), 84.6, 56.4, 53.7, 39.4, 27.4. ^{19}F NMR (282 MHz, CDCl_3) δ -35.6. HRMS (MALDI) $[\text{M}+\text{K}^+]$ calcd for $\text{C}_{16}\text{H}_{17}\text{ClF}_3\text{KNO}_4\text{S}$ 450.0150, found 450.0155. $[\alpha]_D^{20} = +65.4^\circ$ ($c = 0.50$, CHCl_3). Enantiomeric excess = 78% determined by HPLC analysis (CHIRALPAK[®] AS-H column ($\phi 0.46$ cm x 25 cm), *n*-hexane:*i*-PrOH = 96/4, 0.5 mL/min, $t_{\text{major}} = 11.5$ min, $t_{\text{minor}} = 12.3$ min).



tert-butyl (S)-4-(4-bromobenzyl)-5-oxo-4-((trifluoromethyl)thio)isoxazolidine-2-carboxylate (134i)

Following the general procedure with *tert*-butyl 4-(4-bromobenzyl)-5-oxoisoxazolidine-2-carboxylate **133i** (35.6 mg, 0.10 mmol, 1.0 eq.), *N*-(trifluoromethylthio)phthalimide **105** (2.0 eq., 0.20 mmol, 49.4 mg) and catalyst **11** (0.05 eq., 0.005 mmol, 5.4 mg) for 48 hours, the title compound **134i** (36.0 mg, 79%) was obtained a pale yellow oil after column chromatography (minimum amount of silica gel, cyclohexane-ethyl acetate, 20/1 to 10/1).

^1H NMR (300 MHz, CDCl_3) δ 7.49 (d, $J = 8.4$ Hz, 2H), 7.10 (d, $J = 8.4$ Hz, 2H), 4.24 (d, $J = 13.0$ Hz, 1H), 4.07 (d, $J = 13.0$ Hz, 1H), 3.43 (d, $J = 14.5$ Hz, 1H), 3.31 (d, $J = 14.5$ Hz, 1H), 1.51 (s, 9H). ^{13}C NMR (75 MHz, CDCl_3) δ 169.2, 154.5, 131.2, 131.0, 130.8, 127.7 (q, $J = 310.5$ Hz), 121.6, 84.1, 55.9, 53.1, 39.0, 26.9. ^{19}F NMR (282 MHz, CDCl_3) δ -35.6. HRMS (MALDI) $[\text{M}+\text{K}^+]$ calcd for $\text{C}_{16}\text{H}_{17}\text{BrF}_3\text{KNO}_4\text{S}$ 493.9645, found 493.9651. $[\alpha]_D^{20} = +54.7^\circ$ ($c = 0.30$, CHCl_3). Enantiomeric excess = 76% determined by HPLC analysis (CHIRALPAK[®] ID column ($\phi 0.46$ cm x 25 cm), *n*-hexane:*i*-PrOH = 95/5, 1.0 mL/min, $t_{\text{minor}} = 8.0$ min, $t_{\text{major}} = 11.2$ min).

*tert*-butyl**(S)**-4-(4-iodobenzyl)-5-oxo-4-((trifluoromethylthio)isoxazolidine-2-carboxylate (**134j**))

Following the general procedure with *tert*-butyl 4-(4-iodobenzyl)-5-oxoisoxazolidine-2-carboxylate **133j** (40.3 mg, 0.10 mmol, 1.0 eq.), *N*-(trifluoromethylthio)phthalimide **105** (2.0 eq., 0.20 mmol, 49.4 mg) and catalyst **96a** (0.05 eq., 0.005 mmol, 5.4 mg) for 72 hours, the title compound **134j** (32.6 mg, 65%) was obtained as a colorless oil after column chromatography (minimum amount of silica gel, cyclohexane-ethyl acetate, 20/1 to 10/1).

¹H NMR (300 MHz, CDCl₃) δ 7.72 (d, *J* = 8.4 Hz, 2H), 6.99 (d, *J* = 8.4 Hz, 2H), 4.26 (d, *J* = 13.0 Hz, 1H), 4.09 (d, *J* = 13.0 Hz, 1H), 3.44 (d, *J* = 14.4 Hz, 1H), 3.32 (d, *J* = 14.4 Hz, 1H), 1.54 (s, 9H). ¹³C NMR (75 MHz, CDCl₃) δ 169.2, 154.5, 137.2, 131.5, 131.21, 127.7 (q, *J* = 310.4 Hz), 93.2, 84.1, 55.9, 53.0, 39.1, 26.91 ¹⁹F NMR (282 MHz, CDCl₃) δ -35.6. HRMS (MALDI) [M+K⁺] calcd for C₁₆H₁₇F₃IKNO₄S 541.9512, found 541.9526. [α]_D²⁰ = +65.8° (c = 0.50, CHCl₃). Enantiomeric excess = 80% determined by HPLC analysis (CHIRALPAK[®] AS-H column (ϕ0.46 cm x 25 cm), *n*-hexane:*i*-PrOH = 95/5, 0.5 mL/min, *t*_{major} = 16.6 min, *t*_{minor} = 19.6 min).

*tert*-butyl**(S)**-4-(4-methoxybenzyl)-5-oxo-4-

((trifluoromethylthio)isoxazolidine-2-carboxylate

(134k))

Following the general procedure with *tert*-butyl 4-(4-methoxybenzyl)-5-oxoisoxazolidine-2-carboxylate **133k** (30.7 mg, 0.10 mmol, 1.0 eq.), *N*-(trifluoromethylthio)phthalimide **105** (2.0 eq., 0.20 mmol, 49.4 mg) and catalyst **96a** (0.05 eq., 0.005 mmol, 5.4 mg) for 72 hours, the title compound **134k** (8.1 mg, 20%) was obtained as a colorless oil after

column chromatography (minimum amount of silica gel, cyclohexane-DCM, 1/1 to 4/1).

^1H NMR (300 MHz, CDCl_3) δ 7.16 (d, $J = 8.7$ Hz, 2H), 6.90 (d, $J = 8.7$ Hz, 2H), 4.26 (d, $J = 13.0$ Hz, 1H), 4.15 (d, $J = 13.0$ Hz, 1H), 3.83 (s, 3H), 3.45 (d, $J = 14.5$ Hz, 1H), 3.30 (d, $J = 14.5$ Hz, 1H), 1.53 (s, 9H). ^{13}C NMR (75 MHz, CDCl_3) δ 169.6, 158.5, 154.6, 130.5, 127.8 (q, $J = 310.4$ Hz), 123.7, 113.4, 83.9, 55.8, 54.3, 53.5, 38.8, 26.9. ^{19}F NMR (282 MHz, CDCl_3) δ -35.6. HRMS (MALDI) $[\text{M}+\text{K}^+]$ calcd for $\text{C}_{17}\text{H}_{20}\text{F}_3\text{KNO}_5\text{S}$ 446.0646, found 446.0648. $[\alpha]_D^{20} = +9.7^\circ$ ($c = 0.30$, CHCl_3). Enantiomeric excess = 88% determined by HPLC analysis (CHIRALPAK[®] ID column ($\phi 0.46$ cm x 25 cm), *n*-hexane:*i*-PrOH = 95/5, 1.0 mL/min, $t_{\text{major}} = 7.9$ min, $t_{\text{minor}} = 10.4$ min).



tert-butyl (S)-5-oxo-4-((trifluoromethyl)thio)-4-(3,4,5-trimethoxybenzyl)isoxazolidine-2-carboxylate (**134I**)

Following the general procedure with *tert*-butyl 5-oxo-4-(3,4,5-trimethoxybenzyl)isoxazolidine-2-carboxylate **133I** (36.7 mg, 0.10 mmol, 1.0 eq.), *N*-(trifluoromethylthio)phthalimide **105** (2.0 eq., 0.20 mmol, 49.4 mg) and catalyst **96a** (0.05 eq., 0.005 mmol, 5.4 mg) for 72 hours, the title compound **134I** (14.5 mg, 31%) was obtained as a colorless oil after column chromatography (minimum amount of silica gel, cyclohexane-DCM, 1/1 to 4/1).

^1H NMR (300 MHz, CDCl_3) δ 7.26 (s, 1H), 6.40 (s, 2H), 4.28 (d, $J = 13.0$ Hz, 1H), 4.13 (d, $J = 13.0$ Hz, 1H), 3.85 (s, 9H), 3.51 (d, $J = 14.3$ Hz, 1H), 3.23 (d, $J = 14.3$ Hz, 1H), 1.51 (s, 9H). ^{13}C NMR (75 MHz, CDCl_3) δ 169.7, 154.6, 152.5, 137.0, 127.8 (q, $J = 310.8$ Hz), 127.3, 106.4, 84.0, 59.8, 55.4, 55.20, 53.4, 40.1, 26.9. ^{19}F NMR (282 MHz, CDCl_3) δ -35.5. HRMS (MALDI) $[\text{M}+\text{K}^+]$ calcd for $\text{C}_{19}\text{H}_{24}\text{F}_3\text{KNO}_7\text{S}$ 506.0857, found 506.0861.

$[\alpha]_D^{20} = +60.3^\circ$ ($c = 0.3$, CHCl_3). Enantiomeric excess = 70% determined by HPLC analysis (CHIRALPAK[®] ID column ($\phi 0.46$ cm x 25 cm), *n*-hexane:*i*-PrOH = 80/20, 1.0 mL/min, $t_{\text{minor}} = 9.0$ min, $t_{\text{major}} = 15.6$ min).



tert-butyl (S)-5-oxo-4-(thiophen-2-ylmethyl)-4-((trifluoromethyl)thio)isoxazolidine-2-carboxylate (**134m**)

Following the general procedure with *tert*-butyl 5-oxo-4-(thiophen-2-ylmethyl)isoxazolidine-2-carboxylate **133m** (28.3 mg, 0.10 mmol, 1.0 eq.), *N*-(trifluoromethylthio)phthalimide **105** (2.0 eq., 0.20 mmol, 49.4 mg) and catalyst **96a** (0.05 eq., 0.005 mmol, 5.4 mg) for 72 hours, the title compound **134m** (29.9 mg, 78%) was obtained as a colorless oil after column chromatography (minimum amount of silica gel, cyclohexane-ethyl acetate, 20/1 to 10/1).

¹H NMR (300 MHz, CDCl_3) δ 7.33–7.27 (m, 1H), 7.06–7.01 (m, 1H), 7.02–6.95 (m, 1H), 4.33 (d, $J = 13.2$ Hz, 1H), 4.15 (d, $J = 13.2$ Hz, 1H), 3.73–3.57 (m, 2H), 1.55 (s, 9H). ¹³C NMR (75 MHz, CDCl_3) δ 169.3, 154.6, 132.9, 128.1, 127.6 (q, $J = 310.9$ Hz), 126.5, 125.3, 84.0, 56.2, 52.9, 33.9, 26.9. ¹⁹F NMR (282 MHz, CDCl_3) δ -35.7. HRMS (MALDI) $[M+K^+]$ calcd for $\text{C}_{14}\text{H}_{16}\text{F}_3\text{KNO}_4\text{S}_2$ 422.0104, found 422.0111. $[\alpha]_D^{20} = +56.0^\circ$ ($c = 0.50$, CHCl_3). Enantiomeric excess = 84% determined by HPLC analysis (CHIRALPAK[®] ID column ($\phi 0.46$ cm x 25 cm), *n*-hexane:*i*-PrOH = 95/5, 1.0 mL/min, $t_{\text{minor}} = 6.5$ min, $t_{\text{major}} = 9.2$ min).

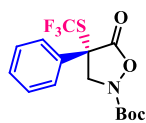


tert-butyl (S)-4-(furan-3-ylmethyl)-5-oxo-4-((trifluoromethyl)thio)isoxazolidine-2-carboxylate (**134n**)

Following the general procedure with *tert*-butyl 4-(furan-3-ylmethyl)-5-oxoisoxazolidine-2-carboxylate **133n** (26.7 mg, 0.10 mmol, 1.0 eq.), *N*-(trifluoromethylthio)phthalimide **105** (2.0 eq., 0.20 mmol, 49.4 mg)

and catalyst **96a** (0.05 eq., 0.005 mmol, 5.4 mg) for 72 hours, the title compound **134n** (12.1 mg, 33%) was obtained as a colorless oil after column chromatography (minimum amount of silica gel, cyclohexane-ethyl acetate, 20/1 to 10/1).

^1H NMR (300 MHz, CDCl_3) δ 7.51–7.40 (m, 1H), 7.40 (s, 1H), 6.33 (s, 1H), 4.32 (d, $J = 13.1$ Hz, 1H), 4.11 (d, $J = 13.1$ Hz, 1H), 3.33 (d, $J = 15.2$ Hz, 1H), 3.22 (d, $J = 15.2$ Hz, 1H), 1.55 (s, 9H). ^{13}C NMR (75MHz, CDCl_3) δ 169.5, 154.6, 142.8, 140.9, 127.7 (q, $J = 310.1$ Hz), 115.6, 110.4, 84.0, 56.0, 52.7, 29.6, 26.9. ^{19}F NMR (282 MHz, CDCl_3) δ -35.7. HRMS (MALDI) $[\text{M}+\text{K}^+]$ calcd for $\text{C}_{14}\text{H}_{16}\text{F}_3\text{KNO}_5\text{S}$ 406.03333, found 406.0333. $[\alpha]_D^{20} = +24.3^\circ$ ($c = 0.30$, CHCl_3). Enantiomeric excess = 66% determined by HPLC analysis (CHIRALPAK[®] AS-H column ($\phi 0.46$ cm x 25 cm), *n*-hexane:*i*-PrOH = 95/5, 0.5 mL/min, $t_{\text{major}} = 11.2$ min, $t_{\text{minor}} = 11.9$ min).



tert-butyl

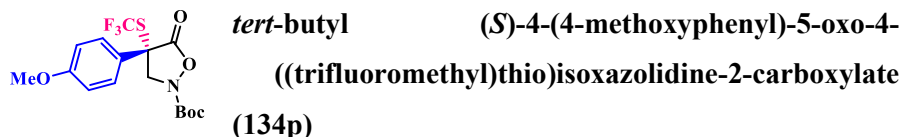
(*S*)-5-oxo-4-phenyl-4-

((trifluoromethyl)thio)isoxazolidine-2-carboxylate (**134o**)

Following the general procedure with *tert*-butyl 5-oxo-4-phenylisoxazolidine-2-carboxylate **133o** (26.3 mg, 0.10 mmol, 1.0 eq.), *N*-(trifluoromethylthio)phthalimide **105** (2.0 eq., 0.20 mmol, 49.4 mg) and catalyst **96b** (0.02 eq., 0.002 mmol, 1.8 mg) for 10 min, the title compound **134o** (30.2 mg, 83%) was obtained as a waxy white solid after column chromatography (minimum amount of silica gel, cyclohexane-ethyl acetate, 20/1 to 10/1).

^1H NMR (300 MHz, CDCl_3) δ 7.68–7.57 (m, 2H), 7.50–7.36 (m, 3H), 4.95 (d, $J = 12.8$ Hz, 1H), 4.59 (d, $J = 12.8$ Hz, 1H), 1.35 (s, 9H). ^{13}C NMR (75 MHz, CDCl_3) δ 170.4, 155.4, 131.7, 130.0, 129.4, 128.5 (q, $J = 310.7$ Hz), 127.4, 85.0, 59.6, 56.6, 27.7. ^{19}F NMR (282 MHz, CDCl_3) δ -36.8. HRMS (MALDI) $[\text{M}+\text{K}^+]$ calcd for $\text{C}_{15}\text{H}_{16}\text{F}_3\text{KNO}_4\text{S}$ 402.0384, found 402.0397.

$[\alpha]_D^{20} = -25.0^\circ$ ($c = 0.50$, CHCl_3). Enantiomeric excess = 68% determined by HPLC analysis (CHIRALPAK[®] AS-H column ($\phi 0.46$ cm x 25 cm), *n*-hexane:*i*-PrOH = 99/1, 0.5 mL/min, $t_{\text{minor}} = 19.5$ min, $t_{\text{major}} = 21.5$ min).



Following the general procedure with *tert*-butyl 4-(4-methoxyphenyl)-5-oxoisoxazolidine-2-carboxylate **133p** (29.3 mg, 0.10 mmol, 1.0 eq.), *N*-(trifluoromethylthio)phthalimide **105** (2.0 eq., 0.20 mmol, 49.4 mg) and catalyst **96b** (0.02 eq., 0.002 mmol, 1.8 mg) for 10 min, the title compound **134p** (33. mg, 84%) was obtained as a waxy white solid after column chromatography (minimum amount of silica gel, cyclohexane-ethyl acetate, 20/1 to 10/1).

¹H NMR (300 MHz, CDCl_3) δ 7.56 (d, $J = 8.9$ Hz, 2H), 6.96 (d, $J = 8.9$ Hz, 2H), 4.97 (d, $J = 12.7$ Hz, 1H), 4.58 (d, $J = 12.7$ Hz, 1H), 3.84 (s, 2H), 1.38 (s, 9H). ¹³C NMR (75 MHz, CDCl_3) δ 169.6, 159.8, 154.4, 127.9, 127.6 (q, $J = 310.8$ Hz), 121.8, 113.7, 83.8, 58.5, 55.42, 54.4, 26.7. ¹⁹F NMR (282 MHz, CDCl_3) δ -36.9. HRMS (MALDI) $[\text{M}+\text{Na}^+]$ calcd for $\text{C}_{16}\text{H}_{18}\text{F}_3\text{NNaO}_5\text{S}$ 416.0750, found 416.0753. $[\alpha]_D^{20} = -31.4^\circ$ ($c = 1.00$, CHCl_3). Enantiomeric excess = 76% determined by HPLC analysis (CHIRALPAK[®] AS-H column ($\phi 0.46$ cm x 25 cm), *n*-hexane:*i*-PrOH = 95/5, 0.5 mL/min, $t_{\text{minor}} = 10.6$ min, $t_{\text{major}} = 11.6$ min).

6.7.5 General procedure for the synthesis of 2-trifluoromethylthio- $\beta^{2,2}$ -amino acid **137a**

In a Schlenk type tube, ammonium formate (10 eq., 1.5 mmol) and Pd/C (10%w/w) (0.10 eq., 0.015 mmol, 16.0 mg) were added to a solution of *tert*-butyl 4-benzyl-5-oxo-4-((trifluoromethyl)thio)isoxazolidine-2-carboxylate **134a** (1.0 eq., 0.15 mmol, 56.6 mg) in *tert*-Butanol (1.5 ml). Then, 3 freeze-pump-thaw cycles were performed, the tube sealed and the reaction mixture was heated at 90 °C overnight. Next, the reaction mixture was filtered through a plug of Celite[®], washed with ethyl acetate (2 x 10 mL) and the filtrate evaporated was washed with brine (3 x 10 mL). The organic phase was dried over MgSO₄, filtered and vacuum to rotavapor, affording the desired product **137a** (51.2 mg, 90%) as a waxy solid.



(S)-2-benzyl-3-((*tert*-butoxycarbonyl)amino)-2-

((trifluoromethyl)thio)propanoic acid (137a**)**

¹H NMR (300 MHz, Methanol-*d*₄) δ 7.25 (s, 5H), 3.65 (d, *J* = 14.5 Hz, 1H), 3.55 (d, *J* = 14.5 Hz, 1H), 3.28–3.17 (m, 2H), 1.44 (s, 9H). ¹³C NMR (75 MHz, CD₃CN) δ 170.6, 155.6, 134.2, 130.5, 130.0 (q, *J* = 307.9 Hz), 128.3, 127.1, 79.1, 62.0, 44.3, 39.5, 27.5. ¹⁹F NMR (282 MHz, Methanol-*d*₄) δ -39.2. HRMS (MALDI) [M+Na⁺] calcd for C₁₆H₂₀F₃NNaO₄S 402.0957, found 402.0972. [α]_D²⁰ = +19.4° (c = 0.50, CHCl₃).

6.7.6 X-Ray data

Compound **105**

A clear colourless prismatic-like specimen of C₁₈H₈F₆N₂O₄S₂, approximate dimensions 0.170 mm x 0.297 mm x 0.308 mm was obtained by slow evaporation of a solution of the compound **105** (5 mg) in hexane:2-propanol 1:1 (5.0 mL) and selected for the X-ray crystallographic analysis.

The X-ray intensity data were measured. The total exposure time was 8.69 hours. The frames were integrated with the Bruker SAINT software package using a narrow-frame algorithm. The integration of the data using an orthorhombic unit cell yielded a total of 30632 reflections to a maximum θ angle of 25.34° (0.83 \AA resolution), of which 1762 were independent (average redundancy 17.385, completeness = 100.0%, $R_{\text{int}} = 2.31\%$, $R_{\text{sig}} = 0.72\%$) and 1731 (98.24%) were greater than $2\sigma(F^2)$. The final cell constants of $a = 5.17410(10) \text{ \AA}$, $b = 9.2140(3) \text{ \AA}$, $c = 20.1869(5) \text{ \AA}$, volume = $962.39(4) \text{ \AA}^3$, are based upon the refinement of the XYZ-centroids of 81 reflections above $20 \sigma(I)$ with $6.886^\circ < 2\theta < 49.18^\circ$. Data were corrected for absorption effects using the multi-scan method (SADABS). The ratio of minimum to maximum apparent transmission was 0.963. The calculated minimum and maximum transmission coefficients (based on crystal size) are 0.8960 and 0.9410. The final anisotropic full-matrix least-squares refinement on F^2 with 145 variables converged at $R1 = 2.60\%$, for the observed data and $wR2 = 9.81\%$ for all data. The goodness-of-fit was 1.059. The largest peak in the final difference electron density synthesis was $0.224 \text{ e}/\text{\AA}^3$ and the largest hole was $-0.215 \text{ e}/\text{\AA}^3$ with an RMS deviation of $0.084 \text{ e}/\text{\AA}^3$. On the basis of the final model, the calculated density was 1.706 g/cm^3 and $F(000)$, 496 e^- .

Table S9. Sample and crystal data for compound 105

Chemical formula	$\text{C}_{18}\text{H}_8\text{F}_6\text{N}_2\text{O}_4\text{S}_2$
Formula weight	494.38 g/mol
Temperature	250(2) K
Wavelength	0.71073 \AA
Crystal size	0.170 x 0.297 x 0.308 mm
Crystal habit	clear colourless prismatic
Crystal system	orthorhombic
Space group	P 21 21 21
Unit cell dimensions	$a = 5.17410(10) \text{ \AA}$ $\alpha = 90^\circ$

	$b = 9.2140(3) \text{ \AA}$	$\beta = 90^\circ$
	$c = 20.1869(5) \text{ \AA}$	$\gamma = 90^\circ$
Volume	$962.39(4) \text{ \AA}^3$	
Z	2	
Density (calculated)	1.706 g/cm^3	
Absorption coefficient	0.365 mm^{-1}	
F(000)	496	

Table S10. Data collection and structure refinement for Compound 105.

Theta range for data collection	2.02 to 25.34°	
Index ranges	-6 ≤ h ≤ 6, -11 ≤ k ≤ 11, -24 ≤ l ≤ 24	
Reflections collected	30632	
Independent reflections	1762 [R(int) = 0.0231]	
Coverage of independent reflections	100.0%	
Absorption correction	multi-scan	
Max. and min. transmission	0.9410 and 0.8960	
Refinement method	Full-matrix least-squares on F ²	
Refinement program	SHELXL-2014/7 (Sheldrick, 2014)	
Function minimized	$\Sigma w(F_o^2 - F_c^2)^2$	
Data / restraints / parameters	1762 / 0 / 145	
Goodness-of-fit on F²	1.059	
Δ/σ_{\max}	0.001	
Final R indices	1731 data; I > 2σ(I)	R1 = 0.0260, wR2 = 0.0742
	all data	R1 = 0.0293, wR2 = 0.0981

Weighting scheme	$w=1/[\sigma^2(F_o^2)+(0.0584P)^2+0.4730P]$ where $P=(F_o^2+2F_c^2)/3$
Absolute structure parameter	0.0(0)
Largest diff. peak and hole	0.224 and -0.215 eÅ ⁻³
R.M.S. deviation from mean	0.084 eÅ ⁻³

Compound 134d

A clear colourless prismatic-like specimen of C₁₆H₁₃F₈NO₄S, approximate dimensions 0.085 mm x 0.262 mm x 0.430 mm, was obtained by slow evaporation of a solution of the compound **134d** (2 mg) in hexane:2-propanol 1:1 (2.0 mL) and selected for the X-ray crystallographic analysis. The X-ray intensity data were measured. The total exposure time was 1.96 hours. The frames were integrated with the Bruker SAINT software package using a narrow-frame algorithm. The integration of the data using an orthorhombic unit cell yielded a total of 23930 reflections to a maximum θ angle of 25.35° (0.83 Å resolution), of which 3592 were independent (average redundancy 6.662, completeness = 99.7%, $R_{\text{int}} = 3.62\%$, $R_{\text{sig}} = 2.12\%$) and 3006 (83.69%) were greater than $2\sigma(F^2)$. The final cell constants of $\underline{a} = 11.5372(5)$ Å, $\underline{b} = 11.7999(5)$ Å, $\underline{c} = 14.4627(6)$ Å, volume = 1968.92(14) Å³, are based upon the refinement of the XYZ-centroids of 5731 reflections above $20 \sigma(I)$ with $5.685^\circ < 2\theta < 41.06^\circ$. Data were corrected for absorption effects using the multi-scan method (SADABS). The ratio of minimum to maximum apparent transmission was 0.922. The calculated minimum and maximum transmission coefficients (based on crystal size) are 0.8960 and 0.9780. The final anisotropic full-matrix least-squares refinement on F^2 with 274 variables converged at $R1 = 3.60\%$, for the observed data and $wR2 = 13.05\%$

for all data. The goodness-of-fit was 1.018. The largest peak in the final difference electron density synthesis was $0.317 \text{ e}^-/\text{\AA}^3$ and the largest hole was $-0.387 \text{ e}^-/\text{\AA}^3$ with an RMS deviation of $0.122 \text{ e}^-/\text{\AA}^3$. On the basis of the final model, the calculated density was 1.577 g/cm^3 and $F(000)$, 944 e⁻.

Table S11. Sample and crystal data for Compound 134d.

Chemical formula	C ₁₆ H ₁₃ F ₈ NO ₄ S	
Formula weight	467.33 g/mol	
Temperature	270(2) K	
Wavelength	0.71073 Å	
Crystal size	0.085 x 0.262 x 0.430 mm	
Crystal habit	clear colourless prismatic	
Crystal system	orthorhombic	
Space group	P 21 21 21	
Unit cell dimensions	a = 11.5372(5) Å	α = 90°
	b = 11.7999(5) Å	β = 90°
	c = 14.4627(6) Å	γ = 90°
Volume	1968.92(14) Å ³	
Z	4	
Density (calculated)	1.577 g/cm ³	
Absorption coefficient	0.261 mm ⁻¹	
F(000)	944	

Table S12. Data collection and structure refinement for Compound 134d.

Theta range for data collection	2.23 to 25.35°
Index ranges	-13 ≤ h ≤ 13, -14 ≤ k ≤ 14, -17 ≤ l ≤ 17
Reflections collected	23930
Independent reflections	3592 [R(int) = 0.0362]

Coverage of independent reflections	99.7%
Absorption correction	multi-scan
Max. and min. transmission	0.9780 and 0.8960
Refinement method	Full-matrix least-squares on F^2
Refinement program	SHELXL-2014/7 (Sheldrick, 2014)
Function minimized	$\Sigma w(F_o^2 - F_c^2)^2$
Data / restraints / parameters	3592 / 0 / 274
Goodness-of-fit on F^2	1.018
Final R indices	3006 data; $R1 = 0.0360$, $wR2 = 0.0950$ $I > 2\sigma(I)$ all data $R1 = 0.0506$, $wR2 = 0.1305$
Weighting scheme	$w = 1 / [\sigma^2(F_o^2) + (0.0757P)^2 + 0.5583P]$ where $P = (F_o^2 + 2F_c^2) / 3$
Absolute structure parameter	-0.0(0)
Largest diff. peak and hole	0.317 and -0.387 $e\text{\AA}^{-3}$
R.M.S. deviation from mean	0.122 $e\text{\AA}^{-3}$

